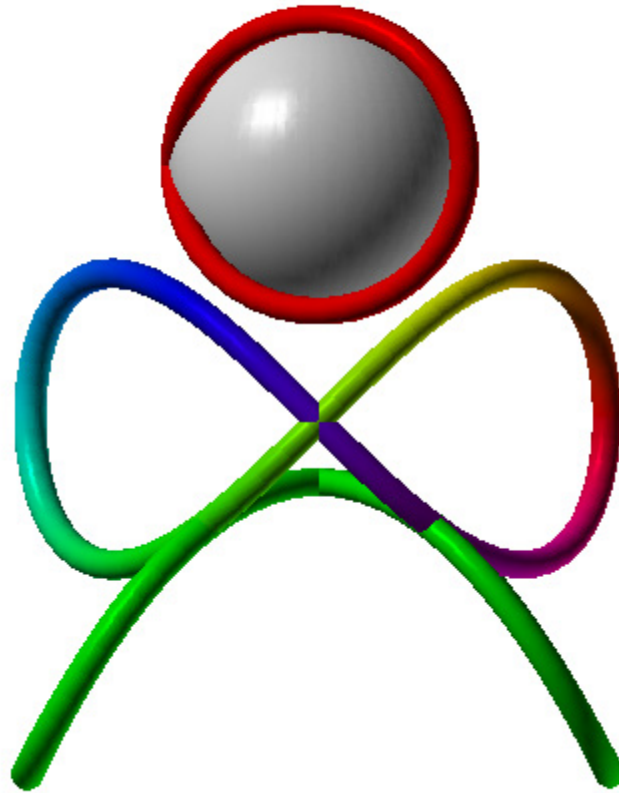


QSO — the Mathematics and Physics of Quasi-Spherical Orbits



Robert G. Chester

QSO – the Mathematics and Physics
of Quasi-Spherical Orbits

Copyright © 2009 by Robert G. Chester

All rights reserved under International and Pan-American Copyright Conventions

Published in the United States

by

Intellectual Property Associates

276 Dennis Street

Tumwater, WA 98501

N914TJ@comcast.net

530.15-dc21

ISBN 978-0-9840727-0-5 (paper)

ISBN 978-0-9840727-3-6 (digital)

Library of Congress Control Number: 2009928577

The index was prepared by

Nancy K. Humphreys

www.wordmapsindexing.com

THIS WORK IS DEDICATED TO



MICHAEL BURKE

“For some unexplained reason [physics professors] seem stuck with the idea that spin is of necessity a 2D phenomenon.”

Contents

Acknowledgments	vii
Rationale	viii
Introduction	ix
<p>The hippoede of Eudoxus (Eudoxus of Cnidus, 408-355 B.C.); The limaçon (Etienne Pascal, 1588-1651); Viviani’s window, aka the “quadrable Florentine sail” (Vincenzo Viviani, 1622 -1703); <i>rhodonea</i> (Guido Grandi, 1671-1742); the lemniscate of Gerono (Camille Christophe Gerono, 1799-1891); Great Circle Railroad Tracks of Energy (Buckminster Fuller, 1895-1983)</p>	
Chapter 1. Curves of Compound Curvature	1
<p>Space Curves; Definition; Alternate Definition; Virtual Sphere; Generating QSOs; Visualization; Generating QSO (1:1) with the Unicycle; Points-of-View; Dynamic Diversity</p>	
Chapter 2. Coordinates and Equations	11
<p>Spherical Coordinates; The QSO Equation in Spherical Coordinates; Limitations of the Spherical Coordinate System – and an Advantage; Cartesian Coordinates; The QSO Equation in Cartesian Notation; Limitations of the Cartesian Coordinate System; The Isotropic Vector Matrix (IVM); Variations on a Theme; Exchanging Axes; Reversing the Polarity of the Axes; Exchanging Rotations; Reversing the Chirality of the Rotations; Exchanging Trig Functions</p>	
Chapter 3. Elements of the QSO	33
<p>The QSO Ratio; Fractional Ratios; Exponential Ratios; Irrational Ratios; Continuously Varying Ratios; Poles; Monopoles; Dipoles; Multipoles; Events; The Event Constellation</p>	

Chapter 4. Events	51
The Intersection Event; Tangent Events; Moving Off-Axis; Dipole Events; A Geometric Anomaly	
Chapter 5. Orbits	68
Orbital Length; Expanding the Envelope; The QSO Landscape; The First 100 Monopole QSOs	
Chapter 6. Displays	78
The First QSO Display; The Kelleher Rotation; The Octamap; Cone & Disk; Globe with Latitude and Longitude; Three-in-One	
Chapter 7. Plane Curves	105
Circle; Parabola; The Lemniscate of Gerono; Cardioid; Limaçon; Epitrochoids; Going Further; Hypotrochoids; Rhodonea	
Chapter 8. Lissajous Figures	133
Lissajous Figures (1:1), (2:1), (3:1), (10:7); Quasi-Cylindrical Orbits	
Chapter 9. Space Curves	145
The Conical Helix; The 3-D Astroid; The Baseball Seam; The Spherical Cardioid; The Clelia; Viviani's Curve	
Chapter 10. Monopole Polygons & Polyhedra	158
First Tetrahedron; The 1(a:1) Series; Chord Lengths; Tipping Angle; The 1(1:b) Series; Chord Lengths; Reversal of Orientation; Loftus QSOs – The L-1(a:1) Series; Loftus QSOs – The L-1(1:b) Series; a-gons & b-gons; The Z-axis; From a-gons and b-gons to Polyhedra	

Chapter 11. The Platonic Solids	185
The QSO 1(3:2) Tetrahedron; The QSO 1(2:3) Octahedron; The QSO 1(2:5) Icosahedron; In Pursuit of the Elusive Dodecahedron	
Chapter 12. Commencement	194
Janus; The Last Platonic; Fuller on Structure; The Analemma	
Appendix 1. Simulating the Unicycle	212
The Fork; The Axle and Two Small Spheres to Give the Axle a Finished Look; The Hub; The Spokes; A Small Sphere That Rotates in Sync With One Spoke; The Wheel; The QSO; Clones; A Tubular QSO	
Appendix 2. Three-Axis Rotation	222
Appendix 3. The Octet Truss	224
Appendix 4. A Brief History of QSO Programming	227
Appendix 5. Drawing QSO Polyhedra	228
QSO 1(1:3), the Oblate Tetrahedron; Chord Lengths; Chords With a Z-Term; QSO 1(2:3), the Prolate Octahedron; QSO 1(2:5), the Prolate Icosahedron; QSO 1(4:5), a 40-hedron; Variables Needed to Write the Chords of the First 25 QSO Monopoles; Derivation of the Total Chord Formula	
References	245
Index	247

Acknowledgments

I must first and foremost recognize the profound creativity of Michael Burke, without whom the study of Quasi-Spherical Orbits would not exist. His insights and guidance have been crucial at every juncture. I must also recognize the contributions of the mathematicians and programmers without whose skills and dedication the exploration of QSOs could not have proceeded: David Loftus, Athol Crosby, John Kelleher, Roland Prodaniuk, Darrell Adams, and Chris Young. Thanks also go to Dr. Vauhn Wittman-Grahler and the students and staff of the Quantitative Reasoning Center, The Evergreen State College, Olympia, WA, and to the reference librarians of the Timberland Regional Library, Olympia, WA, for their assistance in time of need. Finally, I am happily indebted to Ron Avitzur and the crew at Pacific Tech for authoring Graphing Calculator, the Category Five application with which 99⁴⁴/100% of this book is illustrated.

R.G.C.
Tumwater, WA
2009 May 29

Rationale

The purpose of this work is to present a more realistic model for a number of dynamic three-dimensional physical phenomena which are traditionally depicted statically in two dimensions and are therefore misleading. It is also to provide a model for phenomena which are regarded as conceivable only in abstract mathematical terms, and are therefore thought to be permanently inaccessible to the non-specialist. The use of the QSO model will reveal pattern and enable analysis in hitherto untouched areas.

Introduction

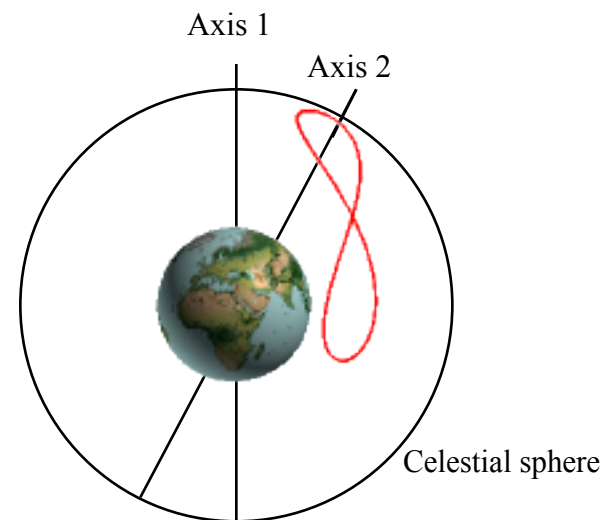
In the fourth century B.C., Greek astronomers had a problem. They had noticed that a handful of the astral lights that filled the night sky moved or wandered¹ across the backdrop of fixed lights. The accepted explanation was that the moving lights were carried on crystal spheres in perfect circles around the Earth. What troubled the sky-gazers was the fact that sometimes the wanderers seemed to reverse their motion. From time to time the lights were distinctly seen to go backward in their heavenly meanderings, only to soon reverse themselves and again resume their customary movement. In the heavens, where all things were perfect, this was clearly unacceptable.

Eudoxus of Cnidus (408-355 B.C.) attempted to explain the motion of the wandering lights with an ingenious scheme involving dual crystal spheres. One sphere, he said, rotated on an axis which passed through the center of the Earth. A second sphere was identical to and concentric with the first, but the axis of the second sphere was determined by two points on the first sphere and *rotated with it*. If the spheres then rotate with equal but opposite angular velocities, a light on the second sphere will describe the figure eight in the sketch. Because it resembles a horse fetter, the curve is called the hippopede² of Eudoxus.³

¹ English *planet* from Greek *planasthai*, to wander

² Greek *hippos*, horse + Latin *impedire*, to entangle, fetter

³ The conventional view of the H. of Eudoxus is seen at <<http://www-groups.dcs.st-andrews.ac.uk/~history/Mathematicians/Eudoxus.html>>

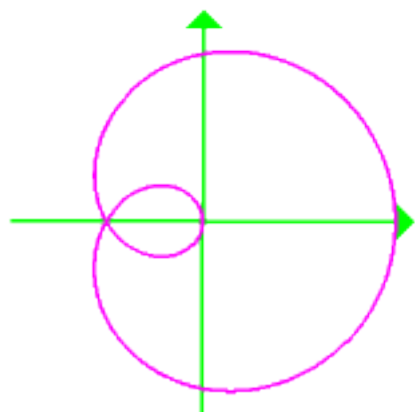


The hippopede of Eudoxus

Eudoxus' curve didn't work too well as an explanation for the retrograde motion of the planets, but he introduced concepts of central importance to the study of Quasi-Spherical Orbits. First, there are two intersecting but noncollinear axes. A point rotates around one axis while that axis rotates around the other. The point thus rotates simultaneously around both axes. The relative angular rates of rotation determine a ratio. In Eudoxus' cosmology this ratio was 1:1, i.e. the angular velocities were equal. Negating one of the velocities as Eudoxus did places the

hippopede in a different quadrant of the sky, but the resulting curve is the same. The axes need not be at 90° to each other (Eudoxus' aren't), and the curve, the hippopede, is the result of a dynamic system.

Twenty-one centuries after Eudoxus, a French lawyer and amateur mathematician, Etienne Pascal (1588-1651), studied curves with an inner loop. In 1650 his contemporary, Gilles de Roberval (1602-1675), named them *limaçon*, which means "snail" in French. It seems unlikely that either man realized that their snails were related to Eudoxus' work.

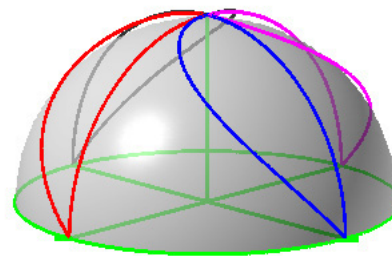


The limaçon -- Pascal's snail

About the same time that Pascal was working with snail-like curves in France, the Italian, Vincenzo Viviani (1622 -1703), published his *Aenigma geometricum*,⁴ which challenged the analysts (mathematicians) of his day to determine on the surface

⁴ Full title: *Aenigma geometricum de miro opificio Testudinis Quadrabilis Hemisphaericae*

of a hemisphere "...four equal windows in such a way that the remaining surface after removal of the windows could be exactly squared." The problem was solved by a number of Viviani's contemporaries, not the least of which was Gottfried Leibnitz.⁵ The problem became known as Viviani's window, but was called the "quadrable Florentine sail" by Viviani himself because of the sail-like appearance of the solution.



Viviani's window, aka quadrable Florentine sail

Viviani's window was and is considered a problem in analytic geometry. There is little or no appreciation of the fact that it is a dynamic phenomenon, or that entire families of curves can be generated from the QSO rotations that create it.

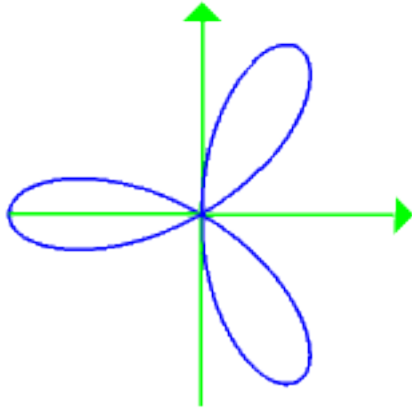
A generation after Viviani, another Italian, Guido Grandi (1671-1742), studied curves which he called *rhodonea*⁶ because they reminded him of roses.

⁵ Loria, G. (1925), p. 201

Roero C. S. (1986), pp. 351-379

Roero C. S. (1988), pp. 803-810

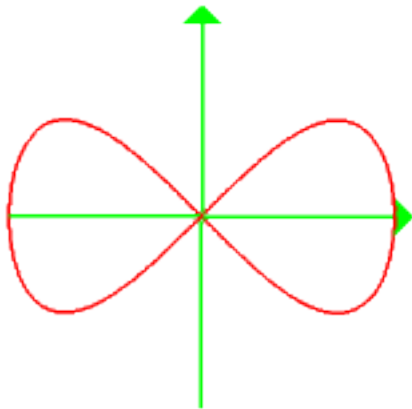
⁶ From Greek *rhodon*, rose.



The trifolium, a three-lobed rhodonea curve

Grandi might be surprised to learn that his beautiful rose curves are the two-dimensional projections of three-dimensional QSOs.

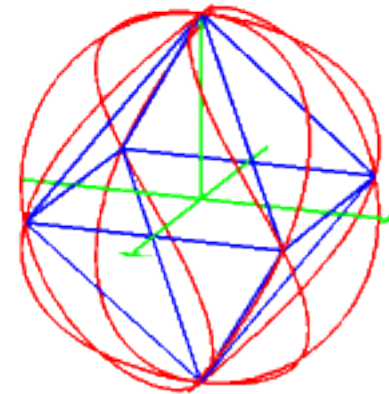
A century after Grandi and Viviani, French mathematician Camille Christophe Geronno (1799-1891) studied what came to be known as the “eight curve.”



The eight curve

Geronno’s ribbon-like curve, which is sometimes called the lemniscate⁷ of Geronno, only superficially resembles Viviani’s window. There is no evidence that they’re related. And yet, both men studied aspects of the same curve, a curve which is, in fact, a QSO.

In 1975 and again in 1979 Buckminster Fuller (1895-1983) discussed what he considered to be the basic energy exchange mechanism in Universe.⁸ Energy, Fuller said, never travels in straight lines. It is stored on and shunted along the multiple “great circle railroad tracks of energy” of the tetrahedron, octahedron, icosahedron, and Vector Equilibrium, Fuller’s name for the cuboctahedron. When energy gets a green light to go from one of the great circles to the next, he said, it can do so by crossing over one of the inter-atomic-sphere bridges, or Grand Central Stations, where the great circles intersect.



Octahedron with great circle railroad tracks of energy

⁷ New Latin, from Latin *lemniscus*, ribbon, from Greek *lemniskos*.

⁸ Fuller, 1975, p. 187

_____, 1979, p. 455

There is always the problem with Bucky's model of how a charge manages to jump from one track to another. He did not explain how the jump was achieved. QSO shows how this happens, and it's not a jump. QSO demonstrates that the charge is sequentially on all the great circles, or on the only one nonsimultaneous great circle. QSO demonstrates that one great circle can pass through all the vertices of a polyhedron. It shows how a single dipole may non-simultaneously constitute an entire system.

* * *

The author must now confess to a small deception. The goal in beginning with these historical antecedents of Quasi-Spherical Orbits was to indicate the range and depth of the QSO concept. Each historical example was illustrated with a sketch. The deception is in the sketches. None of them is based on the original mathematics or physics. Eudoxus' twin crystal spheres were not used to generate the hippopede; the hippopede displayed here is a QSO. Pascal's equations, Viviani's geometry and Grandi's *rhodonea* were not used to generate their curves; they too are QSOs. Likewise for Gerono and Fuller. In every case, the curve illustrating the discoveries of each scientist or mathematician is a Quasi-Spherical Orbit. Although it is unusual to come across a simple concept that subsumes such diverse phenomena, it is not unheard of. Let us proceed to a fuller investigation of these most interesting curves.

Curves of Compound Curvature

Space Curves

QSOs are space curves.¹ They are one-dimensional closed loops which exist in three-dimensional space.

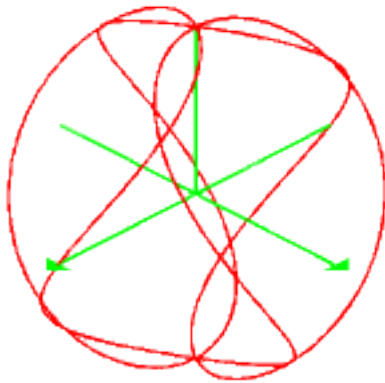


Fig. 1-1a

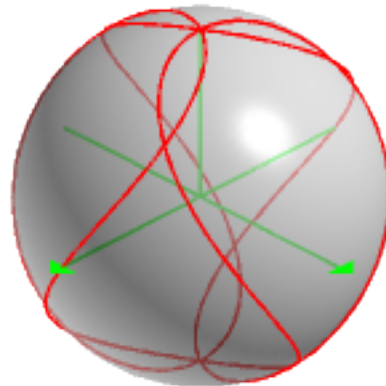


Fig. 1-1b

QSO (2:3)

A one-dimensional QSO space curve

It is difficult to appreciate the three-dimensionality of these curves on a flat page, so a translucent gray sphere has been

¹ The relationship between QSOs and more familiar space curves will be explored in chapter 9.

added to the QSO on the right. The sphere partially blocks the visually confusing overlap of front and back traces and aids depth perception.

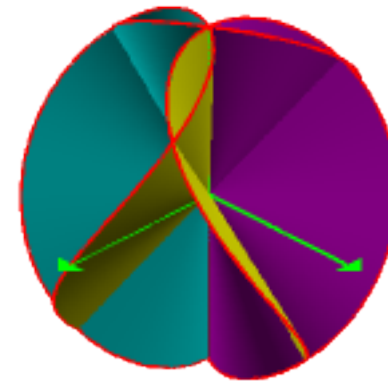


Fig. 1-2
2-D QSO (2:3)

Two-dimensional QSOs are surfaces that exist in three-dimensional space. In figure 1-2, QSO (2:3) is shown again, this time as a self-intersecting two-dimensional surface. Dynamically, the surface corresponds to the sweepout of the radius vector that traces the one-dimensional, linear QSO. For comparison, the one-dimensional QSO in red outlines the two-dimensional multicolored surface.

Three-dimensional QSOs have not been investigated. Such rotations, which presumably trace out volumes of space, offer an excellent opportunity for further exploration.

Definition

A Quasi-Spherical Orbit (QSO) is the path of a particle in orbit simultaneously about two or more axes with a common center.

Alternate Definition

A Quasi-Spherical Orbit (QSO) is the path of a particle in a great circle orbit when a second spin axis is introduced. This causes the great circle to “tumble.” The resultant track appears to be no longer a great circle, but is in fact the synergetic result of the combination of two great circle events or systems.²

² The American Heritage Electronic Dictionary defines “synergy” as:

1. The interaction of two or more agents or forces so that their combined effect is greater than the sum of their individual effects.
2. Cooperative interaction among groups, especially among the acquired subsidiaries or merged parts of a corporation, that creates an enhanced combined effect.

This definition is insufficient for QSOs. Fuller’s (1975) is better.

§101.01 Synergy means behavior of whole systems unpredicted by the behavior of their parts taken separately.

§102.00 Synergy means behavior of integral, aggregate, whole systems unpredicted by behaviors of any of their components or subassemblies of their components taken separately from the whole.

Fuller’s emphasis is not on “an enhanced combined effect,” which may, after all, be quite predictable, but on the unpredicted behaviors of the whole. It includes all such behaviors, not merely additive ones as in the AHED entry.

Although QSOs can be conceived with any number of commonly centered axes, and with various angular orientations, we will limit ourselves here to the simplest case, that is, where there are two axes and they are at 90° to each other.³

Virtual Sphere

QSOs occur on the surface of a virtual sphere. Although the virtual sphere can have any arbitrary size, it simplifies matters considerably if the sphere has a unit radius. Neither of these conventions eliminates the possibility that QSOs may occur on surfaces other than spherical, or that the sphere might have a radius other than unity.

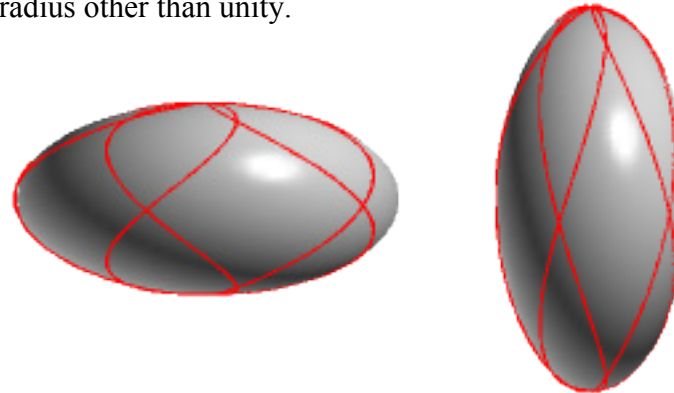


Fig. 1-3a

Fig. 1-3b

Quasi-Elliptical Orbits

QEOs (3:5)

An oblate spheroid, left, and a prolate spheroid, right.

³ Rotation on three mutually perpendicular axes was explored by Kelleher (1991) and by Prodaniuk (1992). See appendix 2.

Two or more QSOs may occur on a single sphere, but a single QSO may not occur on more than one sphere.

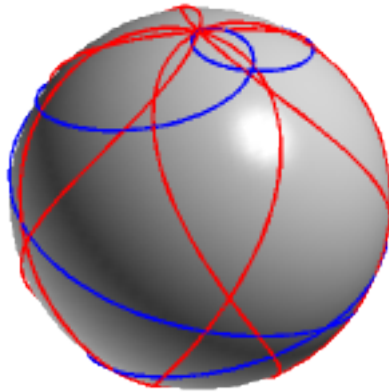


Fig. 1-4
QSO (3:5) [red]
QSO (4:1) [blue]

Generating QSOs

Imagine tying a rock on a string and swinging it around your head. Can you clearly see the path of the rock? Imagine swinging it at the end of your arm, vertically. Again, can you see the path? Now combine the two motions. Imagine swinging the rock *simultaneously* in the vertical and the horizontal planes.⁴ If you're like most people you have no idea what the path of the rock now looks like. Rotation around one axis is a familiar idea. Rotation around two axes sequentially is

⁴ Although it's unfamiliar, it's quite possible to swing an actual rock like this. The key is in knowing where to lead the rock with your arm.

equally familiar, but rotation around two or more axes simultaneously is next to unknown.⁵

Visualization

QSOs are most readily visualized by imagining an inverted unicycle.⁶ The tire has been repaired with a red patch which is at the zenith. One spoke, which points toward the zenith, is colored violet. The seat and pedals have been removed from this unicycle, the better to illuminate the concepts involved.

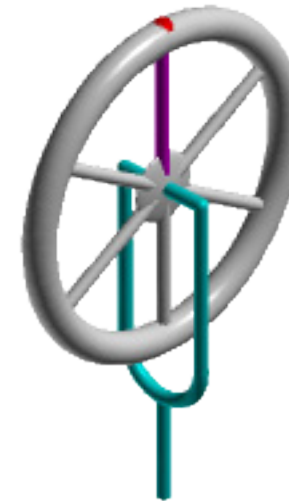


Fig. 1-5
An inverted unicycle

⁵ Technically, rotation about two axes simultaneously is precession.

⁶ See appendix 1 for the mathematics needed to generate the unicycle.

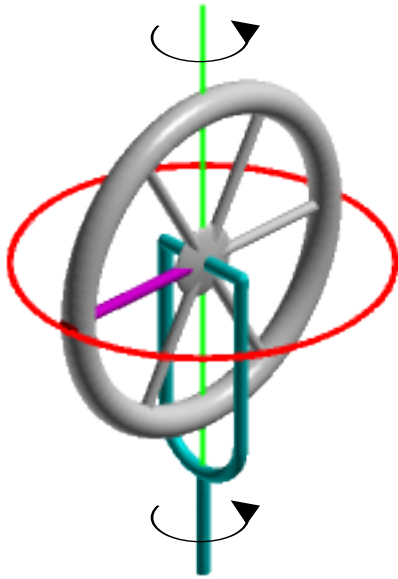


Fig. 1-6
Horizontal orbit

If the patch is placed at the equator and the brake is set, the wheel and fork rotate as a unit about the axis of the seat post. Like the rock around your head, the patch describes a great circle orbit in a horizontal plane. Rotation is in the positive, i.e. the right hand direction.

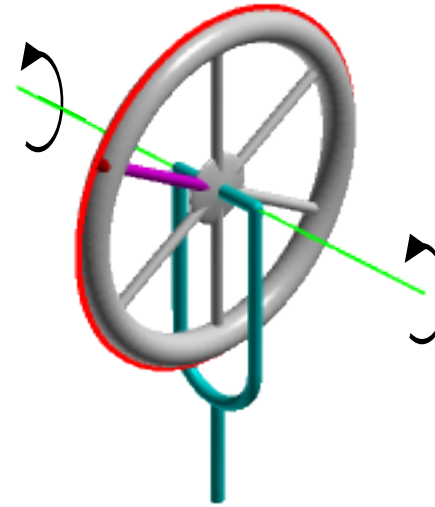


Fig. 1-7
Vertical orbit

When the brake is released and the fork locked, the wheel rotates around its own axle. The patch describes a great circle orbit in a vertical plane as did the rock when you swung it at the end of your arm. Rotation is again in the positive or right-hand direction.

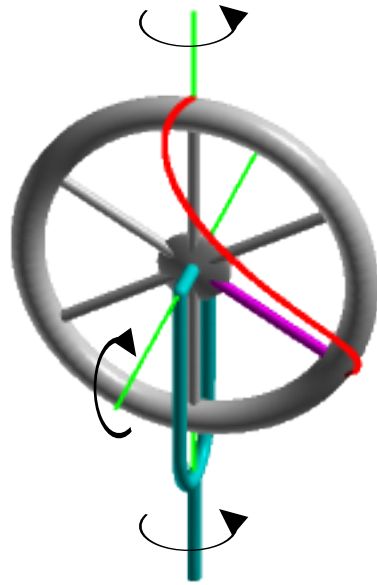
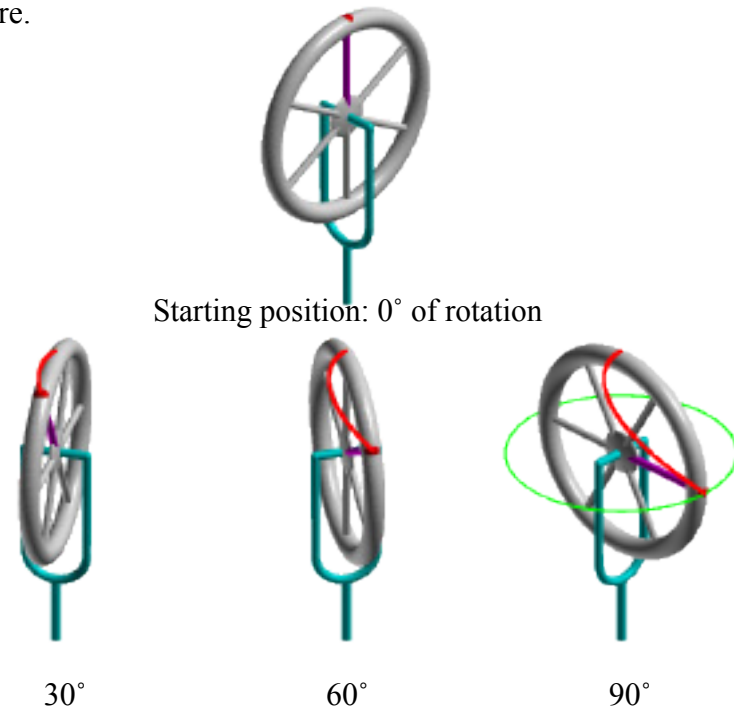


Fig. 1-8
A Quasi-Spherical Orbit

When the wheel and the fork rotate simultaneously, the patch describes an orbital path on the surface of a virtual sphere. The orbital trace seems to be no longer a great circle. It has become a Quasi-Spherical Orbit, or QSO. The precise shape of the orbit is determined by the ratio between the rotational rates on each of the axes.

Generating QSO (1:1) with the Unicycle

Starting with the patch at the vertex, the wheel and fork rotate in the right hand direction around the axis of the seat post. At the same time the wheel also rotates in the right hand direction around its own axle. The rate of rotation on both axes is the same. The *ratio* of the rates of rotation is therefore 1:1 so this is QSO (1:1). Development of the QSO is illustrated next in 30° increments. The patch begins at the north pole of the virtual sphere.



At 90° of rotation (right) the patch reaches the equator of the virtual sphere.

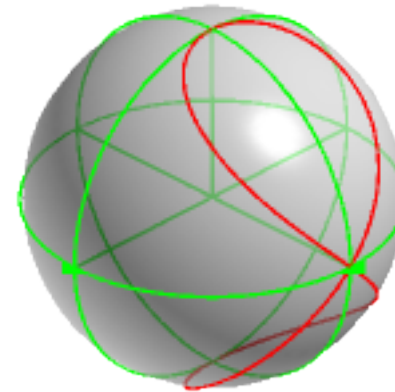
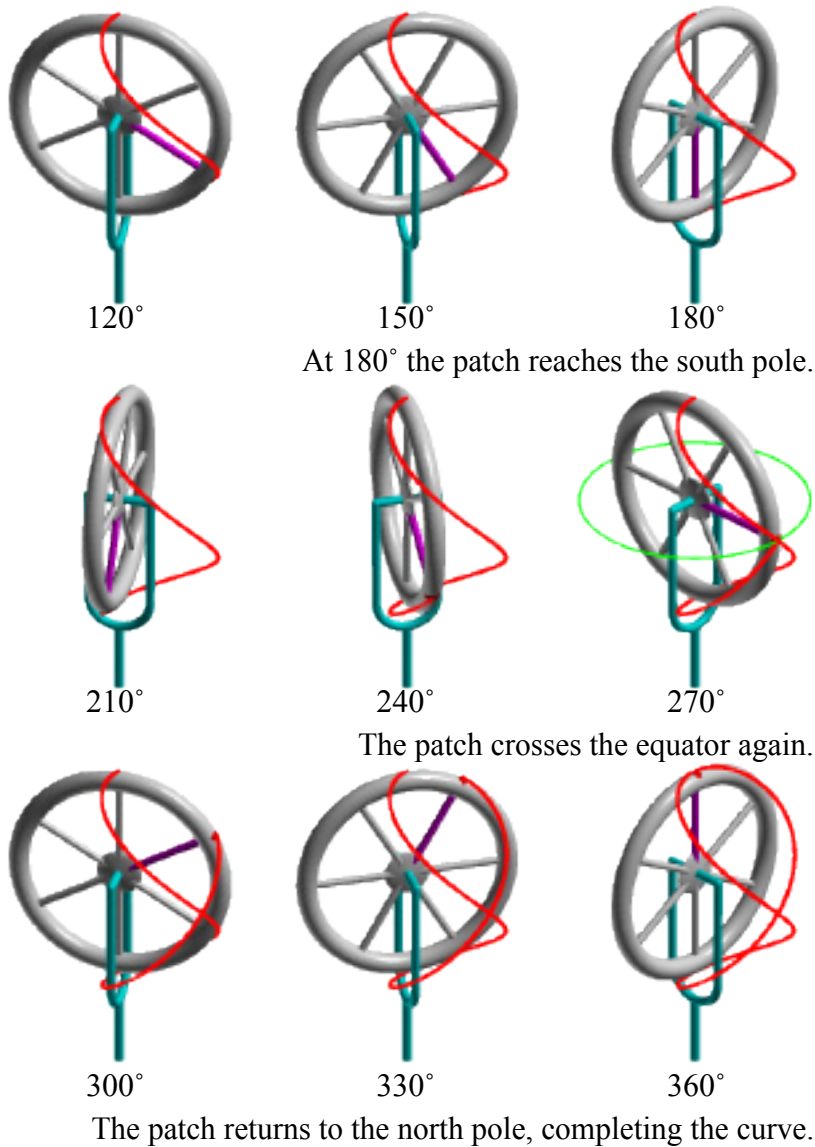


Fig. 1-9
QSO (1:1)

QSO (1:1) is shown on the virtual sphere. The sphere is slightly transparent to allow the full QSO to be seen. Three great circle meridians divide the sphere into octants.

The QSO resembles a bent figure 8. It exhibits symmetry with respect to two of the great circle meridians. The single intersection occurs at the equator where the QSO crosses itself at 90°. All QSOs are self-intersecting. That is, in the course of a single orbit the particle crosses its own trace at least once. The reader may want to turn back now and compare the first quadrant of QSO (1:1) with Viviani's window in the introduction. Four such quadrants comprise Viviani's figure.

Points-of-View

The model particularly accents the importance of considering more than a single point-of-view. In the following illustrations QSO (1:1) is shown again, first as it appears with the unicycle, and then as it appears when seen head-on from each of the three axes of the Cartesian coordinate system.⁷

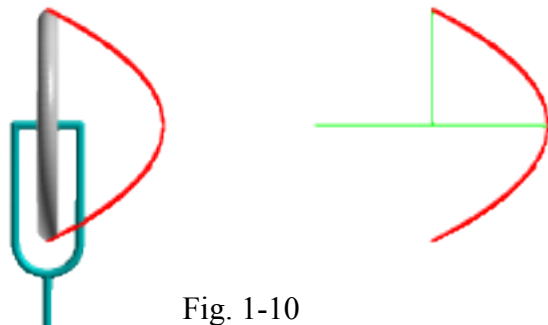


Fig. 1-10
QSO (1:1), view from the x-axis

Seen from the x-axis, QSO (1:1) is an open arc. In chapter 7 the open arc will be shown to be a parabola.

⁷ Software note:

All of the QSOs in this book are generated on Graphing Calculator 3.2 by Pacific Tech <<http://www.PacificT.com/>>. Macintosh and PC versions are available. In Graphing Calculator's 3-D world, the x- and y-axes have arrows that point in the positive direction. The z-axis has no arrow, but Graphing Calculator draws only its positive side.

In the first two sketches that follow, the arrowheads on the positive x- and y-axes are not immediately apparent. They are two-dimensional, and they are drawn in the xy-plane. When seen from any point in this plane, the arrowheads are edge-on. They have no depth. The third illustration, the view from the positive z-axis, clearly shows the arrowheads.

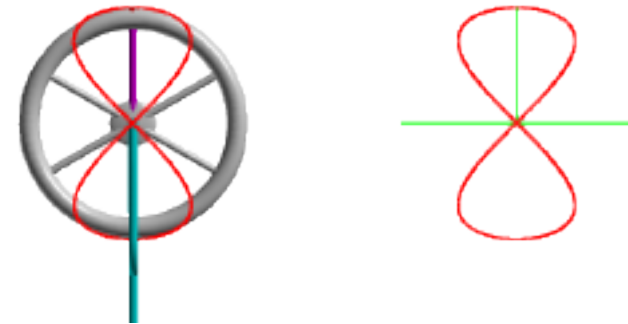


Fig. 1-11
QSO (1:1), view from the y-axis

From the y-axis, the QSO is the figure 8 previously noted. Likewise, chapter 7 will explore the relationship between the figure 8 and the lemniscate of Geronno.



Fig. 1-12
QSO (1:1), view from the z-axis

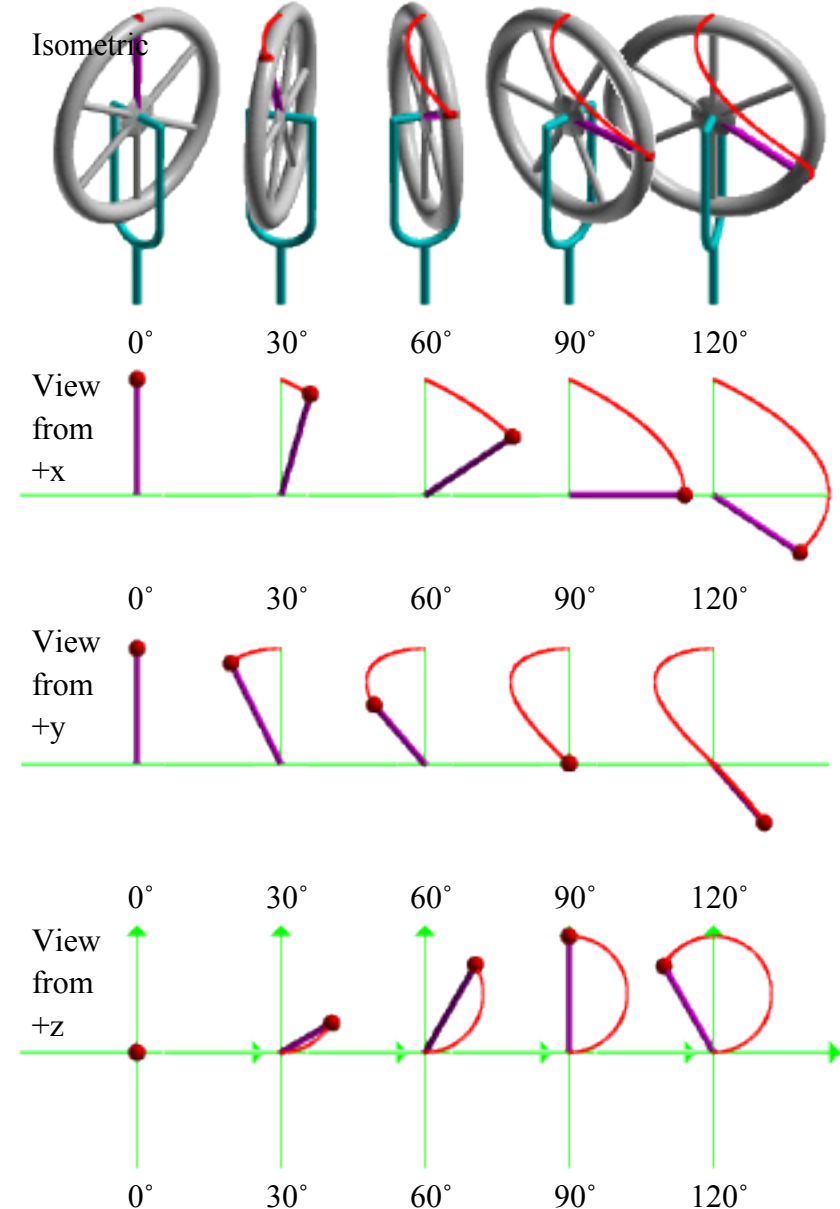
From the z-axis the QSO is a circle. The reader may recognize the cover art on this book as a composite of these three views of QSO (1:1).

Dynamic Diversity

The dynamic picture is equally diverse. The view from the x-axis shows a reciprocating half-wave motion. Looking from the y-axis the particle travels counterclockwise in the northern hemisphere and clockwise in the southern, and from the z-axis the motion seems to be consistently counterclockwise. The x-, y-, and z-views of QSO (1:1) are shown next developing together. The three views, which seem mutually contradictory, must be taken into simultaneous consideration if one is to understand what is really happening. When the wheel, fork, axle and five of the six spokes are removed, the red patch is revealed to be a small sphere rotating at the end of a violet radius. The isometric view with the unicycle is reproduced for comparison.

A Quasi-Spherical Orbit is that trace left by a point rotating simultaneously about two or more intersecting axes where the point of intersection forms a common center of rotation.⁸ The common center of rotation is the Origin of the coordinate system. This appears to be obvious in the two views from the x- and y-axes, but is counterintuitive for the view from the z-axis where the QSO is tracing a circle. Although the center of rotation is at the Origin, the center of the circle is not.

At 90° the QSO has rotated through 1/4 of its total rotation. The *static* pictures seem to show that the elapsed rotation as seen from the x-axis is 90°, although from the y- and z-axes it looks like 180° each.



⁸ See p. 2.

At 180° , half way through, the arc and the circle seem to be complete. Elapsed rotation as seen from the x-axis is apparently -180° . From the y-axis it's $+180^\circ$ followed by -180° , and from the z it appears to be $+360^\circ$. However, stopping here would seriously misrepresent the shape of the orbit.

At 210° the arc and the circle seem to be retracing themselves, but because the QSO is a three dimensional curve this cannot be true. Close examination of the circular trace reveals that the small red sphere is now behind the curve, away from the viewer.

At 270° the QSO intersects itself for the first and only time.

At 300° the small sphere has moved behind the curve in the x-view and in front of it again as seen from +z.

At 360° QSO (1:1) has developed to its fullest extent. The angular sweepout of the particle may be assessed at anything from $\pm 180^\circ$ to $\pm 360^\circ$ to $+720^\circ$! This last angular measure is reminiscent of Fuller's statement that the minimum system is the minimum knot = 720° .^{9,10} QSO (1:1) is the minimum QSO. The model reminds us to look not only at the static picture of the completed curve, but at the video of its dynamic formation.

⁹ Fuller, 1979, p. 403, §1033.665.

¹⁰ Edmondson, 1987, chapter 5.

Coordinates and Equations

Spherical Coordinates

There are three coordinate systems which can be used to graphically illustrate QSOs. Each of these has advantages and disadvantages which we will examine in turn. We begin with the spherical coordinate system.

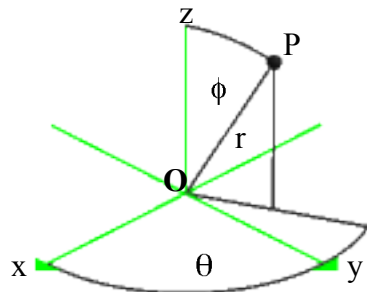


Fig. 2-1

The spherical coordinate system

A fixed point in space is established as the Origin of the system. Three mutually perpendicular axes pass through the Origin. Traditionally the axes are labeled x , y and z , with each axis having positive and negative halves extending to positive and negative infinity. Also by convention the x - and y -axes

define a horizontal plane and the z -axis is perpendicular to that plane.

A point P can be located by measuring its distance from the Origin and its angular displacement from the x - and z -axes. The distance of the point from the Origin is r , the radius of the virtual sphere on which the point lies. In the unicycle model (figure 1–5), r corresponds to the violet spoke which connects the hub of the unicycle to the rotating patch, which here is point P .

The angles from the x - and z -axes are labeled with the Greek letters θ and ϕ . There is sometimes a difference between the way physicists and mathematicians name the angles, so it's necessary to be clear about which is which. For convenience, we adopt the mathematical usage of Graphing Calculator, the primary display software. The angular displacement from the x -axis is expressed as θ . From the z -axis it's ϕ . The location of point P in spherical coordinates is therefore

$$P(r, \theta, \phi)$$

The QSO Equation in Spherical Coordinates

A Quasi-Spherical Orbit is the result of simultaneous rotations around two axes. A vector expression is an efficient way of expressing both rotations along with the radial position of the rotating point.

$$\begin{bmatrix} r \\ \theta \\ \phi \end{bmatrix} = \begin{bmatrix} 1 \\ 1 \\ 1 \end{bmatrix}$$

Eqn. 2-1

The variables r , θ and ϕ appear on the left side of the equation. The order in which the variables appear is also the order in which they're calculated by the software. This is of little concern with respect to the radius which is invariant on the unit sphere. However, the order becomes critically important when dealing with the rotations because in general rotations do not commute. Therefore the order of the QSO rotations assigned by the math is taken as the default order for all QSOs. Specifically, that order is *first theta, then phi*. QSO notation reflects this convention. We write “QSO ($\theta:\phi$),” and *not* “QSO ($\phi:\theta$).” In the natural world the order of the rotations may in fact differ from this convention which is adopted solely to simplify the exploration of QSOs. On the right side of equation 2-1 each variable is assigned a test value of one unit.

Graphing,

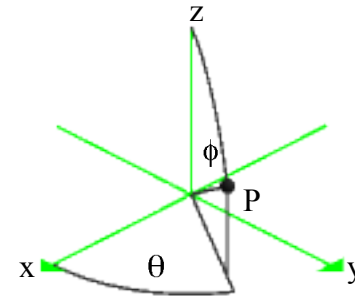


Fig. 2-2

Point (1, 1, 1) in spherical coordinates

The resulting picture shows only point P ; no QSO is evident. Point P is located at a distance r from the Origin and has been rotated θ and ϕ degrees respectively from the x - and z -axes. The default interpretation for angles is radians, so the angles of rotation in degrees are

$$\theta = 1 \text{ radian} = 57.296\dots^\circ$$

$$\phi = 1 \text{ radian} = 57.296\dots^\circ$$

The actual path point P has traveled is revealed by replacing the unit values of the angles with the parametric variable t where $t: 0 \dots 1$.

$$\begin{bmatrix} r \\ \theta \\ \phi \end{bmatrix} = \begin{bmatrix} 1 \\ t \\ t \end{bmatrix}$$

Eqn. 2-2

Graphing,

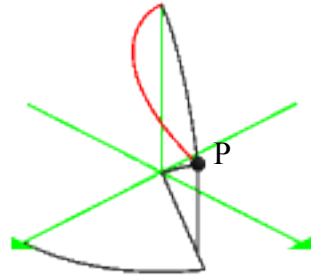


Fig. 2-3
A partial QSO trace

The software calculates and plots the position of P for every value of t from zero to one.¹ Since t is a multiplier of θ and ϕ , and since $\theta = \phi = 1$ radian, the curve exists only from 0° to $57.296\dots^\circ$. In order to see the full curve t needs to encompass the full cycle. There are two ways to accomplish this. We can define $t: 0 \dots 2\pi$, or we can multiply each t in the equation by 2π . The latter method is more instructive.

¹ Compare Fig. 2-3 with Fig. 1-9.

$$\begin{bmatrix} r \\ \theta \\ \phi \end{bmatrix} = \begin{bmatrix} 1 \\ 2\pi t \\ 2\pi t \end{bmatrix}$$

Eqn. 2-3

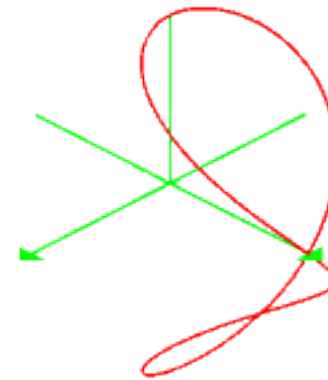


Fig. 2-4
The QSO after one cycle of revolution

The ensuing curve is the familiar QSO (1:1) which results from identical rotations on both axes. To generate QSOs in which the rotations are not identical, we employ variables a and b .² By convention a and b are real numbers. Here they are taken to be positive integers.

² This notation also introduces the possibility of QSOs that have identical but non-unitary rates of rotation, e.g. QSO (15:15).

Equation 2-3 becomes

$$\begin{bmatrix} r \\ \theta \\ \phi \end{bmatrix} = \begin{bmatrix} 1 \\ a2\pi t \\ b2\pi t \end{bmatrix}$$

Eqn. 2-4

For $a = 2$, $b = 3$, the curve is

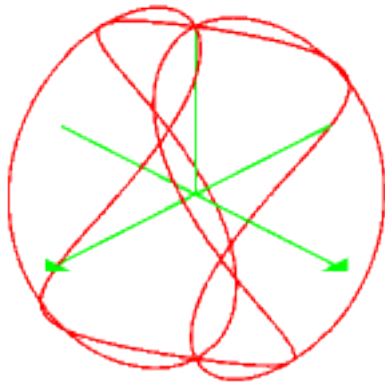


Fig. 2-5
QSO (2:3)

This curve is the one which introduced QSOs in chapter 1, figures 1-1a, b.

So far, so good. We have developed a vector expression using spherical coordinates that will compute and display any QSO whether the rates of rotation are identical or not. Although

technically the QSO is written as “QSO ($a2\pi t:b2\pi t$),” in practice we omit the invariant terms and write only “QSO ($a:b$).”

One last consideration is the fact that QSOs are not static curves that materialize completely developed either on the computer screen or in four-dimensional reality. They are dynamic phenomena which change and evolve over time.

A slider variable n is provided by the Graphing Calculator software. The slider may be used to animate any graph and show how it develops. With n , equation 2-4 becomes

$$\begin{bmatrix} r \\ \theta \\ \phi \end{bmatrix} = \begin{bmatrix} 1 \\ a2\pi nt \\ b2\pi nt \end{bmatrix}$$

Eqn. 2-5

Unlike t , whose range is displayed simultaneously, the range of n is calculated and displayed sequentially.³ If the range of n is set at $n: 0 \dots 1$ with 100 steps allowed between the limits, then each increment of n will represent 1% of the developing QSO.

³ Think of t as a strip of movie film. It shows a series of simultaneous but static pictures of a developing phenomenon. To see the phenomenon actually change, you need a film projector. That’s the role of n .

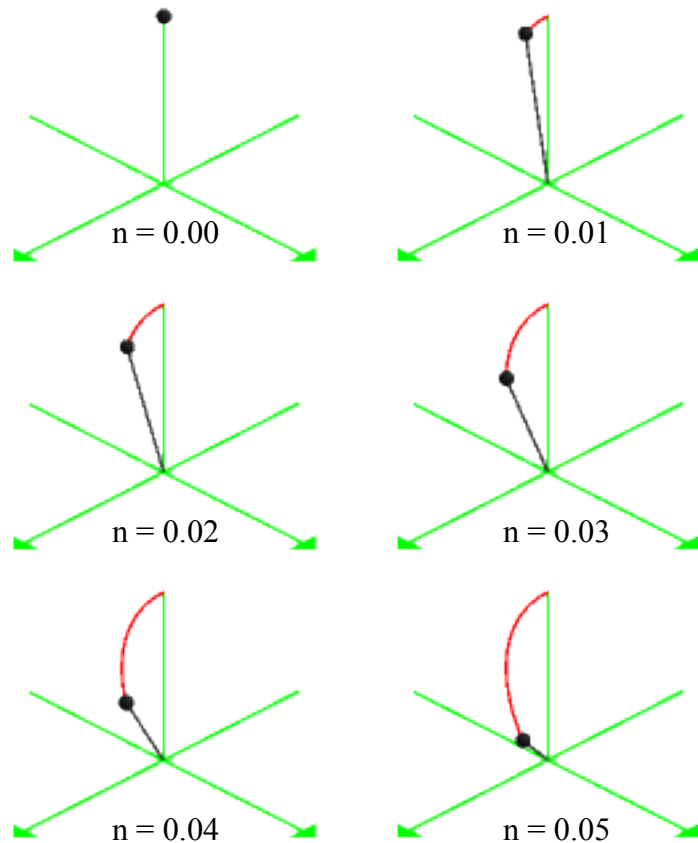


Fig. 2-6
QSO (2:3), $n: 0.00 \rightarrow 0.05$

The effect of watching these frames develop sequentially and rapidly on the screen is exactly that of watching a movie. You *see* the rotations. You *see* the curve develop.

A final step completes the spherical form of the QSO

equation. The term $2\pi n$ may be replaced by the symbol g .

$$g = 2\pi n$$

Substituting,

$$\begin{bmatrix} r \\ \theta \\ \phi \end{bmatrix} = \begin{bmatrix} 1 \\ agt \\ bgt \end{bmatrix}$$

Eqn. 2-6

The QSO equation in spherical notation

Limitations of the Spherical Coordinate System and an Advantage

The limitations of the spherical coordinate system are the same as those of the Cartesian system which will be discussed next. There is a slight advantage to spherical coordinates in that the defined angles are identical to those of QSOs. Thus the spherical expressions for QSOs tend to be somewhat simpler than the Cartesian ones.

Cartesian Coordinates

The Cartesian coordinate system is named after its inventor, René Descartes (1596-1650).

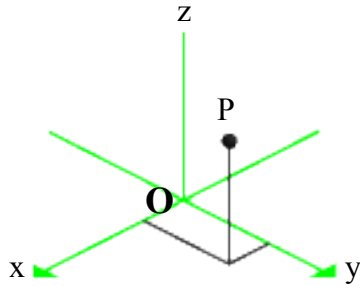


Fig. 2-7

The Cartesian coordinate system

As in spherical coordinates, a fixed point in space is established as the Origin of the system. Three mutually perpendicular axes which pass through the Origin are constructed and labeled as before. A point P is located by measuring first along one axis, then along the second, and finally along the third. The coordinates of P are by convention written as

$$P(x, y, z)$$

The QSO Equation in Cartesian Notation

The derivation of the Cartesian form of the QSO equation is fairly straightforward. We begin with point P in the combined spherical and Cartesian coordinate system.

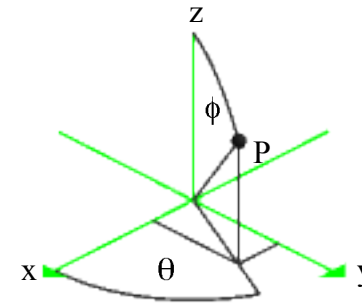


Fig. 2-8

Point P in spherical and Cartesian notation

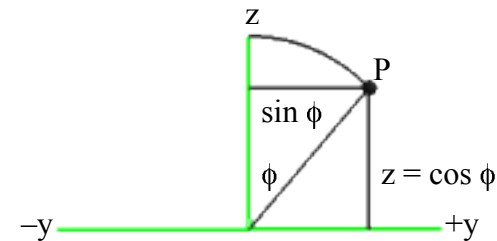


Fig. 2-9

View from the x-axis

The view from the x-axis shows that

$$z = \cos \phi$$

while the horizontal distance of P from the z-axis is $\sin \phi$.

For the x- and y-values we need to look at the point from the z-axis.

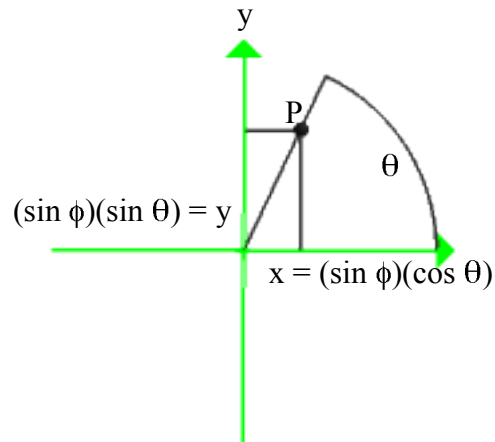


Fig. 2-10
View from the z-axis

Therefore the x- and y-values are

$$x = (\sin \phi)(\cos \theta)$$

$$y = (\sin \phi)(\sin \theta)$$

Writing the vector equation

$$\begin{bmatrix} x \\ y \\ z \end{bmatrix} = \begin{bmatrix} (\sin \phi) (\cos \theta) \\ (\sin \phi) (\sin \theta) \\ \cos \phi \end{bmatrix}$$

Eqn. 2-7

We now face a problem similar to that of equation 2-1. Graphing this equation would yield a single point P , but not a QSO. By a process of reasoning similar to that above, we know that

$$\theta = agt$$

$$\phi = bgt$$

Substituting,

$$\begin{bmatrix} x \\ y \\ z \end{bmatrix} = \begin{bmatrix} (\sin bgt) (\cos agt) \\ (\sin bgt) (\sin agt) \\ \cos bgt \end{bmatrix}$$

Eqn. 2-8a

The QSO equation in Cartesian notation

Limitations of the Cartesian Coordinate System

The Cartesian (and spherical) way of looking at space has two major limitations with respect to QSOs. First, it comes to us from a time when stasis, not movement, was the norm. When René Descartes died in 1650, the *Philosophiae Naturalis Principia*, in which Sir Isaac Newton first published his three Laws of Motion, was thirty-seven years in the future. When Einstein established beyond any doubt that motion, not stasis, is the universal norm, he utterly destroyed even the philosophical basis for Descartes' system. Nevertheless, the system continues to find wide acceptance. Although developments in graphing techniques allow the simulation of motion in the Cartesian system, people still tend to see static pictures.⁴ This is particularly disadvantageous to the study of QSOs which are dynamic and change through time.

The second limitation relates to the ability of the Cartesian system to adequately describe nature. Buckminster Fuller is especially critical: "*The prime barrier to humanity's discovery and comprehension of nature is the obscurity of the mathematical language of science. Fortunately, however, nature is not using the strictly imaginary, awkward, and unrealistic coordinate system adopted by and taught by present-day academic science.*"⁵

⁴ For this reason among others, movies of selected QSOs have been included with this book.

⁵ Fuller's reasons for objecting so strenuously to the orthogonal axis system are beyond the scope of this book. See Fuller, 1979, p. xxiii, p. 566.

Fuller's alternative to Descartes, the Isotropic Vector Matrix, will be outlined next.⁶

The Isotropic Vector Matrix

Despite the convention to limit the discussion to axes that intersect at 90°, the definition of a QSO specifies no such limitation.⁷ Let us briefly explore a coordinate system that was discovered by R. Buckminster Fuller.⁸ To understand Fuller's design we begin with a stack of cannonballs.

⁶ The Cartesian coordinate system is not the only conventional mindset to be challenged by the QSO model. Burke proposes the use of base 720. He writes, "The use of base ten gives us immediate problems as, for instance, 1/3 becomes a recurring fraction and source of imprecision. The use of a much larger base would eliminate a large part of this vagueness. Change of base can reveal otherwise 'encrypted' hidden patterns. I am aware that large bases are considered to be difficult to handle, but... we have a solution to that. In fact I am going to suggest that we use base 720. And use degrees as our subdivisions of the circle. My intuition tells me that this should be as revealing of underlying pattern as the use of base 8 was in analysing the Franklin 16 x 16 square" (personal communication, 1995 Dec 2).

⁷ See p. 2.

⁸ The discussion here presents only the most superficial review of the Isotropic Vector Matrix. For Fuller's own exhaustive treatment, see Fuller (1975, 1979).

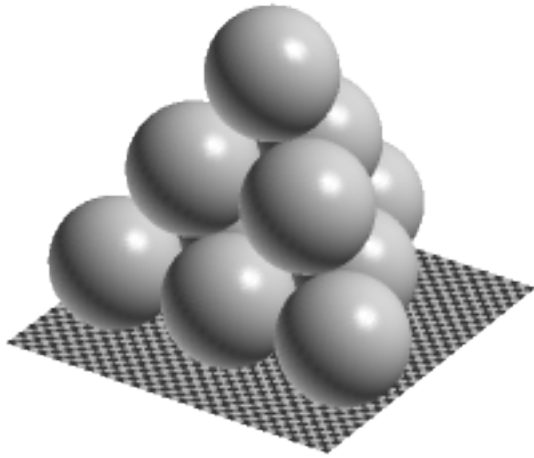


Fig. 2-11
Stacked cannonballs⁹

The figure shows ten cannonballs stacked in omnidirectional closest packing array. Each sphere is tangent to its neighbors and nestles in a valley formed by three others.

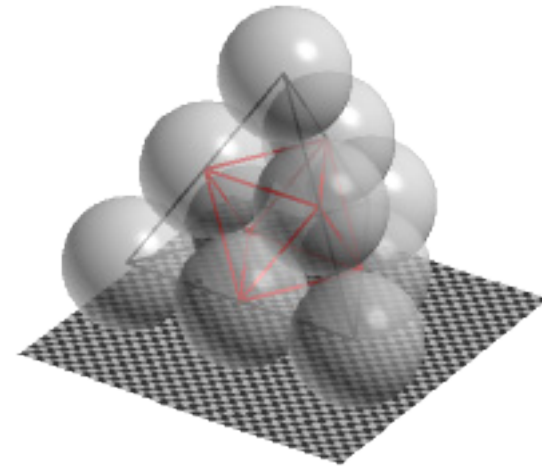


Fig. 2-12
Connecting the centers

The cannonballs have been rendered translucent. Their centers are connected through the points of tangency forming a tetrahedron (black chords) with an embedded octahedron (red chords).

⁹ They can be bowling balls, beach balls, ping-pong balls or stacked fruit. What matters is that they're spherical and have identical radii.

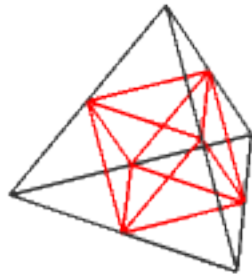


Fig. 2-13

The Isotropic Vector Matrix (IVM)

Removing the spheres and the floor leaves the octa-tetra arrangement. Fuller calls this geometric configuration the Isotropic Vector Matrix, or IVM. All chords meet at 60° , which Fuller identifies as the basic angular relationship in “Scenario Universe.”^{10, 11} Extended indefinitely, this pattern will fill all space without gaps.

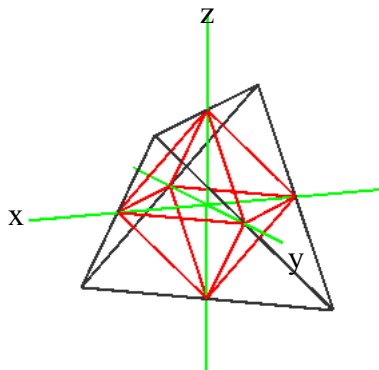


Fig. 2-14

Relationship between orthogonal & IVM systems

It is not immediately apparent that the Isotropic Vector Matrix contains Descartes’ axes. Figure 2-14 shows the IVM rotated to place the orthogonal axes in a more familiar orientation. Specifically, the diagonals of the octahedron comprise the Cartesian coordinate system. Within the tetrahedron, the three bisectors of opposite pairs of edges define the Cartesian system. The Cartesian axes intersect at 90° . The axes of the IVM intersect at 60° . What is needed is not so much a new system as a rotation of the conventional point-of-view into a better relationship with the natural world.

The single greatest failing of this book may be the employment of the Cartesian and spherical coordinate systems to display QSOs. There are two reasons for using them. First, the orthogonal systems are ubiquitous in both mathematics and physics. Their use here facilitates communication. Second, Graphing Calculator, like all other software of its kind, assumes orthogonal axes. As a matter of practicality, we stay with the prevailing system even though orthogonal axes do not adequately reflect reality. Readers are urged to develop QSO theory in the IVM coordinate system. It’s conceivable that such an approach may directly and precisely describe natural phenomena better than anything in the present work.

¹⁰ Fuller (1975), p. 85

¹¹ ——— (1992), p. 38

Variations on a Theme

QSOs can be translated and rotated with ease, as can any space curve generated in Cartesian notation. Additional axes can be considered, as well as multiple rotating points. It is also possible to vary the phase angles of the rotations, or the angle between the axes as in the IVM. We will examine most of these operations in chapter 6. For now let's look at some variations that arise from the Cartesian equation itself.

We can...

- 1) Exchange axes ($x \leftrightarrow y \leftrightarrow z$)
- 2) Reverse polarity of the axes ($+ \leftrightarrow -$)
- 3) Exchange rotations ($a \leftrightarrow b$)
- 4) Reverse chirality of the rotations ($+ \leftrightarrow -$)
- 5) Exchange trig functions (sine \leftrightarrow cosine)

Exchanging axes

($x \leftrightarrow y \leftrightarrow z$)

Exchanging the axes on which a QSO is graphed is as simple as exchanging the terms for those axes in the Cartesian vector equation. The standard form of the vector equation for QSOs is shown next, followed by an expression in which the x- and y-axes have been exchanged.

$$\begin{bmatrix} x \\ y \\ z \end{bmatrix} = \begin{bmatrix} (\sin bgt) (\cos agt) \\ (\sin bgt) (\sin agt) \\ \cos bgt \end{bmatrix}$$

Eqn. 2-8a

$$\begin{bmatrix} x \\ y \\ z \end{bmatrix} = \begin{bmatrix} (\sin bgt) (\sin agt) \\ (\sin bgt) (\cos agt) \\ \cos bgt \end{bmatrix}$$

Eqn. 2-8b

Exchanging x- and y-axes

To abbreviate the equations, let

$$x = (\sin bgt) (\cos agt)$$

$$y = (\sin bgt) (\sin agt)$$

$$z = \cos bgt$$

Equation 2-8a thus becomes $\{x,y,z\}$, and equation 2-8b becomes $\{y,x,z\}$. Curly brackets are used to show that the abbreviated expressions are vector equations and not the Cartesian coordinates of two points.

Graphing,

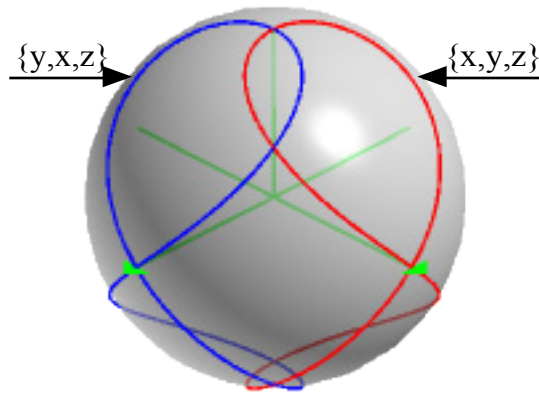


Fig. 2-15

QSOs (1:1) $\{x,y,z\}$, $\{y,x,z\}$ @ 1.0 cycle

Equations 2-8a and 2-8b are shown graphed onto the same unit sphere. Reversal of the x- and y-axes has rotated the original QSO (in red) negative 90° ($\Delta\theta = -90^\circ$). However, that's not the full story. The reversal has also resulted in a change that's not immediately apparent.

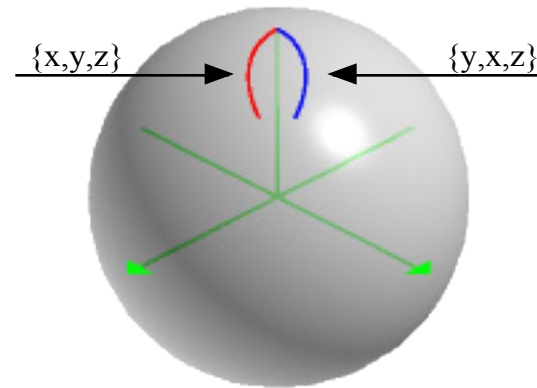


Fig. 2-16

QSOs (1:1) $\{x,y,z\}$, $\{y,x,z\}$ @ 0.1 cycle

At 10% of a cycle it is apparent that the θ -rotation for the blue curve is negative, i.e. left-handed. This curve was generated by exchanging the expressions for the x- and y-axes in equation 2-8a. There are six such permutations, including the original vector equation $\{x,y,z\}$. The abbreviated equations and their graphs are shown next.

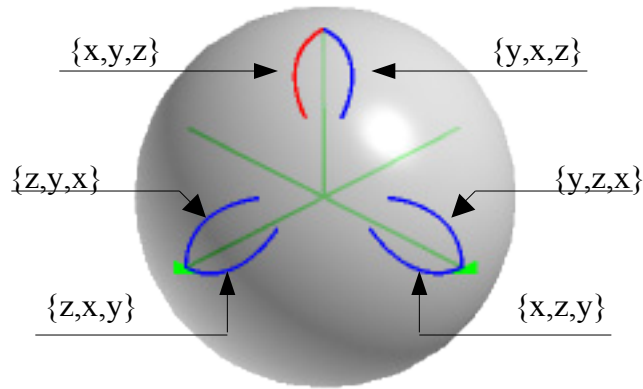


Fig. 2-17

The six axial permutations of QSO (1:1) @ 0.1 cycle

When fully developed, the QSOs look like

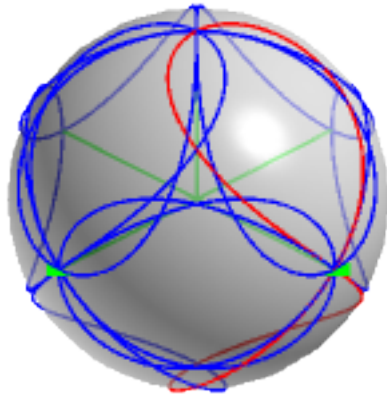


Fig. 2-18

The six axial permutations of QSO (1:1) @ 1.0 cycle

Only the original QSO (1:1) {x,y,z} is graphed in red. All others are blue. Although the curves generated by permutations of the axes range over most of the virtual sphere, they begin only at the positive unit values of the Cartesian axes. To include the negative unit values, we reverse the polarity of the axes.

Reversing the Polarity of the Axes
(+ <-> -)

Reversing the polarity of an axis means that the sign of the term representing that axis is changed.

$$\begin{bmatrix} x \\ y \\ z \end{bmatrix} = \begin{bmatrix} (\sin bgt) (\cos agt) \\ (\sin bgt) (\sin agt) \\ \cos bgt \end{bmatrix}$$

Eqn. 2-8a

$$\begin{bmatrix} x \\ y \\ z \end{bmatrix} = \begin{bmatrix} -(\sin bgt) (\cos agt) \\ (\sin bgt) (\sin agt) \\ \cos bgt \end{bmatrix}$$

Eqn. 2-8c

In equation 2-8a all three axes have a positive sign. Reversing the sign of the term for the x-axis yields equation

2–8c. In the abbreviated vector format the equations are

$$\text{Eqn. 2-8a: } \{x,y,z\}$$

$$\text{Eqn. 2-8c: } \{-x,y,z\}$$

Notice that the *order* of the axes has not changed. Only the *sign* of the x-term has been reversed.

Graphing,

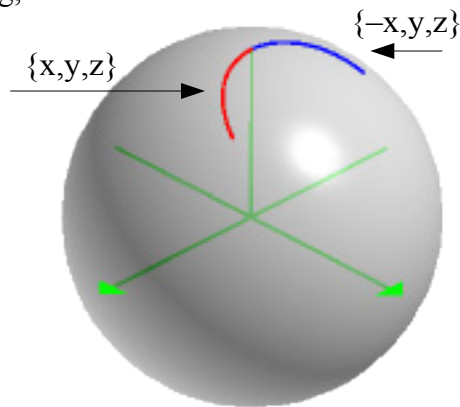


Fig. 2-19

QSOs (1:1) $\{x,y,z\}$, $\{-x,y,z\}$ @ 0.1 cycle

The change in sign has a not unexpected effect. The curve is reflected in the yz-plane. The x-values are now negative while the y- and z-values remain unchanged. Both curves start at (0, 0, 1), but a reversal in one of the rotations is evident; a reflection in the yz-plane also results in a reversal of rotation θ . There are three combinations of positive and negative that have a single negative axis. These are graphed next, along with the

original QSO.

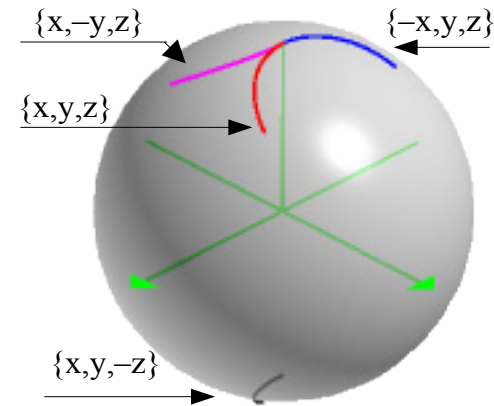


Fig. 2-20

QSOs (1:1) @ 0.1 cycle

Four curves, three with a single negative axis

In each case, in addition to reflection in the corresponding plane, the curve displays the reversal of the θ -rotation previously noted. There are also three combinations that have two negative axes each. These are shown next, along with the original QSO.

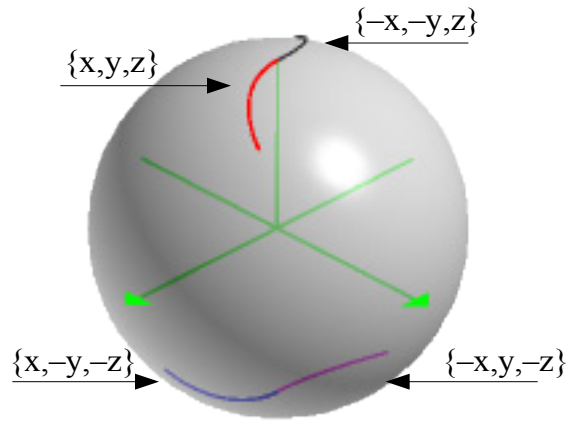


Fig. 2-21

QSOs (1:1) @ 0.1 cycle

Four curves, three with two negative axes each

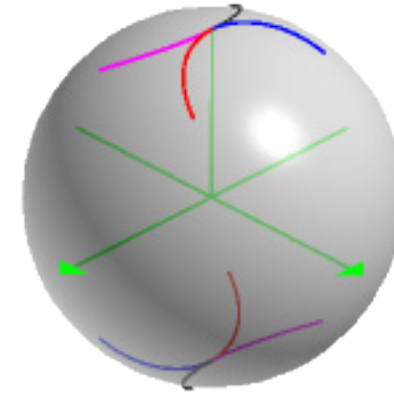


Fig. 2-23

QSOs (1:1) @ 0.1 cycle

The eight combinations of positive and negative axes

And finally, the last curve with negations on all three axes.

Running the rotations forward to one-quarter of a cycle, we get a small surprise.

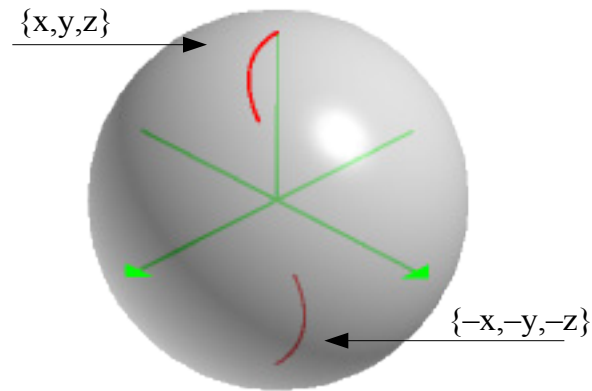


Fig. 2-22

QSO (1:1) with negations on all three axes

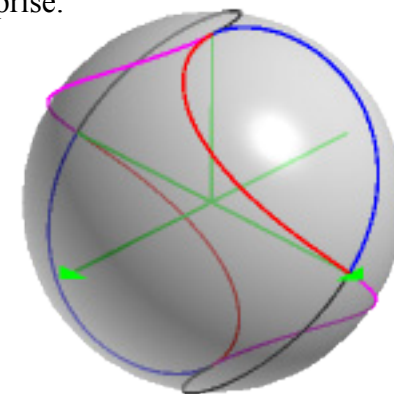


Fig. 2-24

QSOs (1:1)

The eight combinations @ 0.25 cycle

At 25% it looks like only two curves are developing. This cannot be true because all eight colors are visible. Furthermore, each curve differs from the others in its starting point and/or in the rotations which generate it.

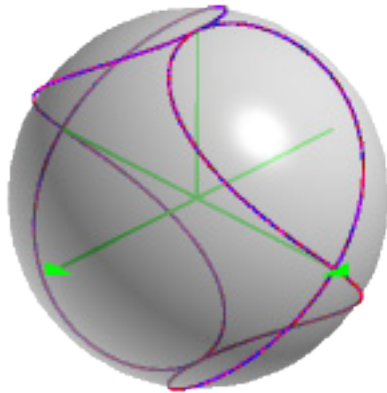


Fig. 2-25
QSOs (1:1) @ 1.0 cycle

The eight combinations of positive – and negative axes

At 100% the colors bleed through, indicating that four curves are present in each hemisphere of the y-axis. When the eight curves resulting from a reversal of the polarity of one or more axes are combined with the six curves from exchanging axes, they create 48 ways to generate a QSO. We leave it to the reader to explore the effects of using QSO ratios other than (1:1)

Exchanging Rotations ($a \leftrightarrow b$)

The standard representation for a Quasi-Spherical Orbit is “QSO ($a:b$),” where a and b represent the rates of increase of angles θ and ϕ . This way of naming QSOs results in equation 2-8a.

$$\begin{bmatrix} x \\ y \\ z \end{bmatrix} = \begin{bmatrix} (\sin bgt) (\cos agt) \\ (\sin bgt) (\sin agt) \\ \cos bgt \end{bmatrix}$$

Eqn. 2-8a

Exchanging a and b results in a single alternative form, QSO ($b:a$).¹²

$$\begin{bmatrix} x \\ y \\ z \end{bmatrix} = \begin{bmatrix} (\sin agt) (\cos bgt) \\ (\sin agt) (\sin bgt) \\ \cos agt \end{bmatrix}$$

Eqn. 2-8d

¹² Variables a and b are not free variables. They represent rotations, of which there are only two. Thus we consider only the systemic change where all variables a are replaced by b and vice versa.

When $a = b$ there is no difference between the two curves.

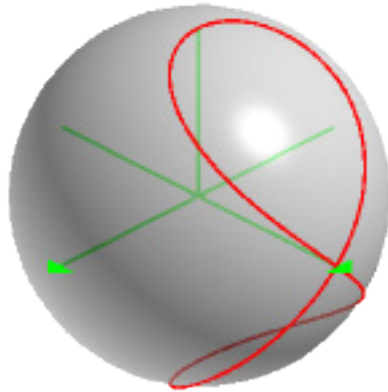


Fig. 2-26a
QSO (1:1) {a:b}

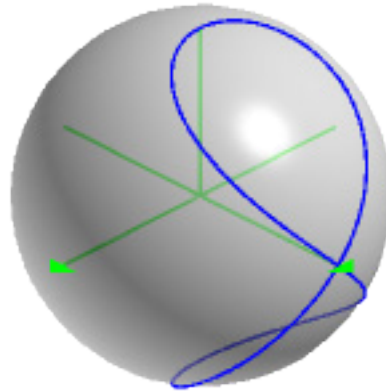


Fig. 2-26b
QSO (1:1) {b:a}

@ 1.0 cycle

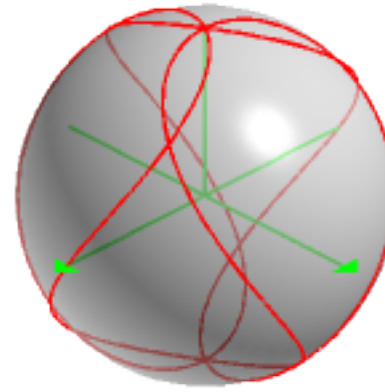


Fig. 2-27a
QSO (2:3)¹³ {a:b}

@ 1.0 cycle

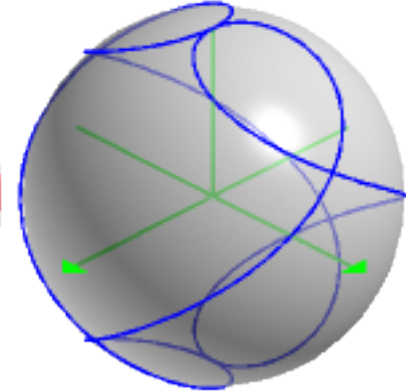


Fig. 2-27b
QSO (3:2) {b:a}

The variables a and b have been exchanged, but you'd never know it. Figure 2-26b is identical to figure 2-26a. They both start at the same point and rotate in the same manner. However, when $a \neq b$, the inverse curve is generated. Compare QSOs (2:3) and (3:2).

The inverse curve is QSO (3:2). The curves start at the same point and rotate in the same manner. However, this time different curves result from the exchange in the order of the rotations. Connecting the intersections of QSO (2:3) forms an octahedron. Connecting the intersections of QSO (3:2) forms a tetrahedron.¹⁴ These and other QSO polyhedra will be discussed in chapters 10 and 11.

¹³ QSO (2:3) was the first QSO used to illustrate the relationship between QSOs and space curves. See Figs. 1-1a, b.

¹⁴ Fuller identifies the tetrahedron and the octahedron as complimentary structures. See: Fuller, 1979, p. 223, § 986.049. —, 1992, p. 53.

There are now six ways of generating QSOs by exchanging the axes, eight by reversing the polarity of the axes, and two by exchanging the rotations. That makes 96 ways so far¹⁵ of generating QSOs that stem directly from equation 2-8a.

Reversing the Chirality of the Rotations

(+ ↔ -)

Chirality¹⁶ refers to the handedness of a pattern or system. For instance, molecules often come in right- and left-handed versions. QSO rotations also come in right- and left-handed versions. Reversing the chirality of a rotation is equivalent to reversing the sign of the variable, but because there are two rotations, four variations result.

As usual, we begin with equation 2-8a.

$$\begin{bmatrix} x \\ y \\ z \end{bmatrix} = \begin{bmatrix} (\sin bgt) (\cos agt) \\ (\sin bgt) (\sin agt) \\ \cos bgt \end{bmatrix}$$

Eqn. 2-8a

If b is negated the equation becomes

$$\begin{bmatrix} x \\ y \\ z \end{bmatrix} = \begin{bmatrix} (\sin (-b) gt) (\cos agt) \\ (\sin (-b) gt) (\sin agt) \\ \cos (-b) gt \end{bmatrix}$$

Eqn. 2-8e

Abbreviating,

Eqn. 2-8e: {a:-b}

The other two variations are

Eqn. 2-8f: {-a:b}

Eqn. 2-8g: {-a:-b}

Once again the curly brackets indicate vector equations.

¹⁵ $6 \times 8 \times 2 = 96$

¹⁶ From Greek *kheir*, hand.

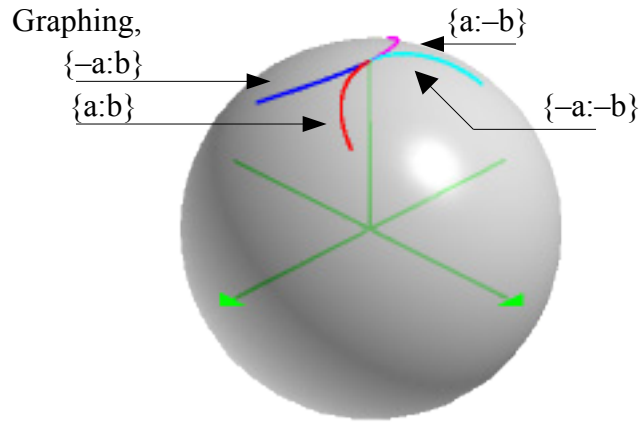


Fig. 2-28

QSOs (1:1) $\{a:b\}$, $\{a:-b\}$, $\{-a:b\}$, $\{-a:-b\}$ @ 0.1 cycle

At 10% four QSOs start from $(0, 0, 1)$ and propagate into the four octants of the positive hemisphere of the z-axis. Next we advance the rotations to 25% of a cycle.

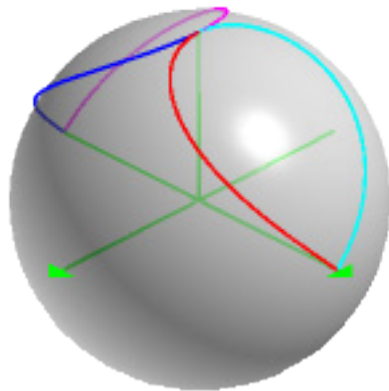


Fig. 2-29

QSOs (1:1) $\{a:b\}$, $\{a:-b\}$, $\{-a:b\}$, $\{-a:-b\}$ @ 0.25 cycle

At 25% the pattern looks suspiciously like that of figure 2-24. The emerging curves seem to be developing only in the positive and negative hemispheres of the y-axis. The difference between that scenario and figure 2-29 is that here there are only four curves whereas in the former there were eight.

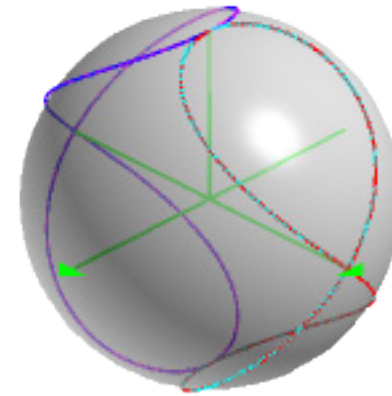


Fig. 2-30

QSOs (1:1) $\{a:b\}$, $\{a:-b\}$, $\{-a:b\}$, $\{-a:-b\}$ @ 1.0 cycle

The colors of the curves after one cycle confirm that each hemisphere of the y-axis contains two overlapping QSOs. Equations $\{a:b\}$ (red) and $\{-a:-b\}$ (light blue) have developed in the positive half, whereas equations $\{-a:b\}$ (dark blue) and $\{a:-b\}$ (violet) are in the negative half. There are now $96 \times 4 = 384$ variations on the theme of equation 2-8a. This is not over yet.

Exchanging Trig Functions (sine \leftrightarrow cosine)

The last of the internal manipulations that generate variations of equation 2-8a is the exchange of the trig functions sine and cosine.

$$\begin{bmatrix} x \\ y \\ z \end{bmatrix} = \begin{bmatrix} (\sin bgt) (\cos agt) \\ (\sin bgt) (\sin agt) \\ \cos bgt \end{bmatrix}$$

Eqn. 2-8a

Here again we consider only the systemic exchange wherein all sines are replaced by cosine and vice versa. Equation 2-8a thus becomes

$$\begin{bmatrix} x \\ y \\ z \end{bmatrix} = \begin{bmatrix} (\cos bgt) (\sin agt) \\ (\cos bgt) (\cos agt) \\ \sin bgt \end{bmatrix}$$

Eqn. 2-8h

The abbreviated forms are

Eqn. 2-8a: {sin cos}

Eqn. 2-8h: {cos sin}

Graphing,

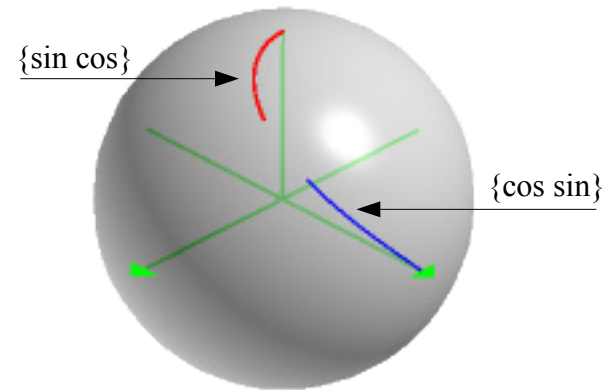


Fig. 2-31

QSOs (1:1), {sin cos}, {cos sin} @ 0.1 cycle

The curves overlap, as they have done before.

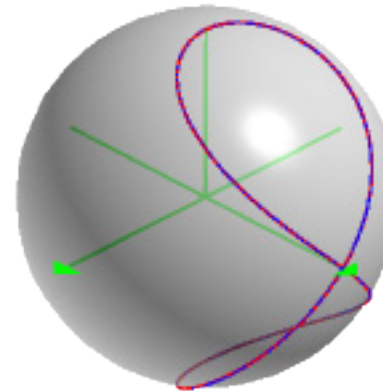


Fig. 2-32

QSOs (1:1), {sin cos}, {cos sin} @ 1.0 cycle

Here, however, there is a difference. The graphic shows only QSO (1:1). Other ratios reveal an interesting pattern. The best vantage point is from the positive z-axis.

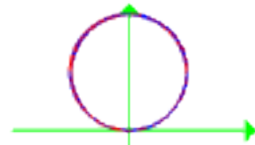


Fig. 2-33

QSOs (1:1), {sin cos}, {cos sin} @ 1.0 cycle
View from the z-axis

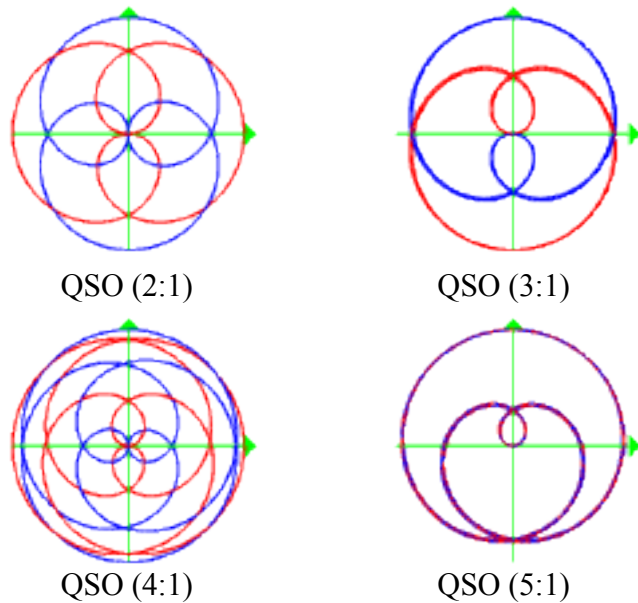


Fig. 2-34

QSOs (2:1), (3:1), (4:1), (5:1), {sin cos}, {cos sin}@ 1.0 cycle
View from the z-axis

Although the curves start in different places and rotate in different ways, they overlap again at QSO (5:1). This is a true congruence, and not an illusion of the point-of-view. The congruencies occur every four increments of α : QSOs (1:1), (5:1), (9:1),... and so on.

It also works the other way.

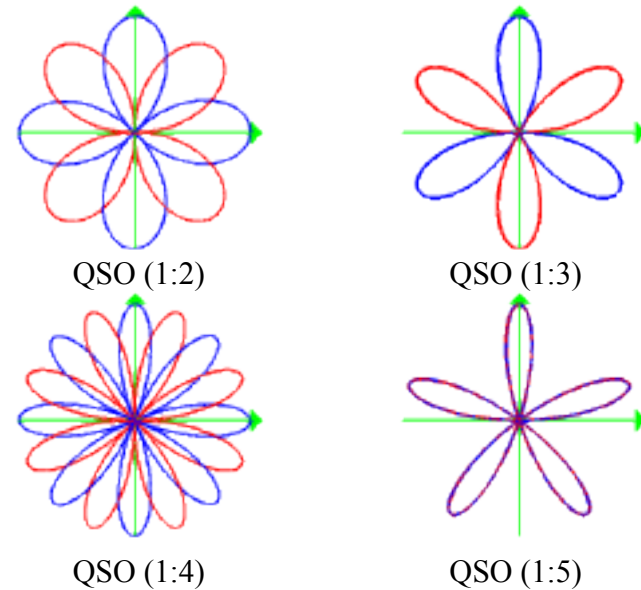


Fig. 2-35

QSOs (1:2), (1:3), (1:4), (1:5), {sin cos}, {cos sin} @ 1.0 cycle
View from the z-axis

Again the curves are congruent every four increments, this time, of b : QSOs (1:1), (1:5), (1:9),... The striking resemblance of the QSO (1:n) series to rhodonea curves will also be discussed in chapter 7.

The number of variations of Eqn. 2-8a now stands at

Exchanging Axes.....	6
Reversing the Polarity of the Axes.....	8
Exchanging Rotations.....	2
Reversing the Chirality of the Rotations.....	4
Exchanging Trig Functions.....	2

Multiplying,

$$6 \times 8 \times 2 \times 4 \times 2 = 768$$

However in each case equation. 2-8a was the common starting point. It appears five times, once in each of the categories. Subtracting 4 from the total leaves equation. 2-8a and 763 variations as the final count.

The take-home lesson in all this shuffling and scrambling of functions and variables is probably to always remember that although equation. 2-8a is the conventional form of the QSO equation, there are 763 other variants out there, some of which might be more interesting, more elegant, or more useful than the standard version. It pays to keep an open mind.

Chapter 3

Elements of the QSO

The QSO Ratio

A Quasi-Spherical Orbit results from the simultaneous rotation of a point about two or more axes. The precise shape of the orbit is determined by the ratio between the rotational rates on each axis. If a and b represent the rates of rotation, the *QSO ratio* is written as $(a:b)$.

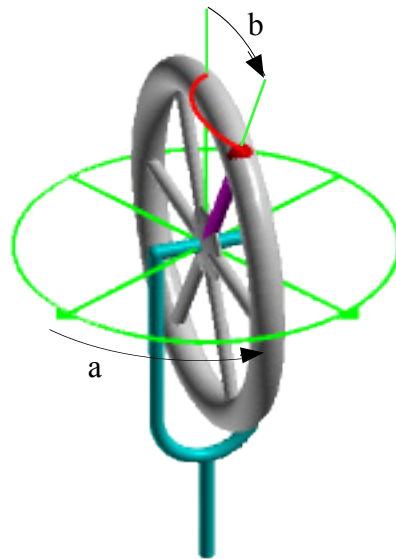


Fig. 3-1

Unicycle showing rotations a and b

In the unicycle model, a controls rotation around the fork while b controls rotation around the axis of the wheel. Much can be learned by manipulating the QSO ratio in a variety of ways. We begin with fractions.

Fractional Ratios

A ratio of $(1:1)$ gives the figure eight curve.

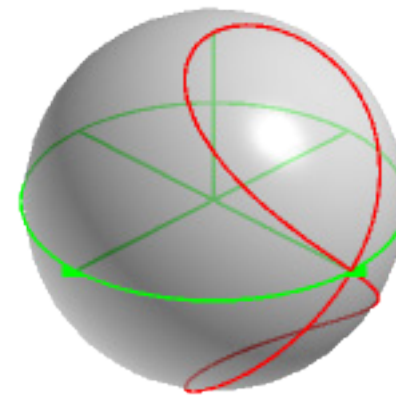


Fig. 3-2
QSO (1:1)

What happens if you divide each element of the QSO ratio in half?

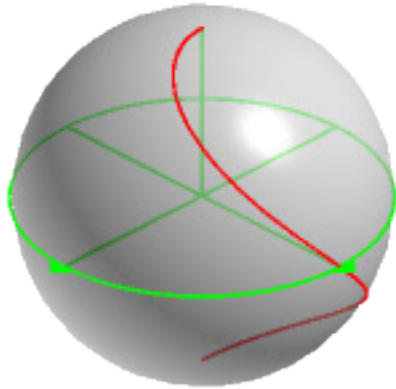


Fig. 3-3
QSO (0.5:0.5)

The tendency is to view figure 3-3 as a static picture. It looks like the curve starts at $(0, 0, 1)$ and rotates to $(0, 0, -1)$ where it stops. It looks like you get half of a (1:1), but in this case looks are deceiving.

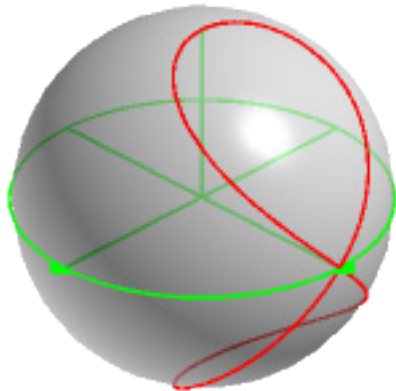


Fig. 3-4
QSO (0.5:0.5) @ 100% of a cycle

The elements of the QSO ratio are rotations, not static displacements. They refer to rates of change over time. When the (0.5:0.5) is given enough time, it results in a curve that, on the static page at least, looks exactly like QSO (1:1). It just takes longer. In fact since QSO (0.5:0.5) rotates half as fast as QSO (1:1), it'll take twice as long to rotate any given amount compared to the (1:1).

Thus QSOs (0.5:0.5), $(1/\pi:1/\pi)$ and $(10^{16}:10^{16})$ all give curves that look alike. However, their rates of rotation are 0.5, $1/\pi$, and 10^{16} angular units per unit time, respectively.

Two conclusions are possible. First, QSOs which differ only in the magnitude of their ratios result in curves which are statically identical. Second, QSOs that are statically identical may still differ dynamically.

If dividing both elements of the QSO ratio by the same number results in a curve that looks the same but differs dynamically from the original, how about dividing only one element or the other?

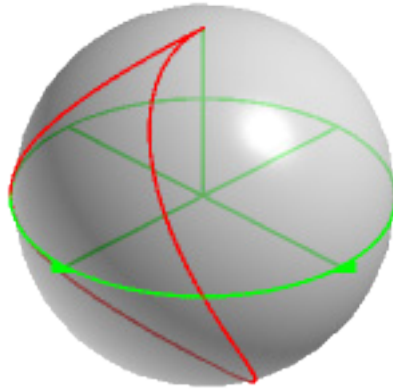


Fig. 3-5a
QSO (0.5:1)

Again the result appears to be an incomplete curve. However, as we just learned, completion is a matter of timing. Let's compare the complete static form of QSO (0.5:1) to the static form of QSO (1:2).

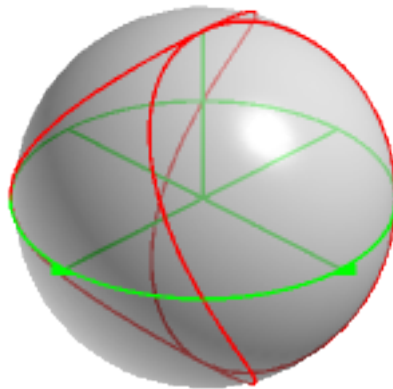


Fig. 3-5b
QSO (1:2)

QSO (0.5:1) has the same static form as the (1:2). For obvious reasons, QSO (1:2) is known as the “baseball seam.”¹ Like the previous example, QSO (0.5:1) rotates at half the speed of QSO (1:2).

Dividing the second element of the (1:1) by 2 gives

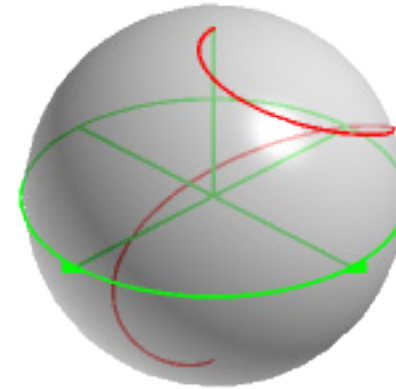


Fig. 3-6a
QSO (1:0.5)

The QSO appears to be a three dimensional spiral beginning at $(0, 0, 1)$ and ending at $(0, 0, -1)$.² Allowing it to go to completion reveals its relationship to QSO (2:1).

¹ The seam on a regulation baseball is not exactly like QSO (1:2). In his delightfully profound book, *Slicing Pizzas, Racing Turtles, and Further Adventures in Applied Mathematics*, author Robert Banks (1999) considers several variations, one of which is, for all intents and purposes, the very thing.

² See chapter 9, Space Curves, QSO (3:1) & the spherical cardioid.

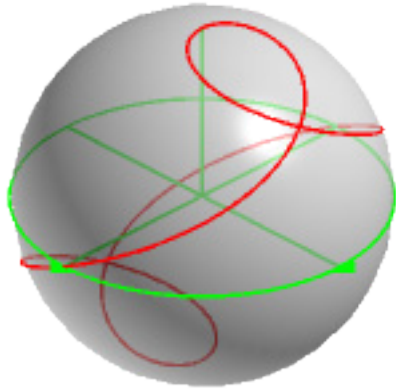


Fig. 3-6b
QSO (2:1)

QSO (2:1) is the “loop-the-loop.” It rotates twice as fast as QSO (1:0.5), but has the same static form.

Exponential Ratios

Exponential QSOs are those QSOs with a ratio of the form $(m^x:n^y)$ where m , x , n and y are real numbers. This is not to say that imaginary numbers are not allowed, but only that such ratios have not been investigated.

QSO (1:2⁰) is one example.³ Since 2⁰ = 1, QSO (1:2⁰) is the same as QSO (1:1).

QSO (1:2¹) is identical to QSO (1:2) which is the baseball seam.

It gets more interesting when the ratio is QSO (1:2^{1.5849625}). Since 2^{1.5849625} = 3, QSO (1:2^{1.5849625}) is identical to QSO (1:3).

³ Since 1^x = 1 for any x , we will ignore this possibility.

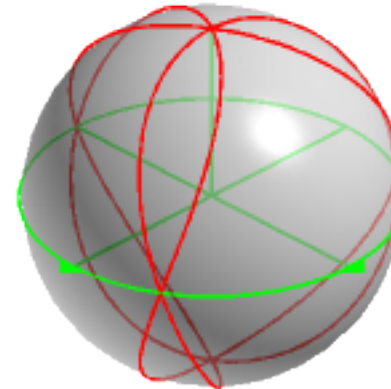


Fig. 3-7
QSO (1:2^{1.5849625}) = QSO (1:3)

In this case there is no caveat about the rate of rotation since 2^{1.5849625} is 3, to whatever degree of accuracy is desired. The only difference between the QSOs is in the expression of the ratio.

QSO (1:2^{1.5849625}), which is identical to the (1:3), intersects itself at (0, 0, ±1) and at three equally spaced points around the equator. Connecting the intersections makes two face-bonded tetrahedra. What may not be immediately apparent is that the 6-hedron is polarized. When the QSO is on the unit sphere, the vectors that extend from the xy-plane to the poles have a length of $\sqrt{2}$. Those that lie in the xy-plane have a length of $\sqrt{3}$. These and other QSO polyhedra will be examined in chapter 10.

QSO (1:3) can also be represented by (1:4^{0.79248125}), (1:5^{0.682606194}), and so on. In fact any QSO with the form (1:n^y) where n^y = 3 will be identical with the (1:3). Similar operations on the first element of the QSO ratio yield similar results.

Irrational Ratios

Until now the focus has been on QSOs with rational ratios.

- QSO (1:1) --> $1/1 = 1$
- QSO (2:1) --> $2/1 = 2$
- QSO (3:5) --> $3/5 = 0.6$

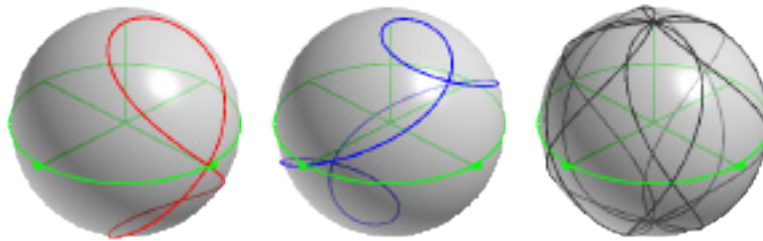


Fig. 3-8

QSO (1:1)

QSO (2:1)

QSO (3:5)⁴

Even QSO ($\pi:\pi$) has a rational ratio, as do QSOs ($1/\pi:1/\pi$), ($3e:e$), ($\sqrt{2}:4\sqrt{2}$) and so on. When the ratio of a QSO is a rational number, the orbit will be finite. It will wind across the virtual sphere only to close upon its point of origin and recycle over the same track, *ad infinitum*. Irrational QSOs are a little harder to characterize.

⁴ Compare QSO (3:5) with Figs. 1-3a, b.

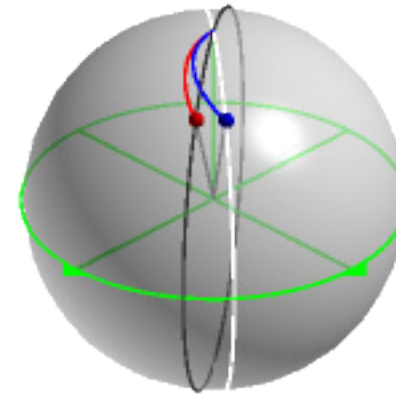


Fig. 3-9a

QSO (1:1) [red], QSO ($\sqrt{2}:1$) [blue] @ 0.1 cycle

QSOs (1:1) and ($\sqrt{2}:1$) are shown on the unit sphere. The curves are generated by two rotating circles which represent unicycle wheels. A black circle generates the (1:1) while a white circle generates the ($\sqrt{2}:1$).⁵ Two radius vectors extend from the center of rotation to small spheres which trace the QSOs. The curves are shown at 10% of completion, which must be carefully defined. Until now, completion for QSOs has been that point in the rotation when the curve returns to its starting point and begins to retrace its previous path. Irrational QSOs demand a more precise definition. Since it makes no sense to talk about a “complete” irrational phenomenon, whether it be a rotation or anything else, we abandon the idea of completion and

⁵ The white circle cannot be seen on the back side of the sphere against the white background of the paper.

instead take up the notion of a cycle.

A cycle is that point in the rotation when the number of trips around each axis equals the multipliers of the respective elements of the ratio.

Thus, a cycle will be tallied for the $(\sqrt{2}:1)$ when the a-rotation totals $\sqrt{2} \times 360^\circ$ and the b-rotation sums to 360° .

Although the definition does not require that a curve repeat itself, it serves for the rational curves as well. Rational curves retrace themselves, the irrationals don't.

In figure 3-9a, both QSOs are shown at less than one cycle of development. The $(1:1)$ has rotated

$$a = 360^\circ/10 = 36^\circ$$

$$b = 360^\circ/10 = 36^\circ$$

while the $(\sqrt{2}:1)$ has rotated

$$a = \sqrt{2} (360^\circ/10) = 50.91\dots^\circ$$

$$b = 360^\circ/10 = 36^\circ$$

The a-rotations differ by $(\sqrt{2} - 1)/10 = 0.0414\dots$ of a cycle. The b-rotations are identical, as can be seen in the figure. The irrational nature of QSO $(\sqrt{2}:1)$ becomes apparent as the rotations continue. The curves are shown in 10% increments of a cycle.

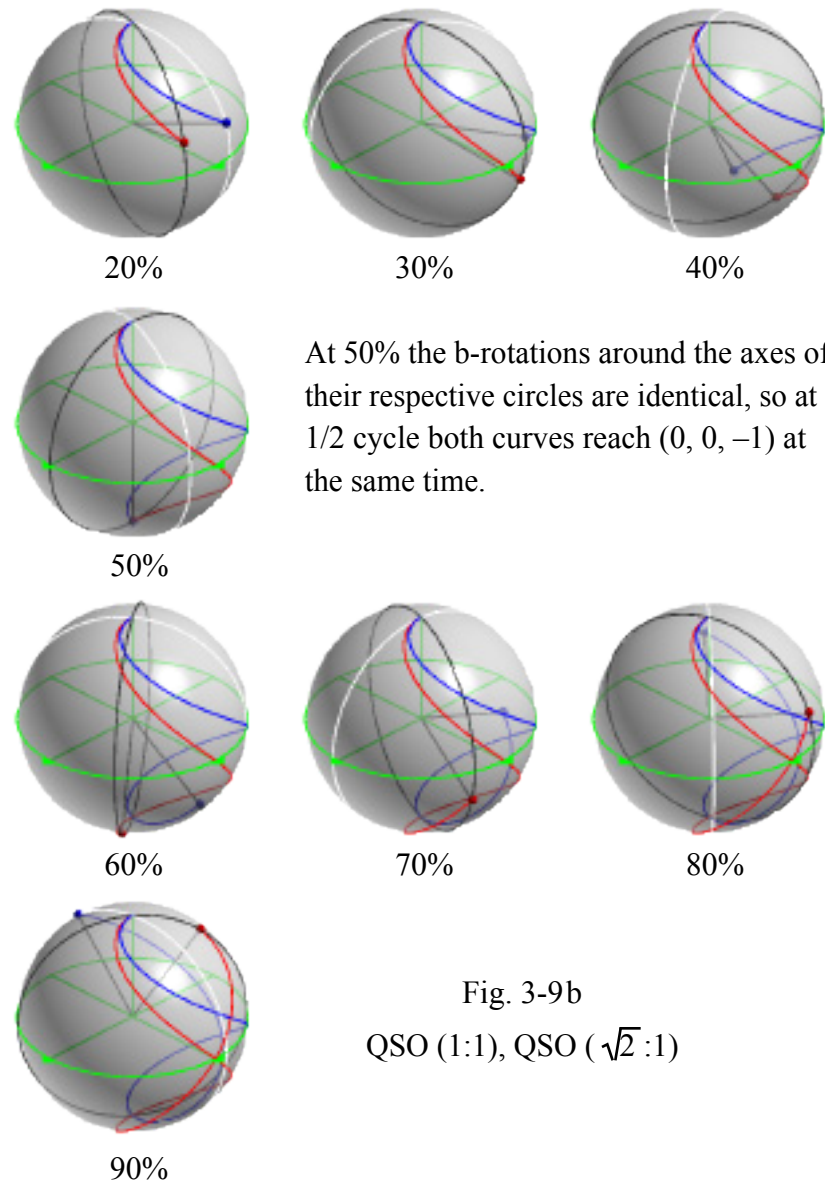


Fig. 3-9b
QSO $(1:1)$, QSO $(\sqrt{2}:1)$

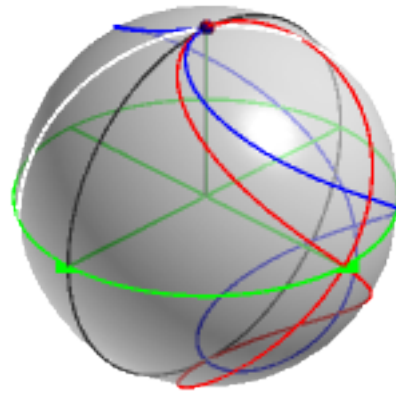


Fig. 3-9c

QSOs (1:1), ($\sqrt{2}$:1) @ 1.0 cycle

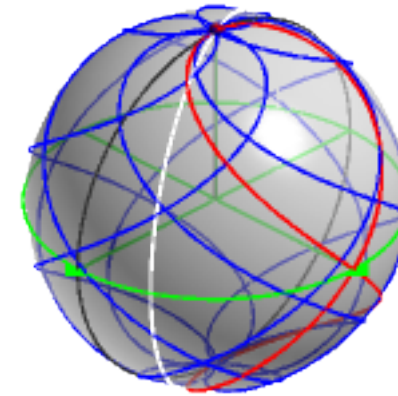
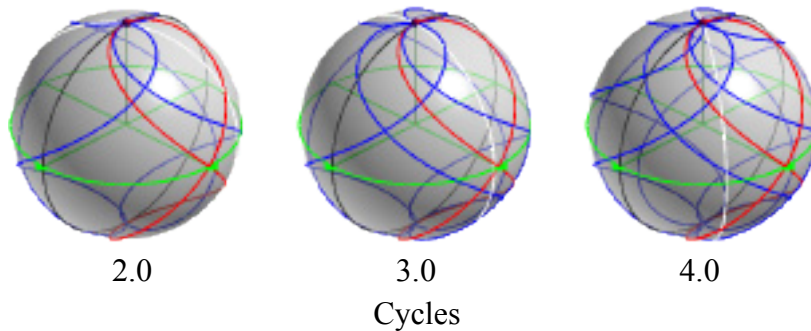


Fig. 3-9d

QSOs (1:1), ($\sqrt{2}$:1) @ 5 cycles of revolution

At the end of one cycle of rotation, both curves have returned to (0, 0, 1). The b-rotations have been 360° each. However the a-rotations have been 360° and $(360 \times \sqrt{2})^\circ$, respectively. While the (1:1) is set to repeat itself, the ($\sqrt{2}$:1) is going off almost 180° in the other direction. It's instructive to let them go for a few more cycles.

While the rational (1:1) is unaffected by the increasing number of cycles, the irrational QSO precesses around the z-axis, adding loops as it goes. What may not be apparent from the sketches, but is amply clear when watching the QSOs develop on the screen, is that the successive loops of the ($\sqrt{2}$:1) are in fact continuous. They are not merely more QSOs added to the first, they *are* the first, ever growing, but never retracing any previous path.



2.0

3.0

4.0

Cycles

The example suggests that if the ratio is irrational, the curve will wander endlessly over the spherical surface, never closing, never precisely recycling. Although this is usually true, there are exceptions. QSO (1:3)⁶ has an irrational ratio, and yet it makes a perfectly well-behaved QSO.

⁶ See Fig. 3-7.

Perhaps the rule should be amended to read that a QSO is irrational if either element is irrational. Not surprisingly, there are still exceptions. QSOs of the form $(n:n)$ where n is irrational are nevertheless rational curves. They do return to the original starting point, and they do recycle endlessly. These QSOs all have the static form of QSO (1:1). Their dynamic properties differ with the multiplier of the ratio.

Some irrational QSOs can be made rational by raising the elements of the ratio to a power. QSO $(\sqrt{2}:1)$, for example, can be made into the very rational QSO (2:1) by raising both elements to the second power. QSO $(1:2^{1/3})$ can be rationalized by raising both elements to the third power, and so on.

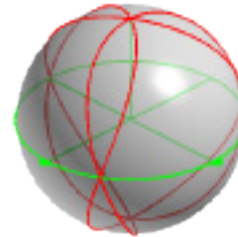
The general rule is that when *one* of the elements of the QSO ratio is an irrational number and the other is rational, then the orbital trace is irrational.⁷ It travels forever across the unit sphere, never retracing its path, never returning to its original conditions. For the present, we will limit the study of Quasi-Spherical Orbits to rational QSOs only. This convention is adopted for the same reason as the others. It will simplify the study of these curves.

Continuously Varying Ratios

At the end of the last chapter we saw that changing the QSO ratio produces differing patterns when seen from the z-axis. In this chapter we have investigated fractional, exponential and irrational ratios. The relationships between the various

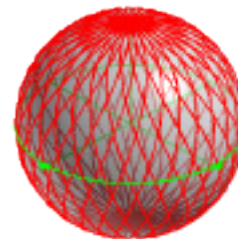
⁷ This insight is credited to D. Loftus, c. 1990.

manipulations of the ratio and the QSOs produced can be summed up by looking at what happens when the ratio is varied continuously. If one element of the QSO ratio is held constant while the other is smoothly varied through an interval on the real number line, the resulting QSOs show an interesting pattern. Since the real number line consists of an infinity of numbers, we can't look at all the QSOs in even the smallest range. We choose instead to start at QSO (1:3) and to change the first element of the ratio by +0.1 until we reach QSO (2:3).



QSO (1:3)

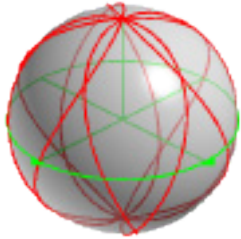
The series begins with QSO (1:3), a fairly simple, easily recognizable curve.



QSO (1.1:3)

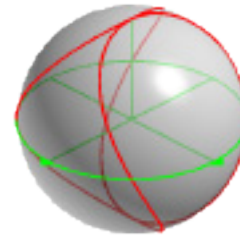
QSO (1.1:3) is considerably more complex. It's a net-like weave with diamond shaped openings oriented generally along the north-south axis.

Elements of the QSO



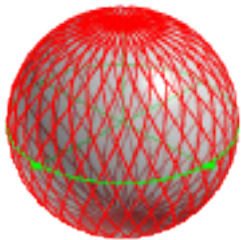
QSO (1.2:3)

QSO (1.2:3) resembles the much simpler (2:5), even though it rotates only 60% as fast.



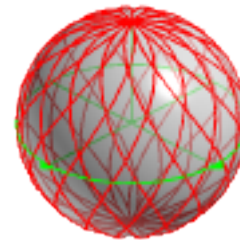
QSO (1.5:3)

QSO (1.5:3) reveals that, given enough time, it looks like the (1:2), statically at least.



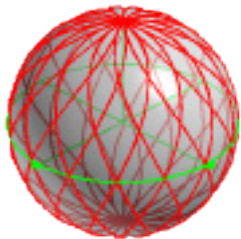
QSO (1.3:3)

QSO (1.3:3) shows a much tighter net bag pattern.



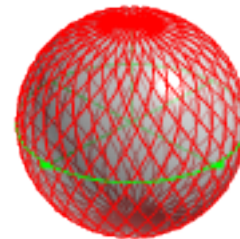
QSO (1.6:3)

QSO (1.6:3) resembles the faster, less complex QSO (8:15).



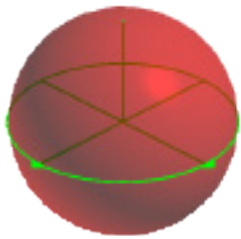
QSO (1.4:3)

Adding 0.1 produces a curve that statically resembles the somewhat less complex QSO (7:15), although it rotates considerably more slowly.

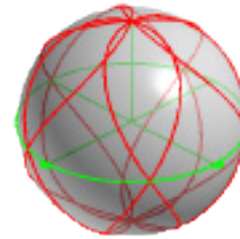


QSO (1.7:3)

The tightest net bag so far. Compare with QSOs (1.1:3) and (1.3:3). Is there a pattern here?

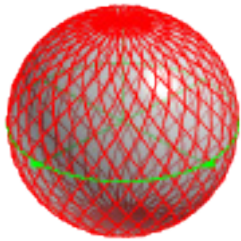
QSO ($\sqrt{2}$:3)

An unscheduled stop at QSO ($\sqrt{2}$:3) discloses an irrational curve that has covered the entire unit sphere (to the resolution of the software, anyway), and shows no sign of stopping any time soon.



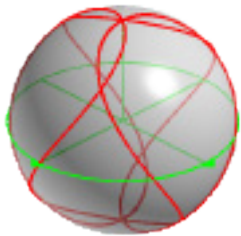
QSO (1.8:3)

Given enough time, QSO (1.8:3) looks like QSO (3:5).



QSO (1.9:3)

QSO (1.9:3), which resembles nothing other than itself, is the most complex curve so far.



QSO (2:3)

However, complexity yields to simplicity as it has all along, and we arrive at our goal, QSO (2:3).

Fig. 3-10

QSO (1:3) goes smoothly to QSO (2:3)

It is possible, of course, to take smaller and smaller increments, and to generate more and more QSOs. The pattern will be the same. The complexity of the QSOs will increase until the ratio can be reduced to some common denominator. The greater the reduction of the ratio, the greater the simplification in the curve itself. Simple curves are bound by complex curves on either side. The simplest curves are bound by the most complex. Smoothly varying the second element of the ratio holds similar lessons. We leave this exercise to the reader.

Poles

The idea of a pole in QSOs is derived from the most common polar system with which people are familiar, the Earth.



Fig. 3-11

The Earth with north & south poles

A diameter, in this case the axis of the Earth, passes through the sphere and defines two points on the surface. The points are designated as the north and south poles. Because it has two poles, the Earth is a bipolar system and the axis itself is a dipole.

Monopoles

A monopole is that point defined by half a diameter, i.e. a radius. A single point rotating at the end of a radius traces a

monopole QSO. Unlike the fixed north and south poles of the Earth, monopole QSOs can and do wander anywhere on the virtual sphere as the point rotates simultaneously about its two axes.

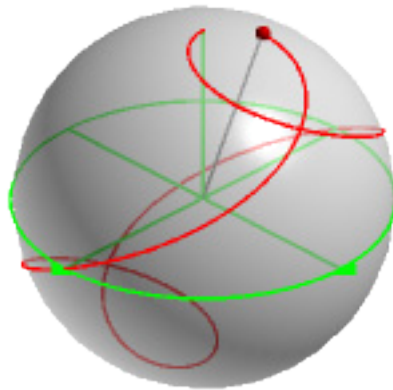


Fig. 3-12
Monopole QSO (2:1) @ 95%

QSO 1(2:1), shown here at 95% of a cycle, is a monopole because it's generated by a single rotating point. Monopole QSOs are written with a leading "1" to indicate the unitary nature of their generation. Monopole QSO (2:1), for instance, is written as *QSO 1(2:1)*.

In figure 3-12 a small sphere has been placed at the rotating point. Its function is to help follow the point. In the simple QSO pictured here the small sphere is not really needed, but in the more complex QSOs to come such visual aids will be useful. The unit sphere has also been placed at the center of the system. Its function, as always, is to help distinguish front from back.

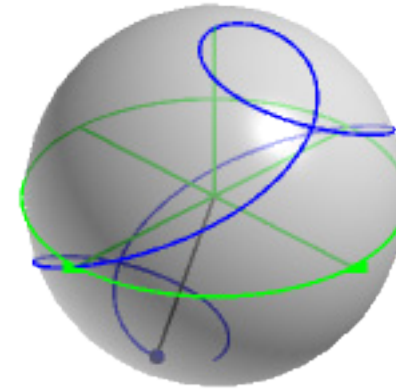


Fig. 3-13
QSO 1(2:1) @ 95%

Monopoles can look deceptively alike. Figure 3-13 shows a blue QSO 1(2:1) which looks like the red QSO 1(2:1) in figure 3-12, but it is not. Overlaying figures 3-12 & 3-13 allows a direct comparison.

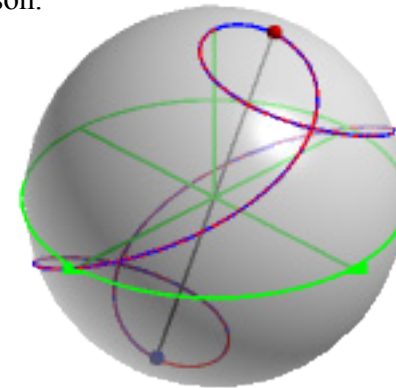


Fig. 3-14
Red QSO 1(2:1) & blue QSO 1(2:1), both @ 95%

The red and blue QSOs considered separately have statically identical forms. Dynamically, they have a phase difference of 180° . The orbiting points have started, red at the north and blue at the south pole respectively. For 90% of the curve the red and blue bleed through. It is only in the as-yet-uncompleted 5% of each QSO that we can appreciate the fact that they are separate curves.

Dipoles

In figure 3-14 both points undergo the same rotations. Because the rotations are identical, the resulting curves can be considered a dipole.⁸ Instead of two monopoles, we have one dipole with two branches.

The dipole in figure 3-14 is written QSO 2(2:1) to indicate that there are two rotating points and that they undergo the same rotations. The branches of the dipole are statically identical but dynamically 180° out of phase. The phase difference of 180° is added to the second rotation of the second pole. Technically, the rotations and phase angles are

	First (red) pole	Second (blue) pole
a-rotation	$2 + 0^\circ$	$2 + 0^\circ$
b-rotation	$1 + 0^\circ$	$1 + 180^\circ$

This notation mixes apples and oranges, rotational rates and phase angles. The preferred form is to specify the rotations and

⁸ When the rotations are not identical, as in Fig. 1-4, the resulting QSOs cannot be considered a dipole.

phase angles separately.

$$\text{QSO } 2(2:1) [0,0] [0,180^\circ]$$

The first set of square brackets specifies the phase angles of the first (red) pole of the dipole. Zero degrees are added to both the a- and b-rotations of the pole. The second set of square brackets likewise specifies the phase angles of the second (blue) pole. Zero degrees are added to the a-rotation, and 180° are added to the b-rotation.

It is of course quite acceptable to express the phase angles in radians. In that case dipole (2:1) would be written as

$$\text{QSO } 2(2:1) [0,0] [0,\pi]$$

In figure 3-14 the branches of the dipole overlap. This is not necessarily so.

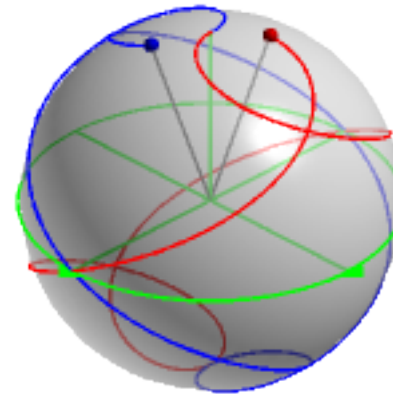


Fig. 3-15

QSO 2(2:1) @ 95%

The addition of a phase angle to the first rotation of the second pole yields a different dipole. In figure 3-15, both rotating points have started at the north pole, but the blue branch of the curve starts 180° ahead of the red one. The rotations and phase angles are

$$\text{QSO } 2(2:1) [0,0] [180^\circ,0]$$

Here again, the preferred form is to specify the rotations and phase angles separately.

Multipoles

QSOs are not limited to two particles of course, and phase angles are not limited to $\pm 180^\circ$. A tripole is shown next with its defining rotations and phases.

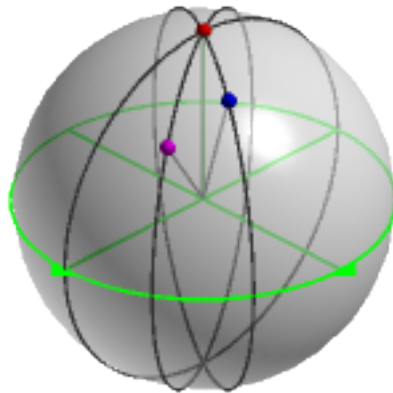


Fig. 3-16
QSO 3(2:1) @ 0%

In the sketch, QSO 3(2:1) is shown at its starting position; the rotations have not yet begun. Three small colored spheres mark the ends of three radii. The spheres are carried on and rotate around three black circles. A small red sphere at the zenith of the system is carried on the first circle, currently in the xz -plane. The corresponding black radius overlays and obscures the green z -axis. Thirty degrees east of the first circle, a second circle carries a violet sphere which is 45° from the zenith. The third circle, at 60° from the x -axis, carries a blue sphere which is 30° from the zenith.

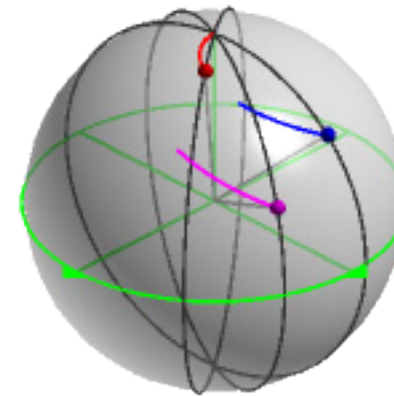


Fig. 3-17
QSO 3(2:1) [0,0] [30°,45°] [60°,30°] @ 5%

At five percent of rotation the QSO traces are beginning to develop.

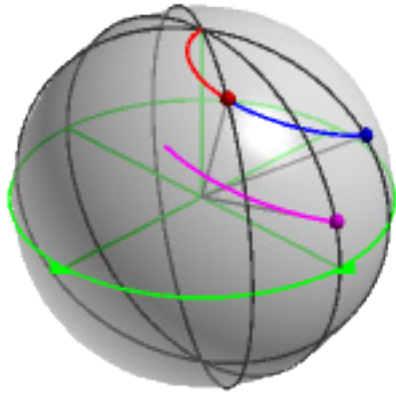


Fig. 3-18

QSO 3(2:1) [0,0] [30°,45°] [60°,30°] @ 8.333...%

We pause the action at eight and one-third percent of the cycle to observe a puzzlement. The red pole of the QSO seems have to caught up with the trace of the blue pole. It looks like the small red sphere is crossing through the starting point of the blue trace. We can ascertain whether this is true or not by calculating the angles.

We know that

$$\begin{bmatrix} r \\ \theta \\ \phi \end{bmatrix} = \begin{bmatrix} 1 \\ a2\pi nt \\ b2\pi nt \end{bmatrix}$$

Eqn. 2-5

Eliminating the parameter t , which is needed only for graphing, leaves

$$\theta = a2\pi n, \phi = b2\pi n$$

where

$$a = 2, b = 1, n = 0.08333\dots$$

Substituting

$$\theta = 2 \times 360^\circ \times 0.08333\dots = 60^\circ$$

$$\phi = 1 \times 360^\circ \times 0.08333\dots = 30^\circ$$

At 8.333...% of a cycle, the a-rotation has carried the small red sphere 60° around the equator. The b-rotation has carried the sphere 30° from the zenith. This is where the blue trace started. Furthermore, because the phase angles of the red and blue branches of the QSO differ by a ratio of 2:1, the traces will overlay each other for the rest of the rotation.

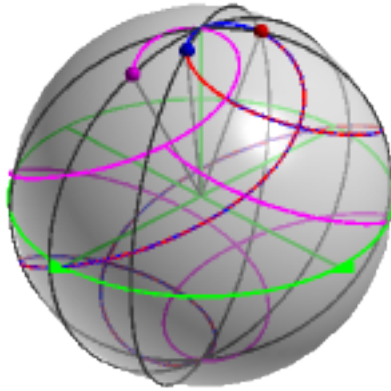


Fig. 3-19
QSO 3(2:1) [0,0] [30°,45°] [60°,30°] @ 95%

With the first cycle nearly complete, it is clear that the red and blue traces have followed the same orbital track with the blue leading and the red following. In the figure the small blue sphere has just passed through the north pole of the system and is closing on its starting point with the red right behind it.

The violet track has also done a couple of interesting things. First, it began, and will therefore complete its orbit, at one of its own intersections. The violet trace also seems to have passed through the starting point of the blue curve, as did the red one. To confirm this we need to calculate the angles of rotation as before. This calculation is left to the reader, but here's a hint. When the a-rotation has carried the small violet sphere 570° from its starting point, the b-rotation has gone through the south pole and the small sphere is now on what started out as the back side of the rotating circle.

To summarize, the general form of a QSO involves a minimum of seven variables. Two of these are the rotations a and b , which are placed within parenthesis: QSO ($a:b$). A third variable, p , indicates the number of poles, and is placed in front of the parenthesis: QSO $p(a:b)$. The rest of the variables are the phase angles. Because there are two rotations, there are two phase angles which must be specified for each pole. In the current notation the phase angles are called out separately. The model accommodates any number of poles, starting points and phase angles. The underlying requirement is that all poles undergo the same rotations, i.e., those within the parenthesis.

Events

The life of a point in a two-dimensional circular orbit⁹ is uneventful. Assuming a constant rate of rotation, there is nothing that differentiates any part of the curve from any other. It's boring. When a point rotates about two axes simultaneously, it passes a minimum of two times through at least one location on the unit sphere. This is known as an *event*. The ratio of the rates of rotation determines the number and locations of the events.

There are two kinds of event. An event can be produced when the orbital trace intersects itself. It can also occur when the orbit is tangent to itself. Sometimes the two kinds of event can occur together. All QSOs have at least one event per orbital cycle. QSO 1(1:1), now written with the leading "1" to indicate a monopole, typifies the intersection event.

⁹ See Figs. 1-6 & 1-7.

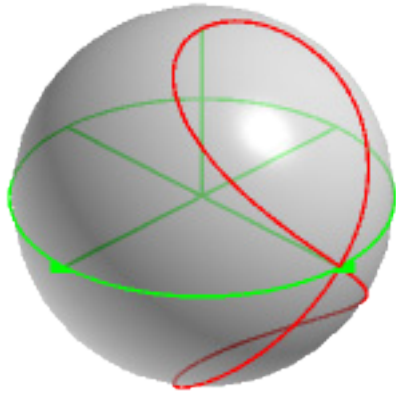


Fig. 3-20

QSO 1(1:1) with a single intersection event.¹⁰

The single event of QSO 1(1:1) occurs at $(0, 1, 0)$ in the Cartesian coordinate system, or at $(1, 90^\circ, 90^\circ)$ in spherical notation. It takes two nonsimultaneous passes of the rotating point to create the event. The timing of the passes is not obvious, nor is it obvious that the angle formed by the two passes is 90° . These and other characteristics of events will be explored in chapter 4.

Tangent events occur when the orbital track is tangent to itself, but does not cross. Two tangent events occur in the baseball seam, one at the north pole of the system, and one at the south.

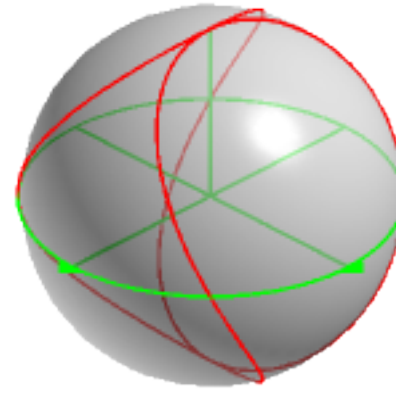


Fig. 3-21

QSO 1(1:2) with tangent events

Again, the events are created by two passes of the rotating point, but it is difficult to see the timing. Also, if it were not known that these are in fact tangent passes, it would be easy to suspect that they might be low angle intersections. Intersection events and tangent events will be discussed in chapter 4.

¹⁰ The full notation for this curve is QSO 1(1:1) [0,0]. We omit the phase angles when their inclusion would obfuscate rather than elucidate.

The Event Constellation

With a single event, QSO 1(1:1) is the simplest QSO. QSO 1(1:2) has two events, as does QSO 1(2:1). QSO 1(1:3) has five events.

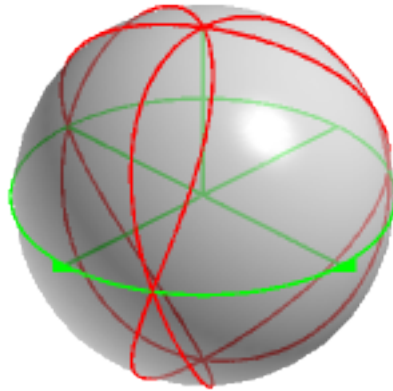


Fig. 3-22
QSO 1(1:3)

QSO 1(1:3) is shown in Fig. 3-22 at 100% of a cycle. The five events are located one each at the north and south poles of the system, and three more equally spaced around the equator.

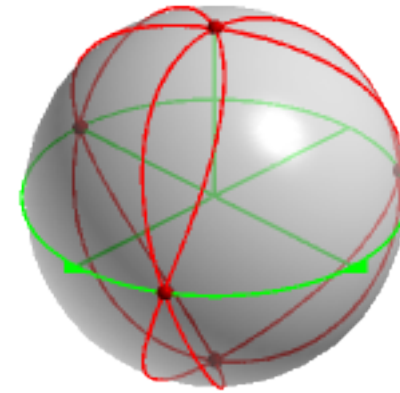


Fig. 3-23
QSO 1(1:3) with small spheres marking the events

Small spheres have been placed at the events. The spheres are red, indicating that the events result exclusively from passes of the red branch of the QSO. This is consistent with the fact that monopole QSOs have only a single branch.

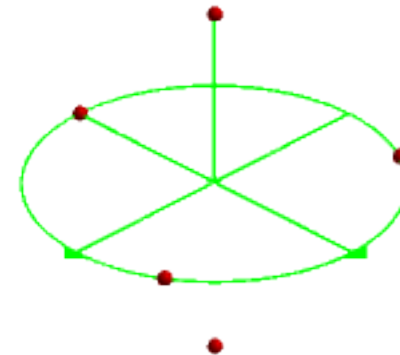


Fig. 3-24
The event constellation of QSO 1(1:3)

In the third sketch the QSO and the central sphere have been deleted, leaving only the small spheres. This arrangement of small spheres in space is called an *event constellation*.

QSO 2(3:1), with phase angles of 0° and 180° added to the second (blue) branch, provides the last example of an event constellation. On the right, the red and blue branches of the QSO have small spheres marking the events. In this illustration, since the events are created in different ways, the colors of the small spheres also differ. Events that are created by two passes of the red branch of the QSO are marked by a red sphere. Events created by two passes of the blue branch get a blue sphere, and events that result from a combination of red and blue passes are marked with a gray sphere.

At the far right the QSO and the unit sphere have been deleted, leaving only the event constellation. From the isometric vantage point the events seem to be randomly distributed throughout space.

In the third graphic the branches of the QSO have been restored. The point-of-view, $(\cos 45^\circ, \sin 45^\circ, 0)$, is achieved by rotating the isometric view until the xy-plane is edge-on to the eye of the reader. Like the twin snakes entwined around the caduceus, the red and blue branches of QSO 2(3:1) wind around

the z-axis and around each other.¹¹ The events define an ellipse while the envelope of the QSO is itself a circle.

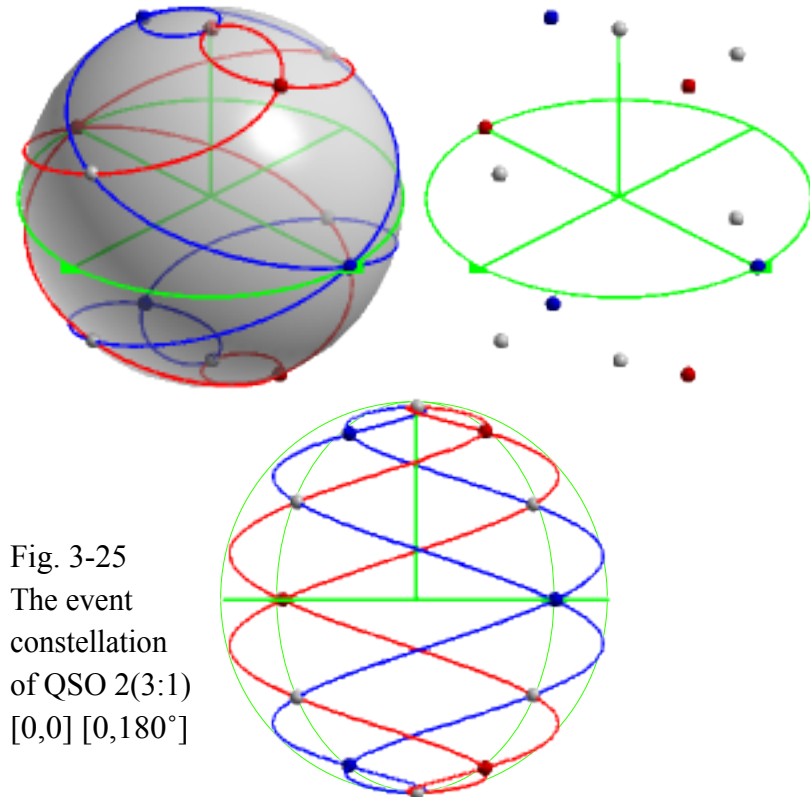


Fig. 3-25
The event
constellation
of QSO 2(3:1)
[0,0] [0,180°]

¹¹ Asclepius was the most important among the Greek gods and heroes who were associated with health and curing disease. The staff of Asclepius with a single coiled serpent is the traditional symbol of medicine. However, in modern times the caduceus, showing twin snakes around a staff with two wings at the apex, has also been used to represent medicine. In Greek (Roman) mythology, the caduceus was the staff of Hermes (Mercury), the god of commerce, eloquence, invention, travel, and theft, and so was a symbol of heralds and commerce, not medicine. Adapted from <<http://www-structmed.cimr.cam.ac.uk/Asclepius.html>>.

Chapter 4

Events

An event is created when the rotating point passes a minimum of two times through at least one location on the unit sphere. There are two kinds of event. An event can be produced when the orbital trace intersects itself. It can also occur when the orbit is tangent to itself. Sometimes the two kinds of event can occur together. All QSOs have at least one event per orbital cycle.

The Intersection Event

QSO 1(1:1) typifies events formed by the intersection of the orbital trace with itself.

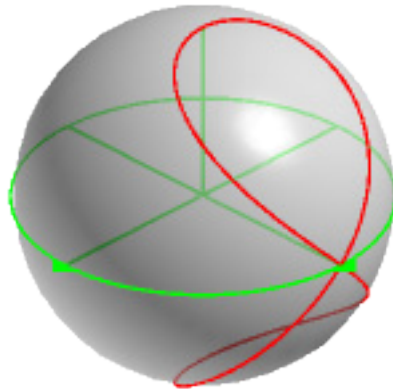


Fig. 4-1

QSO 1(1:1) with a single intersection event

Although the location and nature of the single event in this simple QSO are obvious, it will be instructive nevertheless to follow the development in detail. The first order of business is to identify the poles, ratio and phase angles of the QSO. This is QSO 1(1:1) with phase angles of 0° on both rotations. It has one event, located at $(0, 1, 0)$. In this QSO it's fairly obvious that the rotating point passes twice through the intersection. The timing and direction of those passes are examined next.

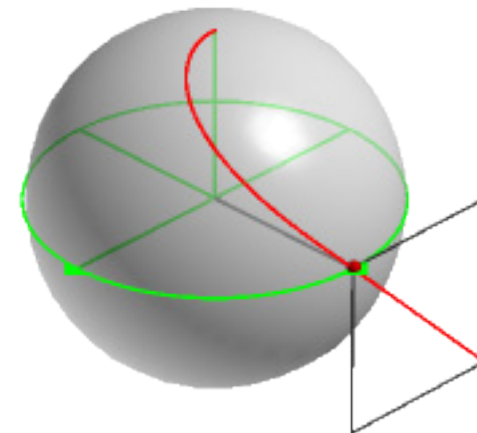


Fig. 4-2a

QSO 1(1:1) at 25% of a cycle

QSO 1(1:1) is shown at two points in its cycle. At 25% the rotating point passes for the first time through the location of the

event. At 75% the second pass completes the event. A vector diagram has been added to the graphics to illustrate the instantaneous velocity of the rotating point. The a and b components of the velocity are shown in black while the velocity vector is red. The event can be analyzed graphically as shown next.

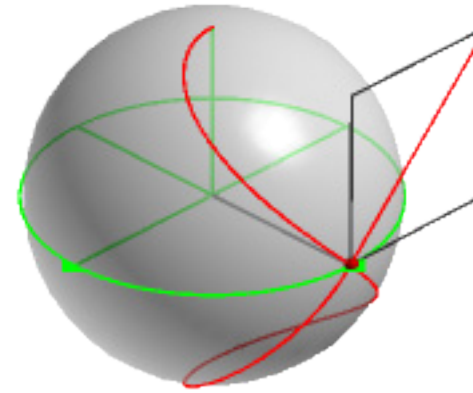


Fig. 4-2b
QSO 1(1:1) at 75% of a cycle


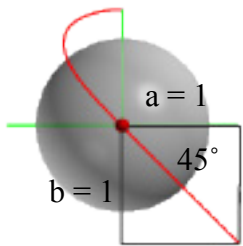
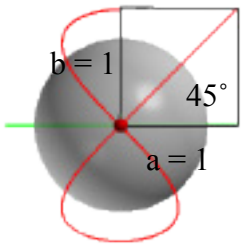
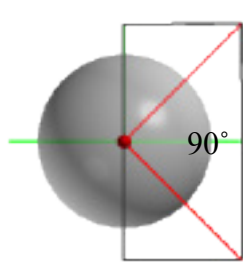
<u>QSO</u> Poles Ratio Phase Angles	<u>Location</u>	<u>Events</u> # of events Branch (color)	<u>Passes</u> Direction Timing		<u>Schematic</u>
			25%	75%	
QSO 1(1:1) [0°,0°]	(0, 1, 0)				

Table 4-1
Graphical analysis of the event of QSO 1(1:1)

In table 4-1 the QSO is identified in the left column. The Cartesian coordinates of the event are next, and in the third column a small colored sphere visually represents the event. The fact that there is only one small sphere tells us that there is only one event. Its color indicates that the event is formed exclusively from passes of the red branch of the QSO.¹

The point-of-view for the vector diagrams is radially outward from the y-axis. Although the isometric view may give a better overall picture, this perspective more clearly illustrates the event itself. At 25% of a cycle, the rotating point passes through the location of the event in a southeasterly direction. The instantaneous track is at an angle of 45° to the xy-plane. At 75% the point passes again through the location of the event traveling this time in a northeasterly direction. The angle of the track at the event is again 45° with respect to the xy-plane. The last column on the right summarizes the two passes of the rotating point and displays them schematically.

It is clear from the table that the event of QSO 1(1:1) is an intersection event. It is located at (0, 1, 0), and is formed by passes that occur at 25% and 75% of the cycle. Each pass makes an angle of 45° with the xy-plane, and the angle between the passes is 90°. The vector diagrams also reveal that the magnitude of the velocity at the event is $\sqrt{2}$. Actually the velocity of the rotating point varies smoothly from $\sqrt{1}$ at the

poles to $\sqrt{2}$ at the event.

Tangent Events

In contrast to the intersection event of QSO 1(1:1), monopole QSO (1:2) features events created by tangential passes of the rotating point.

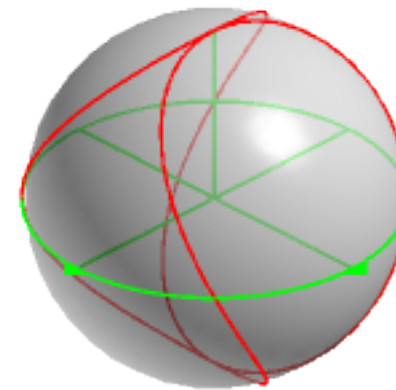


Fig. 4-3
QSO 1(1:2) at 100% of a cycle

The baseball seam, shown above in its static form, has two events, one each at the north and south poles.

¹ Distinguishing which branch of the QSO forms a given event is not so important when there is only one branch to distinguish. However, when considering the events of multipole QSOs, it will become critical to differentiate carefully which branch or branches of the QSO creates them.

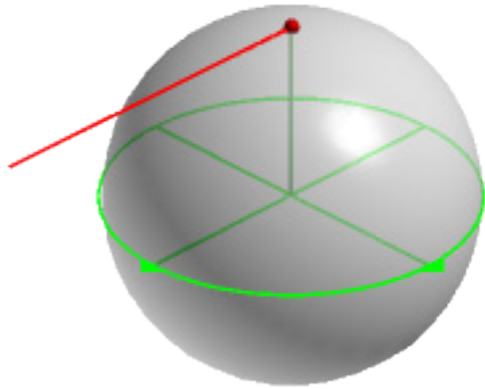


Fig. 4-4a
QSO 1(1:2) at 0% of a cycle

The rotation begins at $(0, 0, 1)$. Since there is no component of the a-rotation at either pole², the motion of the rotating point at the beginning of the orbit is entirely due to the b-rotation. This is QSO 1(1:2), so $b = 2$. The vector diagram consists only of the velocity vector itself. It's in the xz-plane, parallel to the xy-plane, and points with magnitude 2 toward positive x .

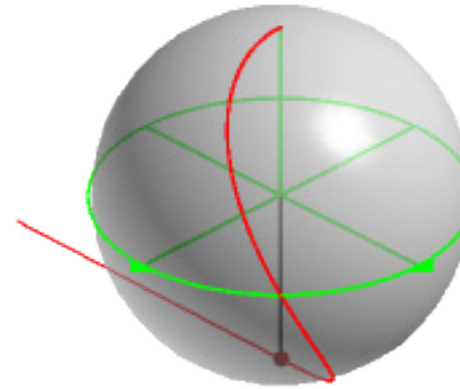


Fig. 4-4b
QSO 1(1:2) at 25% of a cycle

At one-quarter of a cycle the rotating point has reached $(0, 0, -1)$. It's traveling toward negative y with an instantaneous speed of 2. The angle of the velocity vector with respect to the xz-plane is 90° .

² See Fig. 3-1.

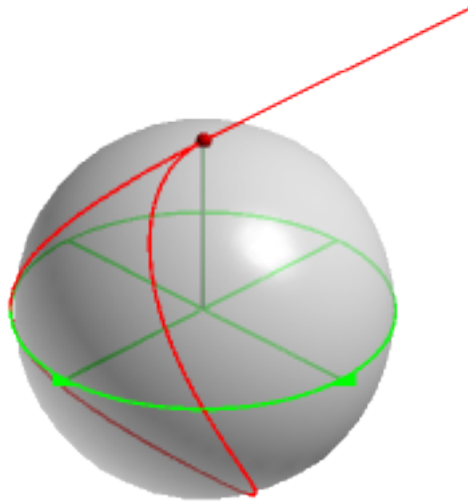


Fig. 4-4c
QSO 1(1:2) at 50% of a cycle

At the halfway point the rotation has again reached the zenith. This time it's heading towards negative x , parallel to the xy -plane and at a 0° angle with respect to the xz -plane.

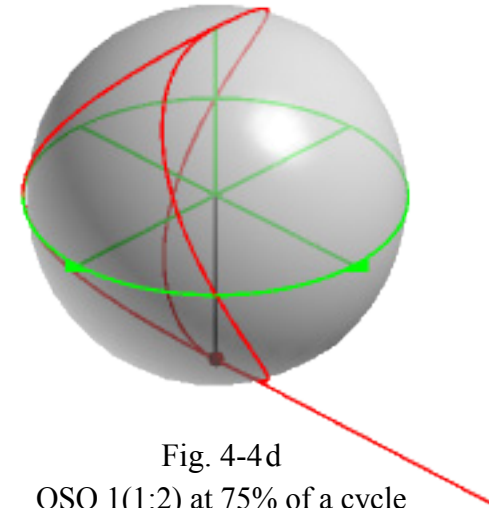


Fig. 4-4d
QSO 1(1:2) at 75% of a cycle

At 75% the rotating point passes for the second time through the south pole of the system, traveling, as may be expected, in the opposite direction from the first pass. These four passes of the rotating point, which create the two events of QSO 1(1:2), are summarized in the following tables.

<u>QSO</u> Poles Ratio Phase Angles	<u>Location</u>	<u>Events</u> # of events Branch (color)
QSO 1(1:2) [0°,0°]	(0, 0, 1)	●
	(0, 0, -1)	●

Table 4-2a
Identification, location and nature
of the events of QSO 1(1:2)

As before, the first column of the table lists the poles, $p = 1$, the QSO ratio, (1:2), and the phase angles, [0°,0°]. The second column locates the events at the north and south poles, respectively, and the third column specifies that both events are created solely by passes of the red branch of the QSO. The timing of those passes differs substantially from the 1(1:1).

Events

<u>Passes</u> Direction Timing				<u>Schematic</u>
0%	25%	50%	75%	
<p>0%</p> <p>$a = 0$ $b = 2$</p> <p>View from +z</p>	<p>25%</p> <p>View from +z</p>	<p>50%</p> <p>View from +z</p>	<p>75%</p> <p>View from +z</p>	<p>50%</p> <p>View from +z</p> <p>0%</p>
<p>View from -z</p> <p>$a = 0$ $b = 2$</p> <p>View from -z</p>	<p>25%</p> <p>View from -z</p>	<p>50%</p> <p>View from -z</p>	<p>75%</p> <p>View from -z</p>	<p>75%</p> <p>View from -z</p> <p>25%</p>

Table 4-2b
Graphical analysis of the events of QSO 1(1:2)

The rotating point oscillates from north to south, picking up half of an event on each oscillation. The passes that create the events are aligned with the x- and y-axes respectively, with an angle of 90° relative to each other. While the view of the northern event is conventional, the view of the event at the south pole is from a point radially outward from the pole.

Moving Off-Axis

The events examined so far have occurred on an axis. The (1:1) event is at $(0, 1, 0)$, and the events of the 1(1:2) are at $(0, 0, \pm 1)$. The 1(2:1) presents the first case of off-axis events. It also imparts a lesson about sequence.

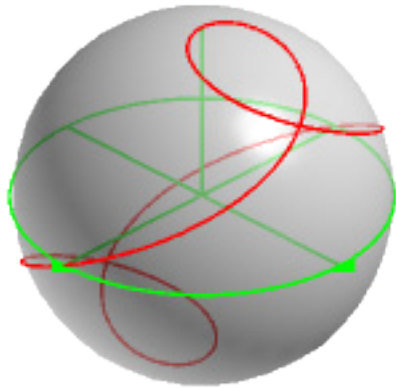


Fig. 4-5a
QSO 1(2:1) @ 100%

The static form of QSO 1(2:1) is shown in figure 4-5a. There are two events. Both are in the yz-plane, and both occur at 45° from the respective north or south pole.³ That is, the event in the positive z-hemisphere is at $(0, \cos 45^\circ, \sin 45^\circ)$, while the one in the negative z-hemisphere is at $(0, -\cos 45^\circ, -\sin 45^\circ)$.

When we analyzed the event of QSO (1:1), there was no ambiguity as to which event to list first; there was only one. When we analyzed the 1(1:2), we intuitively listed the event at $(0, 0, 1)$ first, without much justification. The question now is which event of QSO 1(2:1) should be listed first, and does it make any difference? To help decide that question a new visual aid is needed.

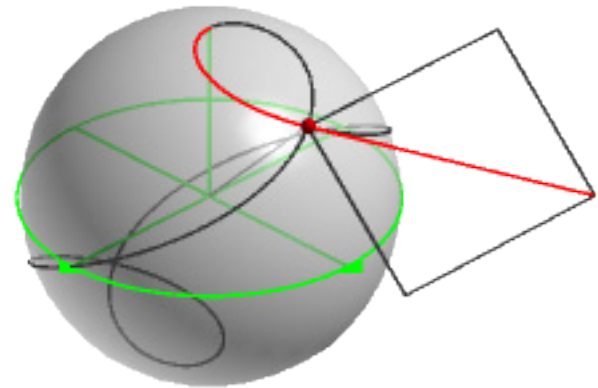


Fig. 4-5b
QSO 1(2:1) at 12.5% with a negative QSO 1(2:1)

A black QSO is generated on the unit sphere. The black QSO is the negative of QSO 1(2:1). As the rotating point traces

³ The coordinates of events will be more fully discussed in appendix 5.

the positive (red) QSO, the negative 1(2:1) disappears. At 12.5% of a cycle, the positive QSO has reached the location of the first event at $(0, \cos 45^\circ, \sin 45^\circ)$.

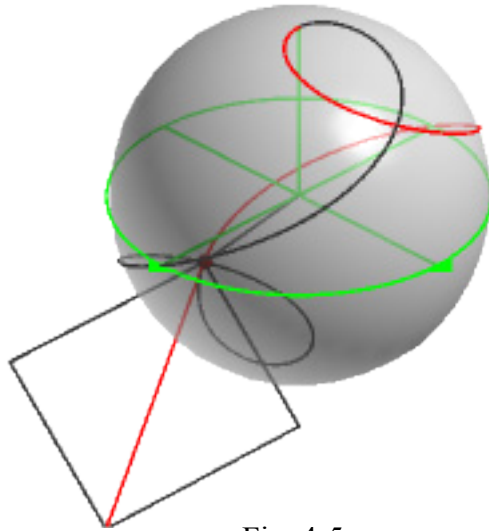


Fig. 4-5c
QSO 1(2:1) at 37.5% of a cycle

One-quarter of a cycle later the QSO has reached the location of the second event at $(0, -\cos 45^\circ, -\sin 45^\circ)$.

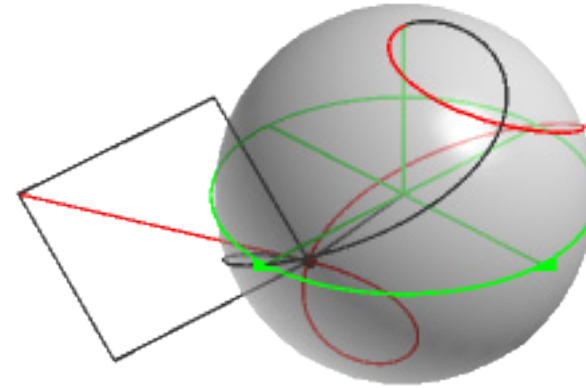


Fig. 4-5d
QSO 1(2:1) at 62.5% of a cycle

The QSO then loops around $(0, 0, -1)$ and goes through $(0, -\cos 45^\circ, -\sin 45^\circ)$ again.

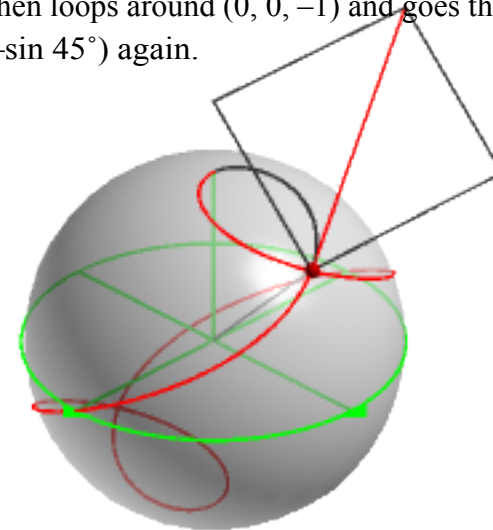


Fig. 4-5e
QSO 1(2:1) at 87.5% of a cycle.

Finally, the QSO returns to $(0, \cos 45^\circ, \sin 45^\circ)$, completing the events. The sequence in which the rotating point passes through the locations of the events suggests a convention: *Events are listed and analyzed in the order in which the rotating point first passes through the location of the event.*⁴ Thus, the events of QSO 1(2:1) are

- 1) $(0, \cos 45^\circ, \sin 45^\circ)$
- 2) $(0, -\cos 45^\circ, -\sin 45^\circ)$

There is now nothing left but to run the analysis.

<u>QSO</u> Poles Ratio Phase Angles	<u>Location</u>	<u>Events</u> # of events Branch (color)
QSO 1(2:1) [0°,0°]	$(0, \cos 45^\circ, \sin 45^\circ)$	•
	$(0, -\cos 45^\circ, -\sin 45^\circ)$	•

Table 4-3a
Identification of the events of QSO 1(2:1)

⁴ Note that this convention also applies to the events of QSOs 1(1:1) and 1(1:2), even though we didn't say so at the time.

Events

<u>Passes</u> Direction Timing				<u>Schematic</u>
12.5%	37.5%	62.5%	87.5%	

Table 4-3b
Analysis of the events of QSO 1(2:1)

The point-of-view in the graphics is in all cases radially outward from the events. This results in unconventional views of both events, but allows a more direct appreciation of the events themselves. The first event of the QSO is formed by passes at 12.5% and 87.5% of the cycle. The second event is

formed by passes at 37.5% and 62.5%. The angle between the passes in each case is just a little less than 70.53° . The magnitude of the velocity vector at the events is $\sqrt{3}$. Although it's not obvious from the current analysis, the velocity varies smoothly from $\sqrt{1}$ at the poles to $\sqrt{5}$ at the equator.

Dipole Events

Dipole events are created by rotations of dipole QSOs. The first example of events in a dipole is provided by QSO 2(1:1) with phase angles of 0° and 0° on the first branch of the QSO and 0° and 180° on the second.

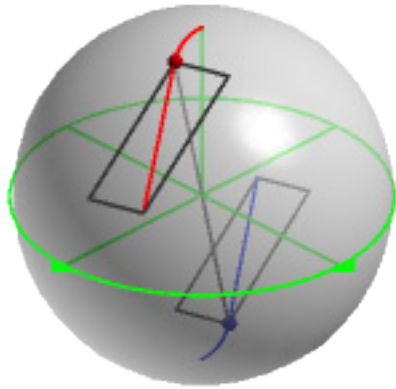


Fig. 4-6a
QSO 2(1:1) [$0^\circ, 0^\circ$] [$0^\circ, 180^\circ$] at 5%

The addition of 180° to the second rotation of the second (blue) branch of the QSO has rotated its starting point to the south pole of the system. At 5% of a cycle the branches of the QSO are seen departing from the north and south poles apparently in diametrically opposed directions, but which are actually the same rotation. The sign of both rotations is still positive. The phase angle has changed the starting point, but not the rotation itself.

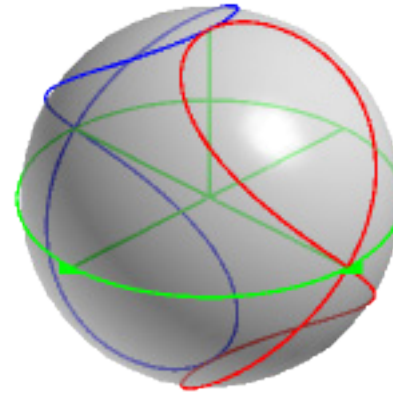


Fig. 4-6b
QSO 2(1:1) [$0^\circ, 0^\circ$] [$0^\circ, 180^\circ$] at 100%

The completed cycle shows each branch of the QSO as a seemingly independent curve. The intersection events at $(0, \pm 1, 0)$ are no surprise, but now there are two more tangent events at the poles. An abbreviated graphical analysis gives the details.

Events

<u>QSO</u> Poles Ratio Phase Angles	<u>Location</u>	<u>Events</u> # of events Branch (color)	<u>Schematic</u>	<u>Location</u>	<u>Events</u> # of events Branch (color)	<u>Schematic</u>
QSO 2(1:1) [0°,0°] [0°,180°]	(0, 0, 1)			(0, 0, -1)		
	(0, 1, 0)			(0, -1, 0)		

Table 4-4

Graphical analysis of the events of QSO 2(1:1) [0°,0°] [0°,180°]

The first column of the table identifies the QSO as the dipole (1:1) and specifies the phase angles. The locations of the events are next. The events themselves are identified by small colored spheres. Those spheres which represent events that are created by passes of the same branch of the QSO take the color of that branch. Those spheres which represent events that are created

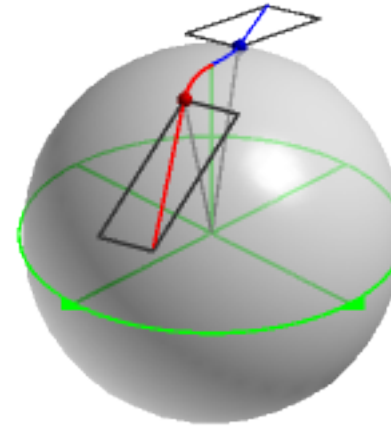
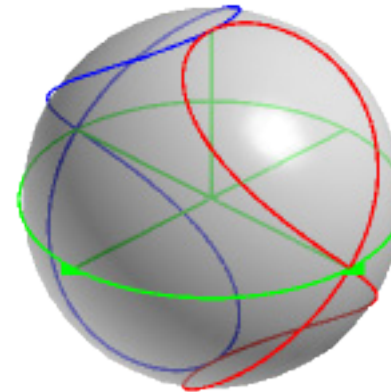
by passes of both branches are colored gray. The graphics in the schematic columns show a large central sphere ($r = 0.75$) which has no meaning other than to help distinguish front from back.

The events are listed in the order in which the first (red) branch of the QSO passes through the location of the event. To see the order, look at the red velocity vector at 0%, 25% and

50% of the cycle. The event that's created solely by passes of the second (blue) branch of the QSO, is listed last. The effect of adding 180° to the b-rotation of the second branch of the QSO is that the blue trace begins at $(0, 0, -1)$. The event at $(0, -1, 0)$ is therefore a simultaneous reflection in space of the event at $(0, 1, 0)$. As before, the passes which create the event at $(0, 1, 0)$ make a 90° angle, as do those at $(0, -1, 0)$. The magnitude of the velocity at these points is $\sqrt{2}$.

The polar events tell a different story. Events there are created by single passes of both branches of the QSO. The north polar event is created by a pass of the first (red) branch of the QSO at 0% of a cycle and by a pass of the second (blue) branch half a cycle later. The angle between the passes is 180° ; they are traveling in opposite directions. The south polar event is similar in timing and orientation, except that red and blue, first and second, are reversed. The magnitude of the velocity vectors at both events is $\sqrt{1}$. The reason for expressing this quantity as a second root rather than the more conventional form of "1" will become apparent in chapters 10 and 11 where a number of second root relationships will be discovered.

QSO 2(1:1) in table 4-4 has phase angles of 0° and 180° on the second branch of the QSO. Reversing the phase angles, both still on the second branch of the QSO, has a subtle effect on the events.

Fig. 4-7a⁵QSO 2(1:1) $[0^\circ, 0^\circ]$ $[180^\circ, 0^\circ]$ at 5%Fig. 4-7b⁶QSO 2(1:1) $[0^\circ, 0^\circ]$ $[180^\circ, 0^\circ]$ at 100%⁵ Compare with Fig. 4-6a.⁶ Compare with Fig. 4-6b.

Events


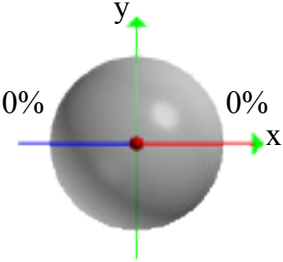

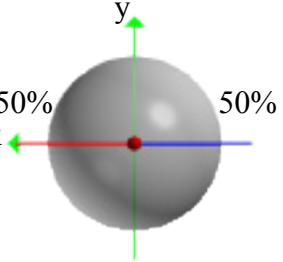

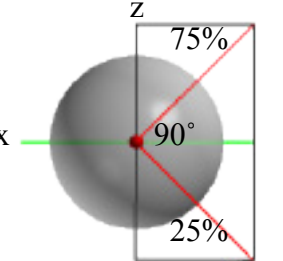

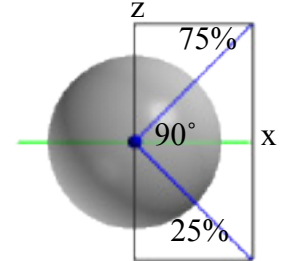
<u>QSO</u> Poles Ratio Phase Angles	<u>Location</u>	<u>Events</u> # of events Branch (color)	<u>Schematic</u>	<u>Location</u>	<u>Events</u> # of events Branch (color)	<u>Schematic</u>
QSO 2(1:1) [0°,0°] [180°,0°]	(0, 0, 1)			(0, 0, -1)		
	(0, 1, 0)			(0, -1, 0)		

Table 4-5

Graphical analysis of the events of QSO 2(1:1) [0°,0°] [180°,0°]

At first glance tables 4-4 and 4-5 look very much alike. However, a moment's inspection reveals that the resemblance is superficial at best. While the orientation of the velocity vectors in all eight schematics is identical, only the event at (0, 1, 0) is the same in each table. The differences, as one might suspect, are in the rotations of the second (blue) branch of the QSO.

With phase angles of 0° and 180° on the second branch, the blue rotating point passes through (0, 0, 1) at 50% of the cycle. Reversing the phase angles has the effect of making the blue rotating point *begin* at (0, 0, 1). With phase angles of 0° and 180°, the blue rotating point begins at (0, 0, -1). Reversing the phase angles puts it there half a cycle later. Even the timing of

the event at $(0, -1, 0)$, which is created solely by the blue branch itself, is reversed from one set of phase angles to the other. These variations are more clearly appreciated on the computer screen or in a video than in the static drawings.

A Geometric Curiosity

QSO 2(1:2) was used in the introduction to illustrate Bucky Fuller’s great circle railroad tracks of energy.⁷ We return to it now to observe a detail with geometric implications.

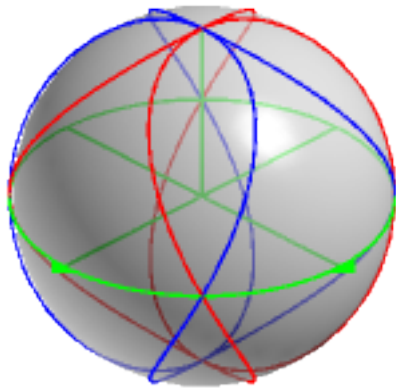


Fig. 4-8
QSO 2(1:2) $[0^\circ, 0^\circ] [0^\circ, 180^\circ]$ at 100%

QSO 2(1:2) consists of two baseball seams where each branch of the QSO is precessed 90° from the other. There are four events spaced equally around the equator, and two more at

⁷ See p. xi.

the poles. The six events are located at the vertices of a regular octahedron. While the equatorial events are created by two intersecting passes of the red and blue branches respectively, the polar events are created by four passes of both branches of the curve.⁸ Let us focus our attention on one of the equatorial events.


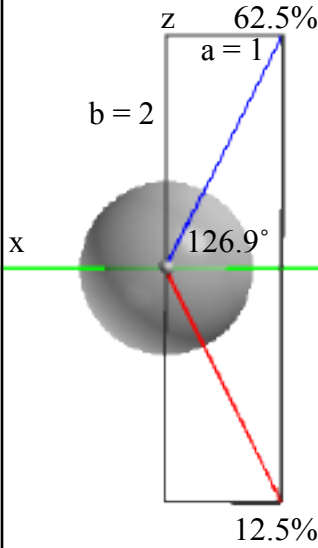
<u>QSO</u> Poles Ratio Phase Angles	<u>Location</u>	<u>Events</u> # of events Branch (color)	<u>Schematic</u>
QSO 2(1:2) $[0^\circ, 0^\circ]$ $[0^\circ, 180^\circ]$	$(\cos 45^\circ,$ $\sin 45^\circ,$ $0)$		

Table 4-6

Analysis of one of the equatorial events of
QSO 2(1:2) $[0^\circ, 0^\circ] [0^\circ, 180^\circ]$

⁸ While examination of the polar events of the 2(1:2) is instructive, the analysis is left to the reader.

The event in the foreground of figure 4-8 is created by a pass of the first (red) branch of the QSO traveling south-southeast at 12.5% of a cycle and by a pass of the second (blue) branch traveling north-northeast half a cycle later. The angle between the passes at the event is just a little less than 126.9° . This doesn't ring any bells until we remember that the central angle of an icosahedron is exactly half of that.

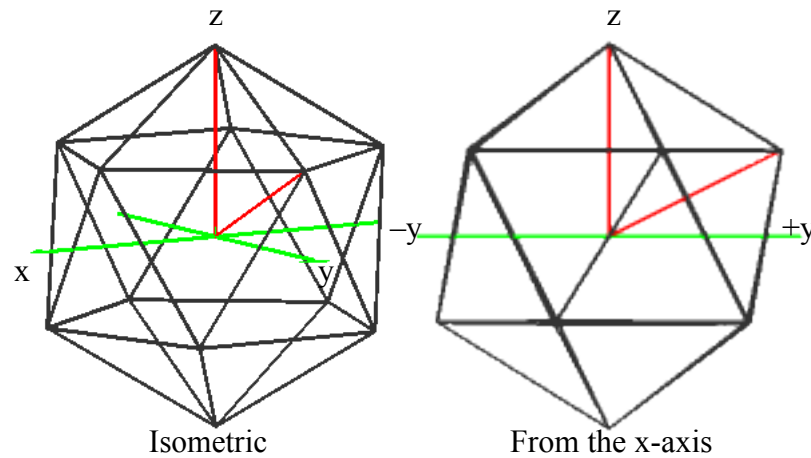


Fig. 4-9

Central angle of the regular icosahedron

A regular icosahedron is shown in figure 4-9. The views are isometric, left, and from the x-axis, right. The central angle of one of the edges is shown in red. From solid geometry we know that the central angle of the icosahedron is $63.43494882\dots^\circ$. But from table 4-6 the angle that either velocity vector makes with the xy-plane is $\tan^{-1}(2/1) = 63.43494882\dots^\circ$. While the

identity of a surface angle of the QSO with a central angle of the icosahedron may come as a surprise, there is a ready, if speculative, explanation.

Fuller showed that the tetrahedron, octahedron, icosahedron and Vector Equilibrium, his name for the cuboctahedron, can be smoothly transformed into one another.⁹ In many cases the surface angles of one figure become the interior angles of another. This may be what's happening here, although confirmation awaits a more detailed examination.

⁹ Fuller, 1975, pp. 190-196.

Orbits

Orbital Length

Rotation around two axes simultaneously produces an orbital trace that differs significantly from planar rotation around a single axis. One of the differences is the length of the orbit. Single axis rotation produces a circular orbit that is always 2π times its radius, whereas the length of a Quasi-Spherical Orbit varies with the QSO ratio. Early efforts to find the length of a QSO involved anything from drawing orbits on large plastic balls and measuring with bits of string to reproducing them on a basketball and using a mapping wheel. These crude methods gave estimates for QSO (1:1) from 1.326 to 1.414 times the length of a planar orbit. Professional mathematicians were of little help. Their estimates for the (1:1) ranged from 1.1 to 1.6 times the circular orbit.

The way out of this conundrum is an integral. Since the first derivative of position is velocity, we can integrate the velocity function for a QSO with respect to time and get the length or distance traveled. In this case it would give the arc length. Unfortunately the integration resulted in what one consultant called, "Quite an ugly mess," which no one involved with QSOs at the time knew how to handle. A recursive algorithm provided a more workable approach. Kenner (1976, p. 60) gives a standard formula for the distance between two points in space.

$$d = \sqrt{r_1^2 + r_2^2 - 2r_1r_2 \{ \cos \theta_1 \cos \theta_2 + \cos(\phi_1 - \phi_2) \sin \theta_1 \sin \theta_2 \}}$$

Eqn. 5-1a

For the spherical case, where $r_1 = r_2 = 1$, this becomes

$$d = \sqrt{2 - 2 \{ \cos \theta_1 \cos \theta_2 + \cos(\phi_1 - \phi_2) \sin \theta_1 \sin \theta_2 \}}$$

Eqn. 5-1b

The equation is in polar coordinates and the distance is calculated in straightforward fashion. One thing to keep in mind is that this formula gives the chord, not the arc. By choosing the points closer and closer together, it is possible to approximate an arc to any required degree of accuracy.

A small routine was written to calculate and sum the successive chords around a QSO. The routine, which ran on a TI-66 handheld programmable calculator, took about 10 seconds to calculate the distance between one pair of points. The problem now becomes a question of how little of an orbit do we actually need to calculate in order to get the whole thing. For QSO (1:1) the answer is 1/4. Since the (1:1) has two symmetrical lobes, and since each lobe is also symmetrical, one need only calculate one quarter of the whole curve and multiply

by four. For our purposes, we need to calculate θ and ϕ from 0° to 90° . The results are interesting so we'll examine all of them. At first, three increments of 30° each were used, then six of 15° , and so on.

# of increments	Degrees each	Time to run	d
3	30°	30 sec.	7.377 606 835
6	15°	60 sec.	7.573 911 027
9	10°	90 sec.	7.610 781 978
18	5°	3.0 min.	7.632 982 429
90	1°	15 min.	7.640 098 925
900	0.1°	2.5 hr.	7.640 392 21
9000	0.01°	25 hrs.	7.640 358 589

Table 5-1
Calculating the orbital length of QSO (1:1)

As the number of iterations of the routine increases and the angular extent of the rotations decreases, the orbital length of QSO (1:1) approaches 7.6403... as a limit. The results are each larger than the just preceding one, which is what one would expect by taking more and smaller increments of the orbit. Thus the slight shrinkage in the last result is a little puzzling. One speculates that accumulated error in the calculator may have had something to do with it, but no definite explanation was ever found. Since the next result, 90,000 iterations at 0.001° would

have taken nearly ten and a half days, it was decided to accept the length of QSO (1:1) as 7.6403 until further notice.

Compared to the length of the circular (flat) orbit, the length of the QSO is

$$7.6403... / 2\pi = 1.2160...$$

With time, the first orbital length program was improved. Ultimately, it could calculate the orbital length of any QSO, whether or not the orbit displayed quadrilateral symmetry. The (1:1) calculation was carried out again, resulting this time in a length of 7.6366..., or 1.2154 times the circumference of a circle.¹

In some ways, the ability to calculate the incremental chords of the orbit is more useful than the integral, which gives only the total length. With the improved program, the increments of QSO (1:1) were calculated at each 1% of rotation ($n = 100$). The results, which are displayed next, show an interesting pattern.

¹ The orbital length of QSO (1:1) has been calculated several times. Slight variations in the method yielded slightly different results each time. For the record, they are:

Chester 1992	7.640 358 589
Kelleher 1994	7.640 395 578
Chester 2003	7.640 357 086
Chester 2006	7.636 551 79

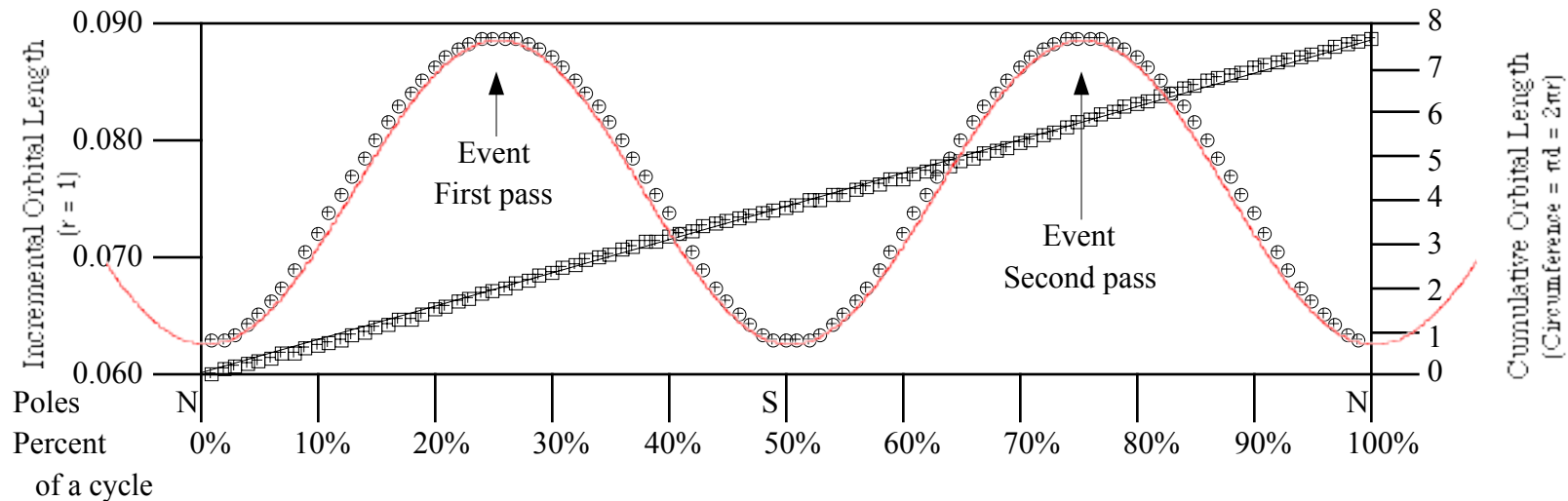


Fig. 5-1
Chordal increments of QSO (1:1)

The black sine-like curve shows how the increments of QSO (1:1) vary with each 1% of rotation. All lengths are a fraction of the radius ($r = 1$). Beginning with an increment of 0.062 821 518, each succeeding increment increases to a maximum of 0.088 799 204 at 25% of the orbital cycle. The increments then decrease to the minimum again at 50% and reach the maximum for the second time at 75%. The rotating point crosses its own trace and forms an intersection event at twenty-five and seventy-five percent of the orbit. At zero and 50% it's at the north or the south pole. The implication is that the velocity and the acceleration of the rotating point vary around the orbit, which is true. However, a detailed examination of the variation is beyond the scope of this volume. The reader is encouraged to do so on

their own.

One might ask whether the obvious resemblance between the incremental plots of the (1:1) and a sine wave is actually a sine or just looks like it. The answer is that it is not a sine. In figure 5–1 a red sine wave has been superimposed on the incremental orbital lengths. It matches at the maxima & minima, but misses elsewhere.

The line formed of small squares is the cumulative total which begins at zero and adds finally to 7.6366... at the right. It's not really a straight line, even though it's close. Because the increments that are being added to the total vary, the total varies too, although the scale of the variation is much smaller than that of the increments themselves.

Expanding the Envelope

We are now in a position to begin calculating QSO orbital lengths wholesale. The orbital lengths of the first twenty-five monopoles are displayed in table 5-2. The 1(1:1) and its equal-rate cousins are revealed as having the absolute shortest orbits. Again a slight shrinkage is noted in the length of the equal rate

curves, this time with increasing rates of rotation, and again we suspect that the shrinkage may be due to accumulated error and not to any real difference in the actual orbital lengths. We mentioned in the introduction and in chapter 2 that QSOs form polygons and polyhedra. Three of the QSOs in table 5-2 are identified as the tetrahedron, the octahedron and the icosahedron. The baseball seam, which forms no polyhedron, is also indicated.

↑ a-rotations	1(5:1)	21.392 780 64	1(5:2)	24.435 133 79	1(5:3)	28.458 273 64	1(5:4)	33.116 355 61	1(5:5)	7.639 434 466
	1(4:1)	17.627 938 1	1(4:2)	10.540 217 8	1(4:3)	25.525 358 16	1(4:4)	7.639 780 453	1(4:5)	35.956 160 41
	1(3:1)	13.974 109 01	1(3:2)	Tetrahedron 17.972 829 11	1(3:3)	7.640 049 563	1(3:4)	28.359 994 73	1(3:5)	34.073 967 99
	1(2:1)	10.540 605 18	1(2:2)	7.640 241 785	1(2:3)	Octahedron 20.794 957 3	1(2:4)	13.317 778	1(2:5)	Icosahedron 32.635 320 46
	1(1:1)	7.640 357 086	1(1:2)	Baseball seam 13.318 195 3	1(1:3)	19.362 358 7	1(1:4)	25.520 179 36	1(1:5)	31.726 334 22
	b-rotations →									

Table 5-2
Orbital lengths of the first twenty-five monopoles

The QSO Landscape

A 3-D graph of the orbital lengths reveals a surprising “landscape.”

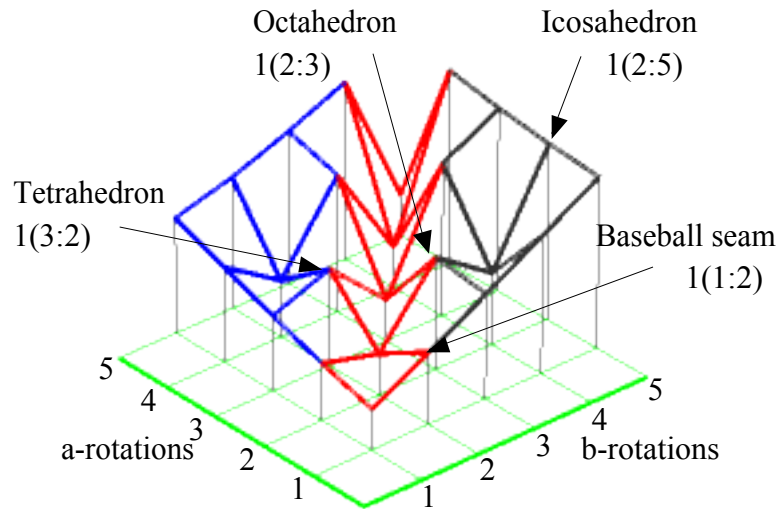


Fig. 5-2

Orbital lengths of the first 25 monopole QSOs

Each QSO occupies the same place in the xy -plane as it does in table 5-2. The lengths of the orbits are graphed vertically. To fit the graph to the space available, the orbital lengths have been reduced by a factor of 12. Connecting the tops of the vertical vectors reveals an “equal-rate valley” ($a = b$) which is displayed in red. In general, the b -rotations have a greater effect on orbital length (black chords) than the a -rotations (blue), since the b -side of the graph grows at a greater rate than the a -side. However,

the appearance of two “dimples” at QSOs (4:2) and (2:4) shows that the relationship is not a linear one. The dimples occur because the orbital *lengths* of QSO (4:2) and the (2:4) are the same as those of QSOs (2:1) and (1:2), although the rotational *rates* of the former are twice those of the latter.

The First 100 Monopole QSOs

Pages 74–77 present the x -, y -, z -, and isometric views of the first 100 monopole QSOs. To save space, labels on the axes have been omitted, although these are the same as in table 5-2 and figure 5-2.

The first thing one notices about the 100-QSO landscape is that the graphs consist of three sections. There is the upper left section (blue) in which $a > b$. There is the lower right section (black) in which $a < b$, and there is the equal rate diagonal (red) in which $a = b$.²

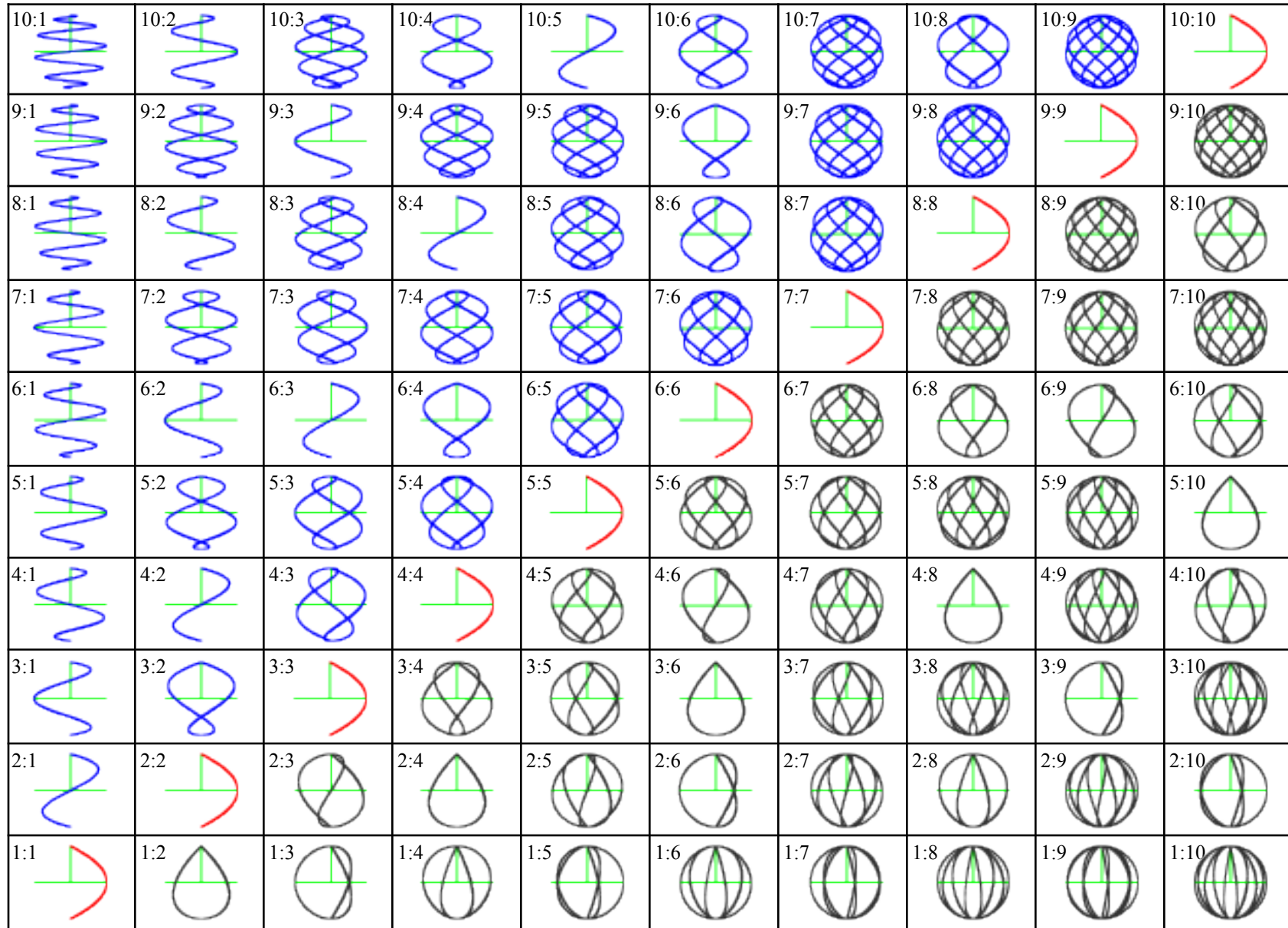
Certain regularities are apparent in all four graphs. The equal rate diagonal is created by multiplying the basic (1:1) ratio by successive integers: 2, 3, 4,.... The same process creates families of statically similar curves of any other basic ratio. For instance, among the blue curves ($a > b$), QSOs (2:1), (4:2), (6:3), (8:4), (10:5),... all look alike. In the black section ($a < b$), QSOs (1:3), (2:6), (3:9),... are also all statically identical. The dimples of figure 5-2 can now be seen as the

² In heraldry, the equal rate diagonal stretching from lower left to upper right would be called a *Bend Sinister*. It passes from the wearer’s upper left side to their lower right. To an observer, of course, left and right are reversed. Compare *sinister* (left) and *dexter* (right).

beginnings of their own “valleys of similarity.” All told, the first 25 QSOs give rise to 19 distinct species, valleys of static similarity which extend indefinitely outward from each basic ratio.

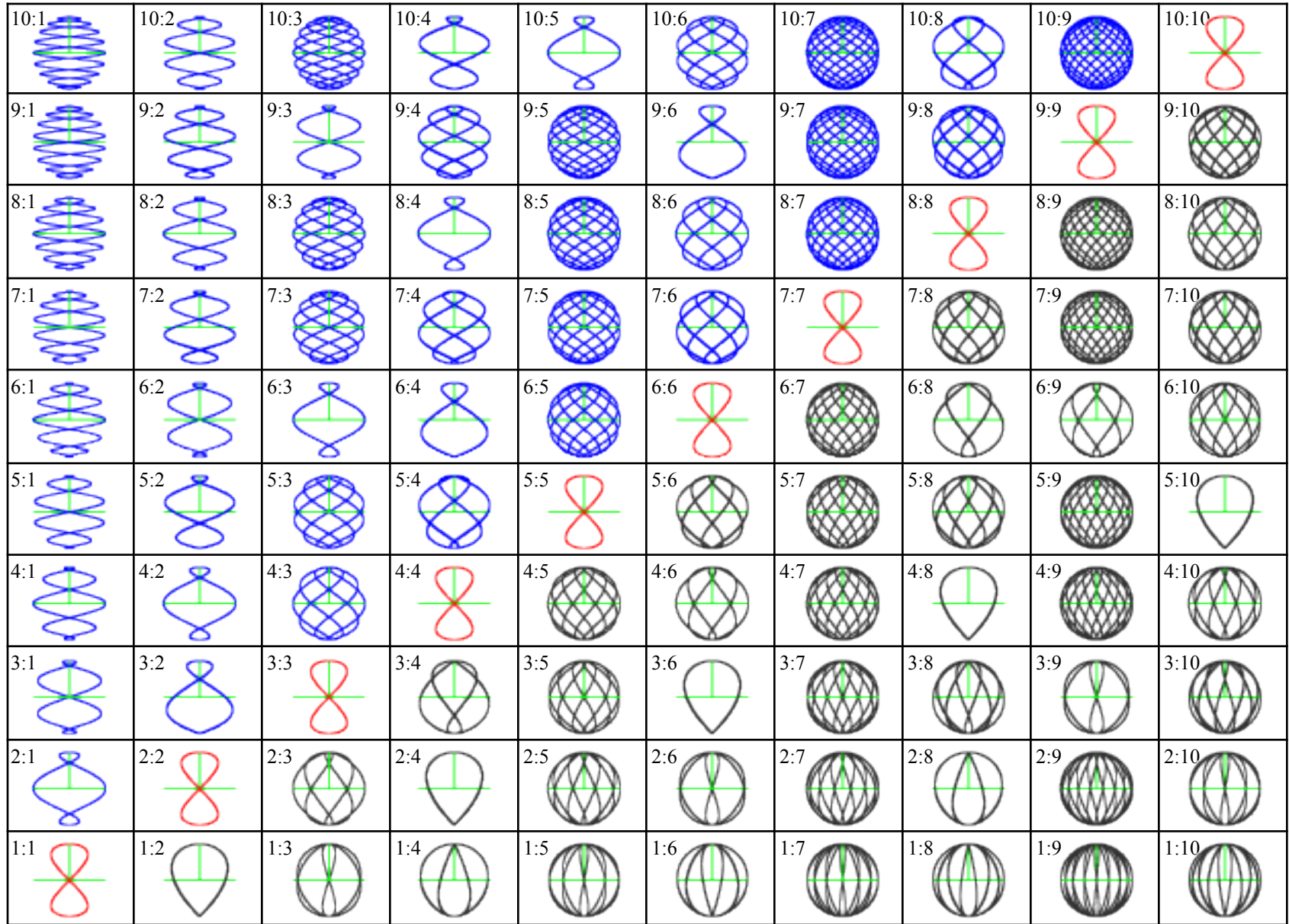
QSO – The Mathematics and Physics of Quasi-Spherical Orbits

Fig. 5-3a The first 100 monopole QSOs View from +x



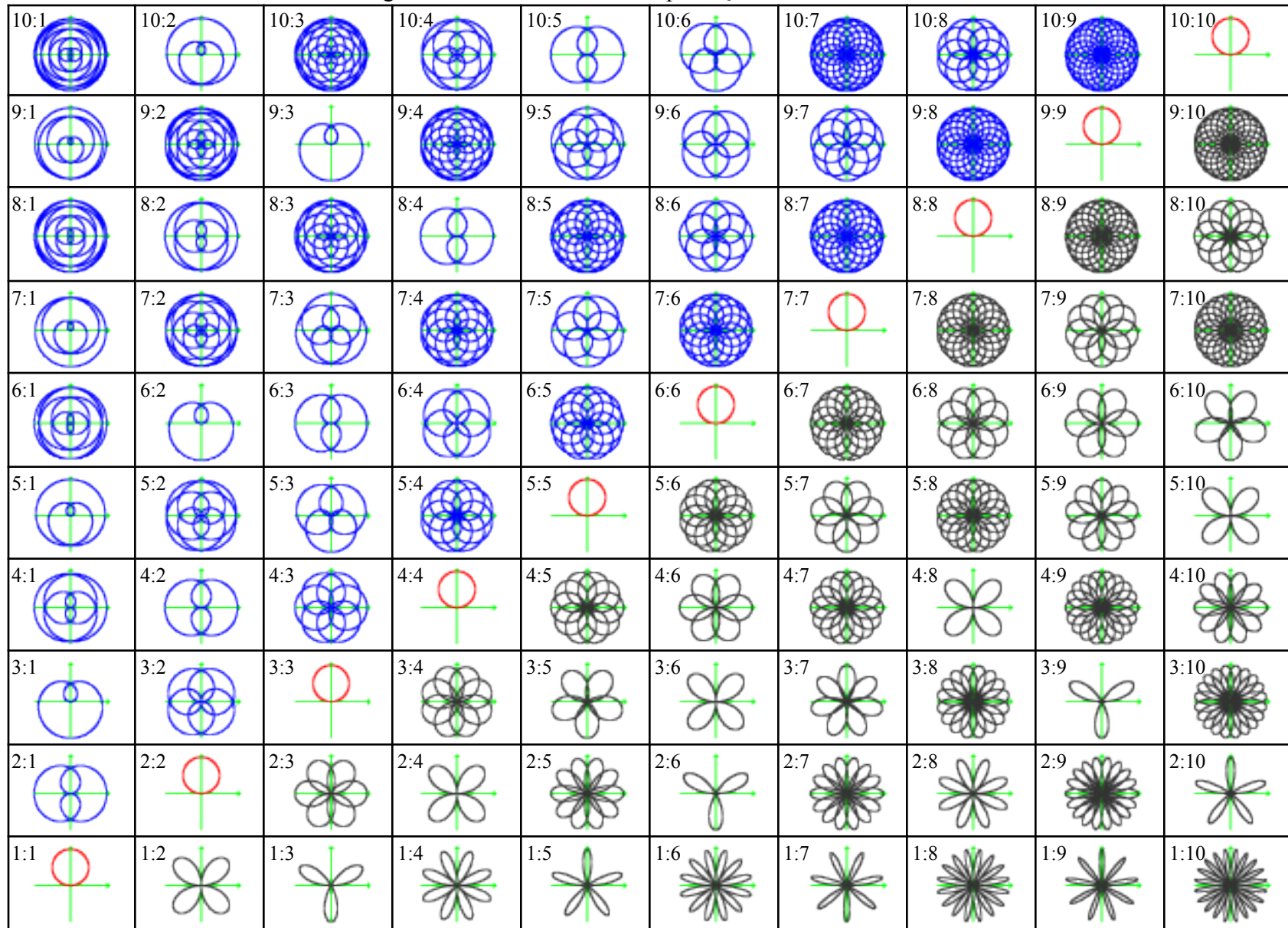
Orbits

Fig. 5-3b The first 100 monopole QSOs View from +y



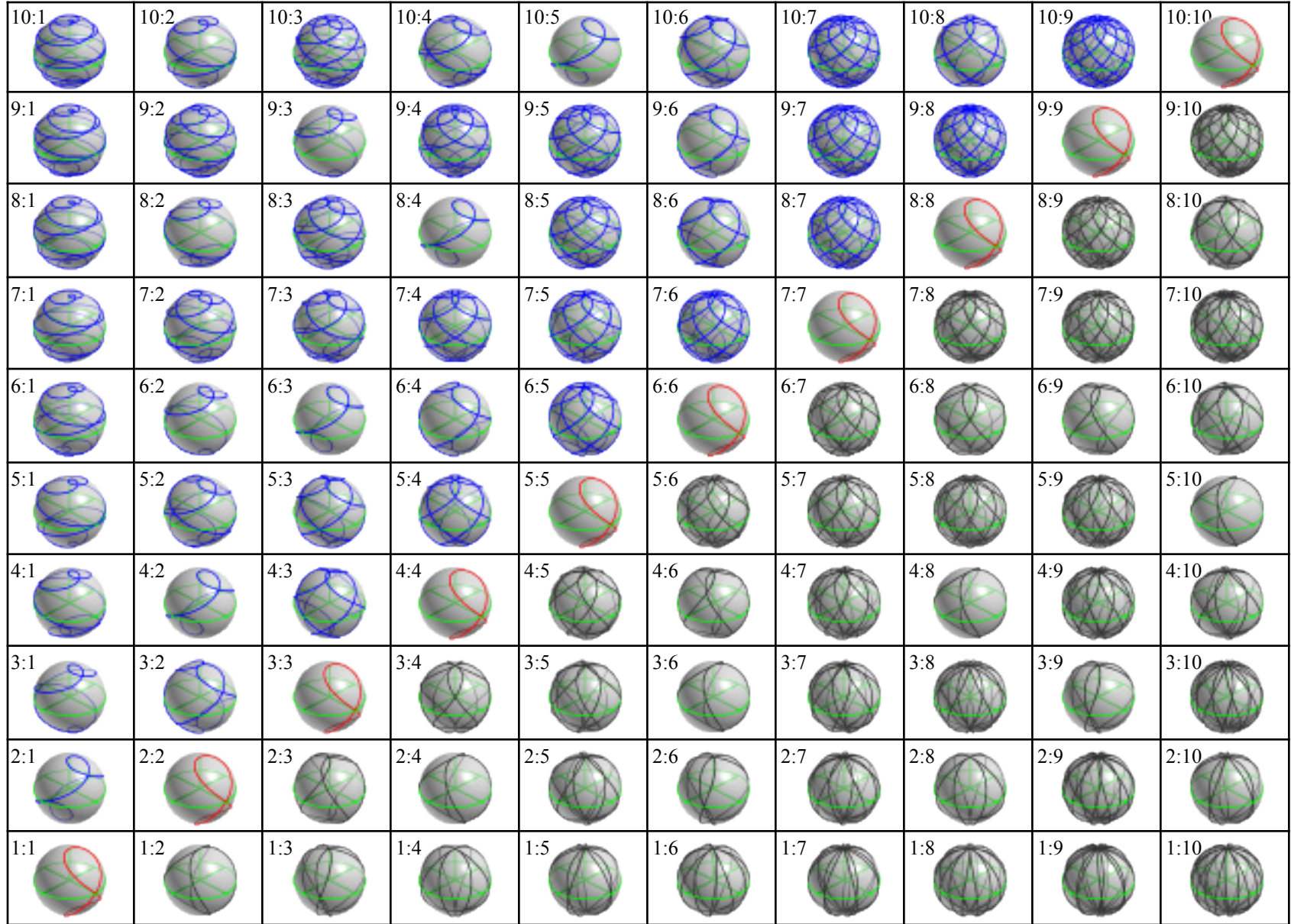
QSO – The Mathematics and Physics of Quasi-Spherical Orbits

Fig. 5-3c The first 100 monopole QSOs View from +z



Orbits

Fig. 5-3d The first 100 monopole QSOs Isometric view



Displays

The First QSO Display

When a new telescope comes online and begins collecting light from the cosmos, astronomers have a name for the occasion. They call it “First Light.” The equivalent for the study of Quasi-Spherical Orbits is the “First QSO.”

As we saw in chapter 2, equation 2-8a is not the only form of the QSO equation. In 1990, Burke approached a young David Loftus and asked him to write a program. “All I gave him,” says Burke, “was ‘imagine the disc with the thing on it and then rotate it and then rotate it on the second axis....’” Loftus, the original QSO programmer, did the math and came up with

$$\begin{bmatrix} x \\ y \\ z \end{bmatrix} = \begin{bmatrix} (\cos t) (\cos t) \\ (\sin t) (\cos t) \\ (\sin t) \end{bmatrix}$$

Eqn. 6-1¹

The original QSO equation

¹ Compare with Eqns. 2-8b & 2-8h.

He then wrote a “3-D Combined Rotation Plotter” in BASIC. It ran on an IBM XT and displayed only one of the three axial views or the isometric view at a time – in monochrome, no less. Loftus’ equation is based solely on geometric and dynamic considerations; he did not begin with spherical coordinates as we did in chapter 2.

For people with a good visual imagination, Burke’s instructions to Loftus would be enough. Eventually though, even people with good visual imaginations need to confirm their vision. Thus was born an effort to display QSOs that continues to this day. The first Quasi-Spherical Orbit that was ever generated on a computer screen was a jagged QSO (1:1).²

² A mechanical device that generated QSO (1:1) was built by Burke long before Loftus’ computer program came along. This and another mechanism will be discussed in chapter 12.

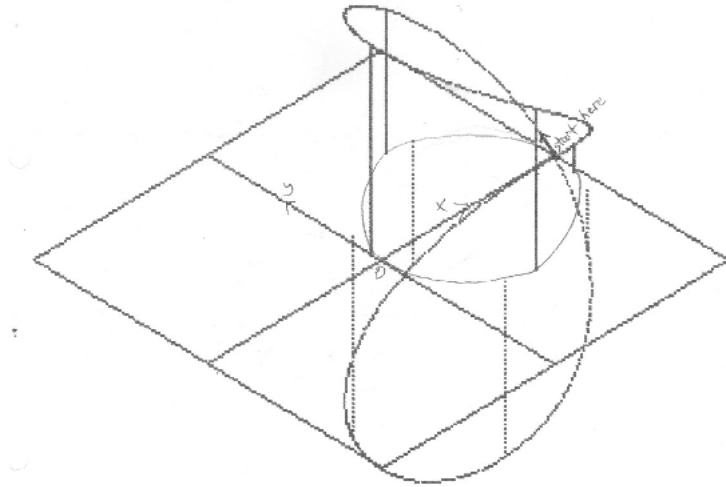


Fig. 6-1
The original QSO (1:1) display

Reproduced here from a 1990 printout, the view is isometric. The positive and negative halves of the x- and y-axes are reversed from their customary orientation while the z-axis, which is not shown, maintains its usual relationship to the horizontal plane. The curve starts at $(1, 0, 0)^3$ and rotates

$$\theta = \text{Pos}, \phi = \text{Neg.}$$

In order to show what was above or below the xy-plane, Loftus' program drew a solid line to the plane from points with a positive z-coordinate and a dotted line from points at negative z. In figure 6-1 the projection of the (1:1) on the horizontal plane

³ Notice "start here" written by hand near the event.

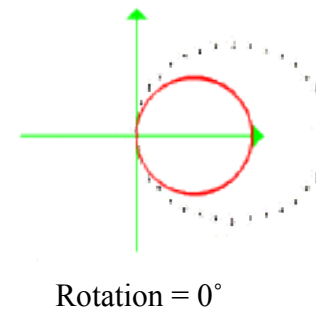
has been drawn in using these marker lines as guides. Although it misses two of the dotted lines, the sketch is a good representation of the circle we now know this projection to be.

When the new 286 PCs with Windows 3.1 became affordable, the second QSO programmer, Athol Crosby, further developed Loftus' program to display and print all four views simultaneously and in color.

The Kelleher Rotation

A year later, John Kelleher, the third QSO programmer, wrote his own display program. Kelleher's program offered another innovative feature, illustrated next.

Like Loftus' display, Kelleher's has also been reproduced from old printouts. The display has no visible axes, but the view from the positive z-axis is conventional. A modern view of QSO (1:1) is included in the first sketch for comparison. The modern QSO, which is drawn in red, has been reduced in size so it doesn't block the view of the older curve.



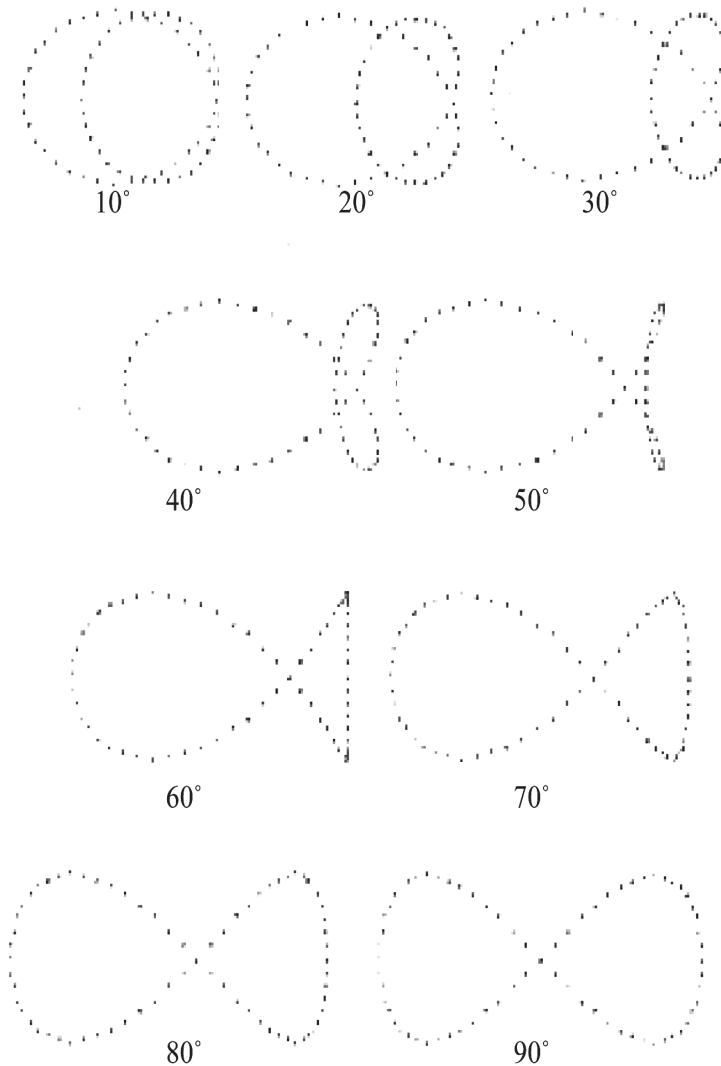


Fig. 6-2
QSO (1:1), the Kelleher rotation

The innovative feature of Kelleher's display was the ability to rotate the axis system. In figure 6-2 QSO (1:1) is seen rotating around the y-axis in 10° increments. Each screen developed dot-by-dot, which took an appreciable amount of time, and had to be printed out before the next screen could be calculated.

The Octamap

It was not easy, when viewing early computer-generated QSOs, to know what one was looking at. The curve, which exists in space, was projected against a nearly flat piece of glass. The observer then had to add back the dimensional information deleted by the computer. The machine helped by giving three views, one from each of the three coordinate axes. These three plus the isometric perspective allowed the viewer with a good imagination to reconstruct the curve in their mind. For the simple QSOs, this process worked fairly well. For the more complex curves, it was difficult, if not impossible, to imagine the trace crossing or not crossing, front or back, going in or heading out, and so on.

In response to these and other concerns, the author developed in 1993 what he calls the Octamap. Each edge of a regular octahedron subtends a 90° central angle. Thus each face of the octahedron represents one octant of the unit sphere. The spherical QSO data can be mapped onto the planar octahedron which can then be unfolded and laid flat to show an entire QSO at one time. It can also be refolded and put together again to see an approximation of the curve in space.

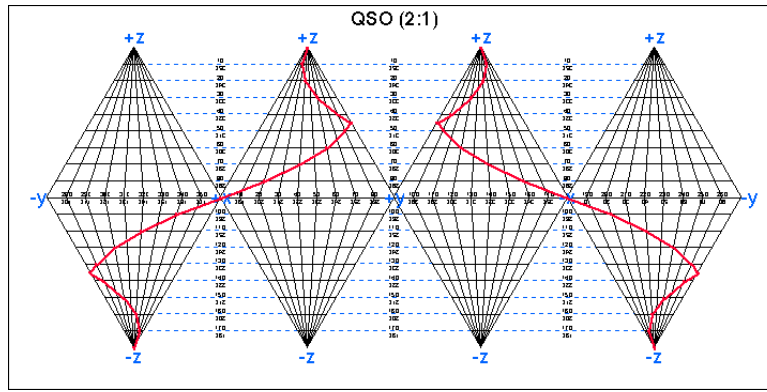


Fig. 6-3
QSO (2:1) Octamap⁴

When appropriately plotted, the Octamap gives a fairly good representation of QSOs. Shown in figure 6-3 is QSO (2:1), the Loop-the-Loop.⁵ It is immediately obvious in the figure that there are two intersections, 180° apart ($\Delta\theta = 180^\circ$). This is not so evident when looking at the flat-screen computer-generated version of the (2:1). The two polar grazings are also clearly 180° apart in ϕ and do not touch, as might be inferred from the computer view along the z-axis. And finally, although the sinusoidal characteristics which are apparent when looking along the x-axis may seem to be absent from the octahedral map, one need only cut out the octa and paste it together to get this information.

⁴ Compare the flat configuration of the Octamap with U.S. Patent 2,393,676 (Dymaxion Airocean World), issued to R. Buckminster Fuller 1946 Jan 29 and updated in 1954 to an icosahedral projection.

⁵ See Fig. 3-6b.

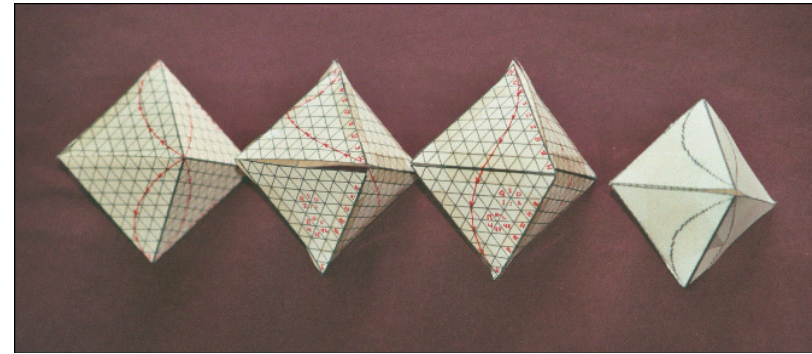


Fig. 6-4
Folded Octamaps

Figure 6-4 shows three Octamaps plotted by hand by the author and one generated by Kelleher on his computer.⁶ Left to right, they are QSO (1:1), (2:1), (1:2) by the author, and QSO (1:1) by Kelleher. Using these and other primitive tools of the day, many discoveries about QSOs were made. Ultimately, more computing power was needed, and for that the author turned to the professionals. In 2002 he purchased the commercial release of Graphing Calculator, version 3.2.⁷ We will explore next some of the more interesting display capabilities made possible by this software.

⁶ If a QSO is plotted on a transparent plastic sheet such as that used in overhead projectors, the sheet can be folded into an octahedron showing the entire QSO at once. For his part, Burke suggested mapping onto a tetrahedron with the poles centered along opposed edges. See Fuller (1979), p.453, §1131.10-13.

⁷ See p. 7, footnote 7.

Cone & Disk

In the first chapter an inverted unicycle was used to visualize QSOs. The purpose of the unicycle was to emphasize the dynamic nature of QSOs and to visually show the dual rotations. As far as it goes, the unicycle metaphor is accurate. It depicts a single QSO developing as the result of simultaneous rotations on two axes. However, the unicycle cannot portray more than two rotations or one resultant QSO. A refinement of the unicycle concept that overcomes these limitations will be developed next.⁸

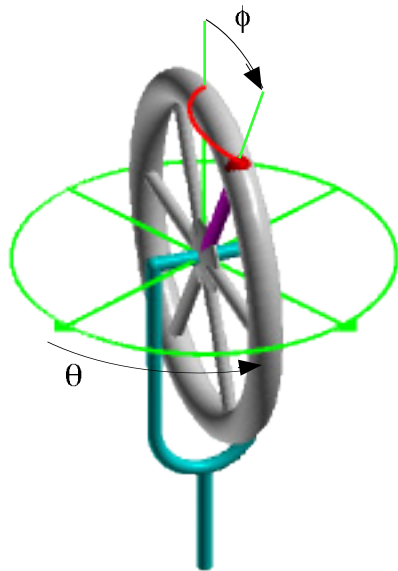


Fig. 6-5
Unicycle with developing QSO

To review briefly, an inverted unicycle appears in figure 6-5. The gray tire has been repaired with a red patch. One spoke, which points toward the patch, is colored violet. As the unicycle rotates simultaneously on the vertical axis of the seat post and on the horizontal axis of the wheel, the patch traces out the orbital path of a QSO. The actual QSO depends on the ratio between the rates of rotation on each of the axes.

The rotations are measured by angles θ and ϕ . Angle θ is the angular displacement in the xy -plane from the positive x -axis, while ϕ is the angular displacement from the positive z -axis.

The unicycle metaphor gives a pretty good picture of θ since the tire rotates θ degrees around the z -axis. However, the unicycle doesn't give much of a visual clue about ϕ . There is only the violet spoke that rotates around the axle of the wheel, and at two places in the rotation, as the wheel goes edge-on to the viewer, the violet spoke is hidden. This disadvantage can be overcome by replacing the tire of the unicycle with a rotating circle.

⁸ For the equations that generate the unicycle itself, see appendix 1.

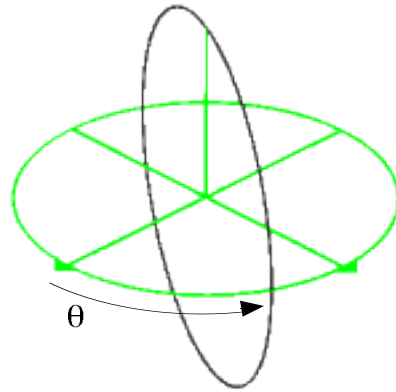


Fig. 6-6

A rotating circle with Cartesian axes and an equator

A black circle which rotates around the z -axis replaces the tire of the unicycle. The circle started in the xz -plane and in this view has rotated about 60° in the positive direction. The angular displacement of rotation is the angle θ . The coordinate system is provided by the software. The equator and the rotating circle need to be generated with appropriate equations. In the case of the circle both the spherical and the Cartesian forms are given for comparison.⁹

⁹ Users of Graphing Calculator please note: When the slider n is activated, all rotations will go to 100% and then reverse and go back to 0% again. To avoid this oscillation and make the rotation continuous in the positive direction, on the Mac, press and hold the option key while you press the “Play” button on the slider. On Windows, it’s one of the other modifier keys. See the online help, under “Special Commands.”

$$\begin{bmatrix} r \\ \theta \\ \phi \end{bmatrix} = \begin{bmatrix} 1 \\ ag \\ 2\pi t \end{bmatrix}$$

Eqn. 6-2a

Rotating circle, spherical notation

$$\begin{bmatrix} x \\ y \\ z \end{bmatrix} = \begin{bmatrix} \cos ag & \sin ag & 0 \\ 0 & 0 & 1 \end{bmatrix} \begin{bmatrix} \sin 2\pi t \\ 0 \\ \cos 2\pi t \end{bmatrix}$$

Eqn. 6-2b

Rotating circle, Cartesian notation

$$\begin{bmatrix} x \\ y \\ z \end{bmatrix} = \begin{bmatrix} \cos 2\pi t \\ \sin 2\pi t \\ 0 \end{bmatrix}$$

Eqn. 6-3

The equator

A radius vector is added to the circle.

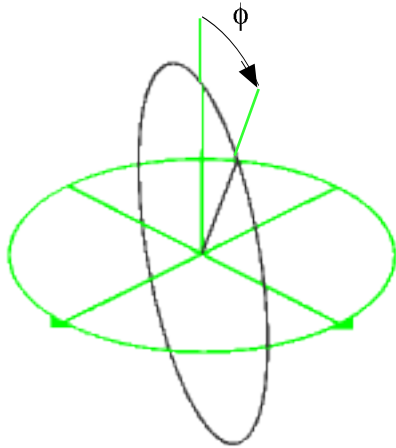


Fig. 6-7

The rotating circle and a rotating radius vector

The radius vector, which represents the violet spoke of the unicycle, rotates around the axis of the circle. The angular displacement of the vector from the z-axis is angle ϕ . Three forms of the vector equation are,

$$\begin{bmatrix} r \\ \theta \\ \phi \end{bmatrix} = \begin{bmatrix} t \\ ga \\ gb \end{bmatrix}$$

$$\begin{bmatrix} x \\ y \\ z \end{bmatrix} = t \begin{bmatrix} \sin(bg) \cdot \cos(ag) \\ \sin(bg) \cdot \sin(ag) \\ \cos(bg) \end{bmatrix}$$

$$\begin{bmatrix} x \\ y \\ z \end{bmatrix} = \begin{bmatrix} \cos ag & \sin ag & 0 \\ \sin ag & \cos ag & 0 \\ 0 & 0 & 1 \end{bmatrix} \begin{bmatrix} 0 & \sin bg & \sin bg \\ 1 & 0 & 0 \\ 0 & \cos bg & \cos bg \end{bmatrix} \begin{bmatrix} 0 \\ 0 \\ t \end{bmatrix}$$

Eqns. 6-4

The rotating radius vector

A small red sphere is placed at the end of the radius vector. The red sphere moves with the intersection of the radius vector and the circle to trace the QSO.

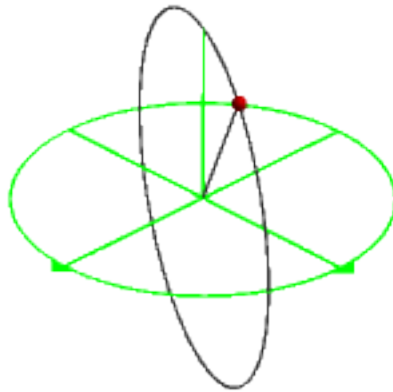


Fig. 6-8

The rotating circle, radius vector and a small red sphere

The sphere represents the patch in the unicycle. It has no structural significance. It's only purpose is to help the eye follow the rotations which produce the QSO. There are two ways to express the small sphere. The equations are,

$$\begin{bmatrix} x \\ y \\ z \end{bmatrix} = 0.04 \begin{bmatrix} \sin \pi u \cdot \cos 2\pi v \\ \sin \pi u \cdot \sin 2\pi v \\ \cos \pi u \end{bmatrix} + \begin{bmatrix} (\sin bg) (\cos ag) \\ (\sin bg) (\sin ag) \\ \cos bg \end{bmatrix}$$

$$\begin{aligned} &((\sin bg) (\cos ag) - x)^2 + ((\sin bg) (\sin ag) - y)^2 \\ &+ (\cos bg - z)^2 = 0.002 \end{aligned}$$

Eqns. 6-5
Small sphere¹⁰

Adding the orbital trace.

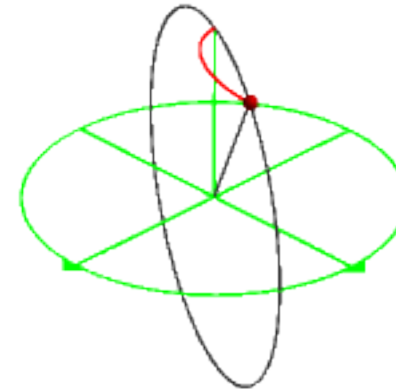


Fig. 6-9

The orbital trace

¹⁰ Users of Graphing Calculator please note: While the implicit form of the small sphere is limited by the space in which Graphing Calculator operates, the parametric form is defined everywhere. In practice, if the QSO rotations carry the implicit sphere beyond the defined space, it will cease to exist. If you get a notice, "No surface found in the coordinate ranges given," and the small sphere does not appear, try increasing the resolution to maximum. If that doesn't work, use the parametric form.

$$\begin{bmatrix} r \\ \theta \\ \phi \end{bmatrix} = \begin{bmatrix} 1 \\ agt \\ bgt \end{bmatrix}, \quad \begin{bmatrix} x \\ y \\ z \end{bmatrix} = \begin{bmatrix} (\sin bgt) (\cos agt) \\ (\sin bgt) (\sin agt) \\ \cos bgt \end{bmatrix}$$

Eqns. 6-6
The orbital trace

In the unicycle graphic the three dimensional tire and spokes help distinguish back from front.¹¹ The model being developed here offers no such visual aid, so we need to put one in. A translucent gray disk fills the interior of the rotating circle and rotates with it.¹²

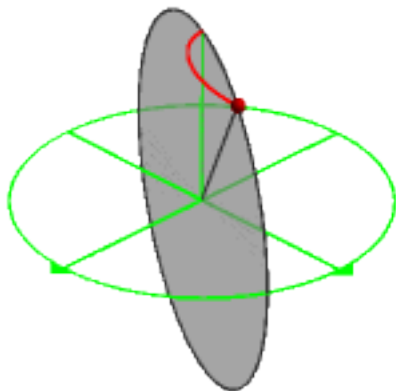


Fig. 6-10

A translucent gray disk fills the rotating circle

¹¹ See chapter 1, Dynamic Diversity, development of QSO (1:1), isometric views from 180° to 360°.

¹² The other visual aid used for this same purpose was a translucent sphere placed at the Origin of the coordinate system. See Fig. 1-1b.

The equation for the translucent disk is simplicity itself.

$$\theta = ag$$

Eqn. 6-7
The rotating disk¹³
 $g = 2\pi n$

Next we introduce a visual effect that was not present in the unicycle.

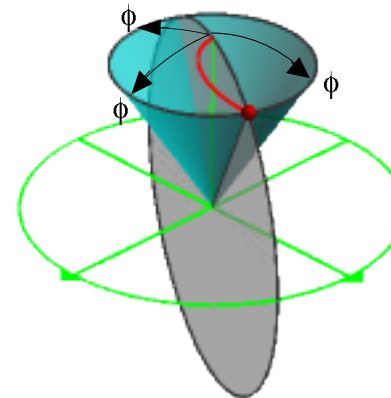


Fig. 6-11

The cone of ϕ

¹³ A further note for users of Graphing Calculator: The default settings are $\theta = 2\pi$, $\phi = \pi$. This makes it necessary to use two equations to draw the complete disk. (The other equation is $\theta = ag + \pi$.) By defining $\phi = 2\pi$, one equation suffices.

Angle ϕ is defined as the angular displacement from the z-axis. There is no restriction on the xy-coordinates of the displacement. Thus ϕ can be represented by a cone centered on the z-axis and opening outward to an extent equal to the displacement. A black circle around the edge of the conical opening shows the intersection of the cone and the unit sphere (not shown). The intersection of the rotating disk and the cone is the radius vector. The intersection of the disk, cone and the unit sphere traces the QSO.

The equations are

$$\phi = bg \quad , \quad \begin{bmatrix} x \\ y \\ z \end{bmatrix} = \begin{bmatrix} v (\sin bg) \cos 2\pi t \\ v (\sin bg) \sin 2\pi t \\ v \cos bg \end{bmatrix}$$

Eqns. 6-8

Cone of ϕ

$$\begin{bmatrix} r \\ \theta \\ \phi \end{bmatrix} = \begin{bmatrix} 1 \\ 2\pi t \\ bg \end{bmatrix} \quad , \quad \begin{bmatrix} x \\ y \\ z \end{bmatrix} = \begin{bmatrix} (\sin bg) \cos 2\pi t \\ (\sin bg) \sin 2\pi t \\ \cos bg \end{bmatrix}$$

Eqns. 6-9

Black circle

In figure 6-11 the disk and the cone intersect in two places. Thus a second QSO may be generated by this same system.

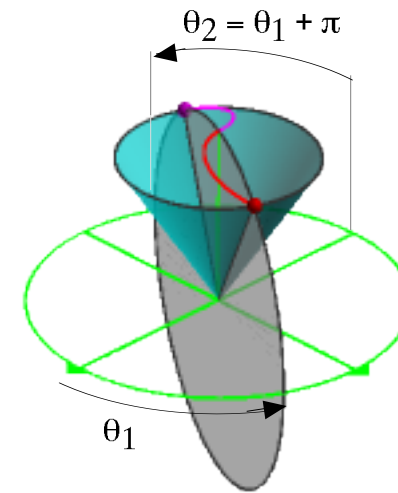


Fig. 6-12
Second orbital trace

In the sketch a dipole QSO is generated from a single disk & cone system. Both branches of the QSO begin at $(0, 0, 1)$ and both have positive θ and ϕ rotations. Both have the same QSO ratio, in this case (2:1). The second branch results from adding 180° to the θ rotation of the first. That is, θ_2 is 180° out of phase with θ_1 .

$$\theta_2 = \theta_1 + 180^\circ$$

In the equations for the second radius vector, small sphere and orbital trace, this addition is equivalent to adding π to the θ -rotation of the first trace.

$$\begin{bmatrix} r \\ \theta \\ \phi \end{bmatrix} = \begin{bmatrix} t \\ ga + \pi \\ gb \end{bmatrix}$$

$$\begin{bmatrix} x \\ y \\ z \end{bmatrix} = \begin{bmatrix} \cos(ga + \pi) & \cos(ga + \pi) & 0 \\ \sin(ga + \pi) & \sin(ga + \pi) & 0 \\ 0 & 0 & 1 \end{bmatrix} \begin{bmatrix} 0 & \sin bg & \sin bg \\ 1 & 0 & 0 \\ 0 & \cos bg & \cos bg \end{bmatrix} \begin{bmatrix} 0 \\ 0 \\ t \end{bmatrix}$$

Eqns. 6-10
Second radius vector

$$\begin{bmatrix} x \\ y \\ z \end{bmatrix} = 0.04 \begin{bmatrix} \sin \pi u \cdot \cos 2\pi v \\ \sin \pi u \cdot \sin 2\pi v \\ \cos \pi u \end{bmatrix} + \begin{bmatrix} (\sin bg) (\cos (ag + \pi)) \\ (\sin bg) (\sin (ag + \pi)) \\ \cos bg \end{bmatrix}$$

$$((\sin bg) (\cos (ag + \pi)) - x)^2 + ((\sin bg) (\sin (ag + \pi)) - y)^2 + (\cos bg - z)^2 = 0.002$$

Eqns. 6-11
Second small sphere¹⁴

$$\begin{bmatrix} r \\ \theta \\ \phi \end{bmatrix} = \begin{bmatrix} 1 \\ agt + \pi \\ bgt \end{bmatrix}, \quad \begin{bmatrix} x \\ y \\ z \end{bmatrix} = \begin{bmatrix} (\sin bgt) (\cos (agt + \pi)) \\ (\sin bgt) (\sin (agt + \pi)) \\ \cos bgt \end{bmatrix}$$

Eqns. 6-12
Second QSO

The model is not limited to a single cone of ϕ . Any number of cones may be accommodated, with phase angles as desired. Next, a second cone of ϕ is added with a phase angle of 180° with respect to the first.

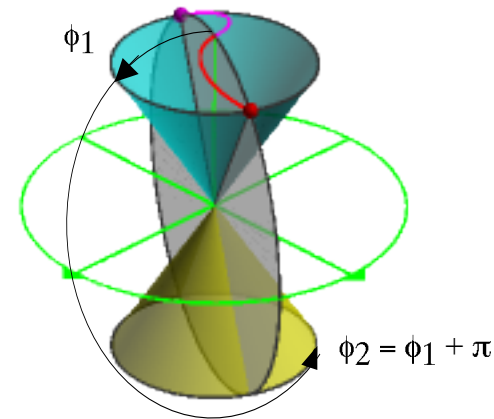


Fig. 6-13
Second cone of ϕ .

¹⁴ The implicit form of the second small sphere is subject to the same limitations as the first. See p. 85, footnote 10.

Like the first cone of ϕ , the second is bounded by a black circle which is the intersection of the cone and the unit sphere. The equations for the cone and the edge circle are

$$\phi = bg + \pi, \quad \begin{bmatrix} x \\ y \\ z \end{bmatrix} = \begin{bmatrix} v (\sin (bg + \pi)) \cos 2\pi u \\ v (\sin (bg + \pi)) \sin 2\pi u \\ v \cos (bg + \pi) \end{bmatrix}$$

Eqns. 6-13

Second cone of ϕ

$$\begin{bmatrix} r \\ \theta \\ \phi \end{bmatrix} = \begin{bmatrix} 1 \\ 2\pi t \\ bg + \pi \end{bmatrix}, \quad \begin{bmatrix} x \\ y \\ z \end{bmatrix} = \begin{bmatrix} (\sin (bg + \pi)) \cos 2\pi t \\ (\sin (bg + \pi)) \sin 2\pi t \\ \cos (bg + \pi) \end{bmatrix}$$

Eqns. 6-14

Second edge circle

Two more radius vectors and two more small spheres are added in the same way that the first and second radius vectors and small spheres were added. A quadripole QSO results from simultaneous rotations in $(\theta:\phi)$ and $(\theta + 180^\circ : \phi + 180^\circ)$.

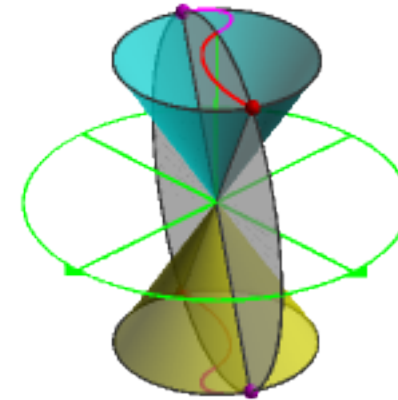


Fig. 6-14a

QSO 4(2:1)

The equations are

$$\begin{bmatrix} r \\ \theta \\ \phi \end{bmatrix} = \begin{bmatrix} t \\ ga \\ gb + \pi \end{bmatrix}$$

$$\begin{bmatrix} x \\ y \\ z \end{bmatrix} = \begin{bmatrix} \cos ag & \cos ag & 0 \\ \sin ag & \sin ag & 0 \\ 0 & 0 & 1 \end{bmatrix} \begin{bmatrix} 0 & \sin (bg + \pi) & \sin (bg + \pi) \\ 1 & 0 & 0 \\ 0 & \cos (bg + \pi) & \cos (bg + \pi) \end{bmatrix} \begin{bmatrix} 0 \\ 0 \\ t \end{bmatrix}$$

Eqns. 6-15

Third radius vector

$$\begin{bmatrix} x \\ y \\ z \end{bmatrix} = 0.04 \begin{bmatrix} \sin \pi u - \cos 2\pi v \\ \sin \pi u - \sin 2\pi v \\ \cos \pi u \end{bmatrix} - \begin{bmatrix} (\sin bg) (\cos ag) \\ (\sin bg) (\sin ag) \\ \cos bg \end{bmatrix}$$

$$((\sin (bg + \pi)) (\cos ag) - x)^2 + ((\sin (bg + \pi)) (\sin ag) - y)^2 + (\cos (bg + \pi) - z)^2 = 0.002$$

Eqns. 6-16
Third small sphere

$$\begin{bmatrix} x \\ y \\ z \end{bmatrix} = \begin{bmatrix} \cos (ga + \pi) & \cos (ga + \pi) & 0 \\ \sin (ga + \pi) & \sin (ga + \pi) & 0 \\ 0 & 0 & 1 \end{bmatrix}$$

$$\begin{bmatrix} 0 & \sin (bg + \pi) & \sin (bg + \pi) \\ 1 & 0 & 0 \\ 0 & \cos (bg + \pi) & \cos (bg + \pi) \end{bmatrix} \begin{bmatrix} 0 \\ 0 \\ t \end{bmatrix}$$

Eqns. 6-18
Fourth radius vector

$$\begin{bmatrix} r \\ \theta \\ \phi \end{bmatrix} = \begin{bmatrix} 1 \\ agt \\ bgt + \pi \end{bmatrix}, \quad \begin{bmatrix} x \\ y \\ z \end{bmatrix} = \begin{bmatrix} (\sin (bgt + \pi)) (\cos agt) \\ (\sin (bgt + \pi)) (\sin agt) \\ \cos (bgt + \pi) \end{bmatrix}$$

Eqns. 6-17
Third orbital trace

$$\begin{bmatrix} x \\ y \\ z \end{bmatrix} = 0.04 \begin{bmatrix} \sin \pi u - \cos 2\pi v \\ \sin \pi u - \sin 2\pi v \\ \cos \pi u \end{bmatrix} - \begin{bmatrix} (\sin bg) (\cos (ag + \pi)) \\ (\sin bg) (\sin (ag + \pi)) \\ \cos bg \end{bmatrix}$$

$$((\sin (bg + \pi)) (\cos (ag + \pi)) - x)^2 + ((\sin (bg + \pi)) (\sin (ag + \pi)) - y)^2 + (\cos (bg + \pi) - z)^2 = 0.002$$

Eqns. 6-19
Fourth small sphere

$$\begin{bmatrix} r \\ \theta \\ \phi \end{bmatrix} = \begin{bmatrix} t \\ ga + \pi \\ gb + \pi \end{bmatrix}$$

$$\begin{bmatrix} r \\ \theta \\ \phi \end{bmatrix} = \begin{bmatrix} 1 \\ agt + \pi \\ bgt + \pi \end{bmatrix}, \quad \begin{bmatrix} x \\ y \\ z \end{bmatrix} = \begin{bmatrix} (\sin (bgt + \pi)) (\cos (agt + \pi)) \\ (\sin (bgt + \pi)) (\sin (agt + \pi)) \\ \cos (bgt + \pi) \end{bmatrix}$$

Eqns. 6-20
Fourth orbital trace

It's a little hard to see the quadripole through the cones and the disk in figure 6-14a. Here it is without those structures.

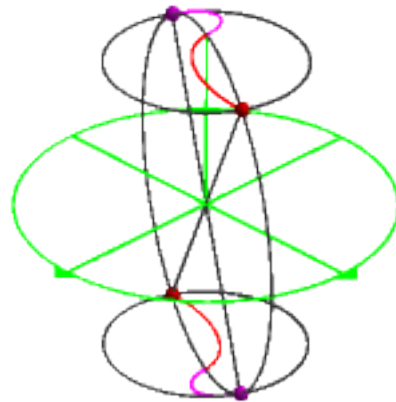


Fig. 6-14b
QSO 4(2:1)

All rotations are positive, even though they begin at different places. Note that the (apparent) dipoles scissor open and closed. It is also possible to generate a quadripole that rotates like a

pinwheel.

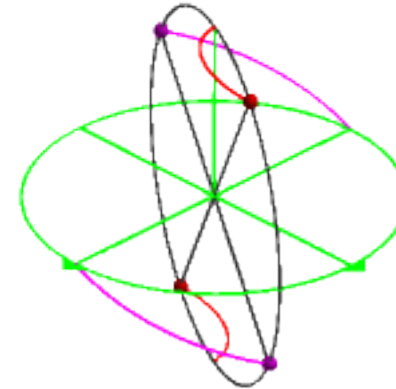


Fig. 6-15
QSO 4(2:1)

It's not immediately obvious that the four branches of the curve are in fact generated from only two rotations of the rotating circle. This can be ascertained by considering where the traces started and where they are now. The first (red) trace starts at $(0, 0, 1)$. The other three are spaced around the rotating circle at intervals of 90° . That is, the rotations for the four QSO traces are $(\theta:\phi)$, $(\theta:\phi + 90^\circ)$, $(\theta:\phi + 180^\circ)$ and $(\theta:\phi + 270^\circ)$. They are all carried on the black rotating circle which rotates positively in θ and ϕ .

It is also possible to estimate the QSO ratio from the figure. The violet traces, which start at $\pm x$, have traveled about $2/3$ of the way to the yz -plane. (Note the position of the rotating circle where it intersects the equator.) The red traces, which start at

$\pm z$, have traveled only about 1/3 of the way to the xy -plane. (Note the position of the diameter that connects them *in* the rotating circle.) Since the violet traces reveal more of the θ -rotation and the red ones show more ϕ , the curve seems to be rotating twice as fast in θ as in ϕ . We can guess that the QSO ratio is (2:1), which is in fact the case.

Just as the model easily accommodates additional cones of ϕ , so too does it allow multiple rotating circles and disks of θ . Next a second rotating circle and disk, precessed at 90° from the first, creates four more QSO traces.

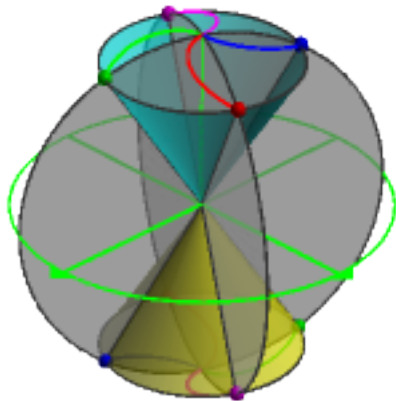


Fig. 6-16a
QSO 8(2:1)

Second rotating circle, second disk, 5th through 8th radius vectors, small spheres & orbital traces

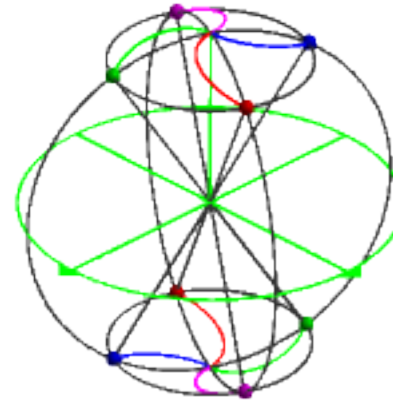


Fig. 6-16b
QSO 8(2:1) without the disks or cones

We leave the discovery of the equations for this 8-trace variation, as well as the 4-trace pinwheel, to the reader.

Globe with Latitude and Longitude

Another useful display is a globe with circles of latitude and longitude. In the next figure the unit sphere ($r = 1$) forms the basis for the display. The equator and the meridians at 0° – 360° and 90° – 180° are green, dividing the sphere into 8 octants. Circles of latitude and longitude at 30° & 60° , N, S, E & W, are blue. All others are black. The interval between each circle is 10° .

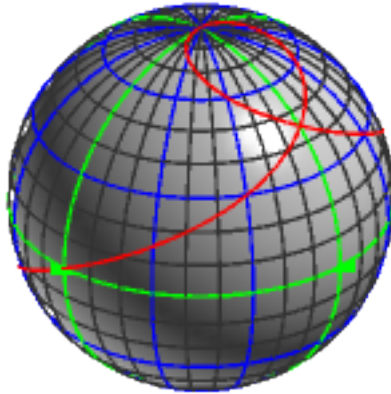


Fig. 6-17
QSO (2:1) on a globe

The globe is a modern version of the Octamap.¹⁵ This display is particularly useful for locating events, the places where the QSO trace passes through the same point at least twice in its orbit. QSO (2:1) has an event at $(1, 90^\circ, 45^\circ)$ in spherical coordinates. Presuming symmetry, there should be another one at $(1, 180^\circ, 135^\circ)$, and in fact there is.

There are only two equations of interest on the globe. They are the equations for the circles of latitude and longitude.

$$\begin{bmatrix} x \\ y \\ z \end{bmatrix} = \begin{bmatrix} (\sin 30^\circ) \cos 2\pi t \\ (\cos 60^\circ) \sin 2\pi t \\ \sin 60^\circ \end{bmatrix}, \quad \begin{bmatrix} x \\ y \\ z \end{bmatrix} = \begin{bmatrix} (\sin 150^\circ) \cos 2\pi t \\ (\cos 60^\circ) \sin 2\pi t \\ -\sin 60^\circ \end{bmatrix}$$

Eqns. 6-21

Circles of latitude north
of the equator

Circles of latitude south
of the equator

The equations are those of a circle. Each has been modified for its position on the globe. The z -term determines the latitude, here 60°N or 60°S . When the latitude goes south of the equator, negating the z -term places the circle in its correct position. The x -term contains angle ϕ . Since latitude is measured from the equator while ϕ is measured from the $+z$ -axis,¹⁶ ϕ for 60°N is the complimentary angle

$$\phi_{60^\circ\text{N}} = 90^\circ - 60^\circ = 30^\circ$$

For a latitude of 60°S , the value of ϕ is

$$\phi_{60^\circ\text{S}} = 90^\circ + 60^\circ = 150^\circ$$

¹⁵ Compare with Fig. 6-3, QSO (2:1) Octamap, and Fig. 6-4, Folded Octamaps, second from left.

¹⁶ See Figs. 2-1, 2-8, 2-9.

The circles of longitude are

$$\begin{bmatrix} x \\ y \\ z \end{bmatrix} = \begin{bmatrix} \cos 2\pi t \cdot \cos 2\pi \left(\frac{40}{360} \right) \\ \cos 2\pi t \cdot \sin 2\pi \left(\frac{40}{360} \right) \\ \sin 2\pi t \end{bmatrix}$$

Eqn. 6-22

Circles of longitude

Again the equation is a modified circle (shown here, 40°–220°). The circles of longitude are spaced every 10° around the equator. The degree of rotation is written as (longitude/360) because it shows more clearly the actual rotation than writing only the result of the division.

This same display affords a variety of other options.

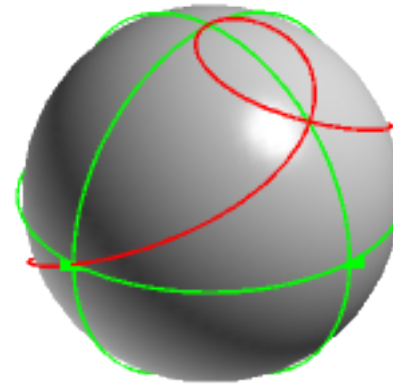


Fig. 6-18

QSO (2:1) with green meridians and the equator

In this view, the black and blue circles of latitude and longitude have been turned off for a less obstructed view of the QSO.¹⁷ The equator and the green meridians can also be turned off. The unit sphere can be reduced in size and made translucent.

¹⁷ Compare with Fig. 1-9.

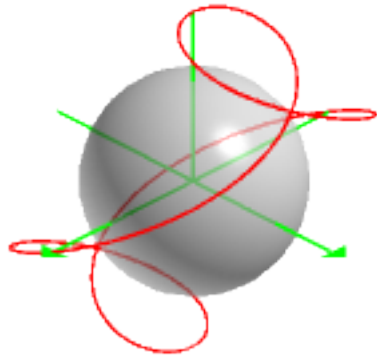


Fig. 6-19

QSO (2:1)¹⁸ with small translucent sphere ($r = 0.6$)

Three-in-One

In chapter one QSO (1:1) was shown developing sequentially from 0° to 360° . The views were from the x-, y- and z-axes, as well as from the isometric perspective. The individual illustrations were generated one at a time and cut and pasted to make up the composite display. To conclude the discussion of QSO display techniques, we will take a look at a method of showing all three axial views at once.

To generate the 3-in-1 display, the first thing to realize is that the software will not create three separate coordinate axis systems and display them from three different perspectives. One must choose a point-of-view and from that point-of-view rotate the curves so that they present the desired profile to the viewer. The point-of-view chosen here is from the positive z-axis.

¹⁸ Compare this translucent sphere with that in Fig. 1-1b.

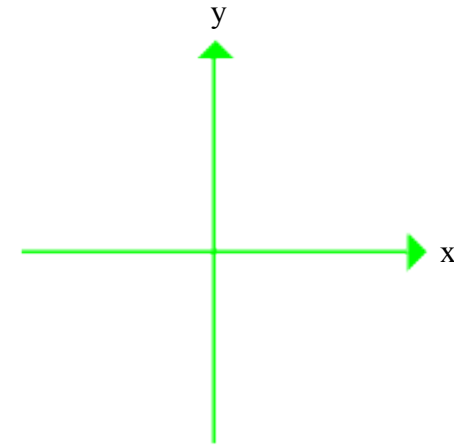


Fig. 6-20

The Cartesian coordinate system
created by Graphing Calculator 3.2
View from +z

This presents an immediate problem. The software creates x- and y-axes with arrowheads indicating the positive direction of each axis. This is fine for displaying curves from a single point-of-view. However, we want the 3-in-1 display to show the view from the x-axis on the left, the view from the y-axis in the center, and the view from +z on the right. While the QSOs themselves can be rotated to give the desired profiles, it would be confusing to have the arrowheads indicating x- and y-axes in the center when what you see from +y are the x- and z-axes, with the positive x-axis pointing to the left no less!. We therefore suppress the axes created by the software and substitute our own.

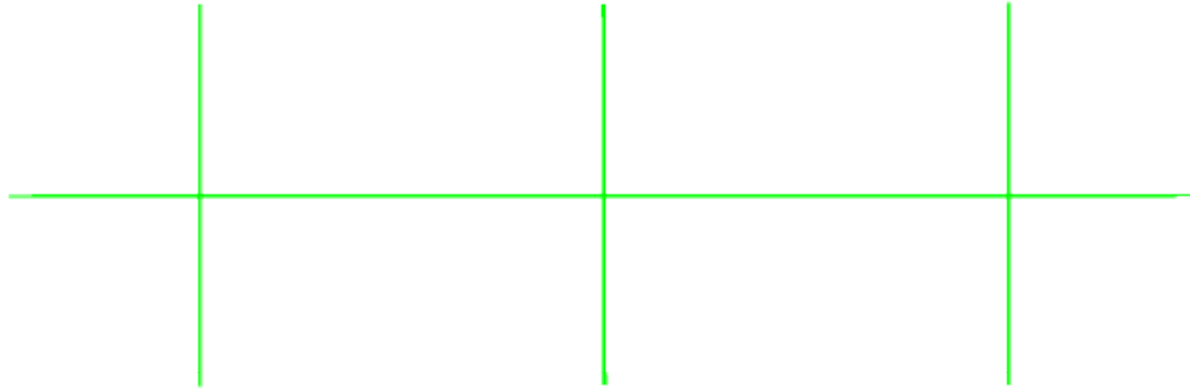


Fig. 6-21

A coordinate system for the 3-in-1 display

The long horizontal axis is drawn by a 2-vector equation

$$\begin{bmatrix} x \\ y \end{bmatrix} = \begin{bmatrix} 6.2t - 3.1 \\ 0 \end{bmatrix}$$

Eqn. 6-23

The long horizontal axis

equations.

$$\begin{bmatrix} x \\ y \end{bmatrix} = \begin{bmatrix} -2.1 \\ 2t - 1 \end{bmatrix}, \quad \begin{bmatrix} x \\ y \end{bmatrix} = \begin{bmatrix} 0 \\ 2t - 1 \end{bmatrix}, \quad \begin{bmatrix} x \\ y \end{bmatrix} = \begin{bmatrix} 2.1 \\ 2t - 1 \end{bmatrix}$$

Left

Middle

Right

Eqns. 6-24

The three vertical axes

The vector is 6.2 units long and is displaced 3.1 units to the left. The rationale for these numbers will become apparent shortly. Because this long axis will represent both the x- and y-axes depending on the view, it's less confusing to leave it unlabeled. Three vertical lines, representing the z-, z-, and y-axes respectively, are drawn by three more 2-vector

The vectors are each two units long ($y = 2t$) and are displaced one unit towards $-y$. The first and third vectors are also translated 2.1 units left and right of the center ($x = \pm 2.1$) while the second vector occupies the center position ($x = 0$).

Displays

Let's add some reference circles.

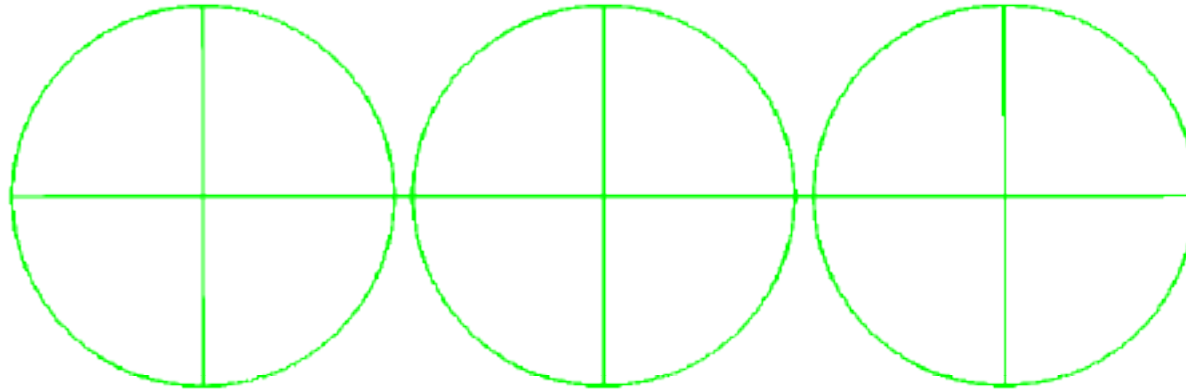


Fig. 6-22

3-in-1 coordinate axes with reference circles

The reference circles are generated by standard 2-vector equations for a circle, each modified for its position in the display.

$$\begin{bmatrix} x \\ y \end{bmatrix} = \begin{bmatrix} \sin 2\pi t \\ \cos 2\pi t \end{bmatrix} + \begin{bmatrix} -2.1 \\ 0 \end{bmatrix}, \quad \begin{bmatrix} x \\ y \end{bmatrix} = \begin{bmatrix} \sin 2\pi t \\ \cos 2\pi t \end{bmatrix}, \quad \begin{bmatrix} x \\ y \end{bmatrix} = \begin{bmatrix} \sin 2\pi t \\ \cos 2\pi t \end{bmatrix} + \begin{bmatrix} 2.1 \\ 0 \end{bmatrix}$$

Eqns. 6-25

Reference circles

left

middle

right

The reason for adding and subtracting 2.1 now becomes clear. Each circle has a diameter of two. Moving them just two units left and right of the center would mean that the circles

would be tangent on the horizontal axis. The extra 1/10 of a unit separates the views slightly and defines them more clearly.

It's time to put in the QSOs, beginning with the view from

the z-axis.

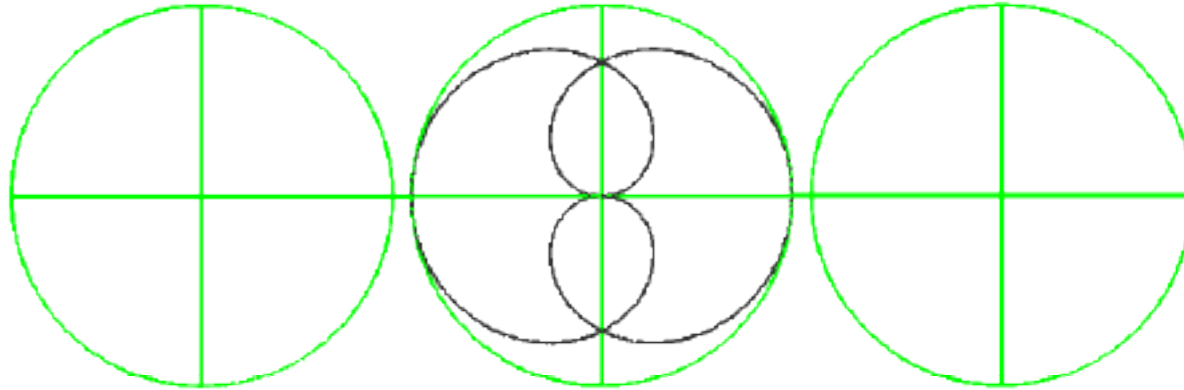


Fig. 6-23

QSO (2:1), view from the z-axis

$$\begin{bmatrix} x \\ y \\ z \end{bmatrix} = \begin{bmatrix} (\sin bgt) (\cos agt) \\ (\sin bgt) (\sin agt) \\ \cos bgt \end{bmatrix}$$

Eqn. 2-8a

The 3-vector form of the QSO equation

The unmodified Cartesian form of the QSO equation which was developed in chapter 2 generates a 3-D QSO. The point-of-view of the software in the 3-in-1 display has been chosen to be

from the z-axis. Thus the 3-vector equation gives the desired projection, but it's in the default position, the center of the display. We want the view from +z to be on the right, so we move it.

$$\begin{bmatrix} x \\ y \\ z \end{bmatrix} = \begin{bmatrix} (\sin bgt) (\cos agt) \\ (\sin bgt) (\sin agt) \\ \cos bgt \end{bmatrix} + \begin{bmatrix} 2.1 \\ 0 \\ 0 \end{bmatrix}$$

Eqn. 6-26

Moving the QSO 2.1 units to the right

Displays

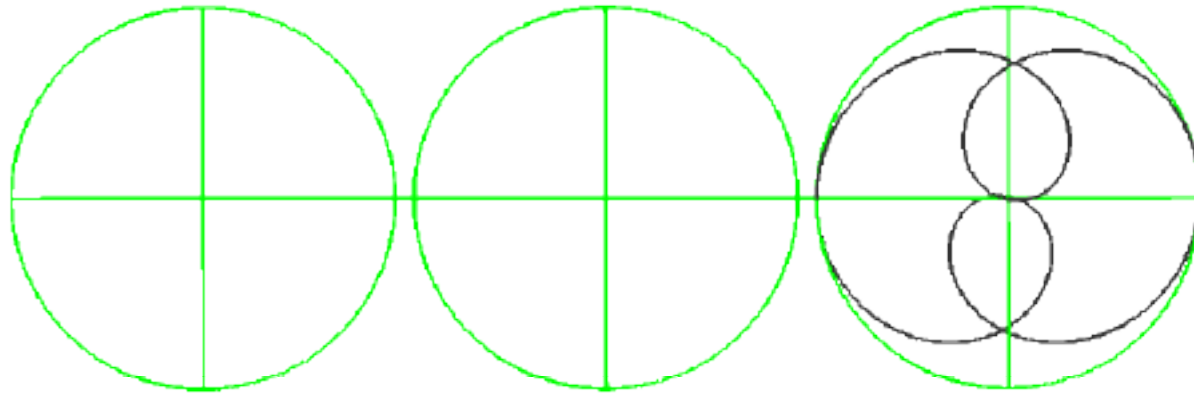


Fig. 6-24

The QSO moves to the right

Adding 2.1 units to the x-term translates the QSO to its desired position. Note that parallax is now evident in the display. The view from +y is next.

In the current environment the standard QSO equation will show the QSO from +z. We could get fancy and use a rotation matrix to display the view from +y, but it's easier to rearrange the terms of the 3-vector equation.

$$\begin{bmatrix} x \\ y \\ z \end{bmatrix} = \begin{bmatrix} (\sin bgt) (\cos agt) \\ (\cos bgt) \\ (\sin bgt) (\sin agt) \end{bmatrix}$$

Eqn. 6-27

Rearranging the terms of the QSO equation to display the view from the y-axis

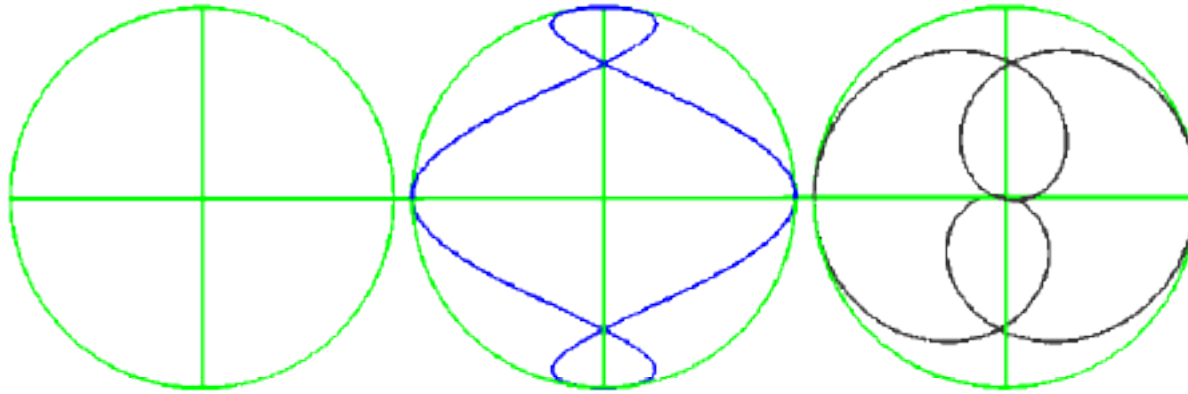


Fig. 6-25
QSO (2:1), views from the y- and z-axes

Although the terms of the equation have been rearranged, it is not necessary to move the orbital trace. It occupies the center default position. On the left, the terms of the QSO equation need to be rearranged again and the trace needs to be moved as well.

$$\begin{bmatrix} x \\ y \\ z \end{bmatrix} = \begin{bmatrix} (\sin bgt) (\sin agt) \\ \cos bgt \\ (\sin bgt) (\cos agt) \end{bmatrix} + \begin{bmatrix} -2.1 \\ 0 \\ 0 \end{bmatrix}$$

Eqn. 6-28
QSO (2:1) on the left

Equation 6-28 modifies equation 2-8a to show the view of QSO (2:1) from the x-axis. It also places the trace in the left position.

Displays

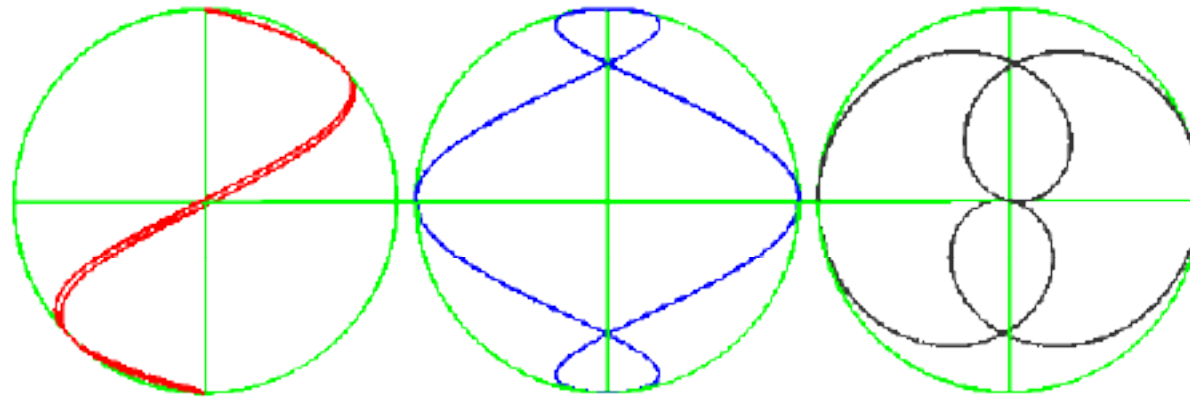


Fig. 6-26

The simultaneous axial views of QSO (2:1)

View from +x

View from +y

View from +z

The orbital trace of QSO (2:1) appears correctly in all three positions and from all three points-of-view. Seen from the x-axis the (2:1) resembles (but is not) a sine wave. From the y-axis it looks like (and may be) a Lissajous figure with a ratio of (1, 3), and from the z-axis it looks like two cardioid curves, back to back. The 2-D projections of QSOs and their relationship to known plane curves will be explored in chapter 7.

Our last task will be to add reference spheres. The easiest way to generate a sphere in the center position is with a simple formula.

$$r = 0.9$$

Eqn. 6-29

The central reference sphere

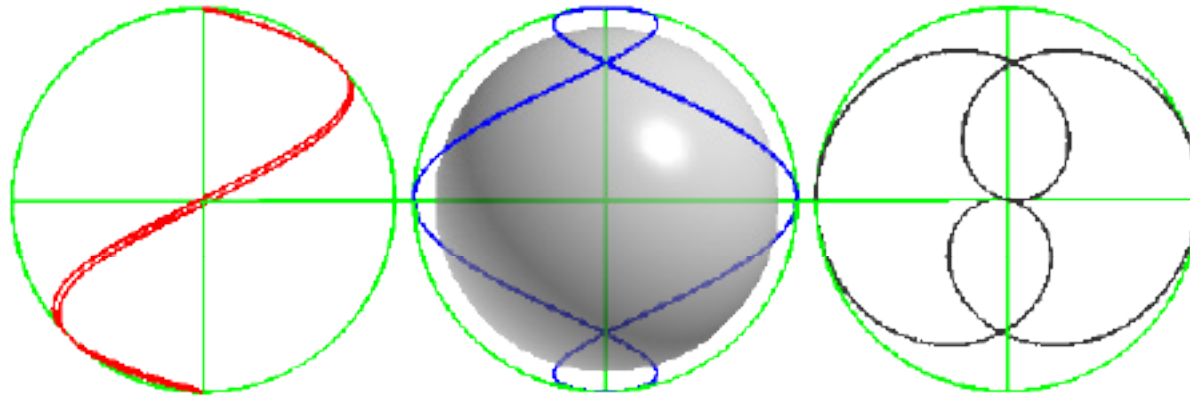


Fig. 6-27

The simultaneous axial views of QSO (2:1) with a central reference sphere

Graphing Calculator's "Use Transparency" command allows the sphere to be made slightly transparent, which allows us to see the front and back lobes of the (2:1). The next step is to generate spheres in the left and right positions. For the left we attempt to subtract 2.1 units from the center sphere.

$$r = 0.9 - 2.1 = -1.2$$

Eqn. 6-30

An attempt to generate a sphere in the left position by subtracting 2.1 from equation 6-29

Unfortunately, subtracting 2.1 from equation 6-29 doesn't work. It just changes the diameter of the sphere. We try a couple of parametric spheres.

Displays

$$\begin{bmatrix} x \\ y \\ z \end{bmatrix} = 0.9 \begin{bmatrix} \sin \pi u \cdot \cos 2\pi v \\ \sin \pi u \cdot \sin 2\pi v \\ \cos \pi u \end{bmatrix} + \begin{bmatrix} -2.1 \\ 0 \\ 0 \end{bmatrix}, \quad \begin{bmatrix} x \\ y \\ z \end{bmatrix} = 0.9 \begin{bmatrix} \sin \pi u \cdot \cos 2\pi v \\ \sin \pi u \cdot \sin 2\pi v \\ \cos \pi u \end{bmatrix} + \begin{bmatrix} 2.1 \\ 0 \\ 0 \end{bmatrix}$$

Eqns. 6-30

Parametric spheres in the left and right positions

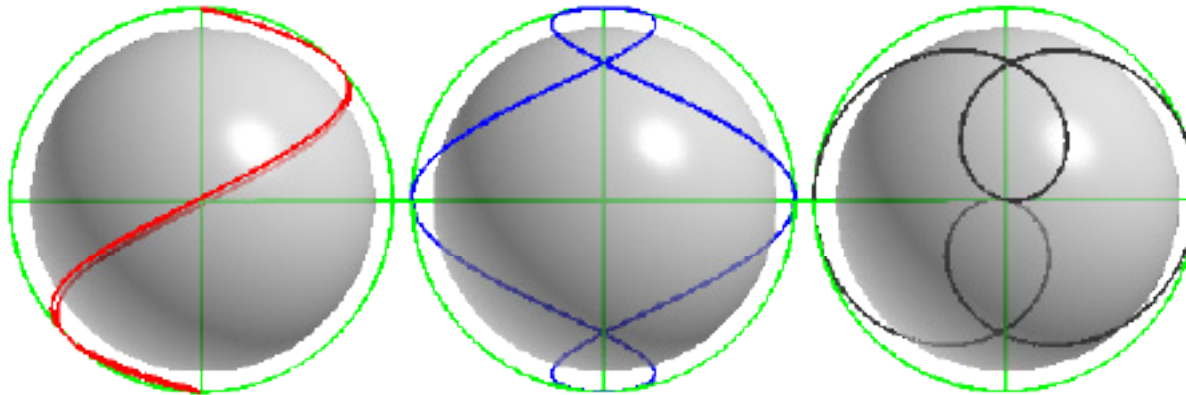


Fig. 6-28

The three simultaneous axial views of QSO (2:1) with reference circles and spheres

View from +x

View from +y

View from +z

The parametric spheres work. Each has a radius of 0.9 and they're properly positioned at ± 2.1 units left and right of center. On the left, looking from the x-axis, the QSO seems to have no depth. It seems to exist just outside of the sphere, between the sphere and the eye of the reader. The three dimensionality of the curve can be appreciated by focusing on the red trace where it

transitions diagonally from lower left to upper right. Because the software draws a true 3-D picture, and because the x-view is shifted to the left of center, parallax allows one branch of the curve to be seen in front of the sphere while the other is behind it. The effect of parallax can also be seen in the view from the z-axis, although there is no doubt there that part of the curve is

in front and part behind the sphere. In the views from the y- and z-axes, the intersections are clearly seen to be 180° apart in θ , although the separation in ϕ is not so certain.

Other display techniques translate and rotate QSOs in 3-space. They can slide back and forth on any axis or spin like propellers. They can grow or shrink as the diameter of the central sphere (which is now no longer a *unit* sphere) is changed. These transformations use standard manipulations which readers may discover for themselves.

Plane Curves

Quasi-Spherical Orbits were introduced in this book with the assertion that many QSOs are identical with, and therefore subsume, some well-known space curves that traditionally have been seen as unrelated. Furthermore, it was said that the projections of specific QSOs on the orthogonal planes are indistinguishable from certain plane curves. It's time to examine those assertions. We begin with curves in the flat, two-dimensional plane of the Greeks.

Circle

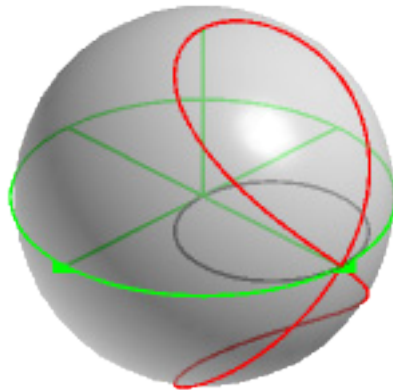


Fig. 7-1
QSO (1:1) @ 100%, isometric view

The projection of the QSO on the xy-plane certainly *looks* like a circle, and we have previously treated it as such.¹ We will show here that the projection is visually congruent with a standard circle. The formal proof will be left to the reader.

One way to generate the QSO is with equation 2-8a.

$$\begin{bmatrix} x \\ y \\ z \end{bmatrix} = \begin{bmatrix} (\sin bgt) (\cos agt) \\ (\sin bgt) (\sin agt) \\ \cos bgt \end{bmatrix}$$

Eqn. 2-8a

The QSO equation in Cartesian notation
 $a = 1, b = 1, g = 2\pi n, n = 1, t: 0 \dots 1.$

Since we're interested only in the xy-plane, the z-term can be deleted, leaving

¹ See pp. 7-9, 74, 87-8, as well as the front cover.

$$\begin{bmatrix} x \\ y \end{bmatrix} = \begin{bmatrix} (\sin bgt) (\cos agt) \\ (\sin bgt) (\sin agt) \end{bmatrix}$$

Eqn. 7-1

The QSO equation on the xy-plane

Then, because we want just the complete curve displayed statically, the unit terms a , b & n can be deleted.

$$\begin{bmatrix} x \\ y \end{bmatrix} = \begin{bmatrix} (\sin 2\pi t) (\cos 2\pi t) \\ (\sin 2\pi t) (\sin 2\pi t) \end{bmatrix}$$

Eqn. 7-2

The static projection for QSO (1:1)
@ 100% of a cycle on the xy-plane

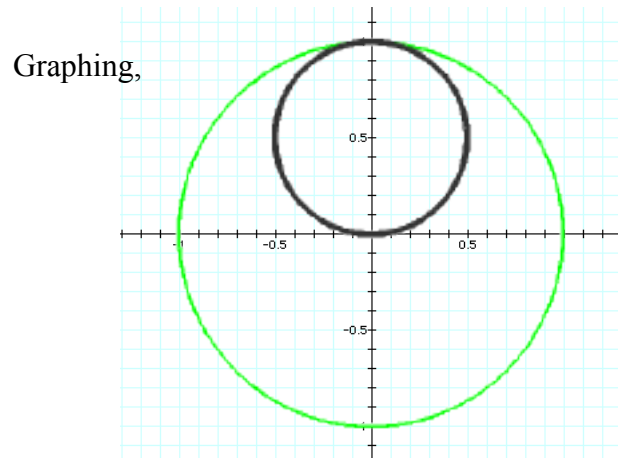


Fig. 7-2

The projection of QSO (1:1) on the xy-plane

The projection of the QSO in black is shown with the green equator from figure 7-1. The equator is a unit circle with the equation

$$x^2 + y^2 = 1$$

In order to fit the projection of the QSO to the unit circle, we multiply by two to increase the radius to $r = 1$.

$$\begin{bmatrix} x \\ y \end{bmatrix} = 2 \begin{bmatrix} (\sin 2\pi t) (\cos 2\pi t) \\ (\sin 2\pi t) (\sin 2\pi t) \end{bmatrix}$$

Graphing,

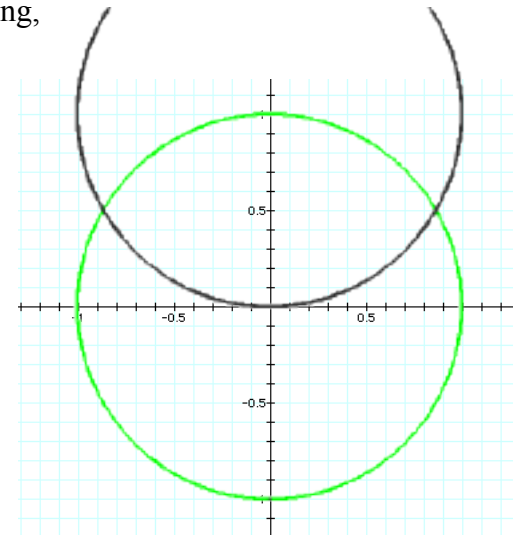


Fig. 7-3

The enlarged projection of QSO (1:1)
on the xy-plane (black) with the equator (green)

The projection has escaped slightly from the picture, but that will be taken care of with the next operation. To overlay the projection of the QSO onto the unit circle, we move the center to the Origin.

$$\begin{bmatrix} x \\ y \end{bmatrix} = 2 \begin{bmatrix} (\sin 2\pi t) (\cos 2\pi t) \\ (\sin 2\pi t) (\sin 2\pi t) \end{bmatrix} + \begin{bmatrix} 0 \\ -1 \end{bmatrix}$$

Graphing,

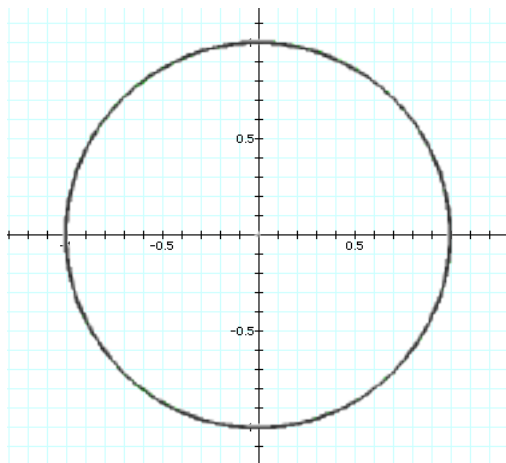


Fig. 7-4

The black projection of QSO (1:1) overlays the unit circle. The formal demonstration of equivalence is left to the reader.

Parabola

The problem is to show the equivalence of the parabola and the projection of QSO (1:1) on the yz -plane. Following the same procedure as the circle, we will show that they are visually congruent. The equation for the parabola is

$$y = x^2$$

Graphing,

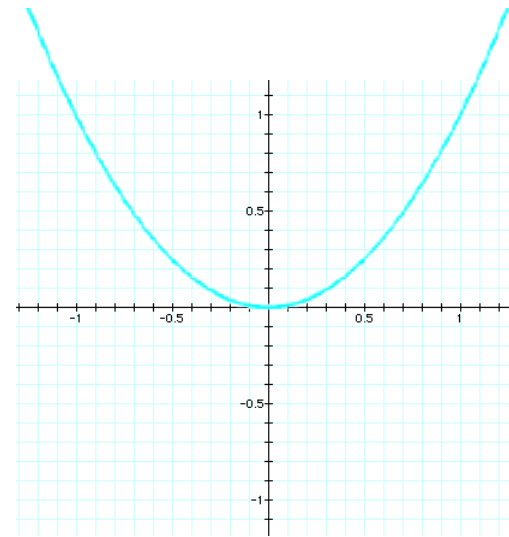


Fig. 7-5

The parabola

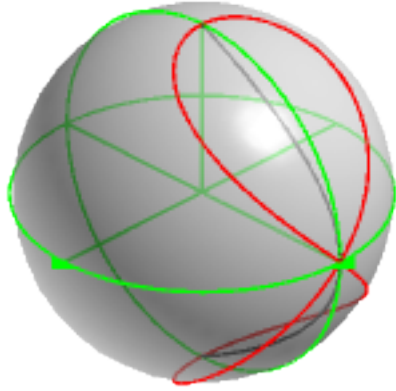


Fig. 7-6

QSO (1:1) @ 100% and its projection on the yz-plane

From the x-axis, the projection of QSO (1:1) on the yz-plane looks like an open letter C written backwards. The red QSO and the green meridian in the yz-plane are on the unit sphere, but the projection is not. We proceed as before by starting with equation 2-8a.

$$\begin{bmatrix} x \\ y \\ z \end{bmatrix} = \begin{bmatrix} (\sin bgt) (\cos agt) \\ (\sin bgt) (\sin agt) \\ \cos bgt \end{bmatrix}$$

Eqn. 2-8a

The QSO equation in Cartesian notation
 $a = 1, b = 1, g = 2\pi n, n = 1, t: 0 \dots 1.$

Since we're interested in the yz-plane, the x-term may be deleted.

$$\begin{bmatrix} y \\ z \end{bmatrix} = \begin{bmatrix} (\sin bgt) (\sin agt) \\ \cos bgt \end{bmatrix}$$

Eqn. 7-3

This gives the projection of the QSO in the yz-plane. We want to compare it with the parabola, which is in the xy-plane, so we need to put the projection also in the xy-plane. This is accomplished by reassigning the first and second terms to the x- and y-axes instead of the y- and z-axes.

$$\begin{bmatrix} x \\ y \end{bmatrix} = \begin{bmatrix} (\sin bgt) (\sin agt) \\ \cos bgt \end{bmatrix}$$

Eqn. 7-4

The unit terms, a , b , and n can be deleted, leaving

$$\begin{bmatrix} x \\ y \end{bmatrix} = \begin{bmatrix} (\sin 2\pi t) (\sin 2\pi t) \\ \cos 2\pi t \end{bmatrix}$$

Eqn. 7-5

Graphing,

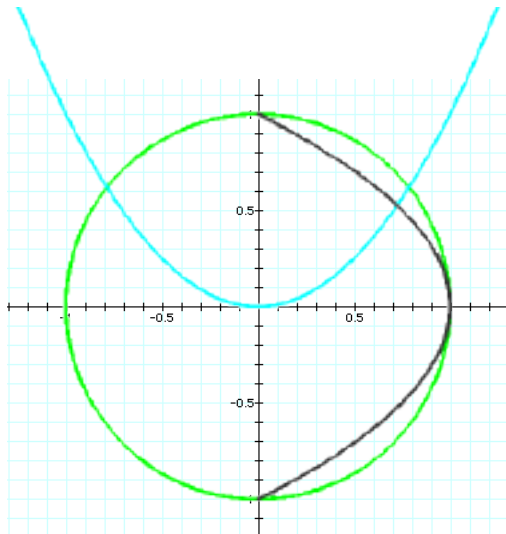


Fig. 7-7

The parabola, the projection of QSO (1:1) and the unit circle

The black projection of QSO (1:1) is drawn on the xy-plane. It is shown with the green unit circle and a blue parabola. Rotating the projection of the QSO so that its axis extends along y-axis,

$$\begin{bmatrix} x \\ y \end{bmatrix} = \begin{bmatrix} \cos 2\pi t \\ -(\sin 2\pi t) (\sin 2\pi t) \end{bmatrix}$$

Eqn. 7-6

In addition to exchanging terms, there is a need to negate the y-term so the projection opens in the positive y-direction.

Graphing,

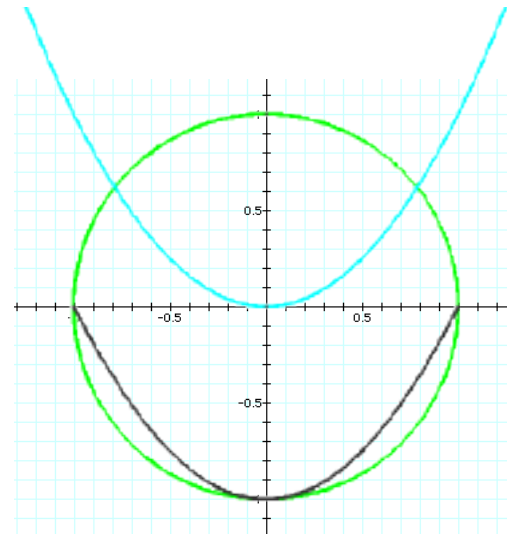


Fig. 7-8

The projection of QSO (1:1) compared to the parabola

The last operation moves the apex of the projection to the Origin.

$$\begin{bmatrix} x \\ y \end{bmatrix} = \begin{bmatrix} \cos 2\pi t \\ -(\sin 2\pi t) (\sin 2\pi t) \end{bmatrix} + \begin{bmatrix} 0 \\ 1 \end{bmatrix}$$

Eqn. 7-7

Graphing,

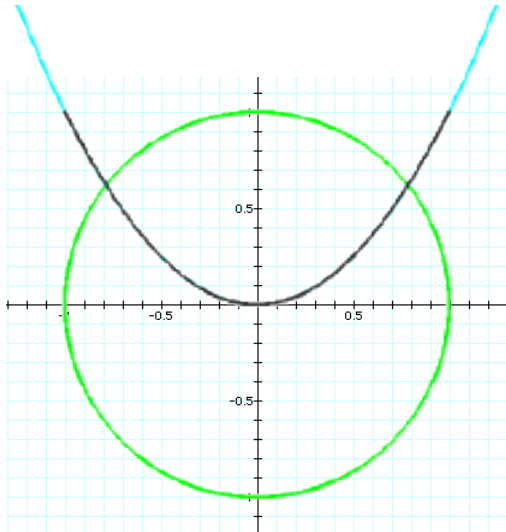


Fig. 7-9

The projection of QSO (1:1) and the parabola

The projection of QSO (1:1), originally on the yz -plane, is now visually congruent with the parabola. The formal proof of congruence is left to the reader.

The Lemniscate of Gerono

The lemniscate² of Gerono, also called the figure eight curve, was studied by the French mathematician Camille Cristophe Gerono (1799-1891).³ The implicit equation for the lemniscate is

$$x^4 = a^2(x^2 - y^2)$$

Eqn. 7-8

where a is a scaling factor

Graphing,

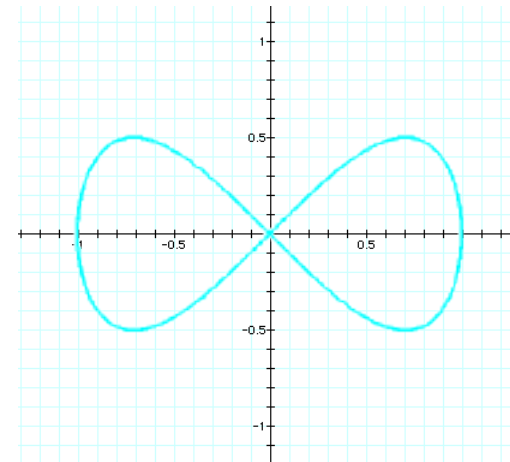


Fig. 7-10

The lemniscate of Gerono

² Latin *lemniscus*, ribbon, from Greek *lemniskos*.

³ Gray (1998) p. 32.

The problem is to show the equivalence of the L. of Gerono and the projection of QSO (1:1) on the xz -plane.

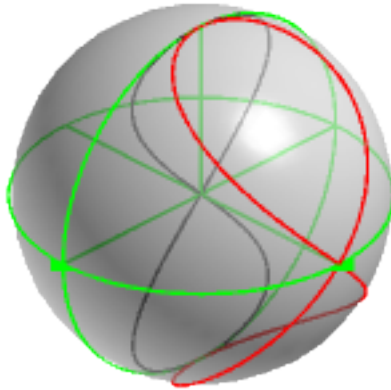


Fig. 7-11
Isometric view of QSO (1:1) at 100%
and its projection on the xz -plane

The projection of QSO (1:1) on the xz -plane is more complex than its projections on the other two planes. It has north and south lobes with a waist apparently at the Origin. At the Origin one would guess that the projected curve intersects itself at a 90° angle as does the QSO.⁴ We proceed as before to write the equation of the projection.

$$\begin{bmatrix} x \\ y \\ z \end{bmatrix} = \begin{bmatrix} (\sin bgt) (\cos agt) \\ (\sin bgt) (\sin agt) \\ \cos bgt \end{bmatrix}$$

Eqn. 2-8a

The QSO equation in Cartesian notation
 $a = 1, b = 1, g = 2\pi n, n = 1, t: 0 \dots 1$

Since this time we're interested in the xz -plane, the y -term may be deleted.

$$\begin{bmatrix} x \\ z \end{bmatrix} = \begin{bmatrix} (\sin bgt) (\cos agt) \\ \cos bgt \end{bmatrix}$$

Eqn. 7-9

Then, deleting the unit terms a, b and n leaves

$$\begin{bmatrix} x \\ z \end{bmatrix} = \begin{bmatrix} (\sin 2\pi t) (\cos 2\pi t) \\ \cos 2\pi t \end{bmatrix}$$

Eqn. 7-10

⁴ See chapter 4, pp. 50–51.

Graphing,

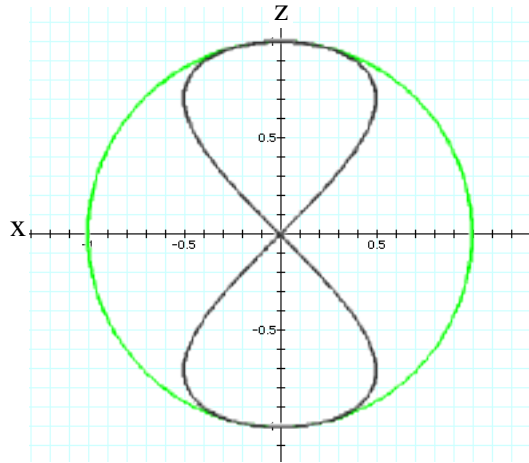


Fig. 7-12

The projection of QSO (1:1) @ 100% on the xz-plane.

Since the projection is symmetrical with respect to the z-axis, we can reverse the x-axis with no distortion. Note the location of the small x labeling the x-axis in each figure.

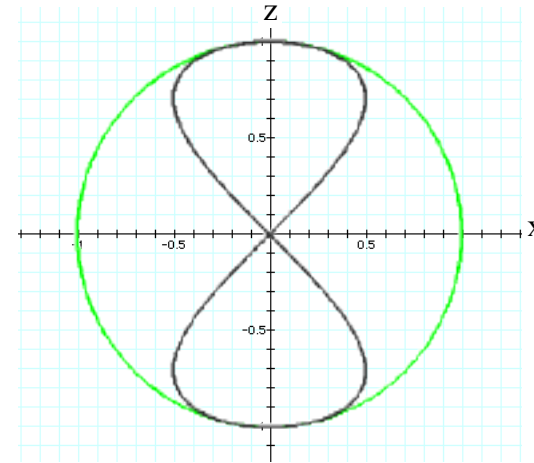


Fig. 7-13

The projection of QSO (1:1) @ 100% on the xz-plane

Next we reassign the terms of the curve to draw it on the xy-plane.

$$\begin{bmatrix} x \\ y \end{bmatrix} = \begin{bmatrix} (\sin 2\pi t) (\cos 2\pi t) \\ \cos 2\pi t \end{bmatrix}$$

Eqn. 7-11

Graphing,

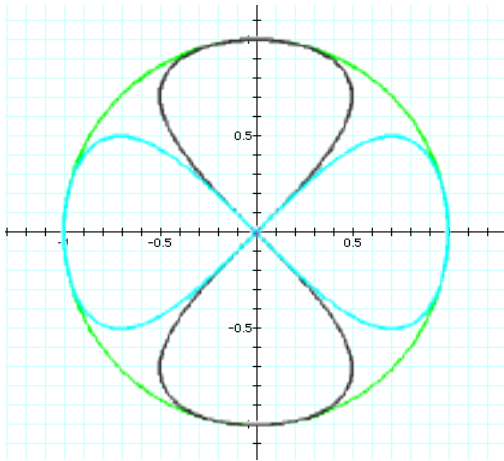


Fig. 7-14

The projection of QSO (1:1) on the xz-plane, translated to the xy-plane and compared to the L. of Gerono

Rotating the projection of the QSO 90°,

$$\begin{bmatrix} x \\ y \end{bmatrix} = \begin{bmatrix} \cos 2\pi t \\ (\sin 2\pi t) (\cos 2\pi t) \end{bmatrix}$$

Eqn. 7-12

Graphing,

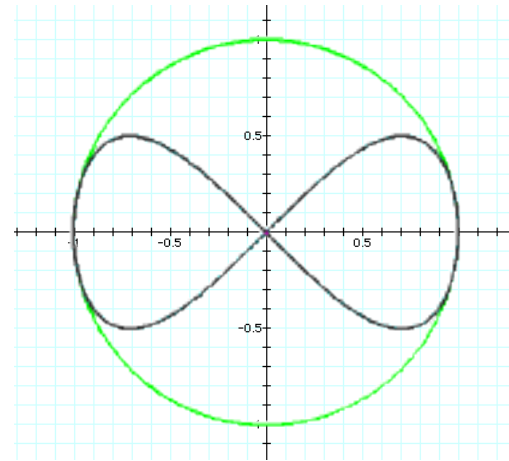


Fig. 7-15

The projection of QSO (1:1) and the L. of Gerono

The projection of the QSO in black overlies the blue lemniscate of Gerono. It is now clear that QSO (1:1) subsumes the circle on the xy-plane, the parabola on the yz-plane, and the lemniscate of Gerono on the xz-plane.

Here are the three projections, together with the QSO.

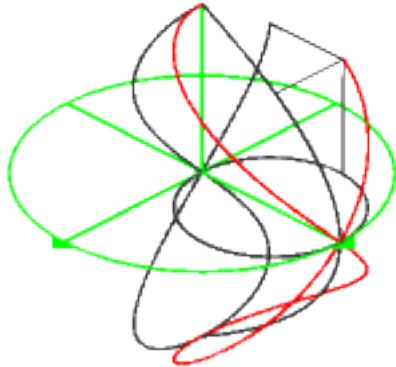


Fig. 7-16
QSO (1:1) @ 87% of a cycle

The QSO simultaneously traces the circle, the parabola and the lemniscate of Gerono. At this point in the cycle the circle and the parabola appear to be complete. We know this is not true because the QSO is yet incomplete.⁵

Cardioid

Although the cardioid⁶ was studied by Roemer in 1674 as a form of gear teeth, the name *cardioid* was first used by de Castillon in 1741.⁷

⁵ See pp. 8–10 for a discussion of this phenomenon.

⁶ Literally, “heart-shaped” [cardi(o)- + -oid].

⁷ Notes from Graphing Calculator 3.2 and
<<http://mathworld.wolfram.com/Cardioid.html>>.

The parametric equation for the cardioid is

$$\begin{bmatrix} x \\ y \end{bmatrix} = d(k + 2c \cos 2\pi t) \begin{bmatrix} \cos 2\pi t \\ \sin 2\pi t \end{bmatrix}$$

Eqn. 7-13

$$c = 0.5, d = 0.5, k = 1.0, t: 0 \dots 1$$

Graphing,

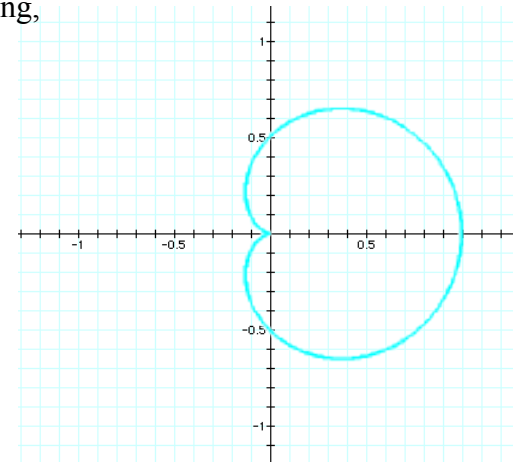


Fig. 7-17
The cardioid

In figure 7-17 the cardioid has a single large lobe which is symmetrical with respect to the x-axis, and which extends along the positive side of that axis. There is a cusp at (0, 0). We compare the cardioid with the projection of QSO (2:1) on the xy-plane.

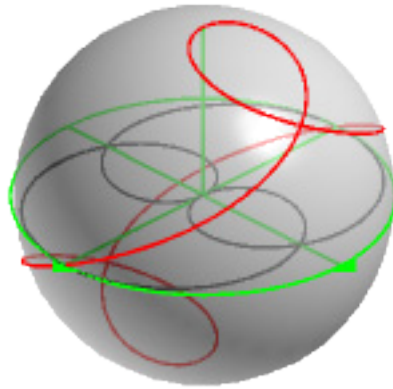


Fig. 7-18
QSO (2:1) at 100% and its projection
on the xy-plane, isometric view

At first glance, the projection of the QSO doesn't look much like a cardioid. To be sure, there are two outer lobes that each resemble the lobe of a cardioid, but the two inner loops seemingly eliminate the possibility of a cusp. Running the QSO backward to 50% of a cycle makes the resemblance more obvious.

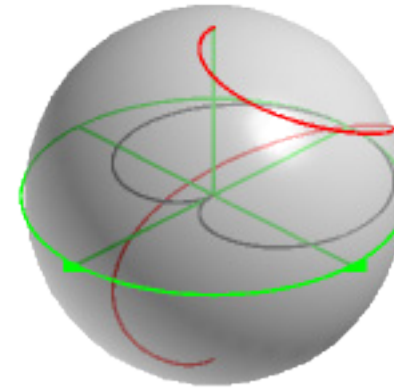


Fig. 7-19
QSO (2:1) at 50% of a cycle and its
projection on the xy-plane, isometric view

There is now a large cardioid-like lobe extending along the negative x-axis, and what appears to be a cusp, again at (0, 0). The equation for the projection is

$$\begin{bmatrix} x \\ y \end{bmatrix} = \begin{bmatrix} (\sin bgt) (\cos agt) \\ (\sin bgt) (\sin agt) \end{bmatrix}$$

Eqn. 7-14

$$a = 2, b = 1, g = 2\pi n, n = 0.5, t: 0 \dots 1$$

Graphing,

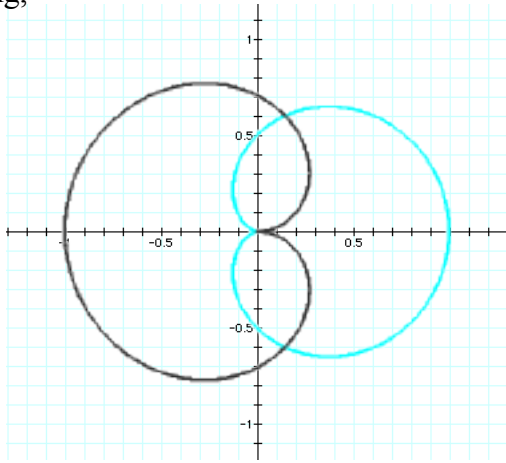


Fig. 7-20

The cardioid and the projection of QSO (2:1)
@ 50% of a cycle on the xy-plane

To more directly compare the projection with the historical cardioid, we reverse the projection left to right by negating the x-term.

$$\begin{bmatrix} x \\ y \end{bmatrix} = \begin{bmatrix} -(\sin bgt) (\cos agt) \\ (\sin bgt) (\sin agt) \end{bmatrix}$$

Eqn. 7-15

Comparing with the cardioid,

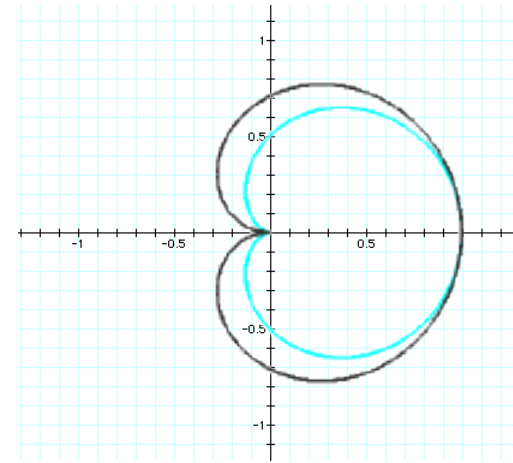


Fig. 7-21

The cardioid and the projection of
QSO (2:1) @ 50% of a cycle

Comparing the historical cardioid (blue) with the projection of the QSO (black), we see that the historical cardioid is everywhere inside or tangent to the projection. The curves are not equivalent. Still, they do have generally similar shapes. Both have a cusp at (0, 0), and both intercept the x-axis at (1, 0). If the classical curve is called a “cardioid,” or the “cardioid of Castillon,” then perhaps the QSO form should be called the “QSO cardioid,” or the “Burchester⁸ cardioid.”

⁸ An amalgam of the names “Burke” and “Chester,” a device we use to refer to collaborative work.

Limaçon

The *limaçon*⁹ (pronounced with a soft *c*) is also called “Pascal’s snail.” It was discovered by Étienne Pascal (1588-1651), the father of Blaise Pascal. It was named by Roberval in 1650 when he used it as an example of his method of drawing tangents.¹⁰

The general form of the parametric equation for the limaçon is the same as for the cardioid. Only the constants change.

$$\begin{bmatrix} x \\ y \end{bmatrix} = d(k + 2c \cos 2\pi t) \begin{bmatrix} \cos 2\pi t \\ \sin 2\pi t \end{bmatrix}$$

Eqn. 7-16

$$c = 1, d = 0.5, k = 1, t: 0 \dots 1$$

Graphing,

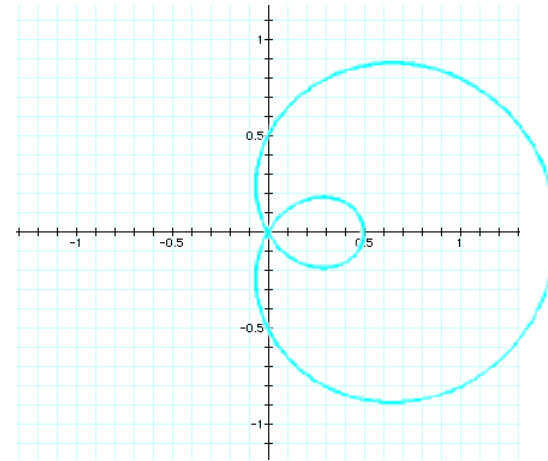


Fig. 7-22
The limaçon

The cardioid is a special case of the limaçon. Where the cardioid has a cusp, the limaçon has an inner loop.¹¹ Of particular interest here is the fact that although the cardioid is not equivalent to the projection of QSO (2:1) on the *xy*-plane, the limaçon, which is the general case, will be shown to be visually identical to the projection of QSO (3:1) on the *xy*-plane.

⁹ Latin *limax*, snail

¹⁰ <http://www-groups.dcs.st-andrews.ac.uk/%7Ehistory/Curves/Limacon.html>

¹¹ <http://en.wikipedia.org/wiki/Lima%C3%A7on>

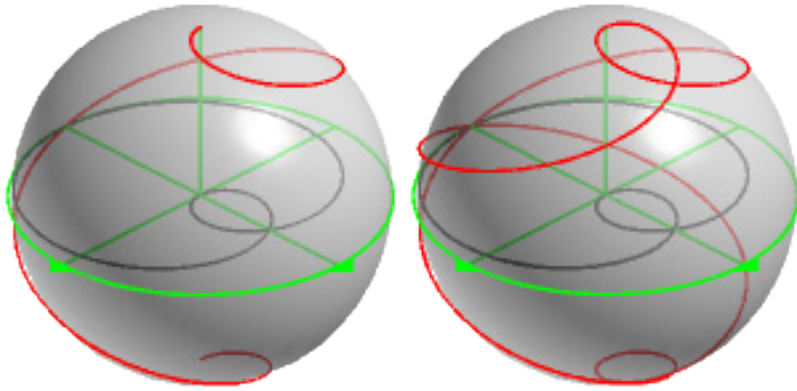


Fig. 7-23
QSO (3:1)

@ 50% of a cycle

@ 100% of a cycle

Between 50% and 100% of a cycle the QSO traces the same projection on the xy-plane. Since it makes no difference which fraction we use, we will choose the full cycle to keep the numbers simple. The QSO is generated by equation 2-8a.

$$\begin{bmatrix} x \\ y \\ z \end{bmatrix} = \begin{bmatrix} (\sin bgt) (\cos agt) \\ (\sin bgt) (\sin agt) \\ \cos bgt \end{bmatrix}$$

Eqn. 2-8a

a = 3, b = 1, g = 2πn, n = 1, t: 0 ... 1

We are interested in the xy-plane, so the z-term may be deleted.

$$\begin{bmatrix} x \\ y \end{bmatrix} = \begin{bmatrix} (\sin bgt) (\cos agt) \\ (\sin bgt) (\sin agt) \end{bmatrix}$$

Eqn. 7-17

Graphing,

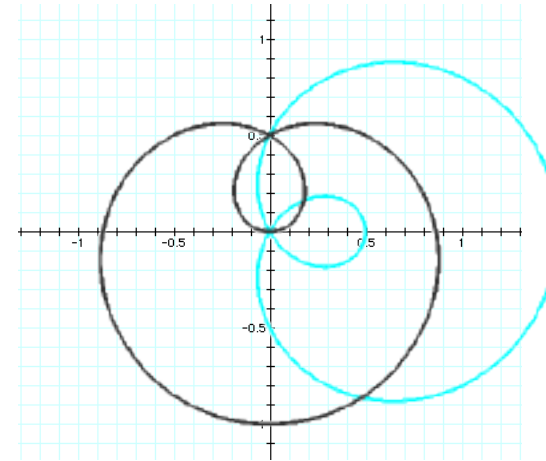


Fig. 7-24

The projection of QSO (3:1) on the xy-plane compared to the limaçon

Rotating the projection so that the inner loop and large outer lobe are oriented along the x-axis,

$$\begin{bmatrix} x \\ y \end{bmatrix} = \begin{bmatrix} (\sin bgt) (\sin agt) \\ (\sin bgt) (\cos agt) \end{bmatrix}$$

Eqn. 7-18

Graphing,

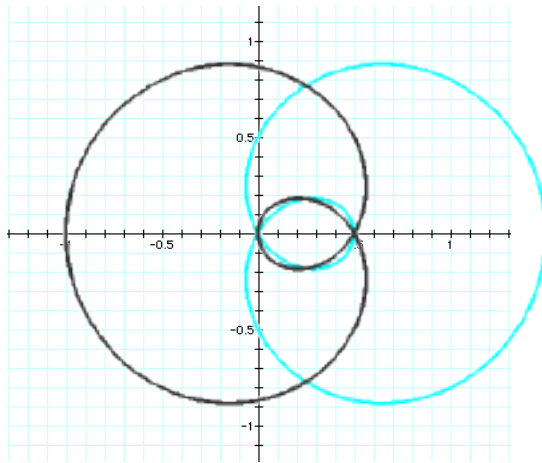


Fig. 7-25

The projection of QSO (3:1) on the xy-plane rotated and compared to the limaçon

Flipping the projection horizontally,

$$\begin{bmatrix} x \\ y \end{bmatrix} = \begin{bmatrix} -(\sin bgt) (\sin agt) \\ (\sin bgt) (\cos agt) \end{bmatrix}$$

Eqn. 7-19

Graphing,

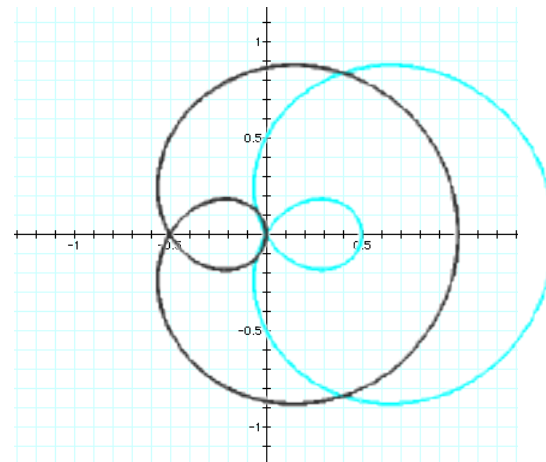


Fig. 7-26

The projection of QSO (3:1) on the xy-plane rotated, reversed left to right and compared to the limaçon

And finally, moving the projection 0.5 to the right,

$$\begin{bmatrix} x \\ y \end{bmatrix} = \begin{bmatrix} -(\sin bgt)(\sin agt) \\ (\sin bgt)(\cos agt) \end{bmatrix} + \begin{bmatrix} 0.5 \\ 0 \end{bmatrix}$$

Eqn. 7-20

Graphing,

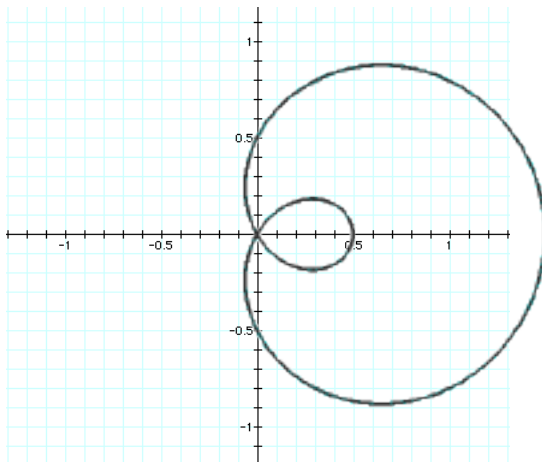


Fig. 7-27

The projection of QSO (3:1) on the xy-plane rotated, reversed left to right, translated and compared to the limaçon

The projection of the QSO is visually congruent with the limaçon.

Epitrochoids

So far the curves have been familiar and easily understood. To explore now the relationship between epitrochoids and QSOs, a little background may be helpful. If a circle rolls along a line without slipping, then a point on the circumference of the circle traces a *cycloid*.

The equation for the cycloid is

$$\begin{bmatrix} x \\ y \end{bmatrix} = \begin{bmatrix} r(\theta - \sin\theta) \\ r(1 - \cos\theta) \end{bmatrix}$$

Eqn. 7-21

where r is the radius of the rolling circle and θ is the angle of rotation of the radius.¹²

Graphing,

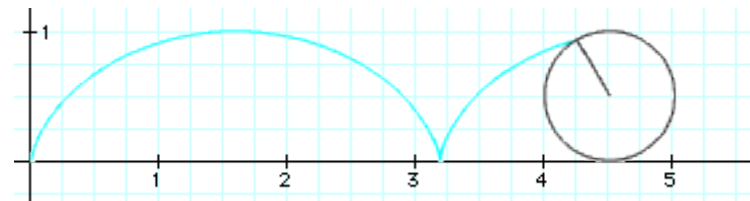


Fig. 7-28

An ordinary cycloid

¹² Readers using Graphing Calculator to explore these curves need to change θ to nt and r to s or some other constant for the curve to display correctly.

You can think of the cycloid as the trace of the valve stem as a tire rolls along the road. If the circle rolls around the outside of a larger fixed circle, the resulting curve is an *epicycloid*.¹³

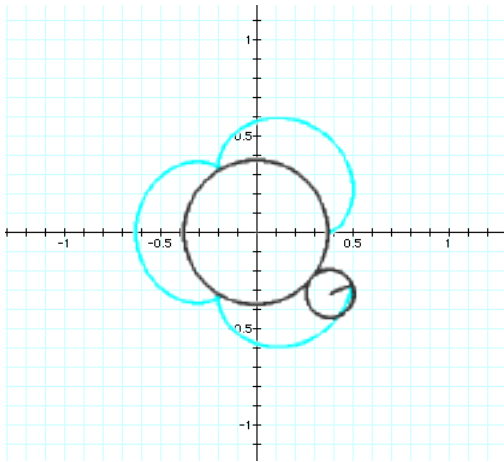


Fig. 7-29
A three-lobed epicycloid

In figure 7-29 the radius of the large fixed circle is three times that of the smaller rolling circle resulting in an epicycloid of three lobes and three cusps.¹⁴ If the radius of the smaller circle is extended without making the circle itself any larger, the resultant curve is an *epitrochoid*.

The equation for the epitrochoid is

$$\begin{bmatrix} x \\ y \end{bmatrix} = \frac{1}{2(R+s)} \begin{bmatrix} (R+s) \cos gt - (R+s) \cos \left(\frac{R+s}{s} gt \right) \\ (R+s) \sin gt - (R+s) \sin \left(\frac{R+s}{s} gt \right) \end{bmatrix}$$

Eqn. 7-22

R is the radius of the inner, fixed circle,
 s is the radius of the outer, rolling circle¹⁵, and

$$g = 2\pi n, n: 0 \rightarrow 1, t: 0 \dots 1.$$

The initial fraction

$$\frac{1}{2(R+s)}$$

is not needed to generate the curve. Its purpose is to normalize the curve so that it falls within the unit circle.

¹³ *epi-* Greek: on, over. Similar to “epicenter,” “epidermis,” etc.

¹⁴ When the circles are of equal size, the cardioid results.

¹⁵ One might suppose that the radius of the smaller circle could be represented by a lower case r , but Graphing Calculator refuses to graph such an equation. Thus, another letter must be used.

If $R = 3$ and $s = 1$, the following curve results.

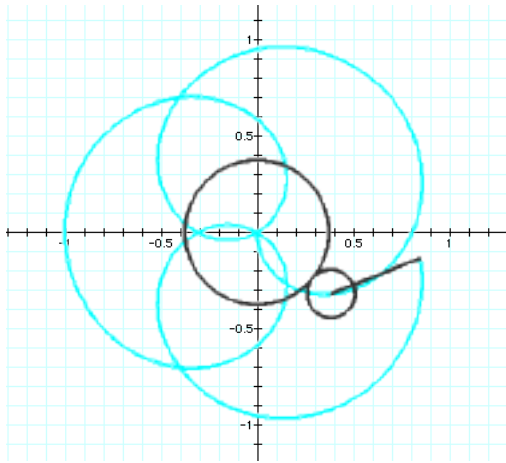


Fig. 7-30
A three-lobed epitrochoid¹⁶

In figure 7-30 the radius of the larger fixed circle is three units, the radius of the smaller rolling circle is one unit, and the extended radius is four units long. An infinite variety of epitrochoids can be generated by manipulating the variables R and s . We will compare this particular curve with the projection of QSO (5:3) on the xy -plane.

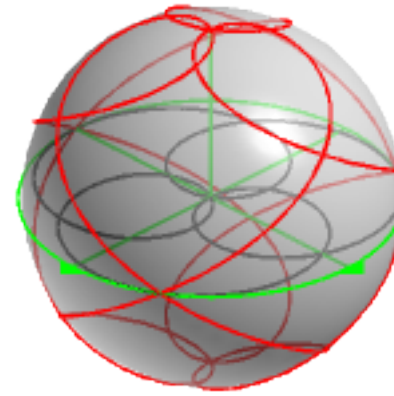


Fig. 7-31
QSO (5:3) @ 100% and its projection on the xy -plane

The projection of the QSO on the xy -plane is a three-lobed figure with three inner loops.

¹⁶ Greek *trokhoeides*, resembling a wheel, wheel like, circular: *trokhos*, wheel.

Next we graph the projection of the QSO together with the epitrochoid from figure 7-30.

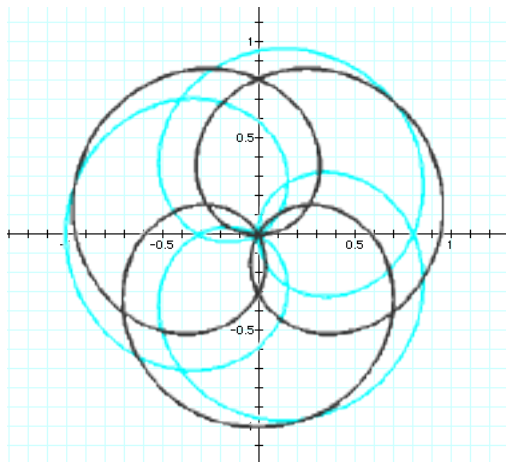


Fig. 7-32

A three-lobed epitrochoid and the projection of QSO (5:3) on the xy-plane

In figure 7-32 the epitrochoid is symmetric with respect to the x-axis while the projection of the QSO is symmetric w.r.t. the y-axis. This is easily remedied. The equation for the projection of the QSO is

$$\begin{bmatrix} x \\ y \end{bmatrix} = \begin{bmatrix} (\sin bgt) (\cos agt) \\ (\sin bgt) (\sin agt) \end{bmatrix}$$

Eqn. 7-23

a = 5, b = 3, g = 2πn, n = 1, t: 0 ... 1

Exchanging axes rotates the projection by 90°.

$$\begin{bmatrix} x \\ y \end{bmatrix} = \begin{bmatrix} (\sin bgt) (\sin agt) \\ (\sin bgt) (\cos agt) \end{bmatrix}$$

Eqn. 7-24

Graphing,

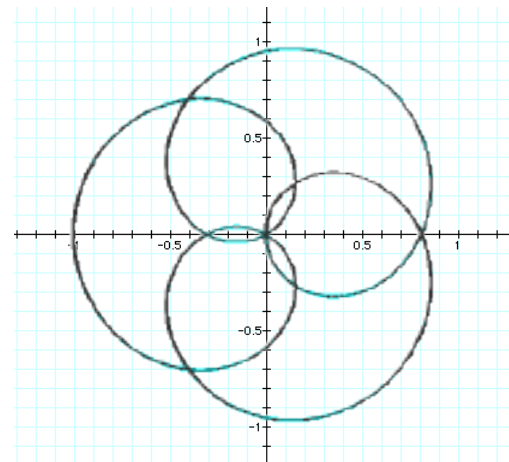


Fig. 7-33

The three-lobed epitrochoid and the projection of QSO (5:3) on the xy-plane

The curves are now visually congruent.

Going Further

Those interested in further exploring the relationship between epitrochoids and QSOs might want to take a look at the following comparisons. For most of the comparisons the projection of the QSO needs to be rotated 90° for visual congruency with the epitrochoid. Some need to be both rotated and flipped left to right.

There are some tempting regularities in the table. It looks as if the QSO corresponding to an epitrochoid with variables (R, s) is of the form QSO (R + 2s : R), but no proof is offered that this is a general pattern.

R	s	QSO expands to -->	QSO
1	1	(3:1)	(3:1)
2	1	(2:1)	(4:2)
3	1	(5:3)	(5:3)
4	1	(3:2)	(6:4)
5	1	(7:5)	(7:5)
1	2	(5:1)	(5:1)
2	2	(3:1)	(6:2)
3	2	(7:3)	(7:3)
4	2	(2:1)	(8:4)
5	2	(9:5)	(9:5)
1	3	(7:1)	(7:1)
2	3	(4:1)	(8:2)
3	3	(3:1)	(9:3)
4	3	(5:2)	(10:4)
5	3	(11:5)	(11:5)

Table 7-1
Comparison of epitrochoids with the
projections of QSOs on the xy-plane

Hypotrochoids

As the name suggests, hypotrochoids are similar to epitrochoids. Whereas epitrochoids are created by a circle rolling around the outside of another circle, hypotrochoids result from one circle rolling around the inside of another.¹⁷ The equations are also similar.

$$\begin{bmatrix} x \\ y \end{bmatrix} = \frac{1}{2(R-s)} \begin{bmatrix} (R-s) \cos gt + (R-s) \cos \left(\frac{R-s}{s} gt \right) \\ (R-s) \sin gt - (R-s) \sin \left(\frac{R-s}{s} gt \right) \end{bmatrix}$$

Eqn. 7-25

R is the radius of the fixed circle,
 s is the radius of the rolling circle, and
 $g = 2\pi n$, $n: 0 \rightarrow 1$, $t: 0 \dots 1$

As before, the initial fraction is not needed to generate the curve. Its function is to normalize the curve so it fits within the unit circle on the xy -plane. If $R = 5$ and $s = 1$, then the graph is

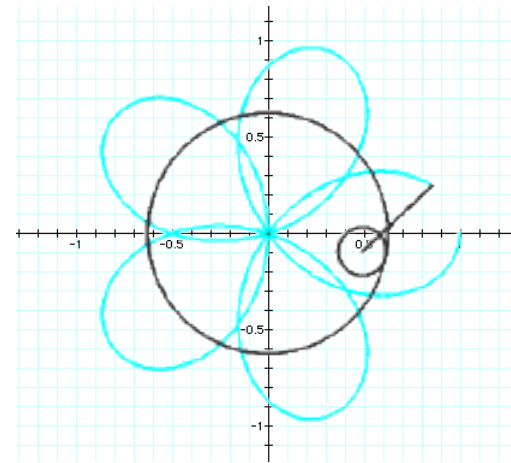


Fig. 7-34

A hypotrochoid with five loops

The radius of the large fixed circle is five units. The radius of the smaller rolling circle is one unit, and the extended radius of the smaller circle is four units long. We will compare this hypotrochoid with the projection of QSO (3:5) on the xy -plane.

¹⁷ hypo-, hyp- from Greek *hupo-*, from *hupo*, under, beneath; for example hypodermic, hypoglycemia

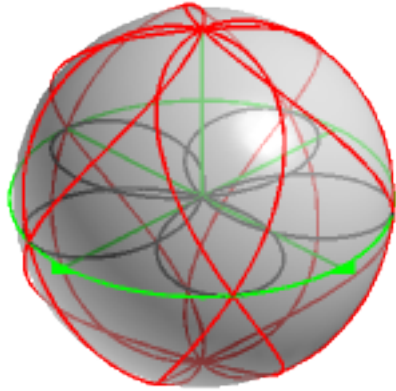


Fig. 7-35

QSO (3:5) and its projection on the xy-plane

The projection of QSO (3:5) has five outer loops arrayed equally around the Origin. Graphing the hypotrochoid and the projection of the QSO together gives,

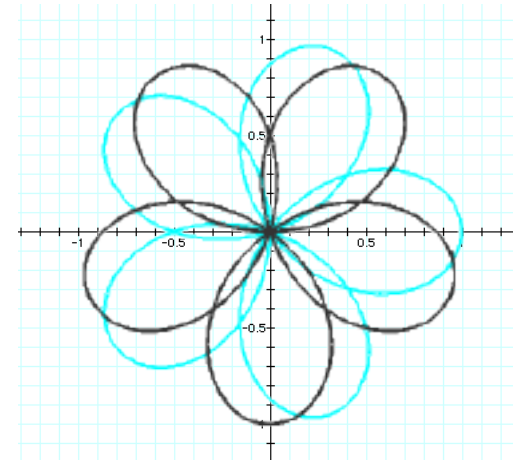


Fig. 7-36

The hypotrochoid $R = 5, s = 1$
and the projection of QSO (3:5) on the xy-plane

Again the trochoid is symmetrical with respect to the x-axis while the projection of the QSO is symmetrical w.r.t. the y-axis, and again the fix is to exchange the terms of the QSO.

$$\begin{bmatrix} x \\ y \end{bmatrix} = \begin{bmatrix} (\sin bgt) (\cos agt) \\ (\sin bgt) (\sin agt) \end{bmatrix}$$

Eqn. 7-26

The projection of QSO (3:5) on the xy-plane

Rotating the projection of the QSO,

$$\begin{bmatrix} x \\ y \end{bmatrix} = \begin{bmatrix} (\sin bgt) (\sin agt) \\ (\sin bgt) (\cos agt) \end{bmatrix}$$

Eqn. 7-27

The projection of QSO (3:5) on the xy-plane rotated 90°

Graphing,

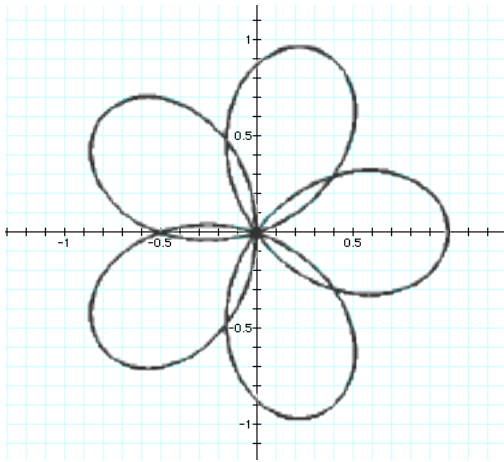


Fig. 7-37

The projection of QSO (3:5) on the xy-plane rotated 90° and compared with the hypotrochoid $R = 5, s = 1$

Once again it's all over but the shouting. For those who want to further explore the relationship between hypotrochoids and QSOs, we offer the following table. For most of the comparisons the projection of the QSO needs to be rotated for visual congruency with the hypotrochoid. Some need to be both rotated and flipped left to right. In table 7-2 the relationship between the hypotrochoids and the projections of the QSOs is even less clear than before. Perhaps a clever reader would like to clarify it.

R	s	QSO
1	1	Does not exist.
2	1	A straight line. x: -1 ... 1
3	1	(1:3)
4	1	(1:2)
5	1	(3:5)
1	2	(3:1)
2	2	Does not exist.
3	2	(1:3)
4	2	A straight line. x: -1 ... 1
5	2	(1:5)
1	3	(5:1)
2	3	(2:1)
3	3	Does not exist.
4	3	(1:2)
5	3	(1:5)

Table 7-2
Comparisons of certain hypotrochoids
with the projections of selected QSOs

Rhodonea

These curves were named *rhodonea*¹⁸ by the Italian mathematician Guido Grandi (1671-1742) because he thought they resembled roses.^{19,20} Rhodonea have the polar equations

$$r = \sin(k\theta)$$

Eqn. 7-28a

or

$$r = \cos(k\theta)$$

Eqn. 7-28b

Since these give identical curves with the exception of a rotation, we will use the first equation to generate curves for this section.

¹⁸ rhodo- from Greek *rhodon*, rose

¹⁹ <http://mathworld.wolfram.com/Rose.html>

²⁰ Legend has it that the rose was created at the birth of the Roman goddess Venus. Botticelli's painting, *The Birth of Venus*, shows the newly minted goddess accompanied by her flower.

When $k = 3$, the curve is a trifolium.²¹

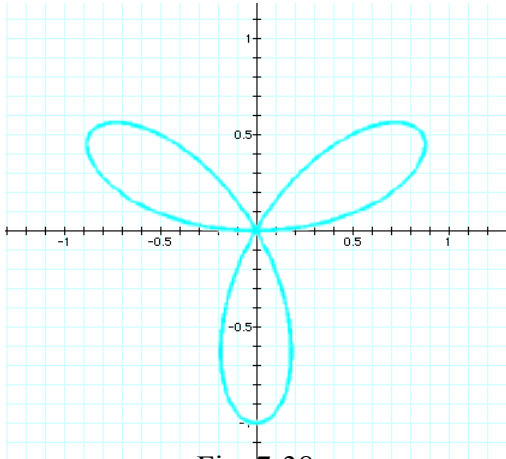


Fig. 7-38
The trifolium, $k = 3$

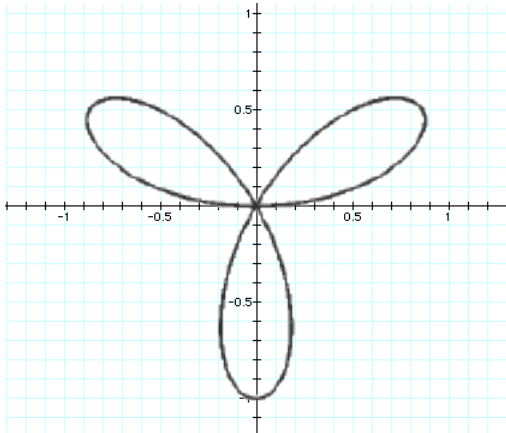


Fig. 7-39
The projection of QSO (1:3) on the xy-plane

When $k = 2$, the curve is a quadrifolium.

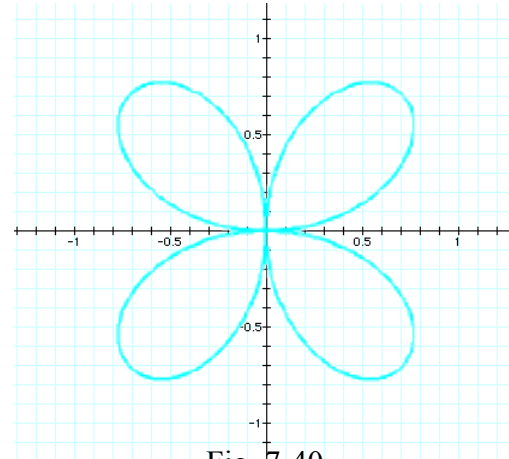


Fig. 7-40
The quadrifolium, $k = 2$

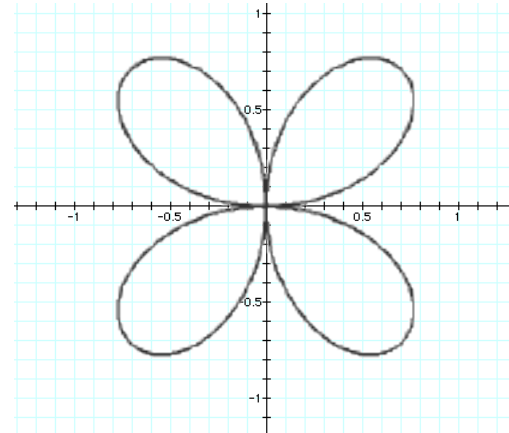


Fig. 7-41
The projection of QSO (1:2) on the xy-plane

²¹ “Three leaves” from Latin and Greek *tri-*, three, + New Latin from Latin *folium*, leaf

In each case the projection of the QSO is, without modification, identical with the Rose curve on the xy-plane. This leads us to suspect that the rhodonea variable k might equate to the second QSO rotation b , and indeed this is so.

$$r = \sin b\theta$$

Eqn. 7-29

The rhodonea equation with QSO variable b

It is possible to take one more step. If k is represented as a fraction,

$$k = \frac{b}{d}$$

where b is the second QSO rotation and d is an integer, then

when $b = 1$ and $d = 2$, the resulting curve is

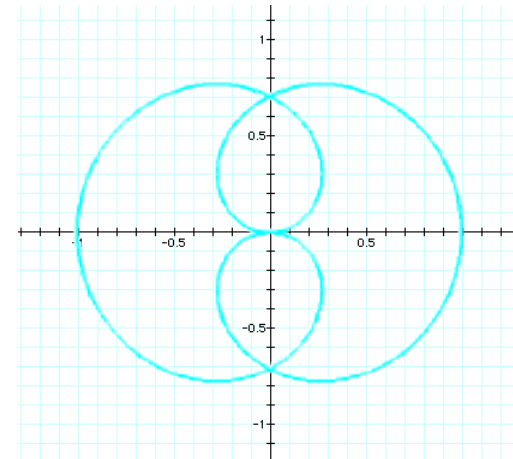


Fig. 7-42

Rhodonea $b = 1, d = 2$

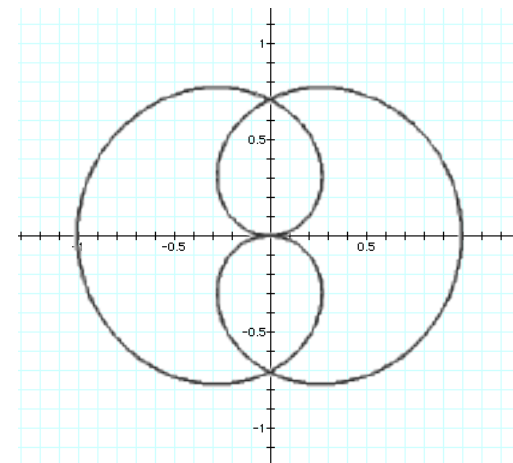


Fig. 7-43

The projection of QSO (2:1) on the xy-plane

When $b = 1$ and $d = 3$, the curve is

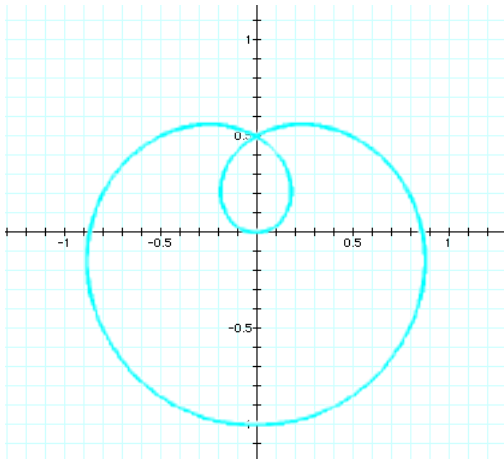


Fig. 7-44

Rhodonea $b = 1, d = 3$

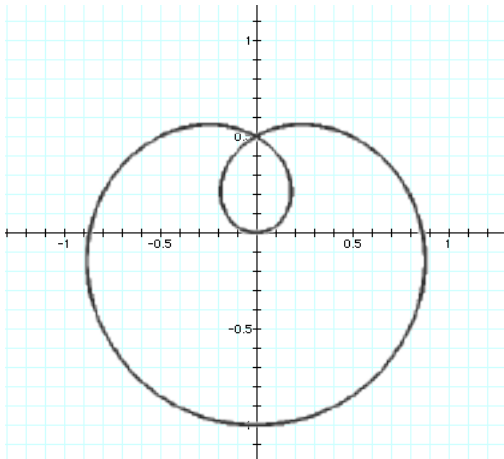


Fig. 7-45

The projection of QSO (3:1) on the xy -plane

The rhodonea curves with $k = \frac{1}{2}$ and $k = \frac{1}{3}$ are identical to

the projections of QSOs (2:1) and (3:1). Therefore we suspect that the general expression for rhodonea using QSO notation is

$$r = \sin\left(\frac{b}{a}\theta\right)$$

Eqn. 7-30

where a and b are the first and second QSO rotations respectively.²² Note also that the rhodonea curve

$$k = \frac{1}{3}$$

is the limaçon, which implies some interesting relationships not only between rhodonea, QSOs and the limaçon, but the trochoid curves as well.²³

²² Wikipedia gives a good accounting of the first 49 rhodonea which are also QSOs. See <http://en.wikipedia.org/wiki/Rose_curve>.

²³ See Tables 7-1 & 7-2.

We close with an example of the intersection between art and life. Although QSO (1:2) gives the quadrifolium on the xy -plane²⁴, when graphed as a surface of revolution and viewed in 3-D with appropriate color and shading, it truly resembles a rose bud.

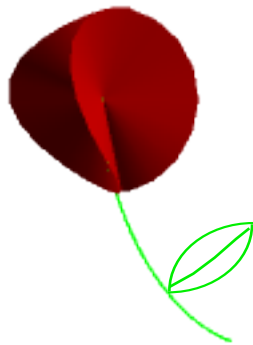


Fig. 7-46

QSO (1:2) as a surface of rotation, isometric view

The green stem and leaf have been added to enhance the illusion. The equation for the “bud” is

$$\phi = 2\theta$$

Eqn. 7-31

where $\theta: 0 \dots 2\pi$

²⁴ See p. 129.

Chapter 8

Lissajous Figures

French physicist Jules Antoine Lissajous (1822-1880), like many of his contemporaries, was interested in demonstrations of vibration that did not depend on the sense of hearing. Lissajous' most important research, first published in 1855, described a way to study acoustic vibrations by reflecting a ray of light from a vibrating object onto a screen. Lissajous produced two kinds of luminous curve. The second kind, named the "Lissajous figure," is the more useful of the two. A ray of light is successively reflected from mirrors on two tuning forks that vibrate about mutually perpendicular axes. If the light ray is projected onto a screen, persistence of vision causes various curves to appear. The shapes of these curves depend on the relative frequency, phase and amplitude of the vibrations of the tuning forks.

Lissajous figures are plane curves and could reasonably be grouped with the plane curves in the last chapter. They're created by independent sinusoidal oscillations on two mutually perpendicular axes. As such, they might seem to be a shoo-in for congruency with the projections of at least some QSOs. Yet, congruency is not automatic and surprises abound, so we will investigate the relationship between QSOs and Lissajous figures separately from the other plane curves.

L-figures are generated by any combination of sine and cosine on two axes.

$$\begin{bmatrix} x \\ y \end{bmatrix} = \begin{bmatrix} \sin (c) \\ \sin (s) \end{bmatrix}, \quad \begin{bmatrix} x \\ y \end{bmatrix} = \begin{bmatrix} \sin (c) \\ \cos (s) \end{bmatrix}$$

8-1a 8-1b

$$\begin{bmatrix} x \\ y \end{bmatrix} = \begin{bmatrix} \cos (c) \\ \sin (s) \end{bmatrix}, \quad \begin{bmatrix} x \\ y \end{bmatrix} = \begin{bmatrix} \cos (c) \\ \cos (s) \end{bmatrix}$$

8-1c 8-1d

Eqns. 8-1

Equations for Lissajous figures

where c and s are the relative frequencies of the vibrations. We will take equation 8-1c as the basis for discussion.

Adding amplitudes and a phase angle,¹

$$\begin{bmatrix} x \\ y \end{bmatrix} = \begin{bmatrix} C \cos (c + \theta) \\ S \sin (s) \end{bmatrix}$$

Eqn. 8-2

Graphing Calculator uses radians, so 2π is needed to see the complete curve. The variable t is included so that a trace is generated rather than a vector field.

$$\begin{bmatrix} x \\ y \end{bmatrix} = \begin{bmatrix} C \cos (2\pi ct + \theta) \\ S \sin (2\pi st) \end{bmatrix}$$

Eqn. 8-3

For the moment we will assume that $C = S = c = s = 1$, and that the phase angle $\theta = 0$.

¹ A second phase angle could be added to the oscillation on the y-axis, but it would not materially change the patterns generated.

Lissajous Figure (1:1)

The simplest Lissajous figure, like the simplest QSO, is L-fig. (1:1).

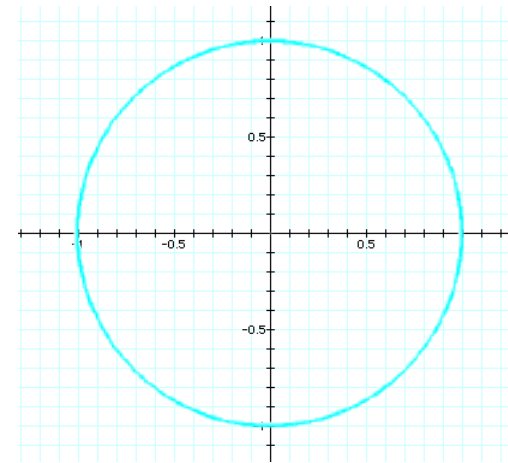


Fig. 8-1

L-fig. (1:1), $C = S = 1$, $\theta = 0$

The result is a circle with a radius of one and centered on the Origin. We have already seen that the projection of QSO (1:1) on the xy-plane is a circle,² so we'll skip a repeat demonstration here. Of more interest is what happens as the phase angle changes.

² See p. 117.

Lissajous Figures

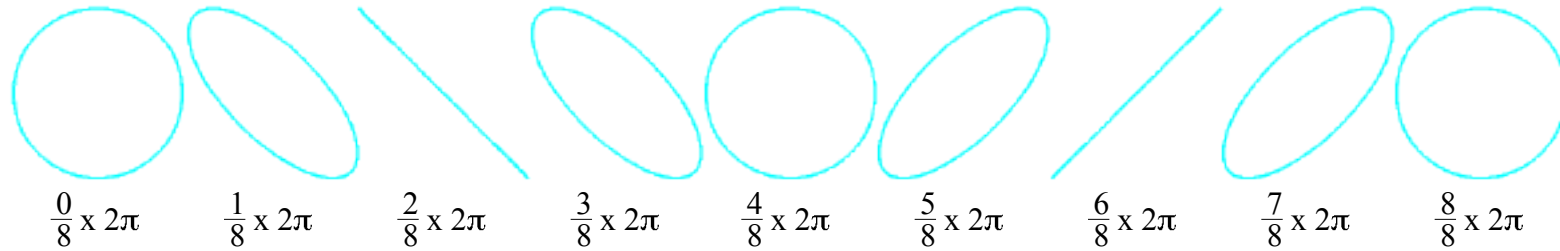


Fig. 8-2

L-fig. (1:1), $C = S = 1$, $\theta: 0 \dots 2\pi$

Lissajous figure (1:1), like all L-figures, oscillates between two distinct patterns as the phase angle varies.³ In this case, the patterns are a circle and a diagonal line. The diagonal line lies first along the line $y = -x$, and then, π radians later, along the line $y = x$. Although the slope changes, both are diagonal lines. For our purposes here, we will not distinguish between the two.

Also, there are ellipses between the circle and the diagonal line. They vary in eccentricity and orientation, but again we will not distinguish. In fact, since the ellipses are all intermediate between the circle and the diagonal line, we won't bother with them at all.⁴

Lissajous Figure (2:1)

Turning now to L-fig. (2:1), familiar sights emerge.

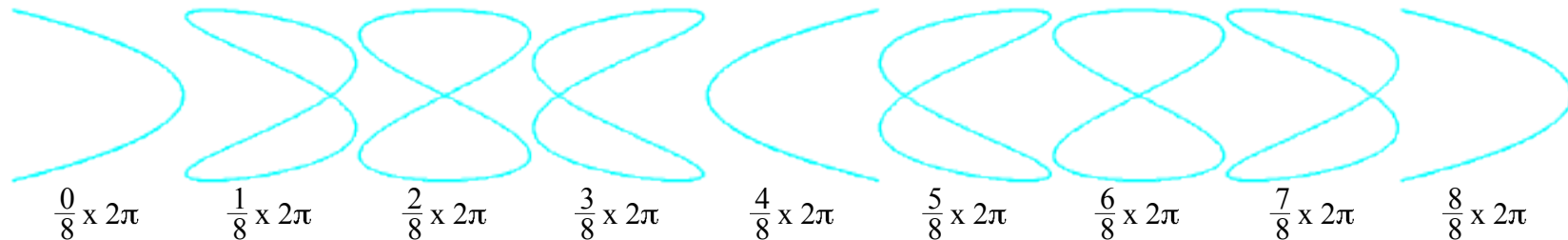


Fig. 8-3

L-fig. (2:1), $C = S = 1$, $\theta: 0 \dots 2\pi$

³ The nonstandard labeling of the phase angle deserves an explanation. The full cycle of the L-fig. goes to completion in 2π radians. For display purposes, the cycle is divided into eight steps, and each step is labeled as $1/8$ of the cycle.

⁴ QSO (0:1) @ 100% gives a circle in the xz -plane, which, when rotated around the z -axis, produces a series of elliptical views. See p. 4, Fig. 1-7.

The L-fig. oscillates between a parabola at $\theta = 0$, and a figure-eight curve at $\theta = \pi/2$, where the figure eight curve is reminiscent of the lemniscate of Gerono.⁵ Comparing the L-fig. at $\theta = 0$ and $\theta = \pi/2$ with the corresponding projections of QSO (1:1), we get

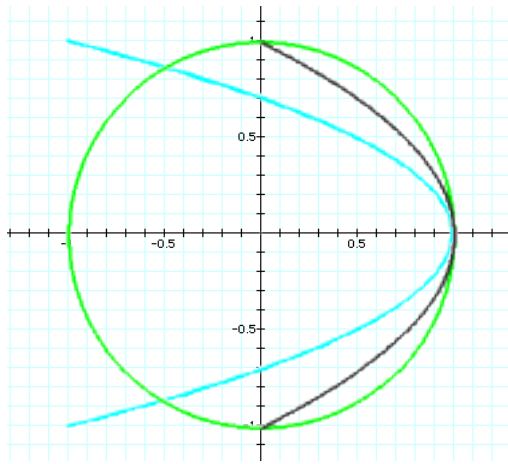


Fig. 8-4

L-fig. (2:1) [blue], $C = S = 1$, $\theta = 0$
 QSO (1:1) @ 100% [black], view from the x-axis,
 projected onto the xy-plane

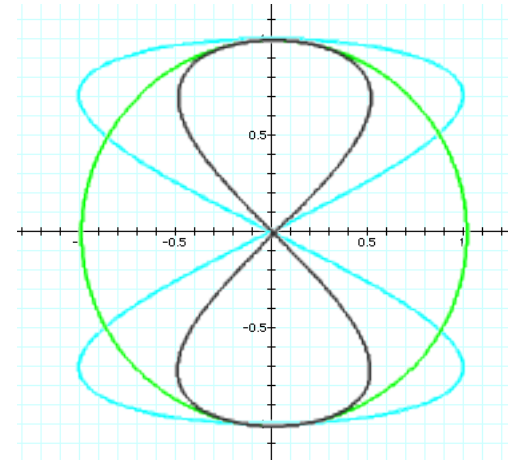


Fig. 8-5

L-fig. (2:1) [blue], $C = S = 1$, $\theta = \pi/2$
 QSO (1:1) @ 100% [black], view from the y-axis,
 projected onto the xy-plane

It looks in each case as if the L-fig. is just a wider version of the corresponding projection of the QSO. To test this observation, we let $C = 0.5$.

⁵ See pp. 119, 122.

The L-figs. become

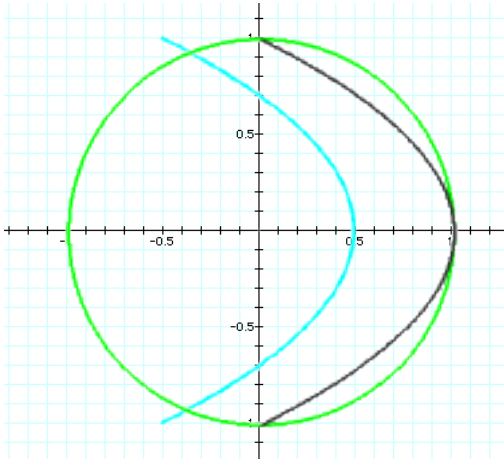


Fig. 8-6

L-fig. (2:1) [blue], $C = 0.5$, $S = 1$, $\theta = 0$
 QSO (1:1) @ 100% [black], view from the x-axis,
 projected onto the xy-plane

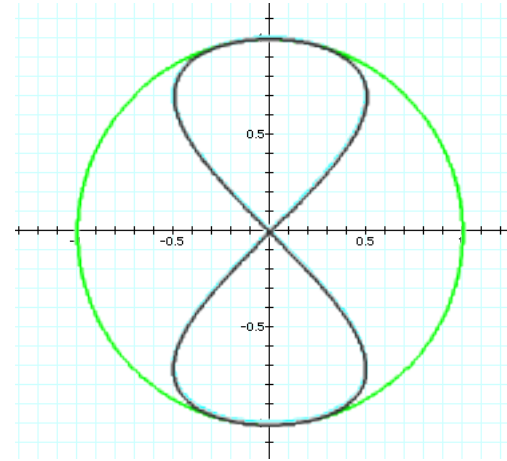


Fig. 8-7

L-fig. (2:1) [blue], $C = 0.5$, $S = 1$, $\theta = \pi/2$
 QSO (1:1) @ 100% [black], view from the y-axis,
 projected onto the xy-plane

The L-fig. (2:1) parabola occurs to the left of the QSO (1:1) parabola, but they are otherwise identical. The L-fig. (2:1) figure eight underlies the QSO (1:1) lemniscate of Geronno to the extent that they are visually indistinguishable. We note in passing that reversing c and s in the L-fig. rotates the static patterns 90° , but does not otherwise alter them.

Lissajous Figure (3:1)

Lissajous figure (3:1) oscillates between a sort of double hourglass pattern at $\theta = 0$ and an upper-case letter “S” at $\theta = \pi/2$, or an upper-case letter “Z,” π radians later.

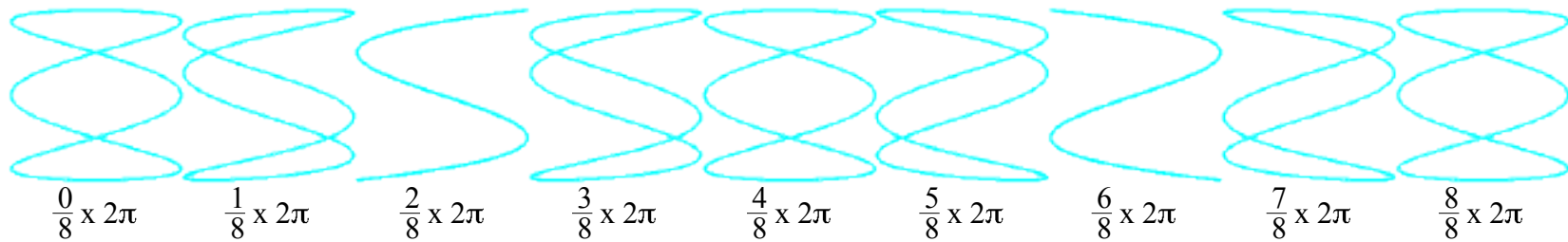


Fig. 8-8

L-fig. (3:1), $C = S = 1$, $\theta: 0 \dots 2\pi$

The double hourglass and the Z look like the y- and x-axis views of QSO (2:1) respectively, so we compare them.

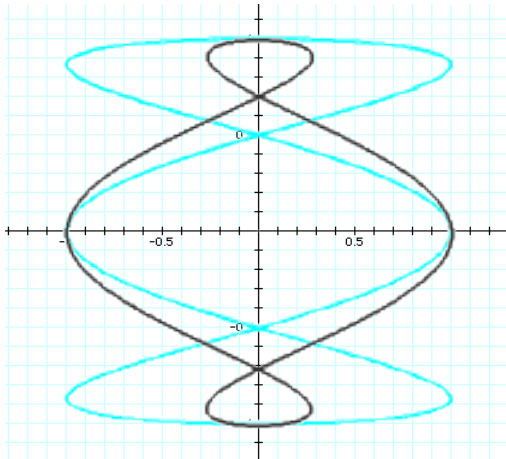


Fig. 8-9
 L-fig. (3:1) [blue], $C = S = 1$, $\theta = 0$
 QSO (2:1) @ 100% [black], view from y-axis,
 projected onto the xy-plane

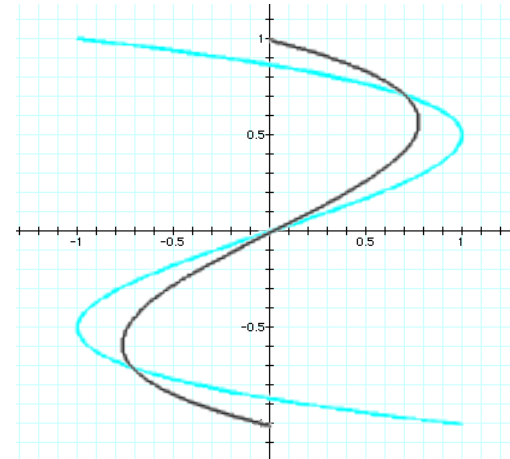


Fig. 8-10
 L-fig. (3:1) [blue], $C = S = 1$, $\theta = 3\pi/2$
 QSO (2:1) @ 100% [black], view from x-axis

Again the L-figures seem to be wider versions of their QSO cousins. Unfortunately, squeezing them on the x-axis doesn't do the trick this time.

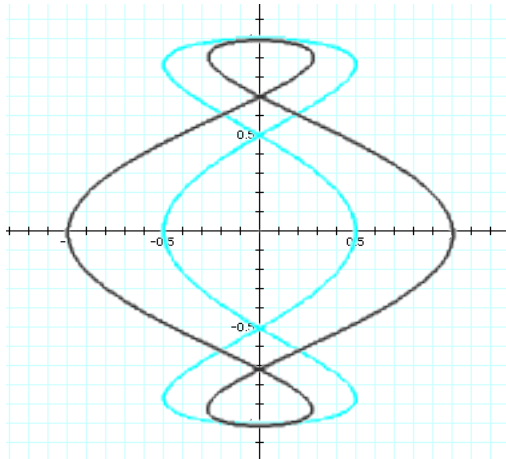


Fig. 8-11

L-fig. (3:1) [blue], $C = 0.5$, $S = 1$, $\theta = 0$
 QSO (2:1) @ 100% [black], view from y-axis

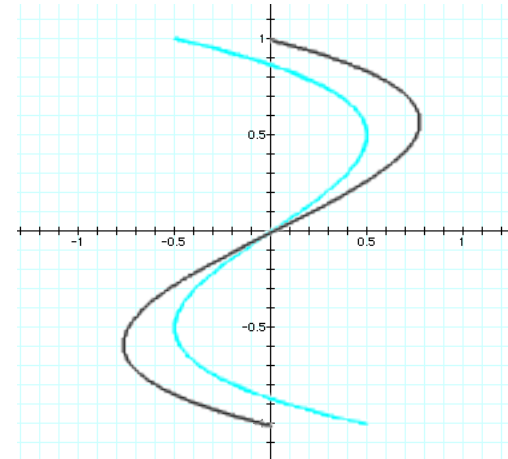


Fig. 8-12

L-fig. (3:1) [blue], $C = 0.5$, $S = 1$, $\theta = 3\pi/2$
 QSO (2:1) @ 100% [black], view from x-axis

The problem becomes clear when we look at a higher order curve.

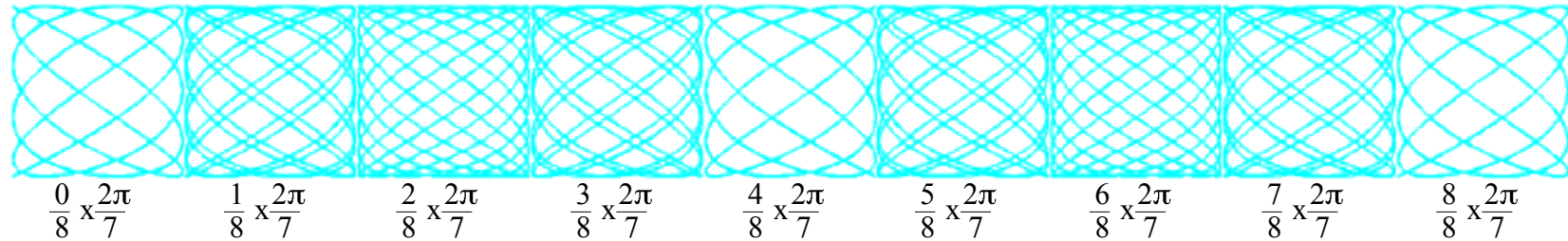
Lissajous Figure (10:7)

Fig. 8-13

L-fig. (10:7), $C = S = 1$, $\theta: 0 \dots 2\pi/7$

Lissajous figure (10:7) oscillates between an open weave and a closed weave pattern.^{6, 7} The reason that this and all similar Lissajous figures cannot be squeezed into congruency with any projection of any QSO is that the L-figures occur on a square field whereas the projections of the QSOs are drawn on a circular field.⁸ The congruency of the squeezed versions of L-fig. (2:1) with two of the projections of QSO (1:1) is thus revealed as an exception to the general rule, not to be repeated as the frequencies increase.

At this point one might concede that the superficial

⁶ Note that the open weave pattern comes in left- and right-handed versions, whereas the closed weave is statically symmetrical.

⁷ A further note on the labels for the phase angle. In general, the number of times an L-fig. oscillates between its two identifiable patterns is controlled by the frequency on the axis that does not have the phase angle. In the present examples, the phase angle is added to the x-axis, so the frequency on the y-axis controls the oscillation. For L-fig. (10:7), that's seven cycles in 2π radians.

⁸ See Figs. 8-4, 8-5, 8-6, 8-7.

resemblance of low-order Lissajous figures to some of the projections of QSOs is simply coincidence – and they would be right, to a point. Still, much remains to be said before we leave the topic of L-figures and their relationship to QSOs.

Quasi-Cylindrical Orbits

By definition, *Quasi-Spherical* Orbits occur on a sphere. Equation 2-8a guarantees that.

$$\begin{bmatrix} x \\ y \\ z \end{bmatrix} = \begin{bmatrix} (\sin bgt) (\cos agt) \\ (\sin bgt) (\sin agt) \\ \cos bgt \end{bmatrix}$$

Eqn. 2-8a

The QSO equation in Cartesian notation

However, the QSO can be unwrapped from the sphere by removing the $(\sin bgt)$ terms from the expressions for x and y .

$$\begin{bmatrix} x \\ y \\ z \end{bmatrix} = \begin{bmatrix} \cos agt \\ \sin agt \\ \cos bgt \end{bmatrix}$$

Eqn. 8-4

The parametric equation for Quasi-Cylindrical Orbits

The effect of this modification is to create a Quasi-Cylindrical Orbit, or QCO.⁹ The QCO equation, on the x - and y -axes at least, looks very much like equation 8-1c which generates L-figures. The difference between QCOs and QSOs is immediate and dramatic.

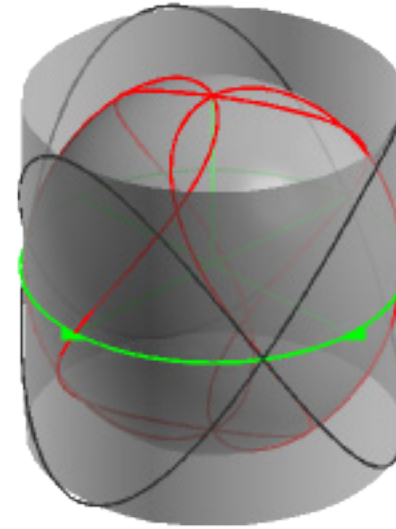


Fig. 8-14
QSO (2:3) [red]
QCO (2:3) [black]

In figure 8-14, QSO (2:3) appears conventionally on the unit sphere. The Quasi-Cylindrical Orbit (2:3) appears on the unit cylinder, where $r = 1$ and $z: -1 \dots 1$.

⁹ Kelleher (1994) wrote an equation very similar to Eqn. 8-4. Neither of us realized at the time that it generated a curve on a cylinder rather than on a sphere.

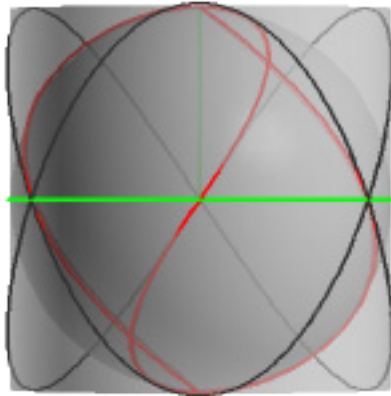


Fig. 8-15
QSO (2:3) [red]
QCO (2:3) [black]
View from the x-axis

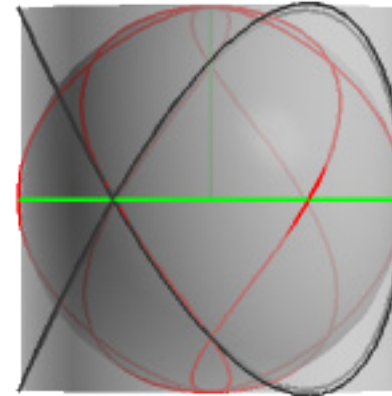


Fig. 8-16
QSO (2:3) [red]
QCO (2:3) [black]
View from the y-axis

The comparison is between QCO (2:3) and L-fig. (2:3). First the L-fig.,

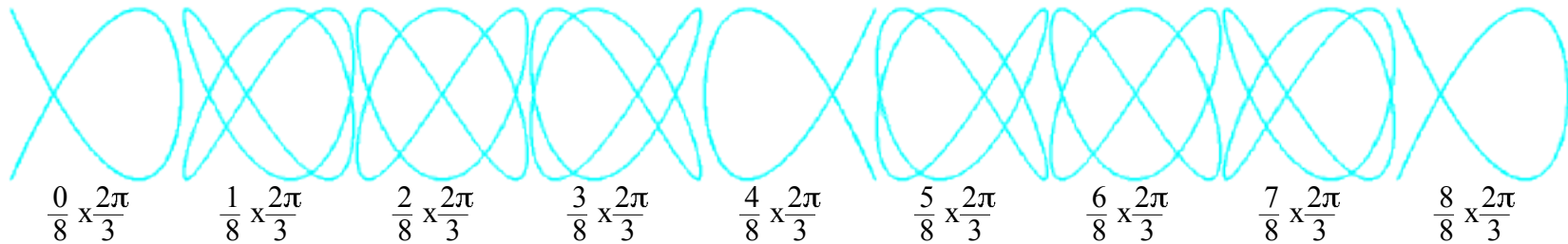


Fig. 8-17
L-fig. (2:3)

...and then the QCO.

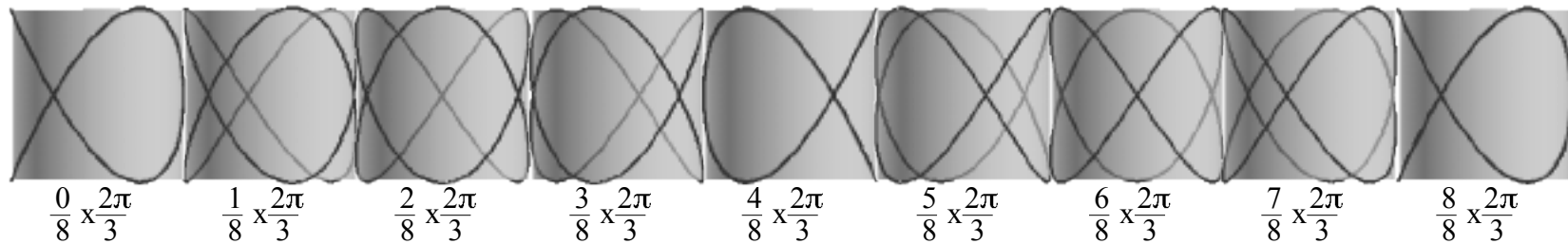


Fig. 8-18
QCO (2:3)

The view of the QCO is from the y-axis, but since this is an actual 3-D curve, we can rotate it around the z-axis. The QSO, the unit sphere, and the equator are all suppressed, but the unit cylinder is left in to give a sense of front and back. The 2-D aspects of the QCO and the L-fig. are for all intents and purposes identical, and both curves change three times faster than L-figures with the form (n:1) where n is a positive integer.

Extrapolating from the present example, we can predict that Lissajous figures are in general the 2-D projections of 3-D Quasi-Cylindrical Orbits. Both curves will have the form (c, s), and both will go through the same number of cycles in 2π radians. The formal proof of these observations, as always, is left to persons more mathematically adventurous than the author.

Space Curves

Space curves are one-dimensional curves that exist in three-dimensional space. All QSOs are space curves, but not all space curves are QSOs.

and helices grow without limit whereas QSOs and the projections of QSOs are bound in the first case by the unit sphere and in the second by the unit circle. Even the irrational QSOs are bound this way, while spirals and helices are not. The 3-D astroid is a different matter.

The Conical Helix

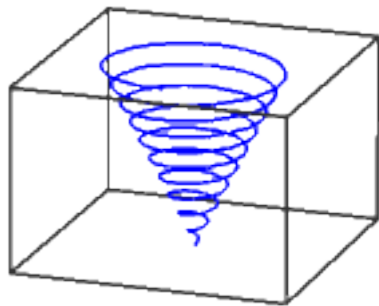


Fig. 9-1

The conical helix

$$\begin{bmatrix} x \\ y \\ z \end{bmatrix} = \begin{bmatrix} jt \cos mt \\ kt \sin mt \\ lt \end{bmatrix}$$

Eqn. 9-1¹

The conical helix, for example, is not and cannot be related to any QSO. Even in its two-dimensional embodiment as Archimedes' spiral, it cannot correspond to the projection of any QSO. No spiral can. The reason is found in the fact that spirals

¹ The equations for the space curves in this chapter are from Gray, 1998, appendix B. Equivalent expressions are found in many places. Although Gray uses the conventional "a, b, c, d..." for his variables, we replace them here with "j, k, l, m..." because "a, b..." etc. are already in use for QSOs.

The 3-D Astroid

The 3-D astroid is the three-dimensional analog of the 2-D astroid, which itself is a hypocycloid.²

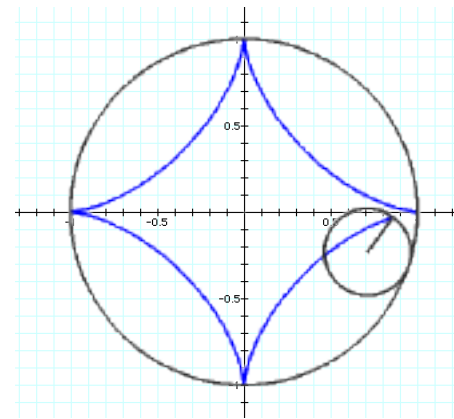


Fig. 9-2

The 2-D astroid @ 95% of a cycle³

$$\begin{bmatrix} x \\ y \end{bmatrix} = \begin{bmatrix} j (\cos t)^3 \\ k (\sin t)^3 \end{bmatrix}$$

Eqn. 9-2

² For a discussion of hypocycloids, see Hypotrochoids, p. 125.

³ See Gray, 1998, p. 892.

A circle of radius $r/4$ rolls around the inside of a circle of radius r . A point on the circumference of the rolling circle traces the 2-D astroid.

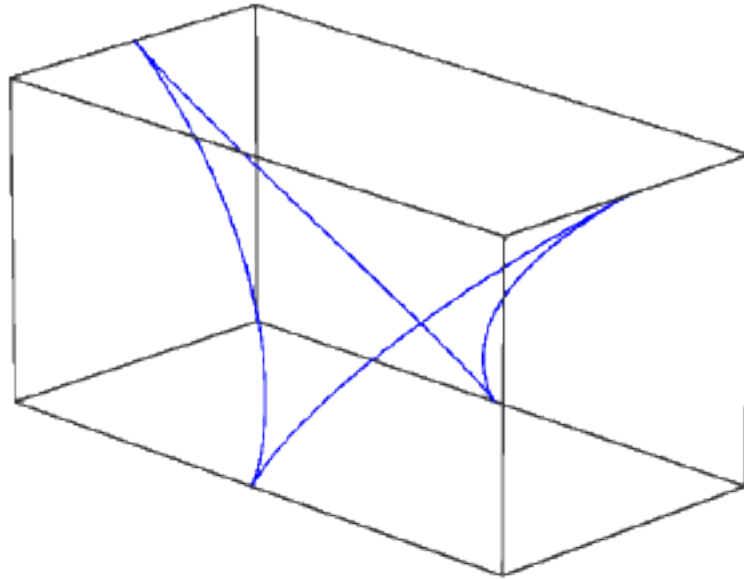


Fig. 9-3
The 3-D astroid⁴

$$\begin{bmatrix} x \\ y \\ z \end{bmatrix} = \begin{bmatrix} j(\cos gt)^3 \\ k(\sin gt)^3 \\ l(\cos 2gt) \end{bmatrix}$$

Eqn. 9-3
The 3-D astroid

⁴ See Gray, 1998, p. 927.

To generate the 3-D astroid we add a cosine term to the z -axis. The coefficient k on the y -axis has arbitrarily been set to 2 in order to display the curve more effectively.

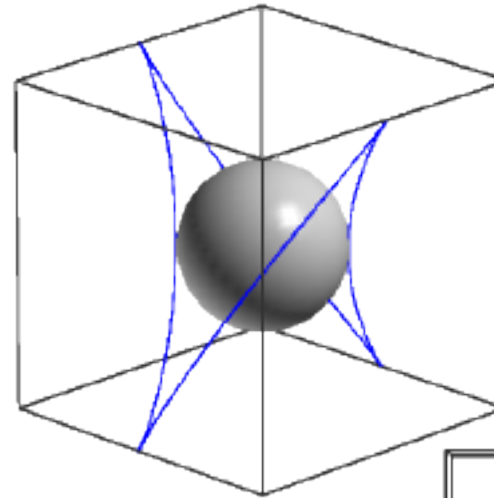


Fig. 9-4a
Isometric view

The 3-D astroid in a cube

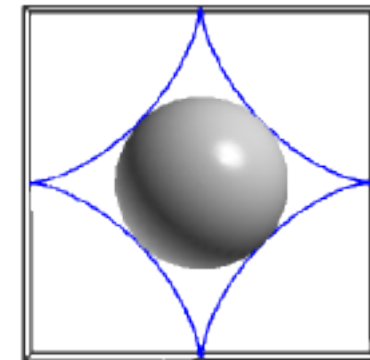


Fig. 9-4b
View from +z

Returning the coefficients of the x -, y -, and z -axes to unity yields a 3-D astroid that now occupies a cubical space. An

opaque sphere ($r = 0.5$) has been added to help tell front from back. The sphere is tangent to all four branches of the astroid. As we saw in chapter 6, page 103, Graphing Calculator draws a true 3-D picture, so we see all 12 edges of the cube in the foreshortened view from the z-axis. Close examination of this sketch reveals that the 3-D astroid has two cusps on the edges of the cube nearest the reader, and two on the edges away from the reader.

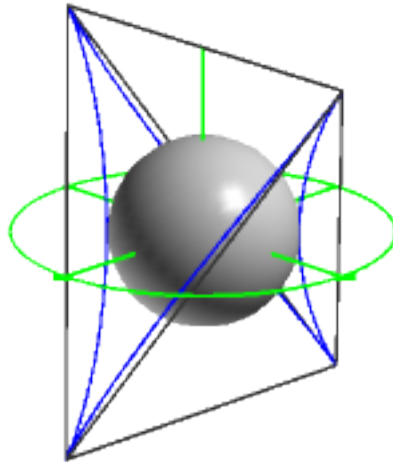


Fig. 9-5
The cubical 3-D astroid
with its circumscribed tetrahedron and inscribed sphere

Connecting the cusps of the cubical 3-D astroid results in a tetrahedron. The short horizontal edges of the tetra are 2 units long, while the longer edges are $\sqrt{6}$ units long. In this view the cubical box has been replaced by the standard orthogonal axes and an equator ($r = 1$).

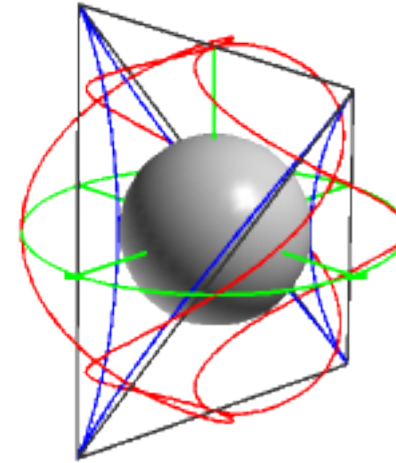


Fig. 9-6
The cubical 3-D astroid
with its circumscribed tetrahedron, inscribed sphere,
and QSO 1(3:2) @ 100% of a cycle

We mentioned in chapter 2 that connecting the events of QSO 1(3:2) makes a tetrahedron, so we add this QSO to the display.⁵

⁵ See also chapter 10, p. 158, and chapter 11, p. 185.

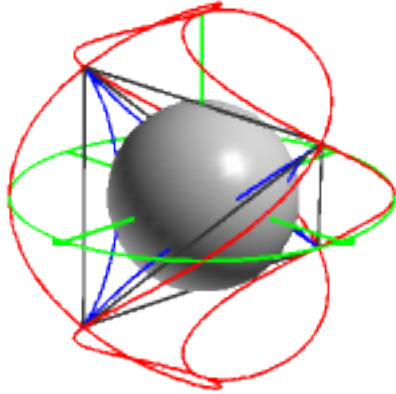


Fig. 9-7
The QSO astroid
with its circumscribed tetrahedron
and QSO 1(3:2) @ 100% of a cycle

The 3-D astroid and its circumscribed tetrahedron can be fitted to the QSO by letting

$$\begin{aligned} j &= \cos 30^\circ \\ k &= \cos 30^\circ \\ l &= \sin 30^\circ \end{aligned}$$

The central sphere is now tangent to the horizontal edges of the tetrahedron, but at $r = 0.5$ it's no longer inscribed in the astroid.

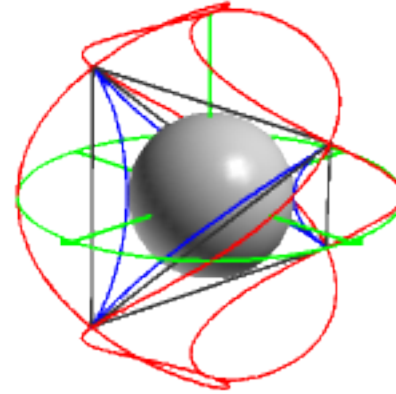


Fig. 9-8
Fitting the central sphere to the QSO astroid

The final step is to fit the central sphere to the QSO astroid by setting $r = (\cos 30^\circ)/2$. Although the relationship between some space curves and certain QSOs may seem at first farfetched, there is sometimes a surprising connection.

The Baseball Seam

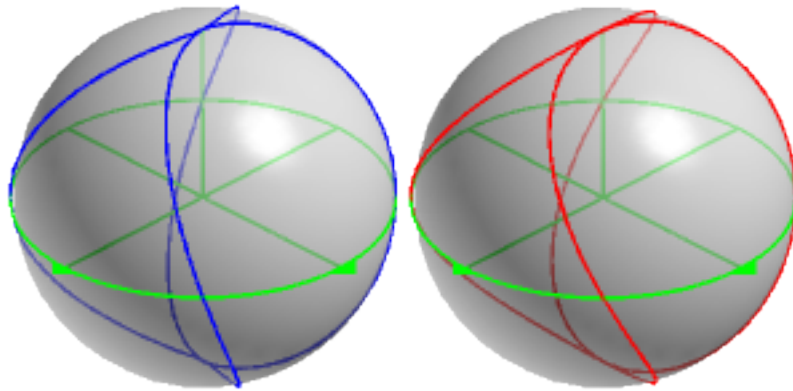


Fig. 9-9

The baseball seam by Gray (1998) The QSO baseball seam

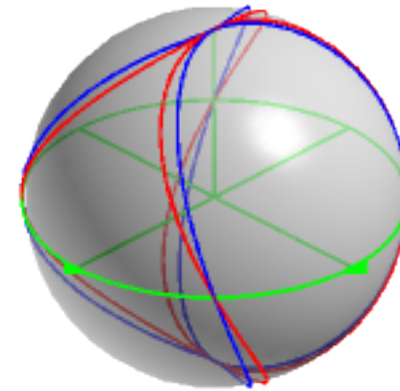


Fig. 9-10

Gray's baseball seam and QSO 1(1:2)

$$\begin{bmatrix} x \\ y \\ z \end{bmatrix} = \begin{bmatrix} j \left(\sin \left(\frac{\pi}{2} - \left(\frac{\pi}{2} - k \right) (\cos t) \right) \right) \left(\cos \left(\frac{t}{2} + k \sin 2t \right) \right) \\ j \left(\sin \left(\frac{\pi}{2} - \left(\frac{\pi}{2} - k \right) (\cos t) \right) \right) \left(\sin \left(\frac{t}{2} + k \sin 2t \right) \right) \\ j \left(\cos \left(\frac{\pi}{2} - \left(\frac{\pi}{2} - k \right) (\cos t) \right) \right) \end{bmatrix}$$

Eqn. 9-4, $j = 1, k = 0, t: 0 \dots 4\pi$

The baseball seam (Gray, 1998)

However, graphing the curves together reveals that they are not identical. Although they both begin at the north pole and both cross the equator at the same four places, a less obvious difference makes it unlikely that Gray's baseball seam can ever be massaged into the QSO.

Gray (1998) gives a fairly complex expression for a curve he calls the baseball seam. At first glance it looks a lot like QSO 1(1:2).

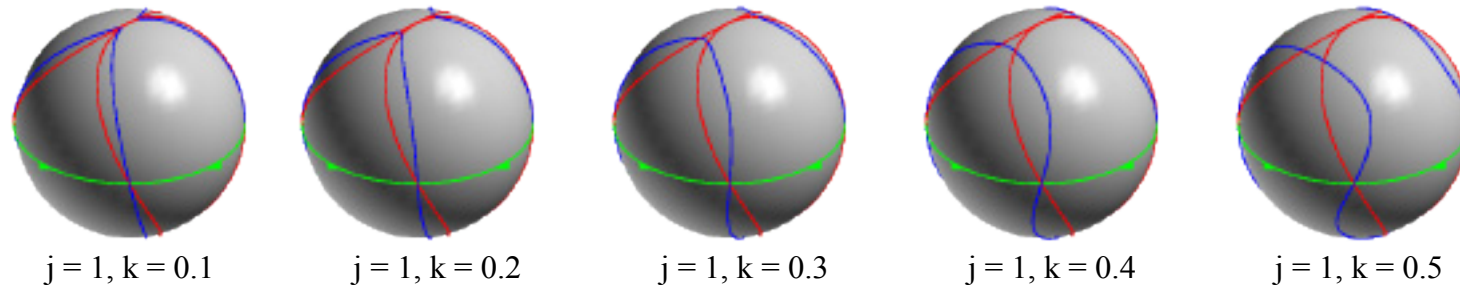
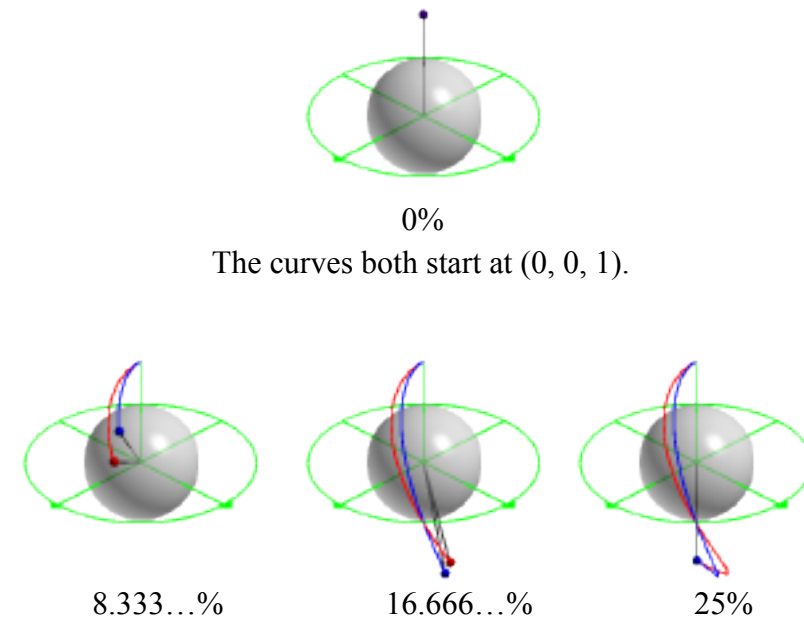


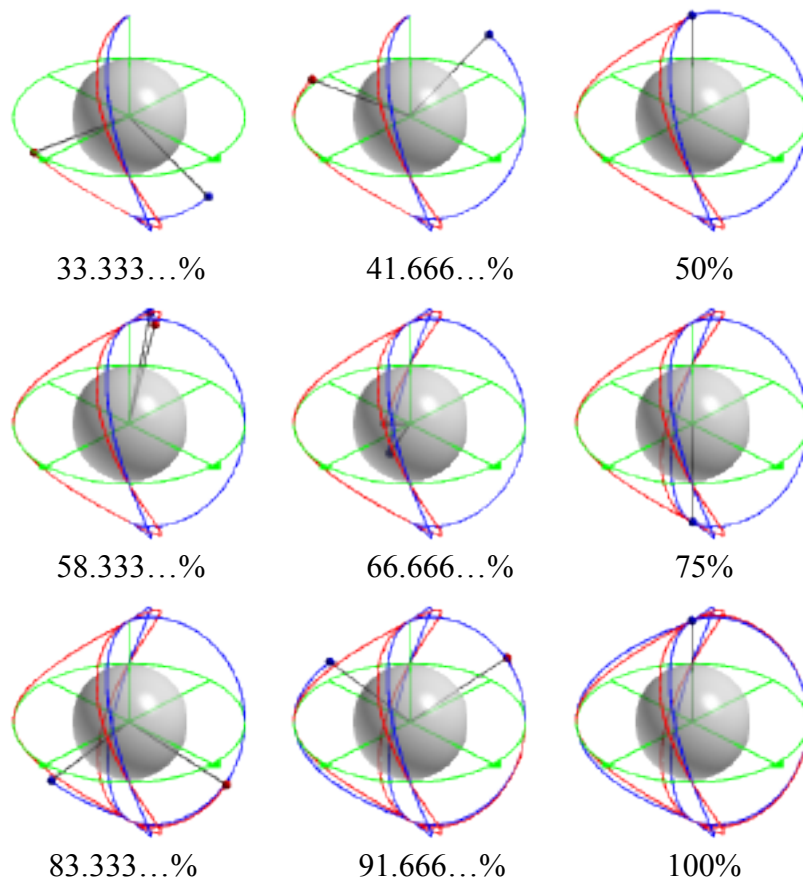
Fig. 9-11
Transforming Gray's baseball seam

Holding $j = 1$ while increasing k 0.1 unit at a time reveals that what appear to be polar events in Gray's baseball seam are actually cusps. As k increases slowly, the cusps withdraw from each other and transform into lobes until, at about $k = 0.4$, Gray's curve approximates the seam on a real baseball.⁶ The transformation does not stop there, of course. There are some interesting curves as k increases even further. There are also some interesting curves at negative k , but these seem less and less related to QSOs and are left for the reader to explore.

Holding $j = 1$, $k = 0$ and animating the curves, we find that the dynamics of Gray's curve and QSO 1(1:2) reveal insights not available from the static analysis. In the following illustrations the rotational rates have been adjusted so Gray's baseball seam and the QSO both go to completion in 2π radians.

⁶ Banks (1999, pp. 232–46) derives a formula for the length of a baseball seam that includes a quantity called the "minimum latitude." For a real baseball, the minimum latitude is 25° . For the monopole QSO (1:2) it's 0° . See also chapter 3, p. 35, footnote 1.





Gray's baseball seam (blue) and QSO 1(1:2) (red) are shown as orbital traces developing around a translucent central sphere ($r = 0.5$). They begin together at $(0, 0, 1)$. Although the QSO seems to be leading, both curves cross the equator simultaneously and at the same point at 12.5% of the cycle (not shown). They also reach the south pole at the same time, but then the major difference between the curves shows becomes apparent. While the QSO continues smoothly through the pole, Gray's curve "bounces." It reverses course and takes off in a direction approximately diametrically opposed to the QSO, confirming, if there was any doubt, that the polar trace is a cusp.

At 50% of the cycle the curves reach the north pole. We pause here to note that if we were to consider only the static appearance of the curves, we could easily come to believe that they are the same curve, one branch of which has experienced two 90° rotations compared to the other. But they're not the same curve, which is apparent as the traces continue to develop. Gray's curve bounces again, and then travels to the south pole where it bounces once more. It then returns to the north pole where it would form the fourth cusp if it were to go into the second cycle of rotation.

Fig. 9-12
QSO 1(1:2) and Gray's baseball seam

The Spherical Cardioid

Like the 3-D astroid, the spherical cardioid is the three-dimensional analog of the 2-D cardioid.

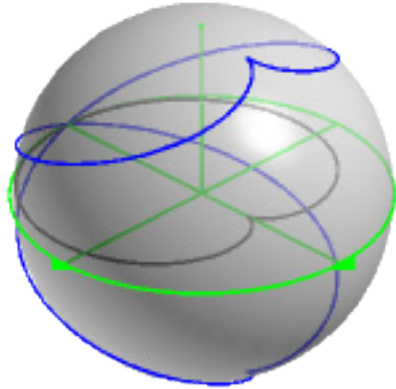


Fig. 9-13

The 2-D cardioid⁷ (black) and the 3-D cardioid (blue)

$$\begin{bmatrix} x \\ y \end{bmatrix} = d(k + 2c \cos 2\pi t) \begin{bmatrix} \cos 2\pi t \\ \sin 2\pi t \end{bmatrix}$$

Eqn. 7-13

The 2-D cardioid

$$\begin{bmatrix} x \\ y \\ z \end{bmatrix} = \begin{bmatrix} 2j(\cos gt) - j(\cos 2gt) \\ 2j(\sin gt) - j(\sin 2gt) \\ \sqrt{k} - j\left(\cos \frac{gt}{2}\right) \end{bmatrix}$$

Eqn. 9-5

The 3-D cardioid

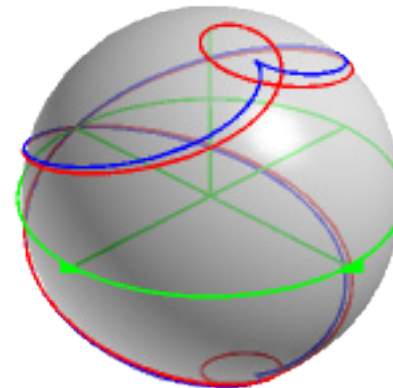


Fig. 9-14

The 3-D cardioid and QSO 1(3:1) @ 100%

In chapter 7 we learned that the plane cardioid was not congruent with the projection of QSO 1(2:1) on the xy-plane.⁸ We suspect that's true here as well, so we'll try something different. QSO 1(3:1) is shown above with the spherical cardioid. It's obvious that they don't fit either.

⁷ Deleting the z-term in Gray's equation gives the same curve as Equation 7-13.

⁸ See p. 116, Fig. 7-21.

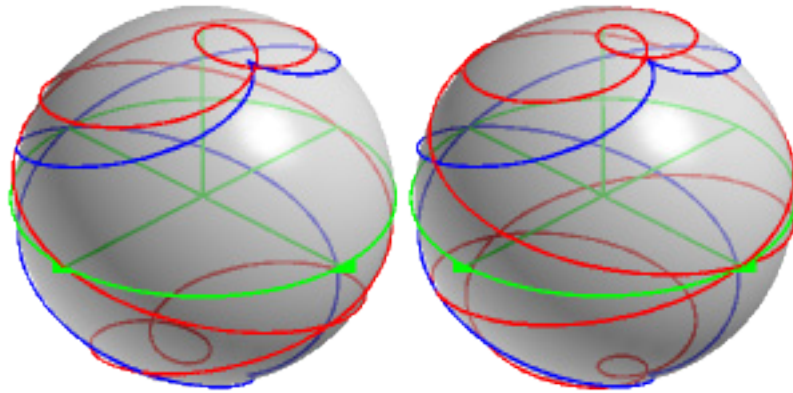


Fig. 9-15a

Fig. 9-15b

The spherical cardioid with QSOs 1(4:1), left, and 1(5:1), right.

It may seem that increasing the α -rotation of the QSO ratio might ultimately result in a QSO that has an event at the same point as the spherical cardioid. Whether this is true or not is a moot point, because such an increase results in multiple loops of the QSO around the unit sphere, eliminating all hope that the two could ever match.

Dynamically, we find in figure 9-16 that the spherical cardioid behaves very much like Gray's baseball seam.

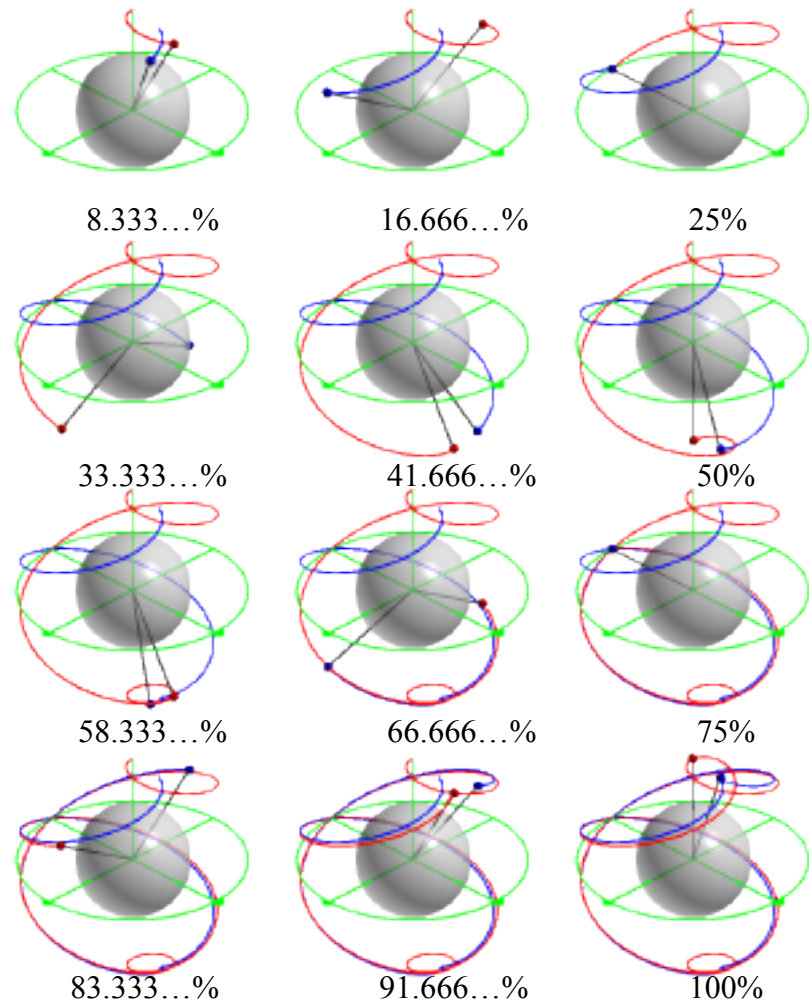
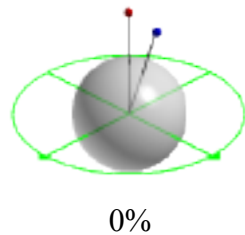


Fig. 9-16

The spherical cardioid and QSO 1(3:1)

While the QSO goes smoothly through its events, the cardioid bounces off its cusps, as did Gray's curve. If one is willing to relax the restriction that the spherical cardioid be identical with a QSO, some other interesting things happen. For instance, the square root spreads the curve vertically. For $j = 1/3$, $k = 0$ you get the 2-D cardioid. For $j = 1/3$ and $k = 8$, the spherical cardioid is on the unit sphere. If you delete the initial twos in the x- and y-terms, the curve has polar loops like QSO (3:1), but is not on the unit sphere. If you delete the initial twos, let $j = 0.5$, and $k = 4$, the curve is identical to QSO 1(3:1), but it's no longer the spherical cardioid.

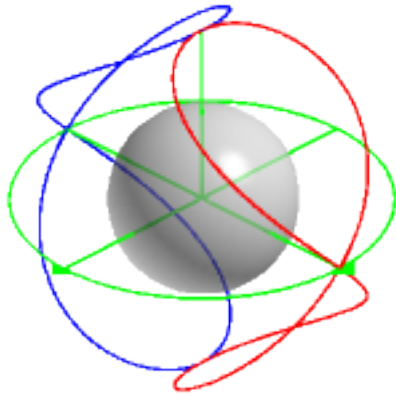


Fig. 9-17

A modification of the spherical cardioid (blue)
that looks like QSO 1(1:1) (red)

$$\begin{bmatrix} x \\ y \\ z \end{bmatrix} = \begin{bmatrix} (\cos gt) - 0.5 (\cos gt) \\ (\sin gt) - 0.5 (\sin gt) \\ (\cos \frac{gt}{2}) \end{bmatrix} + \begin{bmatrix} -0.5 \\ 0 \\ 0 \end{bmatrix}$$

Eqn. 9-6, $g = 4\pi$, $t: 0 \dots 1$

A modification of the spherical cardioid
that looks like QSO 1(1:1)

Deleting the twos in the arguments of the trig functions results in a curve that resembles QSO (1:1) precessed 180° around the z-axis, above, and if you delete the initial twos, let $j = 0.5$, and $k = 0$, the spherical cardioid becomes the limaçon.

The Clelia

The Clelia was named by Grandi (1671-1742) after the Countess Clelia Borromeo.⁹ It is a rosette space curve with multiple lobes emanating from (0, 0, 1). The Clelia curve occurs only on the positive side of the z-axis. It is the 3-D analog of the rhodonea curves.¹⁰

⁹ O'Connor, J. J. and Robertson, E. F.

¹⁰ Grandi also studied rhodonea. See chapter 7, p. 128.

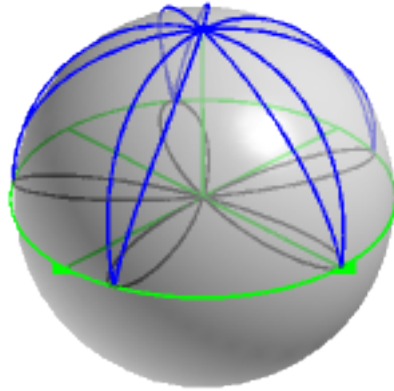


Fig. 9-18a
The Clelia (blue)

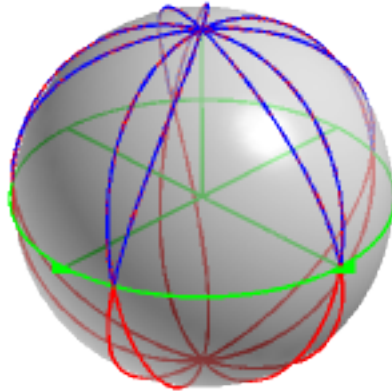


Fig. 9-18b
QSO 1(1:5) @ 100% (red)

A five-lobed Clelia is shown above left with its rhodonea projection on the xy-plane. The lobes of the Clelia terminate in cusps at the equator, but the lobes of the rhodonea are smoothly rounded at the same points. We learned in chapter 7 that the rhodonea curves correspond to the projections of QSOs of the form (1:b). Mapping the five-lobed Clelia together with QSO (1:5) in figure 9-18b confirms that they match, at least north of the xy-plane. The reason for this equivalence is not hard to find.

$$\begin{bmatrix} x \\ y \\ z \end{bmatrix} = \begin{bmatrix} jk (\cos t) (\sin mt) \\ jk (\sin t) (\sin mt) \\ j\sqrt{1 - (k \sin mt)^2} \end{bmatrix}$$

Eqn. 9-7
The Clelia

$$\begin{bmatrix} x \\ y \\ z \end{bmatrix} = \begin{bmatrix} (\sin bgt) (\cos agt) \\ (\sin bgt) (\sin agt) \\ \cos bgt \end{bmatrix}$$

Eqn. 2-8a
The parametric QSO equation

The expression for the Clelia, left, is similar to that for QSOs, right. Both have a sine-cosine term on the x-axis and a sine-sine term on the y-axis. The terms on the z-axis differ only in the expression for the cosine. The QSO expresses the cosine directly, and thus exists in the range $z: -1 \dots 1$. The Clelia uses an expression for the cosine from the identity

$$(\sin \theta)^2 + (\cos \theta)^2 = 1$$

Solving for the cosine,

$$\cos \theta = \sqrt{1 - (\sin \theta)^2}$$

Because the root is forever positive, the Clelia exists only at positive z .

The variable m in equation 9-7 controls the number of lobes of the Clelia curve. It corresponds to QSO rotation variable b when a is fixed at unity. At $m = 5$, as in figure 9-18a, the lobes of the Clelia perfectly match the northern half of QSO 1(1:5). Here, with $m = 4$, the Clelia has eight lobes, only the left or right half of which overwrite the QSO. Both curves go to completion in 2π .

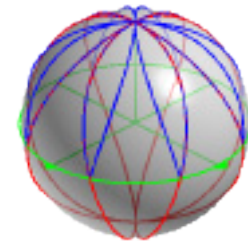
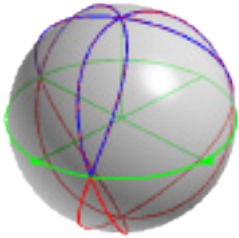


Fig. 9-19
Clelia, $m = 4$, $t: 0 \dots 2\pi$, with QSO 1(1:4) @ 100%



For $m = 3$, the correspondence of the Clelia with the northern half of the QSO is again perfect. Although the Clelia completes a cycle in π radians, the QSO still takes 2π .

Fig. 9-20

Clelia, $m = 3$, $t: 0 \dots \pi$, with QSO 1(1:3) @ 100%

At $m = 2$ the Clelia has $2m$ lobes, but only half of each lobe maps onto the QSO. The Clelia and the QSO both complete their cycles in 2π radians. Note that the Clelia outlines half of a regular octahedron. This corresponds to the northern half of the regular octahedron formed by QSO 2(1:2) $[0,0] [0,\pi]$.

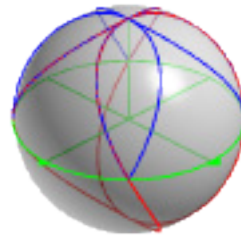
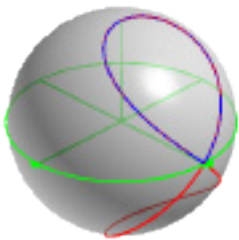


Fig. 9-21

Clelia
 $m = 2$, $t: 0 \dots 2\pi$,
with QSO 1(1:2) @ 100%



At $m = 1$ the Clelia is identical to the northern half of QSO 1(1:1). It takes π radians to draw the single lobe of the Clelia. The QSO takes 2π to draw its two lobes.

Fig. 9-22

Clelia, $m = 1$, $t: 0 \dots \pi$, with QSO 1(1:1) @ 100%

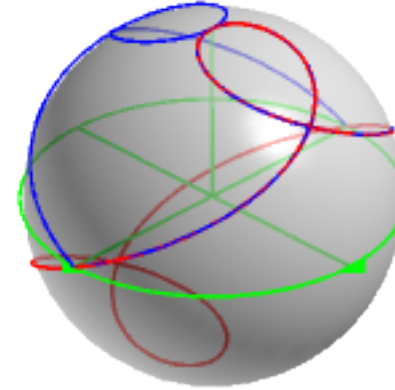


Fig. 9-23

Clelia, $m = 0.5$, $t: 0 \dots 4\pi$,
with QSO 1(2:1) @ 100%

There is also some interesting math in the range $m: 0 \dots 1$. Here, with $m = 0.5$, the Clelia conforms to the northern half of QSO 1(2:1). Other correspondences await the curiosity of the reader.

Viviani's Curve

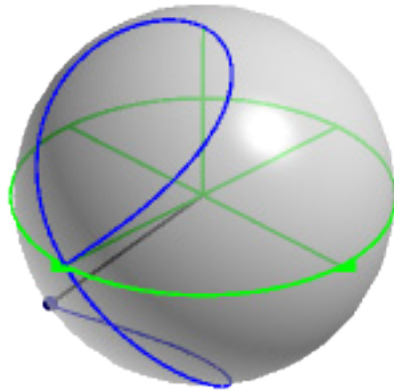


Fig. 9-24a
Viviani's curve (Gray, 1998)
@ 90%

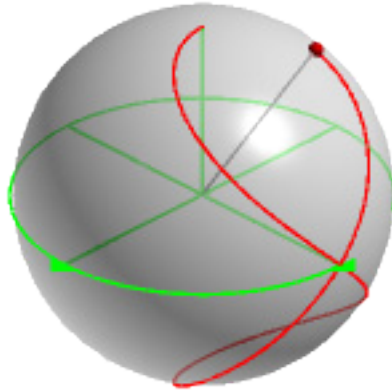


Fig. 9-24b
QSO 1(1:1)
@ 90%

The final comparison is between our old friend QSO (1:1) and Viviani's curve. The expression for Viviani's curve given by Gray (1998, p. 933) is

$$\begin{bmatrix} x \\ y \\ z \end{bmatrix} = \begin{bmatrix} a(1 + \cos t) \\ a(\sin t) \\ 2a\left(\sin \frac{t}{2}\right) \end{bmatrix}$$

Eqn. 9-8
Viviani's curve (Gray, 1998)

This results in a curve that begins at (1, 0, 0) and rotates like Loftus' original QSO, but which is statically indistinguishable from QSO 1(1:1).¹¹

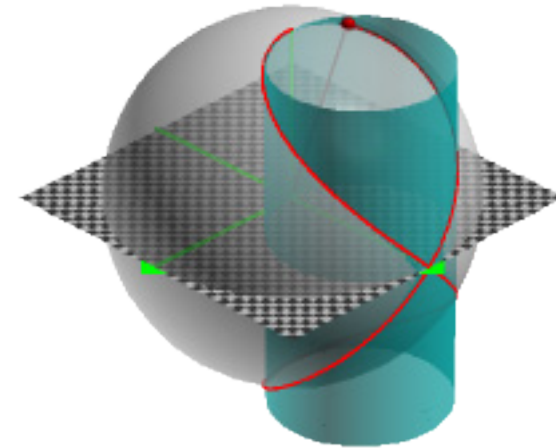


Fig. 9-25
Viviani as the intersection of a sphere and a cylinder.
Shown @ 95% of a cycle

Banchoff (1998) points out that another way of looking at Viviani is as the intersection of a sphere of radius r and a cylinder of radius of $r/2$. He calls this construction "The Temple of Viviani."¹²

¹¹ See chapter 1, pp. 5-10, chapter 6, pp. 79-80.

¹² The Temple of Viviani <<http://alem3d.obidos.org/en/struik/viviani/comm>>. See also <<http://www.math.umbc.edu/~rouben/dynagraph/gallery/viviani.jpg>>.

Monopole Polygons & Polyhedra

First Tetrahedron

In early 1991 the only tool available for studying QSOs was David Loftus' "3-D Combined Rotation Plotter."¹ About that time Michael Burke wrote, "[The program] clutters the screen with orbital track when all I really want is to see the Crossings or Events (and to triangulate them) all of which I now have to do by peering and counting."² But peer and count he did, and in the spring of that year he made an astounding discovery. QSOs were not only beautiful and intriguing curves, but when you connected the "Crossings or Events" you got known geometric figures. The first of these was a tetrahedron.

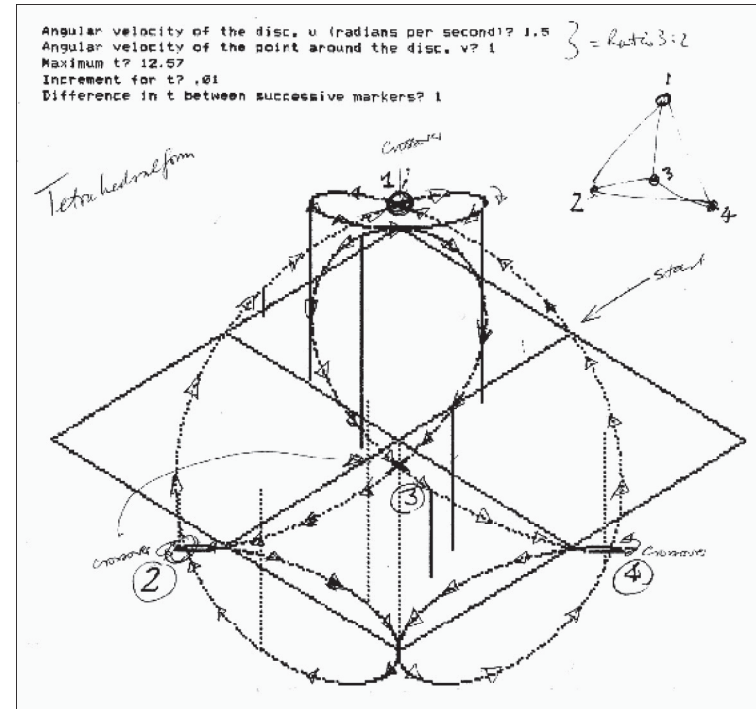


Fig. 10-1

The first QSO tetrahedron

Here reproduced from the original printout is what Burke saw when he graphed "QSO 1.5:1." Burke's handwritten annotation affirms that this is "Ratio 3:2." Although he got the

¹ See p. 78.

² 1991 Jun 7. Letter from Michael Burke to the author.

direction of the rotations wrong for part of the curve, nevertheless he definitely recognized the tetrahedron. He wrote “Tetrahedral form” in the upper left quadrant of the paper and sketched a tetra in the upper right. Years later I asked him, “Were you looking for a tetra?” He replied, “No, this was pure luck. It was a Eureka moment. I said, ‘By God, we’ve got something going on here!’”³ But for our purposes now the QSO (3:2) tetrahedron is not a good place to start. Instead we will begin the study of QSO geometric figures along the edges of the QSO landscape.

The QSO landscape consists of all possible combinations of the QSO ratio (positive integers only!) beginning with QSO (1:1) in the lower left corner. Variable a increases as you move from bottom to top. Variable b increases as you move from left to right. Table 10-1 shows only the first 36 ratios. A variant of this landscape was seen in table 5-2 and figure 5-2. The (a:1) series refers to those QSOs in the first column on the left, QSOs (1:1), (2:1), (3:1), etc., where a is changing, but b is held constant at $b = 1$. By placing a “1” in front of the ratio, we limit the curves – for the time being – to monopoles.

The 1(a:1) Series

	(6:1)	(6:2)	(6:3)	(6:4)	(6:5)	(6:6)
	(5:1)	(5:2)	(5:3)	(5:4)	(5:5)	(5:6)
	(4:1)	(4:2)	(4:3)	(4:4)	(4:5)	(4:6)
	(3:1)	(3:2)	(3:3)	(3:4)	(3:5)	(3:6)
	(2:1)	(2:2)	(2:3)	(2:4)	(2:5)	(2:6)
	(1:1)	(1:2)	(1:3)	(1:4)	(1:5)	(1:6)
(a:b)	$b \longrightarrow$					

Table 10-1
The QSO landscape

We saw at the end of chapter 3 that the events of the dipole (3:1) lie on an ellipse when viewed from 45° between the x- and y-axes. In that case the projections of the events onto the flat page were connected with a smooth curve. We look now at the monopole (3:1) where we will connect the actual events in space with straight lines.

³ 2004 Jan 16 & 19 Interview of Michael Burke by the author.

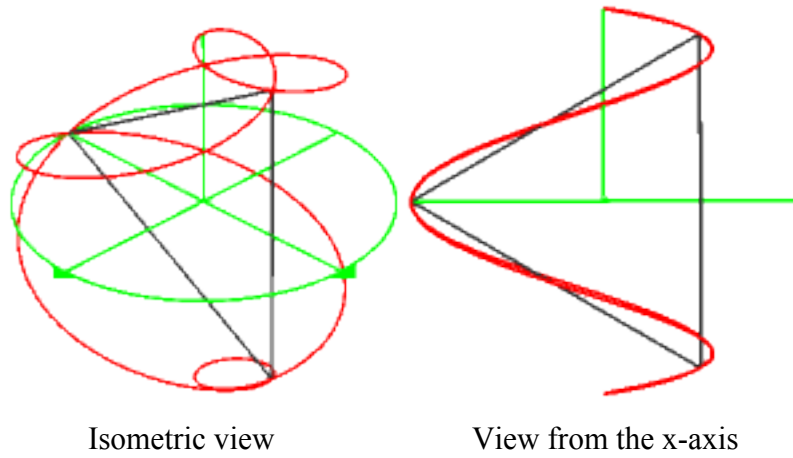


Fig. 10-2
QSO 1(3:1)

Connecting the three events of QSO 1(3:1) gives a triangle in the yz-plane. One vertex is at $(0, -1, 0)$, while the other two are at $(0, \cos 60^\circ, \pm \sin 60^\circ)$. Compared to the radius of the unit sphere, the sides of the triangle are each $1.73205\dots$, or $\sqrt{3}$ units long.

Although the vertices are located at the events of the QSO, it is evident from the side view that two of the three event-vertices do not coincide with the wave crests of the projection of the curve in the yz-plane. The first six QSOs of the 1(a:1) series are shown next with their inscribed polygons.

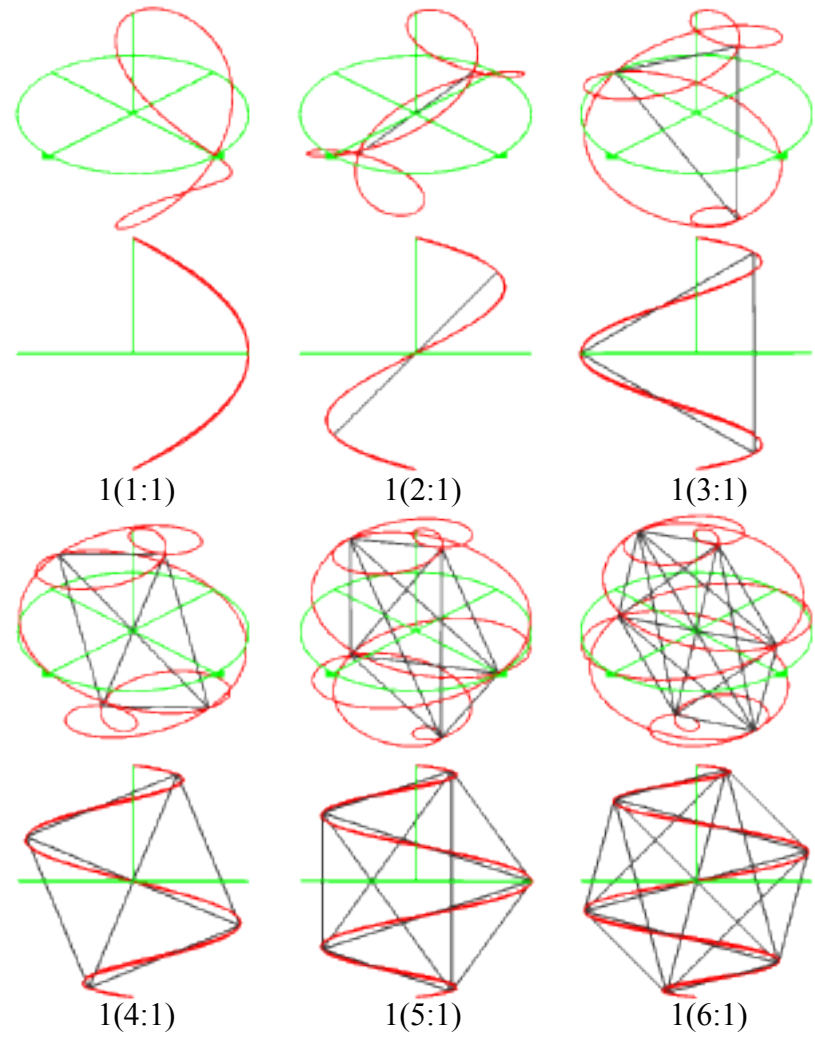


Fig. 10-3
The first six 1(a:1) QSOs and their inscribed polygons
Isometric (above) From the x-axis (below)

The first six QSO polygons of the 1(a:1) series reveal the classic point-line-plane progression. The “polygon” formed by QSO 1(1:1) is merely the point at the event. QSO 1(2:1) has two events. Connecting them gives a line segment which passes through the center of the system. It is thus a diameter. QSO 1(3:1) and all ensuing QSOs have three or more events disposed equally around a single great circle in the yz-plane. Given that the QSO ratio is (a:b), each curve of the form 1(a:1) generates *a* events. When these are connected, they form regular polygons having *a* sides.

Chord Lengths

The chord lengths of a polygon are calculated in a straightforward manner. If *C* represents the central angle subtended by a chord, then the general expression for the length *d* of any chord of a unit circle is

$$d = 2\sin\frac{C}{2}$$

Eqn. 10-1
Chord length *d*

In the QSO 1(6:1) hexagon there are six short chords around the circumference of the hexagon. These subtend central angles of 60° each. There are six intermediate chords that span two of the short chords and subtend 120°, and three diameters that span three circumferential chords and subtend 180°.

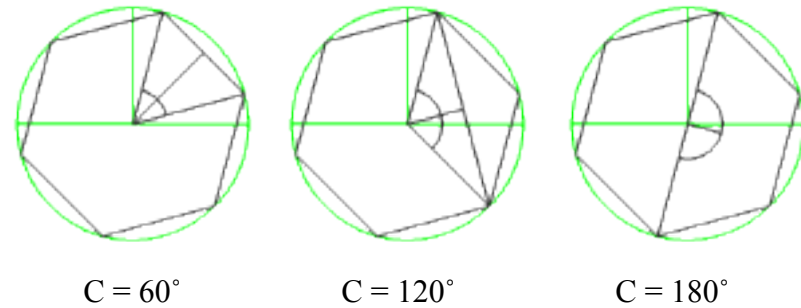


Fig. 10-4a
The three unique chords of the 1(6:1) hexagon and their central angles

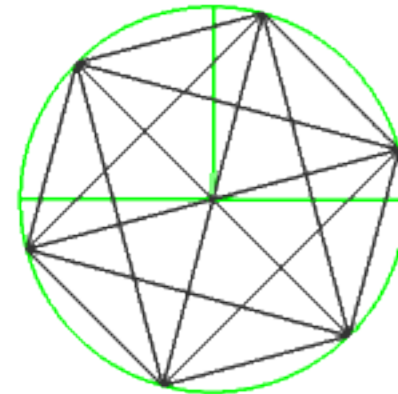


Fig. 10-4b
The 15 chords of the 1(6:1) hexagon

Calculating,

Short chords: $d = 1.00000\dots (= \sqrt{1})$

Intermediate chords: $d = 1.73205\dots (= \sqrt{3})$

Diameters: $d = 2.00000\dots (= \sqrt{4})$

In this way all the chords of the first six 1(a:1) polygons may be found.

QSO	Polygon	Number of chords & their lengths (d)
1(1:1)	Point	0 @ 0.00000... ($= \sqrt{0}$)
1(2:1)	Line	1 @ 2.00000... ($= \sqrt{4}$)
1(3:1)	Triangle	3 @ 1.73205... ($= \sqrt{3}$)
1(4:1)	Square	4 @ 1.41421... ($= \sqrt{2}$) 2 @ 2.00000... ($= \sqrt{4}$)
1(5:1)	Pentagon	5 @ 1.17557... ($2 \sin 36^\circ$) 5 @ 1.90211... ($2 \sin 72^\circ$)
1(6:1)	Hexagon	6 @ 1.00000... ($= \sqrt{1}$) 6 @ 1.73205... ($= \sqrt{3}$) 3 @ 2.00000... ($= \sqrt{4}$)

Table 10-2

The first six 1(a:1) QSO polygons and their chords

In table 10-2 most of the chord lengths can be expressed as second roots. These are just the sides of the respective polygon. The two that don't fit, the sides and diagonals of the pentagon, have no simple second root representation.

Tipping Angle

In figure 10-3 the x-axis is perpendicular to the page. It sticks directly out at the reader. In these illustrations the polygons are all rotated around the x-axis, resulting in figures that seem to be tipped from their vertical positions. The polygon 1(4:1) provides the example.

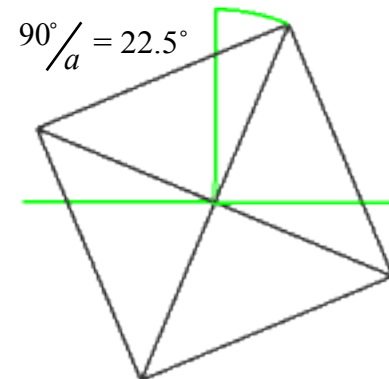


Fig. 10-5

The QSO 1(4:1) square rotated around the x-axis

In the QSO ratio (a:b), variable a controls the number of edges of the polygon. Thus, the QSO 1(4:1) polygon has four edges which are equally disposed around a great circle in the yz -plane. This makes the figure a square. Variable a also

controls rotation of the QSO around the z-axis. In chapter 2 we called this the θ -rotation. Likewise, variable b controls rotation *from* the z-axis, or what we called the ϕ -rotation in chapter two.⁴ It may be a little surprising then, to find that a , not b , controls the rotation of the QSO polygons around the x-axis. In general, the expression $90^\circ/a$ gives the number of degrees from (0, 0, 1) to the first event of the QSO. This in turn marks the location of a vertex of the polyhedron.

The inverse relationship between a and the angle of rotation results in diminishing angles as a increases. If the series 1(1:1) ... 1(6:1) is read backwards, even the “polygon” of QSO 1(1:1), which is only a single point, fits the progression.

Variable a	$90^\circ/a$
6	15°
5	18°
4	22.5°
3	30°
2	45°
1	90°

Table 10-3

The tipping angles for QSO polygons 1(6:1) through 1(1:1)

⁴ See Fig. 2-1, Eqn. 2-4.

The 1(1:b) Series

If the monopole (a:1) series of QSOs generates polygons in the yz-plane, one might expect the 1(1:b) series to do something similar.

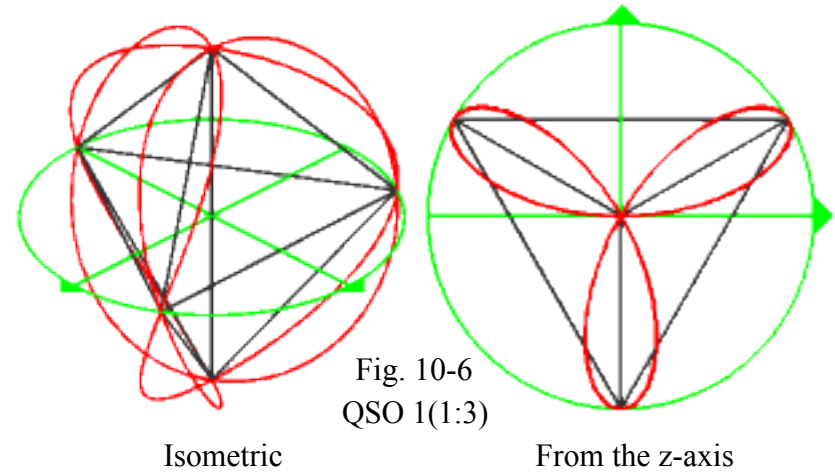


Fig. 10-6
QSO 1(1:3)

The 1(1:3), which from the z-axis is identical to the trifolium of chapter 7, generates a triangle in the xy-plane.⁵ Furthermore, when the two polar events are taken into account, there is a chord along the z-axis from $z = -1$ to $z = 1$. Connecting the two polar and three planar events yields a hexahedron, or two face-bonded tetrahedra.⁶ We have moved into the third dimension.

⁵ See p. 129.

⁶ In his amazingly detailed and apparently endless reviews of the basic polygons, Buckminster Fuller made practically no reference at all to the face-bonded pair of tetrahedra which seems to fall between the tetrahedron and the octahedron. One wonders why it was of so little interest. Didn't it fit?

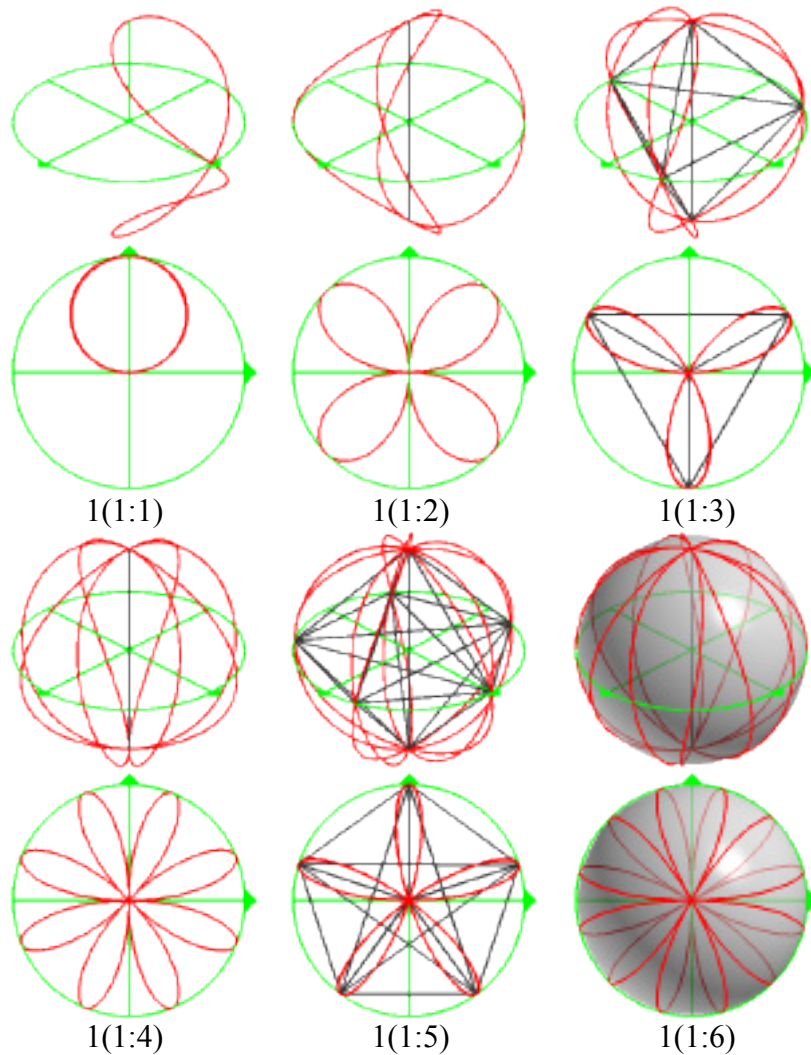


Fig. 10-7

The first six 1(1:b) QSOs and their inscribed polyhedra
 Isometric (above) From the z-axis (below)

The first six QSOs of the 1(1:b) series and their inscribed polyhedra illustrate the similarities and the differences between these and the monopole (a:1) curves. For instance, all of the 1(1:b) polyhedra show the chord along the z-axis, while none of the former curves have this feature. The 1(1:b) polyhedra develop polygons in the xy-plane, whereas the 1(a:1) series has them in the yz-plane.

However the most striking difference between the two series is probably that the 1(1:b) curves generate polyhedra only when b is odd, whereas in the former series every curve generates a polygon. Translucent unit spheres added to the views of the 1(1:6) help show why this curve and its even numbered cousins generate only the polar diameter. There are simply no equatorial events, a fact that becomes increasingly difficult to appreciate as b increases.

Chord Lengths

The lengths of the chords of the 1(1:b) polyhedra can be calculated in the same way as those of the 1(a:1) series. A tabulation of the results shows that many of the chords are identical to those previously calculated.

QSO	Polygon	Number of chords & their lengths (d)
1(1:1)	Point	0 @ 0.00000... (= $\sqrt{0}$)
1(1:2)	Line	1 @ 2.00000... (= $\sqrt{4}$)
1(1:3)	Hexahedron (2 face-bonded tetrahedra)	6 @ 1.41421... (= $\sqrt{2}$) 3 @ 1.73205... (= $\sqrt{3}$) 1 @ 2.00000... (= $\sqrt{4}$)
1(1:4)	Line	1 @ 2.00000... (= $\sqrt{4}$)
1(1:5)	Decahedron (2 face-bonded hexahedra)	10 @ 1.41421... (= $\sqrt{2}$) 5 @ 1.17557... (2 sin 36°) 5 @ 1.90211... (2 sin 72°) 1 @ 2.00000... (= $\sqrt{4}$)
1(1:6)	Line	1 @ 2.00000... (= $\sqrt{4}$)

Table 10-4
The first six 1(1:b) QSO polygons and their chords

Table 10-4 reveals that the chords in the xy-plane, if they exist, are identical to the corresponding chords of the 1(a:1) series in the yz-plane. New in the 1(1:b) series are the diameters along the z-axis and the chords in the positive and negative

z-hemispheres. A number of second roots are again apparent, but any relationship between these and the elements of the QSOs remains undiscovered.

Reversal of Orientation

The 1(1:b) polyhedra and polygons do not show rotation around any axis as do the 1(a:1) polygons. Instead, there is a periodic reversal of the orientation of the polyhedron with respect to the y-axis. The event of QSO 1(1:1) is at $y = 1$. For the 1(1:3) polygon, there is an event at $y = -1$. For 1(1:5), it's back to $y = 1$ again. Every other odd b results in a polyhedron with an event the other end of the y-axis.

Loftus QSOs: The L-1(a:1) Series

All of the QSOs and their inscribed polygons and polyhedra seen thus far have been generated with equation 2-8a.

$$\begin{bmatrix} x \\ y \\ z \end{bmatrix} = \begin{bmatrix} (\sin bgt) (\cos agt) \\ (\sin bgt) (\sin agt) \\ \cos bgt \end{bmatrix}$$

Eqn. 2-8a

The QSO equation in Cartesian notation

However, in chapter 2 it was pointed out that there are at least 763 variations of this equation. The original QSO equation by Loftus combines two of these.⁷

$$\begin{bmatrix} x \\ y \\ z \end{bmatrix} = \begin{bmatrix} (\cos t) (\cos t) \\ (\sin t) (\cos t) \\ (\sin t) \end{bmatrix}$$

Eqn. 6-1

The original QSO equation

Like equation 2-8b, Loftus' equation exchanges the x- and y-axes. It also exchanges the sine and cosine functions, as in equation 2-8h. The resulting QSOs and their inscribed figures are statically and dynamically quite different from those generated with equation 2-8a. For one thing, QSOs generated with equation 2-8a begin at (0, 0, 1), whereas those generated with Loftus' equation begin at (1, 0, 0). To keep things simple, we will look here only at the static curves at 100% of a cycle.⁸ To distinguish Loftus' curves from those generated by equation 2-8a, we will place an upper case "L" for "Loftus" in front of the QSO ratio, e.g. QSO L-1(a:b). We begin with QSO L-1(3:1).

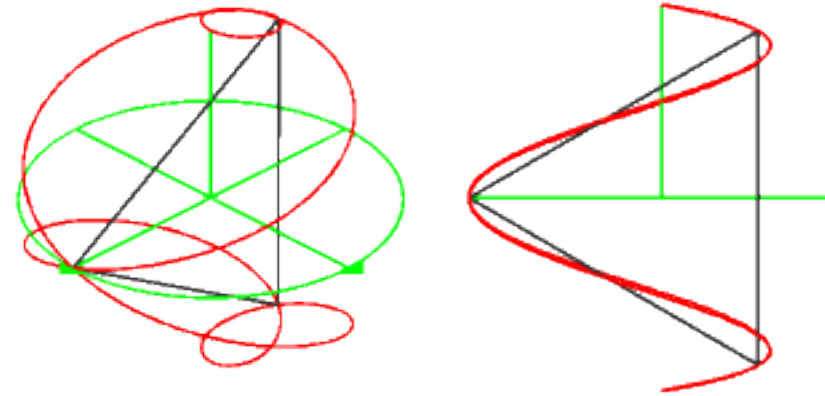


Fig. 10-8
QSO L-1(3:1)

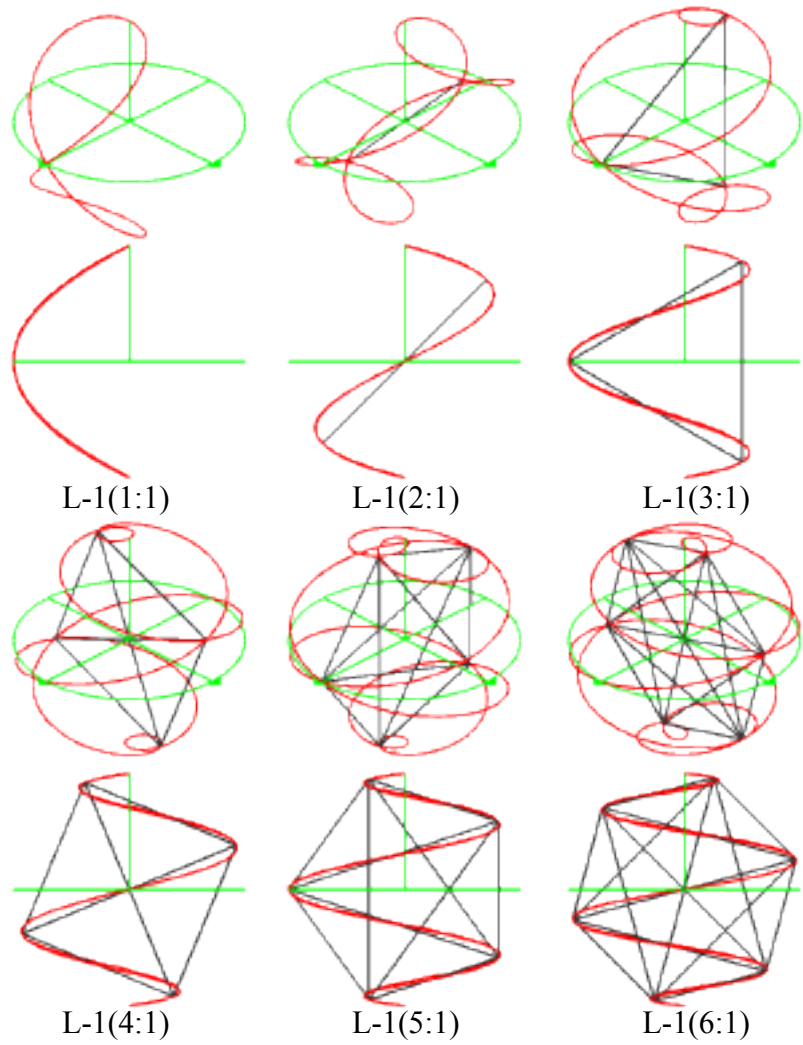
Isometric

From the y-axis

The L-1(3:1) has three events. One event is at (1, 0, 0), while the other two are at $(-\cos 60^\circ, 0, \pm \sin 60^\circ)$. Connecting these events gives a triangle in the xz-plane. This is in contrast to the QSO 1(3:1) of figure 10-2 which had the triangle in the yz-plane. The sides of the triangle are again 1.73205... each, or $\sqrt{3}$ units long relative to the radius of the unit sphere. The first six QSOs of the L-1(a:1) series are shown next with their inscribed polygons.

⁷ See p. 87.

⁸ For equation 2-8a, $t: 0 \dots 1$. However, for Loftus' equation to display a complete curve on Graphing Calculator, the range of t must be defined as $t: 0 \dots 2\pi$.



L-1(1:1) L-1(2:1) L-1(3:1)

L-1(4:1) L-1(5:1) L-1(6:1)

Fig. 10-9

The first six L-1(a:1) QSOs and their inscribed polyhedra
 Isometric (above) From the y- or x-axis (below)

On first impression, the L-1(a:1) polygons seem to be flip-flopping between planes. The single event of QSO L-1(1:1) is in the xz-plane. QSO L-1(2:1) draws a diameter in the yz-plane, and for the L-1(3:1), it's back to the xz-plane again. Looking more closely, the reason for this behavior becomes apparent. The northernmost loop that connects the z-axis with the event nearest to (0, 0, 1) tells the story. For the QSO L-1(1:1), the loop "points" toward +x. It points toward +y in the L-1(2:1), but in the L-1(3:1), the loop points toward -x. The loop of L-1(4:1) points toward -y, and so on. The L-QSOs are actually precessing around the z-axis. One may speculate that irrational or fractional L-QSOs exist between the vertical planes, but are not observable. The rational L-QSOs may then become apparent only as the precession passes through increments of 90°. It's interesting to observe that even while the L-QSOs are pirouetting around the z-axis, the chord lengths and the angle of rotation from the z-axis to the first event, what we called the tipping angle above, retain the same values they had in the previous 1(a:1) series.

Loftus QSOs: The L-1(1:b) Series

Like the monopole (1:b) series of QSOs based on equation 2-8a, the Loftus 1(1:b) QSOs generate polyhedra with a regular polygon in the xy-plane. They also alternate between polyhedra and a single chord along the z-axis. The exploration of L-1(1:b) polyhedra begins with the L-1(1:3).

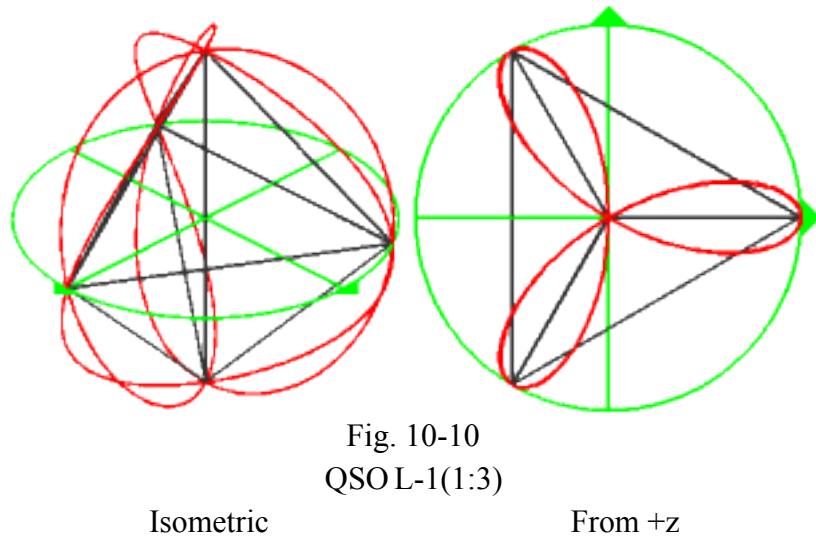


Fig. 10-10
QSOL-1(1:3)

The L-1(1:3) polyhedron looks very much like the variant generated with equation 2-8a. Two face-bonded tetrahedra occur in the positive and negative hemispheres of the z-axis with a vertical diameter between their apexes. The difference here is the orientation of the polyhedron around the z-axis. The former 1(1:3) hexahedron had a vertex at (0, -1, 0), whereas this time it's at (1, 0, 0). The polyhedron seems to have been rotated either 30° clockwise or 90° counterclockwise around the z-axis. The first six QSOs of the form L-1(1:b) show the same puzzling rotation around the z-axis suggested by the L-1(1:3). To emphasize the fact that the L-QSOs generate only the vertical diameter when *b* is even, a translucent gray unit sphere has been added to the views of the Loftus monopole (1:6).

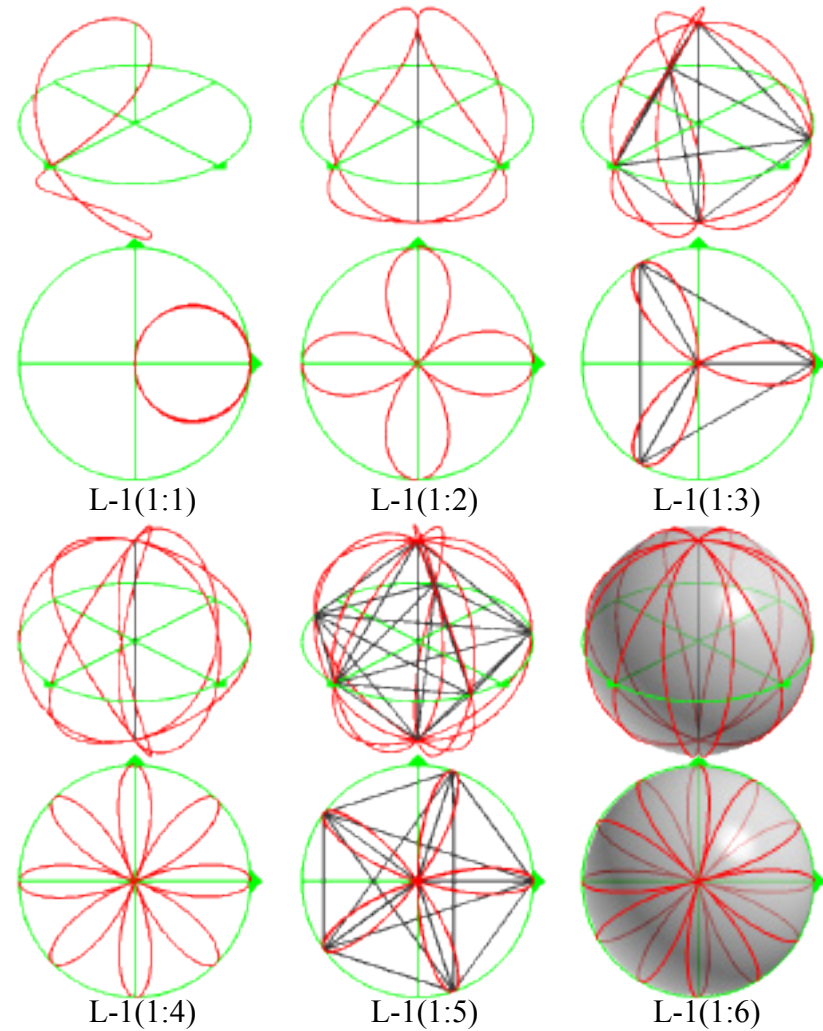


Fig. 10-11

The first six L-1(1:b) QSOs and their inscribed polyhedra
Isometric (above) From the z-axis (below)

Compared to the 1(1:b) series, the L-1(1:1) has been rotated either 90° clockwise or 270° counterclockwise. The L-1(1:2) has been rotated 45° one way or the other, and the L-1(1:3), as we said, shows either a 30° clockwise or a 90° counterclockwise rotation. Applying Ockham’s Razor⁹ we choose the simpler of the two explanations. Looking at only the clockwise rotations, the L-1(1:1) rotates 90°, the L-1(1:2) rotates 45°, the L-1(1:3) rotates 30° and so on. The angles of rotation are similar to the tipping angles listed in table 10-3, and are calculated the same way, as are the chord lengths. We leave these diversions for the reader.

a-gons & b-gons

The 1(a:1) polygons all occur in the yz-plane. Ignoring for the moment the chords along the z-axis and their related triangular faces, the 1(1:b) polygons occur in the xy-plane. Loftus’ L-1(1:b) series follows suit, while the precessing polygons from his L-1(a:1) series appear in the xz- or yz-planes and nowhere else.

	1(a:1)	1(1:b)
Eqn. 2-8a	yz	xy + z-axis
Loftus	xz or yz	xy + z-axis

Table 10-5

Planes of monopole (a:1) and monopole (1:b) polygons

QSOs along the edges of the QSO landscape seem to create polygons in a single plane. To test whether this observation is generally applicable, we need to go inland. We begin with QSO 1(1:5) and its attendant pentagon.

⁹ *Entia non sunt multiplicanda praeter necessitatem.* (Entities should not be multiplied beyond necessity.) Attributed to William of Ockham, English philosopher of the early 14th century. Often called the Law of Parsimony, in modern English it might come out as the KISS principle: “Keep it simple, Simon!”

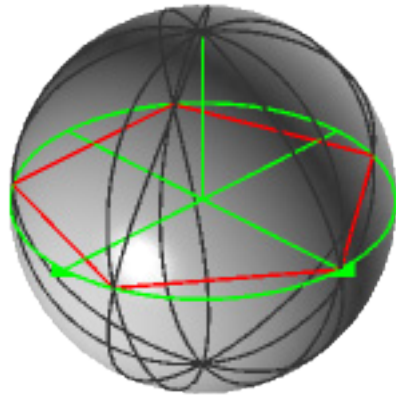


Fig. 10-12
QSO 1(1:5) and its attendant pentagon¹⁰

¹⁰ To emphasize the chords inside the QSO, the colors for the QSO and the chords have been reversed. The opaque form of the standard unit sphere is employed with the difference that the front hemisphere, i.e. that part of the sphere toward the reader, has been removed. The QSO trace is retained as a reference, but it's not the focus of attention it was previously. The point-of-view remains unchanged.

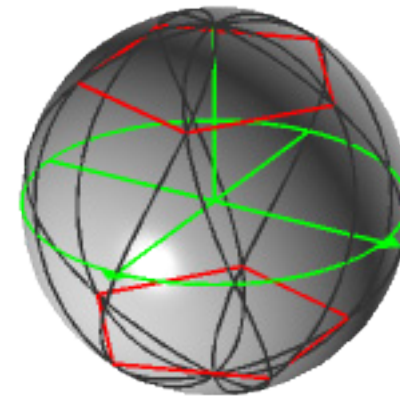
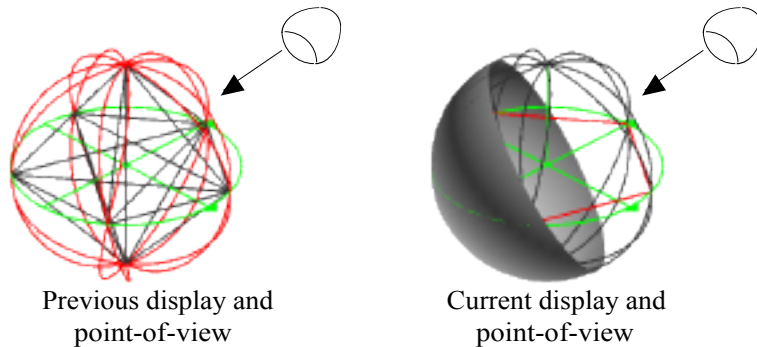


Fig. 10-13
The two 5-gons of QSO 1(2:5)¹¹

QSO 1(1:5) is shown in figure 10-12. In order to focus on the pentagon, the chords connecting events in the xy -plane with the polar events have been deleted, as have the interior chords of the pentagon itself. Missing also is the chord along the $\pm z$ -axis. Given that the QSO ratio is $(a:b)$, there are a “ b -gons,” or one 5-gon, created by the QSO. The QSO ratio predicts the number and kind of figures to be found within the curve. The 5-gon lies in the xy -plane. Its edges are $1.17557\dots$ with respect to the unit radius, and there is a vertex at $(0, 1, 0)$

QSO 1(2:5) offers two 5-gons. They lie in planes parallel to the xy -plane and at a distance of $\pm \sin 45^\circ$ from it.

($\phi = 90^\circ/a = 45^\circ$. Then $90^\circ - 45^\circ = 45^\circ$ measured from the

¹¹ To better show the figures in the QSO, the coordinate system has been rotated slightly from the isometric view.

xy-plane.) The edges of both 5-gons are 0.831254... w.r.t. the unit radius. Although they appear to be 180° out of phase, a rotation of $72^\circ/2 = 36^\circ$ around the z-axis by either of them would bring them into alignment.

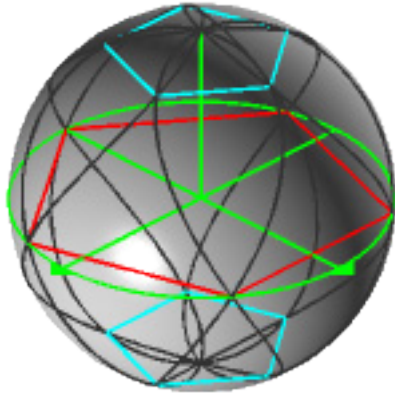


Fig. 10-14
The three 5-gons of QSO 1(3:5)

QSO 1(3:5) has three 5-gons. The larger of these lies in the xy-plane. It is identical to the 1(1:5) pentagon, and appears to be 180° out of phase with it. Where the 1(1:5) pent has a vertex at $(0, 1, 0)$, the large pent of the 1(3:5) has a vertex at $(0, -1, 0)$. However, a rotation of 36° around the z-axis would make it congruent with the former polygon. The two smaller 5-gons lie in planes parallel to the xy-plane and $\pm \sin 60^\circ$ from it.

($\phi = 90^\circ/a = 30^\circ$. Then, $90^\circ - 30^\circ = 60^\circ$ measured from the xy-plane.) Their sides are 0.587785... w.r.t. the unit radius. They are in phase with each other, and 36° out of phase with the

large 5-gon.

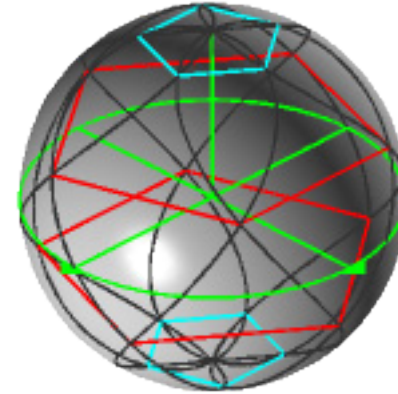


Fig. 10-15
The four 5-gons of QSO 1(4:5)

QSO 1(4:5) has four 5-gons. The two large 5-gons lie in planes parallel to the xy-plane and $\pm \sin 22.5^\circ$ from it. ($\phi = 3(90^\circ/a) = 67.5^\circ$. Then, $90^\circ - 67.5^\circ = 22.5^\circ$ from the xy-plane.) They are 36° out of phase, and their edges are 1.08608... w.r.t. the unit radius. The two smaller 5-gons lie in planes parallel to the xy-plane and at a distance of $\pm \sin 67.5^\circ$ from it. ($\phi = 90^\circ/a = 22.5^\circ$. Then $90^\circ - 22.5^\circ = 67.5^\circ$ from the xy-plane.) The edges of the smaller 5-gons are 0.449871... w.r.t. the unit radius. They are 36° out of phase w.r.t. each other and also w.r.t. the nearest large 5-gon.

In each case the ratio (a:b) predicts the polygons within the QSO. Variable a determines how many n-gons there will be while variable b specifies the number of edges they will have. In

the examples, all of the 5-gons occur either in the xy-plane or in planes parallel to it, decreasing in size as they near the poles. Each is out of phase with its nearest neighbor, but in phase with its next nearest, if any. Put another way, the phase angles of the pentagons oscillate by 36° along the z-axis.

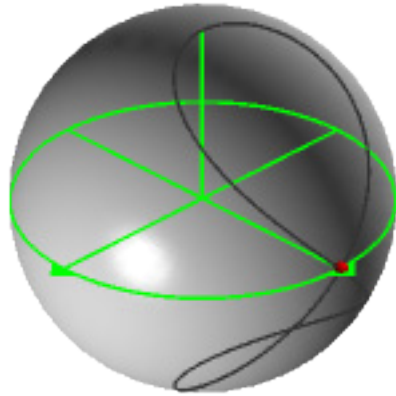


Fig. 10-16
QSO 1(5:5)

With QSO 1(5:5), the prediction formula seems to fail. There is only the single event at $(0, 1, 0)$, identified here by a small red sphere. No pentagons are visible, and certainly not the five pentas predicted by the ratio. The difficulty can be partially resolved by remembering the definition of an event from chapter four. *An event is created when the rotating point passes a minimum of two times through at least one location on the unit sphere.* This definition implies that two or more passes through the same point create only a single event. If instead we count

each pair of passes as an event, then the 1(5:5) creates, not a single 10-pass event, but 5 two-pass events per cycle. Next, when a is odd the 1(a :5) QSOs all have a 5-gon in the xy-plane. Thus the five events of the 1(5:5) can be seen as a pentagon that has collapsed into the point at $(0, 1, 0)$. This analysis still leaves four 5-gons unaccounted for.

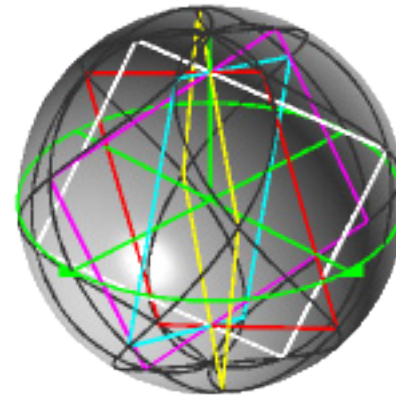


Fig. 10-17
The five 4-gons of QSO 1(4:5)

Having climbed up the QSO ratio from 1(1:5) to 1(5:5), let's now turn around and climb back down. Figure 10-17 shows QSO 1(4:5) again. Recently we saw that this QSO creates four 5-gons, a fact predicted by the QSO ratio read left to right. Here, reading the ratio in reverse, i.e. right to left, we see that it also predicts five 4-gons *in the same QSO*. Each of the 4-gons is a square with sides of $1.41421\dots$ w.r.t. the unit radius. The squares lie in vertical planes which are disposed around the

z-axis every 72° of arc. The angles at which the 4-gons are tipped from the vertical are calculated as above.

$$90^\circ/a = 22.5^\circ$$

Previously, we called the pentagons of the 1(a:5) series “b-gons,” after the variable that determines the number of edges. The present figures, and all figures similarly predicted by the QSO ratio read in reverse, are “a-gons” because the rotation variable a determines how many edges each will have.

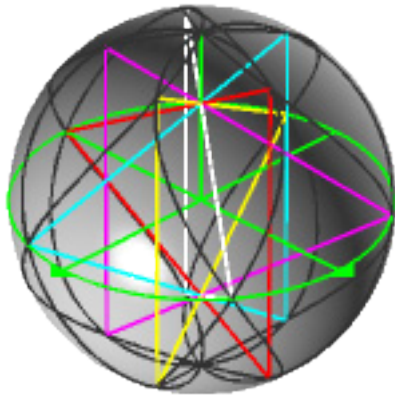


Fig. 10-18
The five 3-gons of QSO 1(3:5)

The five 3-gons of QSO 1(3:5) are equilateral triangles. Like the five 4-gons of the 1(4:5), the five 3-gons are in vertical planes arrayed around the z-axis every 72° . The tipping angles are all 30° and the edges are uniformly 1.73205... w.r.t. the unit

radius. One edge of each triangle is vertical; the opposite vertex is on the equator.

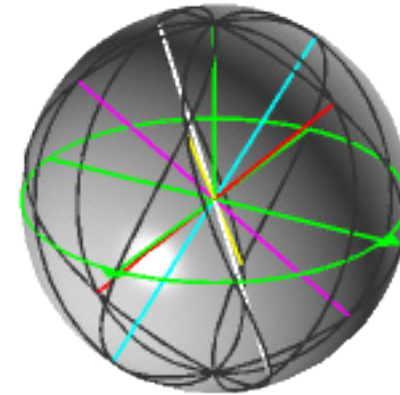


Fig. 10-19
The five 2-gons of QSO 1(2:5)

Reading the QSO ratio right to left, there should be five 2-gons in QSO 1(2:5). Although the concept of a “2-gon,” a two-sided polygon, is unfamiliar, it’s not unreasonable. Perhaps the math is telling us to count, not sides or edges, but vertices. In that case a 2-gon consists of two vertices with a single relationship between them. That is, a 2-gon is two QSO events connected by a single chord. There are five such objects in the present QSO. They are diameters, each of which connects a non-polar event in the northern hemisphere with its diametrical opposite event in the southern hemisphere.

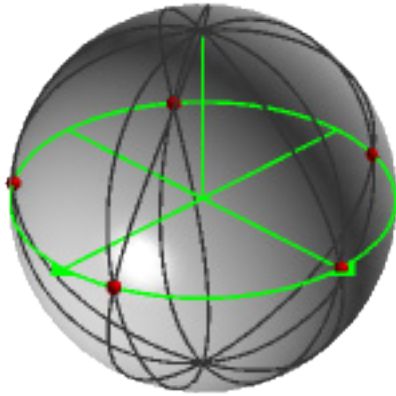


Fig. 10-20
The five 1-gons of QSO 1(1:5)

By the revised definition of a polygon developed for the 1(5:5), the five 1-gons of QSO 1(1:5) are the five events in the xy-plane, here identified by five small red spheres. They are counted, not as a single group of five, which would yield one 5-gon, but as five individual points – five 1-gons.

The z-axis

The 1(a:5) QSOs all form polar events. Yet none of these events has figured in the polygons just discussed. The question becomes, is the z-axis *ever* needed in constructing a-gons or b-gons? Previously we began with QSO 1(1:5). To investigate the involvement of the z-axis in a- and b-gons, we begin with the inverse of QSO 1(1:5), which is to say, QSO 1(5:1). The plan will be to work our way across the 1(5:b) row and back, just as we've gone from 1(1:5) to 1(5:5) and back.

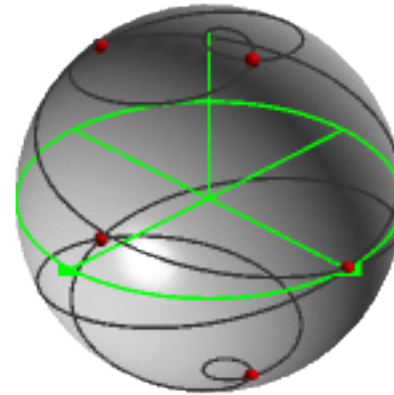


Fig. 10-21
The five 1-gons of QSO 1(5:1)

The QSO ratio read left to right predicts five 1-gons in QSO 1(5:1). These consist of the five events of the QSO, taken individually. They are in the yz-plane and occur every 72° around the x-axis. In the figure the five 1-gons are marked by small red spheres. There are no events at the poles, and the z-axis is not needed to satisfy the prediction formula.

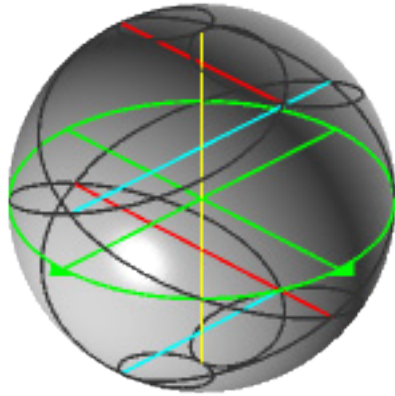


Fig. 10-22a
Five 2-gons of QSO 1(5:2)

The five 2-gons of QSO 1(5:2) consist of four horizontal lines connecting the non-polar events of the curve two at a time. The z-axis, which connects the north and south polar events, is needed to complete the total of five 2-gons. In figure 10-22a there is one long chord and one short chord in each vertical plane. The red chords are in the yz-plane; the blue ones are in the xz-plane. The long chords are 1.90211... w.r.t. the unit radius; the short ones are 1.17557.... We recognize the short chords as the sides of inscribed pentagons, while the long chords are diagonals.¹² The actual pentagons will appear shortly. The long chords are $\pm \sin 18^\circ$ from the xy-plane and parallel to it. The short chords are $\pm \sin 54^\circ$ from the xy-plane, and also parallel to it. The chords in the southern hemisphere are precessed 90° around the z-axis from their northern

¹² See Tables 10-2 & 10-4.

counterparts. Finally, the yellow chord corresponds to the diameter ($d = 2.0000\dots$) of the unit sphere along the $\pm z$ -axis.

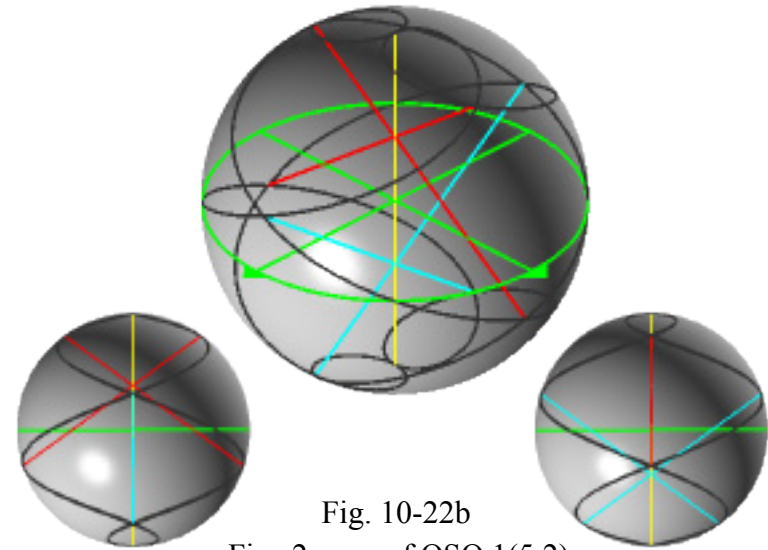


Fig. 10-22b
Five 2-gons of QSO 1(5:2)

Fig. 10-22c
View from the x-axis

Fig. 10-22d
View from the y-axis

Alternately, four of the five 2-gons in the 1(5:2) can be counted as the four diagonal lines which connect an event in the northern hemisphere with one in the southern hemisphere. The red and blue chords are in the same vertical planes as in figure 10-22a. The red chords are in the yz-plane and the blue chords are in the xz-plane. In contrast, here all four chords are the same length, $d = 1.90211\dots$, which we again recognize as the diagonal of a pentagon. As in figure 10-22a, the z-axis is needed to complete the total of five b-gons. Figures 10-22c &

10–22d show the x- and y-axis views of figure 10-22b. Many other ways of connecting the events of QSO 1(5:2) with five 2-gons are possible. Some of these involve the z-axis and some do not. These alternatives have not been explored.

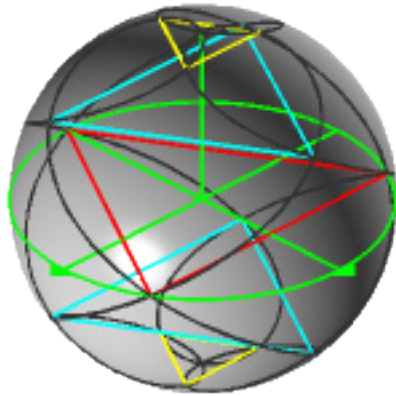


Fig. 10-23
The five 3-gons of QSO 1(5:3)

Reading the QSO ratio forward, QSO 1(5:3) forms five 3-gons. The chord connecting the polar events is not needed. The largest of the 3-gons is in the xy-plane with a vertex at $y = -1$. Edges of the large 3-gon are $1.73205\dots$, thus making it identical to the 3-gon of QSO 1(1:3). The next largest 3-gons are $120^\circ/2 = 60^\circ$ out of phase with the large one, but in phase with each other. They're in planes parallel to the xy-plane and $\pm\sin 36^\circ$ from it. Edges are $1.40125\dots$. The small yellow 3-gons near the poles echo the orientation of the large red one and of each other. They are in planes parallel to the xy-plane

and $\pm\sin 72^\circ$ from it. The edges of the yellow 3-gons are $0.535233\dots$. It's worth noting that the five 3-gons of QSO 1(5:3) read forwards are not the same as those of the 1(3:5) read in reverse. The 3-gons in the present example are in horizontal planes whereas those of the former QSO are in vertical planes. In general, the a- or b-gon of a given QSO is not identical to the b- or a-gon of its inverse.

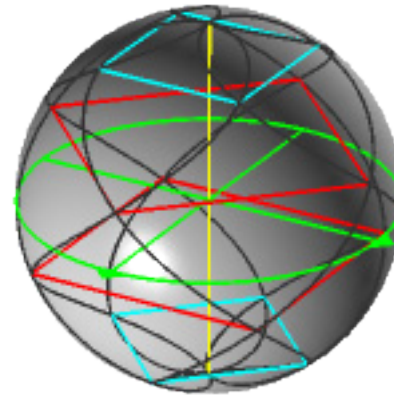


Fig. 10-24
The five 4-gons of QSO 1(5:4)

Four of the five 4-gons of the QSO are immediately apparent. There are two large squares with sides of $1.34499\dots$ at distances of $\pm\sin 18^\circ$ from the xy-plane. They are out of phase by $90^\circ/2 = 45^\circ$. There are also two smaller 4-gons with sides of $0.831254\dots$ at distances of $\pm\sin 54^\circ$. These too are out of phase by 45° with each other and also with their nearest large neighbor. This leaves the z-axis to complete the fifth 4-gon. By

the revised definition of an event, there are four passes of the rotating point at each of the poles which create two events at each pole. Thus the z-axis connects four events, two at $z = 1$ and two at $z = -1$, making the 4-gon.

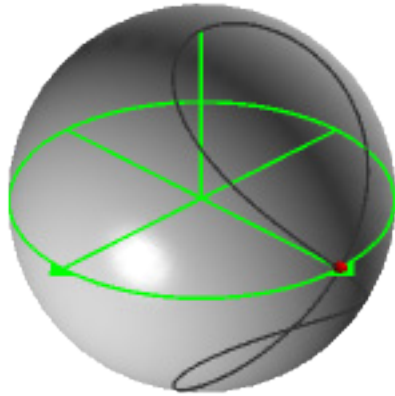


Fig. 10-25
QSO 1(5:5)

The problem with QSO 1(5:5) is the same as before. There should be five 5-gons, but even with the revised definition of an event, only one can be found. Where are the other four? A similar situation occurs in all of the equal ratio QSOs. One a- or b-gon will be found, but not the multiples suggested by the QSO ratio.

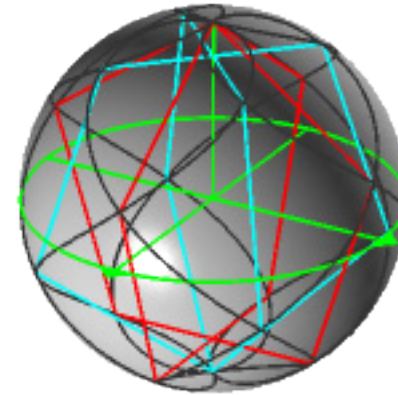


Fig. 10-26
The four 5-gons of QSO 1(5:4)

As advertised, we'll now take a look at the 1(5:b) series reading the QSO ratio in reverse. The first of these is QSO 1(5:4) which creates four 5-gons. They are arrayed around the z-axis in vertical planes 45° apart. In the illustration, two red pentagons are in the xz- and yz-planes, and two blue ones are in vertical planes rotated 45° from the orthogonal planes. The two red 5-gons have vertices at $z = 1$, while the blue ones have vertices at $z = -1$. The sides of all four figures are 1.17557.... The z-axis is not needed.

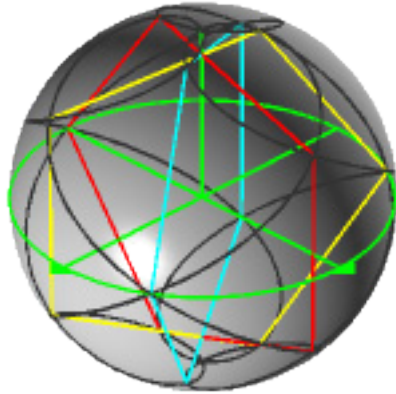


Fig. 10-27

The three 5-gons of QSO 1(5:3)

The three 5-gons of QSO 1(5:3) are arrayed in vertical planes every 120° around the z -axis. The red 5-gon is in the yz -plane with a vertex at $y = -1$. The yellow 5-gon is rotated -120° , and the blue one is rotated $+120^\circ$ from the y -axis. The tipping angle for all three is $\phi = 90^\circ/a = 18^\circ$, while the edges are all $1.17557\dots$ relative to the unit radius. Again the z -axis is not needed to make any of the polygons.

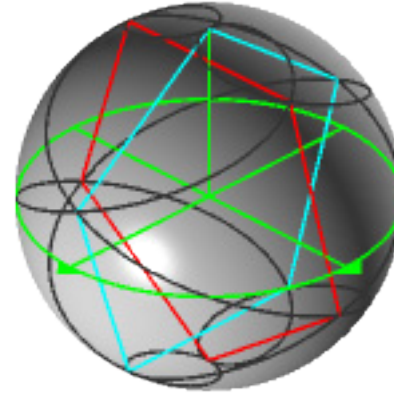


Fig. 10-28

The two 5-gons of QSO 1(5:2)

The two 5-gons of QSO 1(5:2) occur in the xz - and yz -planes. The red 5-gon in the yz -plane has a vertex at $z = -1$, whereas the blue one in the xz -plane has a vertex at $z = 1$. The sides of the pentagons are $1.17557\dots$, as usual. Each 5-gon can be seen as tipped from the pole opposite the pole with the vertex. The tipping angle in both cases is $\phi = 2(90^\circ/a) = 36^\circ$. A chord along the z -axis is not needed to make either 5-gon.

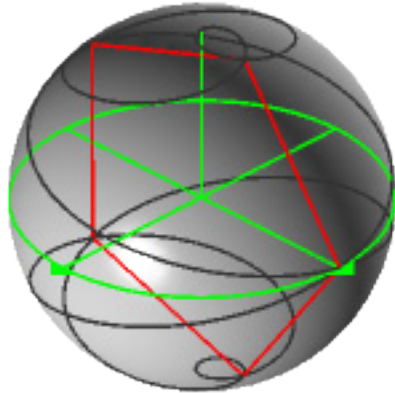


Fig. 10-29
The single 5-gon of QSO 1(5:1)

The five events of QSO 1(5:1), when taken together, make a single 5-gon in the yz-plane. The edges are $1.17557\dots$ w.r.t. the unit radius, and it's tipped at $\phi = 90^\circ/a = 18^\circ$ from the north pole.

So far the 1(a:5) and the 1(5:b) QSOs have shown little propensity to form n-gons with the z-axis. Only the 1(5:2) and the 1(5:4) have such chords, and even that's only when the QSO ratio is read left to right. Fortunately, with a little patience this dearth of data can be turned into a pattern.

Left to right	N	Y	N	Y	N
The QSO ratio	5:1	5:2	5:3	5:4	5:5
Right to left	N	N	N	N	N
Left to right	N	N	N	N	N
The QSO ratio	4:1	4:2	4:3	4:4	4:5
Right to left	N	N	N	N	N
Left to right	N	Y	N	Y	N
The QSO ratio	3:1	3:2	3:3	3:4	3:5
Right to left	N	N	N	N	N
Left to right	N	N	N	Y	N
The QSO ratio	2:1	2:2	2:3	2:4	2:5
Right to left	N	N	N	Y	N
Left to right	N	Y	N	Y	N
The QSO ratio	1:1	1:2	1:3	1:4	1:5
Right to left	N	N	N	N	N

Table 10-6
z-axis chords in the QSO landscape

The pattern of z-chord involvement in the polygons of the first 25 QSOs is revealed in table 10-6. An upper case "N" for "No" indicates that the z-chord is not present, whereas an upper case "Y" for "Yes" indicates that it is. The table tabulates only the presence or absence of a chord along the z-axis. No other attributes of the curves are recorded. As noted above, even with the revised definition of an event, the equal rate QSOs seem to be missing some polygons. However, outside the central diagonal, the pattern seems to be that the z-chord occurs only when the QSO ratio is read left to right, a is odd and b is even. This is deceptive, though. The 1(2:4) uses a z-chord coming and going,

while the 1(4:2), does not need the z-chord at all. Curiously, neither of these curves makes the full compliment of chords predicted by the QSO ratio. The 1(2:4) read left to right makes only one 4-gon, not the two predicted by the ratio. Similarly, the 1(4:2) read left to right makes only two 2-gons, not the anticipated four. Reading right to left, the 1(2:4) creates only two of the four predicted 2-gons, while the 1(4:2) has only half of its presumed compliment of two 4-gons. One wonders if the landscape were extended whether this pattern would persist at higher frequencies.

From a-gons and b-gons to Polyhedra

Although this chapter is entitled “Monopole Polygons & Polyhedra,” we have seen precious few polyhedra. Burke’s 1(3:2) tetrahedron was mentioned on the first page. The 1(1:3) hexahedron and the 1(1:5) decahedron appeared briefly in both their incarnations, that of equation 2-8a and Loftus’ version, but that’s about it. Intending no slight to the three dimensional objects, we will next assemble the a-gons, b-gons, diagonals and diameters to make a complete polyhedron. The example will be QSO 1(3:4).

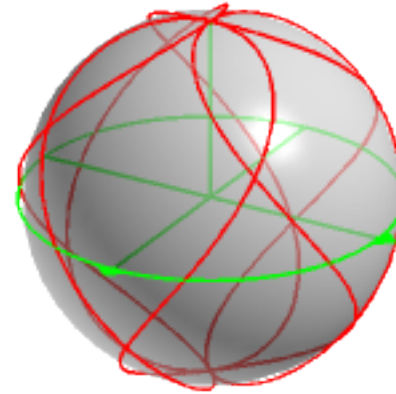


Fig. 10-30
QSO 1(3:4)

QSO 1(3:4), seen here slightly rotated from the isometric view, has four non-polar events in the northern hemisphere and four more in the southern. Each of these is a two-pass event, i.e. they are created by two passes of the rotating point. The events at the poles are created by four passes of the rotating point. Thus there are two events at each pole. Statically, the QSO appears to have 10 events; dynamically it has 12. The QSO is displayed on a translucent unit sphere. The sphere has no structural meaning. It’s only purpose is to help differentiate front from back.

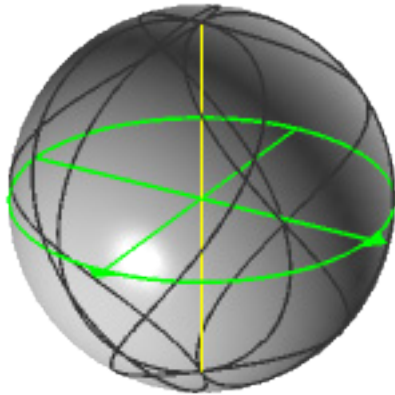


Fig. 10-31
 The QSO 1(3:4) polyhedron
 One chord @ 2.00000... ($= \sqrt{4}$)

We begin with the longest chords of the polyhedron, those between the poles. Statically, we connect the north pole and the south pole with a single chord. However, dynamically we're connecting two events at the north pole with two more at the south pole. There are six relationships between four points.¹³ Thus there are at least two chords present, and, if one counts all the possibilities, as many as six. There are four nonzero-length chords between the north and south poles, a zero-length chord between the two north polar events and another between the two south polar ones. The nonzero chords are 2.00000... long with respect to the unit radius.

¹³ The tetrahedron and the square are the classic examples of four events with six relationships between them.

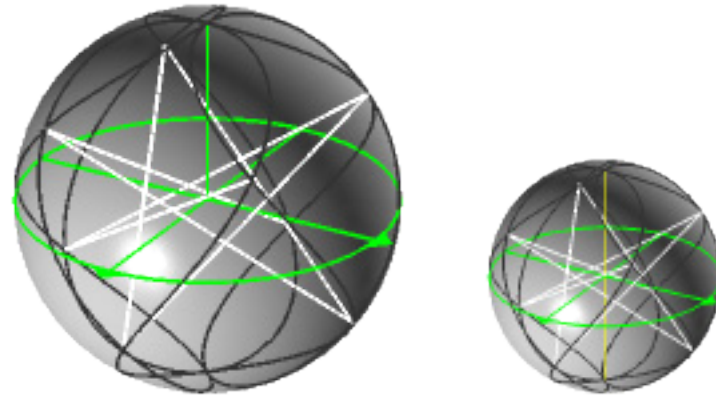


Fig. 10-32
 The QSO 1(3:4) polyhedron
 Eight chords @ 1.88697...

The next longest chords are those that connect the non-polar events in one hemisphere to those in the other. There are eight such chords, shown above in white. They are 1.88697... long. We do not try to connect a given event in either hemisphere to all non-polar events in the opposite hemisphere. To do so would require chords that differ in length from those illustrated. The small graphic keeps a running account of the chords as we build the polyhedron.

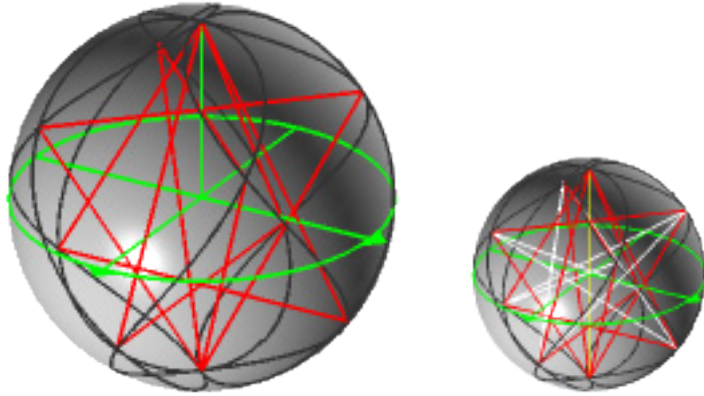


Fig. 10-33

The QSO 1(3:4) polyhedron

Twelve chords @ $1.73205\dots (= \sqrt{3})$

The next chords are those of the four 3-gons predicted by the QSO ratio read right to left. There are four equilateral triangles in vertical planes 45° apart. The two in the xz - and yz -planes have a vertex at $z = 1$. Those in planes rotated 45° from the xz - and yz -planes have a vertex at $z = -1$. These chords are all $1.73205\dots$ w.r.t. the unit radius.

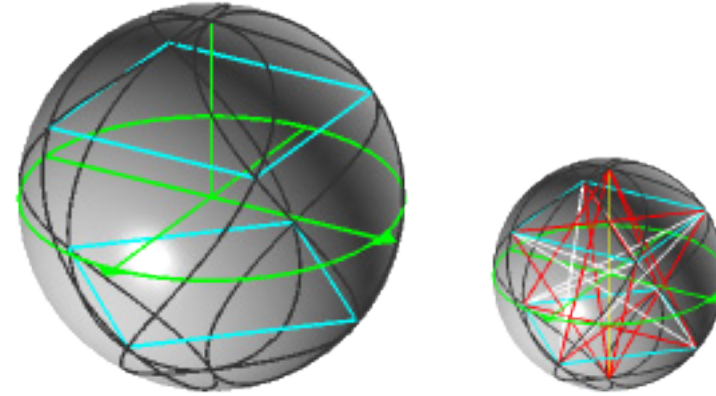


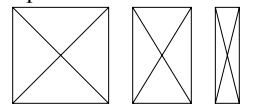
Fig. 10-34

The QSO 1(3:4) polyhedron

Eight chords @ $1.22474\dots (= \sqrt{1.5})$

The QSO ratio read left to right predicts three 4-gons. Two of these are shown above, with edges of $1.22474\dots$. The edges of the 4-gon in the northern hemisphere are parallel to the x - and y -axes. The diagonals of the one in the southern hemisphere are similarly parallel to the x - and y -coordinate axes. Both 4-gons are in planes parallel to the xy -plane and $\pm \sin 30^\circ$ from it. The third 4-gon is the collapsed polygon along the $\pm z$ -axis.¹⁴

¹⁴ The polygon along the z -axis can be seen as the result of the collapse of a square.



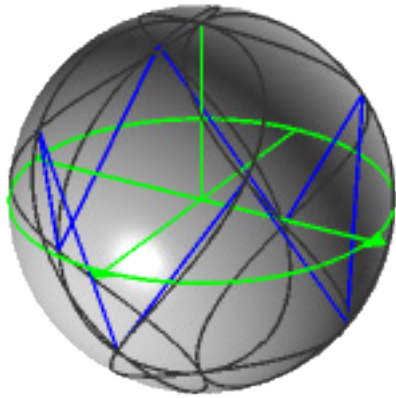


Fig. 10-35
The QSO 1(3:4) polyhedron
Eight chords @ 1.19972...

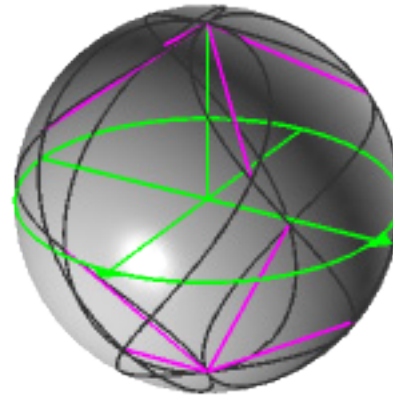
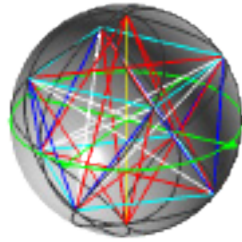
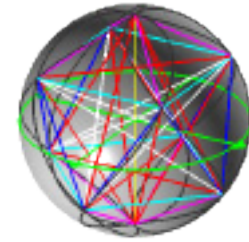


Fig. 10-36
The QSO 1(3:4) polyhedron
Eight chords @ 1.00000... (= $\sqrt{1}$)



The next to shortest chords are those that connect a non-polar event in one hemisphere with its two nearest neighbors in the opposite hemisphere. These eight chords are 1.19972... long. They form a jagged ring around the equator of the QSO. The small graphic shows an increasingly complex figure.

The shortest chords in the 1(3:4) polyhedron are those that connect the two polar events in a given hemisphere with the four non-polar events in the same hemisphere. These are 1.00000... long.

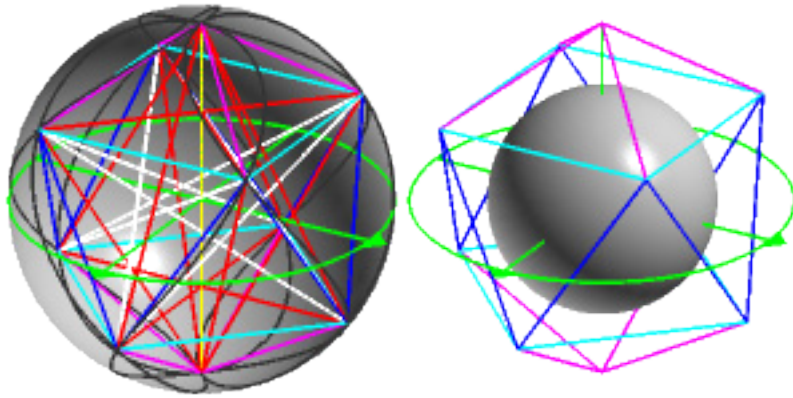


Fig. 10-37

The QSO 1(3:4) polyhedron
66 (45) chords The 16-hedron

Figure 10-37 on the left shows the complete QSO 1(3:4) polyhedron against a backdrop of the concave opaque unit hemisphere. Sixty-six chords are needed to connect its 12 events. However, only ten of these events are distinguishable to the eye, so it appears as if there are only 45 chords in the sketch. The reader is invited to figure out which chords are doubled and/or quadrupled to account for the 21 chord difference.

In figure 10-37 on the right the three sets of the longest chords have been deleted, as well as the QSO trace and the background hemisphere. This leaves only the surface chords. The polyhedron looks like a fairly ordinary 16-hedron. The opaque sphere ($r = 0.6$) helps give depth to the figure.

The conventional approach to a polyhedron typically sees only the surface chords as depicted on the right. In chapter one

we learned that we need to pay attention to all views of a QSO. Looking at them from only one point-of-view gives incomplete information and leads to misunderstanding. Here the lesson is to pay attention to all the chords of QSO polyhedra. Otherwise we again have incomplete information and may seriously underestimate the complexity of the objects.

The Platonic Solids

The Platonic solids are the five-and-only-five regular convex polyhedra with congruent faces, edges and angles. Although evidence suggests that at least some of them have been known since prehistoric times, they figure prominently in the philosophy of Plato after whom they are named.



Fig. 11-1
The Platonic solids¹

Reading counterclockwise from lower left, figure 11-1 shows the tetrahedron, octahedron, hexahedron or cube,

icosahedron and dodecahedron. When the polyhedra all have equal edges, as they do in Fig. 11-1, their volumes range from the tetrahedron, which has the smallest volume, to the dodecahedron, which has the greatest. We began the last chapter with Burke's discovery that QSO 1(3:2) generates a tetrahedron when the events of the QSO are connected by straight lines. It's time to revisit that discovery.

The QSO 1(3:2) Tetrahedron

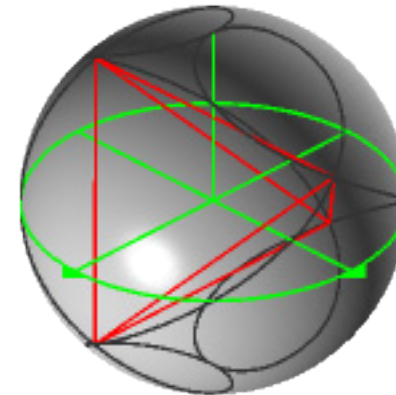


Fig. 11-2a
QSO 1(3:2) and its inscribed tetrahedron

¹ Photograph © David S. Gunderson, 2003. Used with permission.

Ignoring for the moment the events at $\pm z$, when each of the four non-polar events is connected to the other three they generate a tetrahedron. The first thing we notice about the QSO tetrahedron is its orientation. Although the Platonic solids are often depicted as sitting on a face as in figure 11-1, the QSO tetra has an edge-zenith orientation.²

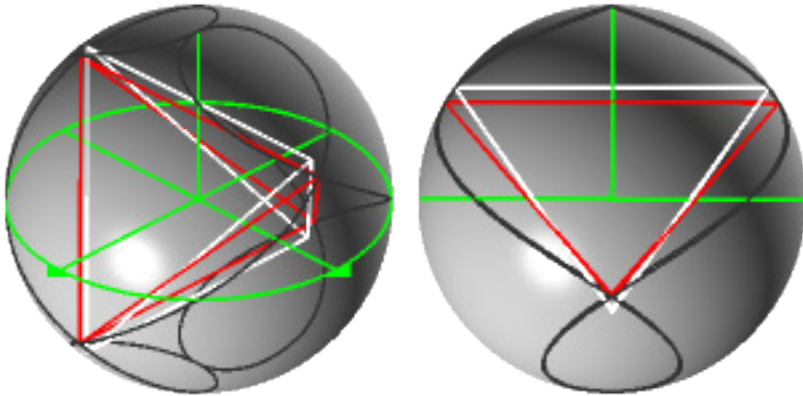


Fig. 11-2b

QSO 1(3:2) and its inscribed tetrahedron (red)

compared to a regular tetrahedron (white)

Isometric view

View from the x-axis

What may not be so obvious is that the QSO tetrahedron is polarized. The two horizontal edges are 1.73205... with respect to the radius of the unit sphere,³ while the other four are 1.58114.... Thus, the QSO polyhedron is not the Platonic solid, but a polarized analog of that figure. The QSO

² This chapter continues the practice of displaying the chords connecting the events of the QSO inside a hollow unit radius hemisphere.

³ See also Figs. 10-3 & 10-9, and Tables 10-2 & 10-4.

polyhedron is an oblate tetrahedron. Its vertical dimension is less than its equatorial diameter. By way of comparison, the edges of the regular tetrahedron, when inscribed in the unit sphere, are 1.63299... w.r.t. the unit radius.

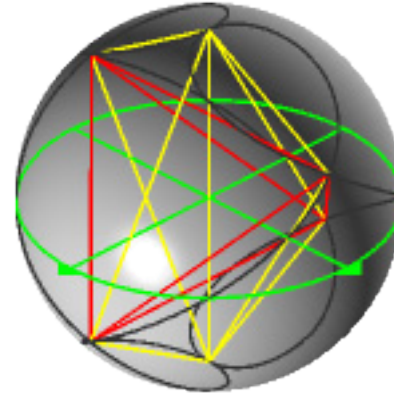


Fig. 11-2c

QSO 1(3:2) with the fully connected inscribed polyhedron

To complete the polyhedron, each event must be connected to every other event. Since there are six total events, there are fifteen total chords.⁴ Put another way, each event must connect to five others. This makes a fairly complex figure. In addition to the original tetrahedron, there are two low altitude isosceles triangles at the poles and two equilateral triangles, one in the xz -plane and one in the yz -plane. Last, there is a chord along the z-axis connecting north and south poles. The QSO 1(3:2)

⁴ The number of unique chords T_n needed to connect n events is

$$T_n = \frac{n(n-1)}{2} \text{ See also Fig. 10-4b and Table 10-2.}$$

tetrahedron is shown above in red with the additional chords to and from the polar events in yellow. Structurally and conceptually there is no difference between the red and yellow chords. They all represent a linear relationship between two events. Color is used solely to distinguish the tetrahedron from the chords added later. Chord lengths are tabulated in the following table.

The QSO 1(3:2) polyhedron
4 @ 1.0000... (= $\sqrt{1}$)
4 @ 1.58114... (= $\sqrt{2.5}$)
6 @ 1.73205... (= $\sqrt{3}$)
1 @ 2.0000... (= $\sqrt{4}$)
The regular tetrahedron
6 @ 1.63299... (= $\sqrt{\frac{8}{3}}$)

Table 11-1
The chords of the QSO 1(3:2) polyhedron compared to those of the regular tetrahedron

The QSO 1(2:3) Octahedron

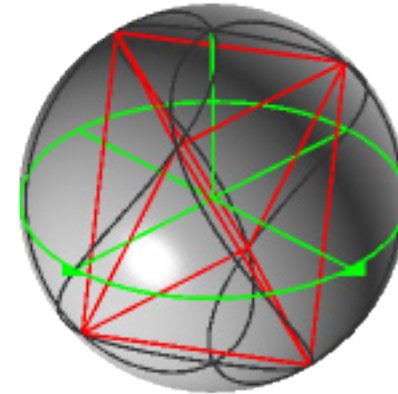


Fig. 11-3a
QSO 1(2:3) and its inscribed octahedron

The inverse of QSO 1(3:2) is QSO 1(2:3), which also generates an analog of a Platonic solid. Ignoring again the events at $\pm z$, the three non-polar events in the northern hemisphere, when connected to the three non-polar events in the south, form an octahedron. This is not the octahedron that was used to illustrate Bucky Fuller’s great circle railroad tracks of energy in the introduction, a topic to which we will return briefly in the next chapter. The orientation is more conventional than that of the QSO 1(3:2) tetrahedron. The QSO 1(2:3) octahedron sits on a face with the opposite face toward the zenith.

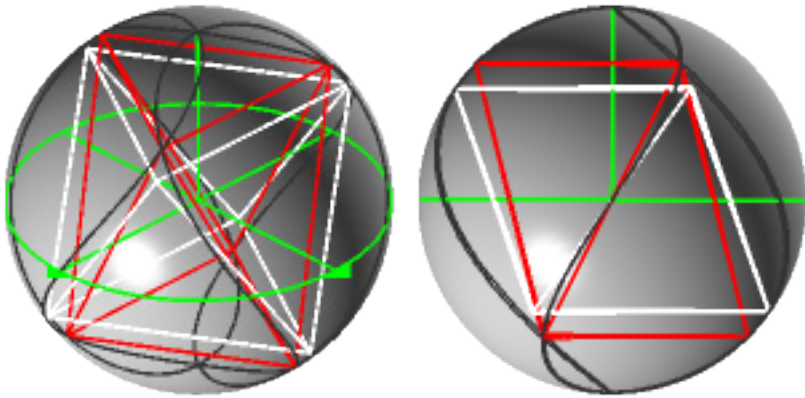


Fig. 11-3b

QSO 1(2:3) and its inscribed octahedron (red)
compared to a regular octahedron (white)

Isometric view

View from the x-axis

Like the QSO 1(3:2) tetrahedron, the QSO 1(2:3) octahedron is also polarized. Unlike the QSO tetrahedron, the QSO octa is clearly taller and skinnier than its regular counterpart. It's a prolate octahedron with the vertical dimension greater than the equatorial diameter. The six horizontal chords in the northern and southern hemispheres are 1.22474... while the six chords connecting them are 1.58114... compared to the unit radius.

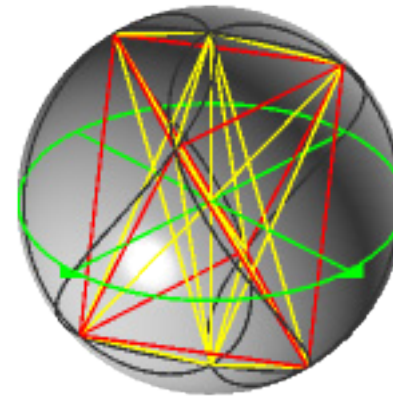


Fig. 11-3c

QSO 1(2:3) with the fully connected inscribed polyhedron

There are 28 total chords in the QSO 1(2:3) polyhedron.⁵ Connecting the polar events to the three non-polar events in their own hemisphere adds two low-altitude tetrahedra at the north and south poles. Connecting each polar event with the three non-polar events in the opposite hemisphere yields two more isosceles tetrahedra,⁶ and connecting each of the four northern events with its southern counterpart creates four diameters. As before, there is nothing structurally or conceptually different about the red and yellow chords. They all connect two events. Color is used solely to distinguish the octahedron from the

⁵ See p. 186, footnote 4.

⁶ The conventional meaning of “isosceles” is “having two equal legs.” However, the notion of “two” is absent from *iso-* [equal, identical, similar], as it is from *skelos* [leg]. Thus we may permit ourselves to identify a tetrahedron having three isosceles triangles as faces as an “isosceles tetrahedron.” Note that the two low-altitude tetrahedra at the north and south poles are also isosceles tetras.

chords added later. The chord lengths are tabulated next.

The QSO 1(2:3) polyhedron
6 @ 0.765367... (= 2 sin 22.5°)
6 @ 1.22474... (= $\sqrt{1.5}$)
6 @ 1.58114... (= $\sqrt{2.5}$)
6 @ 1.84776... (= $\sqrt{2 + \sqrt{2}}$)
4 @ 2.0000... (= $\sqrt{4}$)
The regular octahedron
12 @ 1.41421... (= $\sqrt{2}$)

Table 11-2
The chords of the QSO 1(2:3) polyhedron compared to those of the regular octahedron

The QSO 1(2:5) Icosahedron

For reasons which will become apparent in the next chapter, we will skip the cube for now and go directly to the icosahedron.

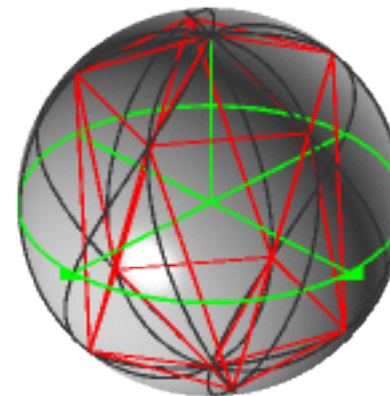


Fig. 11-4a
QSO 1(2:5) and its inscribed icosahedron

An icosahedron is generated by QSO 1(2:5). The five non-polar events in the northern hemisphere, when connected to the north polar event, form a pentacap of the icoso. The same is true of the five non-polar events in the southern hemisphere. Connecting the five non-polar events in each hemisphere with their opposite number completes the figure.

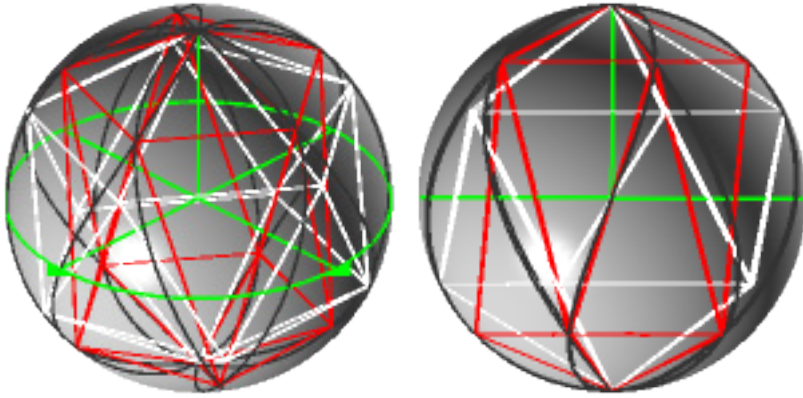


Fig. 11-4b

QSO 1(2:5) and its inscribed icosahedron (red)
compared to a regular icosahedron (white)

Isometric view

View from the x-axis

Again we see that a QSO polyhedron is polarized compared to its regular counterpart. The QSO 1(2:5) icosahedron is clearly prolate, perhaps even more so than the 1(2:3) octahedron. The 10 chords connecting the north and south poles with the five nearest events in each hemisphere are $0.765367\dots$. The 10 horizontal chords in each hemisphere are $0.831254\dots$, and the 10 connecting the hemispheres are $1.4802\dots$ w.r.t. the unit radius.

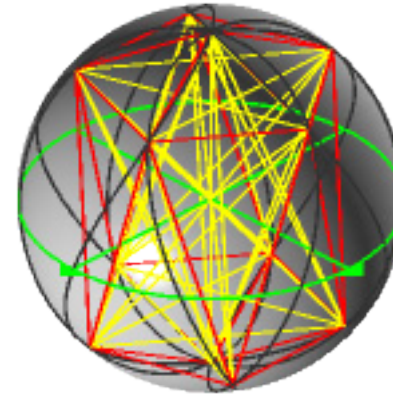


Fig. 11-4c

QSO 1(2:5) with the fully connected inscribed polyhedron

Like its regular counterpart, the QSO 1(2:5) icosahedron has twenty faces, twelve vertices and thirty edges. However, the twelve event-vertices imply a total chord count, not of thirty, but of sixty-six chords necessary to complete the figure. Above without further analysis is the fully connected 1(2:5) polyhedron. The 66 chords of the fully connected polygon are tabulated next.

The QSO 1(2:5) polyhedron
10 @ 0.765367... (= 2 sin 22.5°)
10 @ 0.831254... (= (cos 45°)(2 sin 36°))
10 @ 1.3445...
10 @ 1.4802...
10 @ 1.81907... (= $\sqrt{3 + \cos 72^\circ}$)
10 @ 1.84776... (= $\sqrt{2 + \sqrt{2}}$)
6 @ 2.00000... (= $\sqrt{4}$)
The regular icosahedron
30 @ 1.05146... (= 2 sin (0.5 tan ⁻¹ 2))

Table 11-3
The chords of the QSO 1(2:5) polyhedron compared to those of the regular icosahedron

In Pursuit of the Elusive Dodecahedron


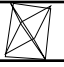

	(6:1)	(6:2)	(6:3)	(6:4)	(6:5)	(6:6)
	(5:1)	?	(5:3)	(5:4)	(5:5)	(5:6)
	(4:1)	(4:2)	(4:3)	(4:4)	(4:5)	(4:6)
	(3:1)		(3:3)	(3:4)	(3:5)	(3:6)
	(2:1)	(2:2)		(2:4)		(2:6)
$a \uparrow$	(1:1)	(1:2)	(1:3)	(1:4)	(1:5)	(1:6)
(a:b)	$b \rightarrow$					

Table 11-4
The QSO landscape with the three QSO analogs to the Platonic tetrahedron, octahedron and icosahedron

A polarized tetrahedron is created by QSO 1(3:2). Its inverse, QSO 1(2:3), creates a polarized octahedron. It seems reasonable then, to look for the dodecahedron, polarized or not, in the inverse of QSO 1(2:5), which is to say QSO 1(5:2).⁷

⁷ Inversion is a better tool to look for the dodecahedron than is the concept of duals. The dual of the tetrahedron is the tetrahedron itself, which says nothing about the octahedron. The dual of the octahedron is the cube, which we haven't found yet, and, while the dual of the icosahedron is the dodecahedron, knowing that gives no indication of where to look for it.

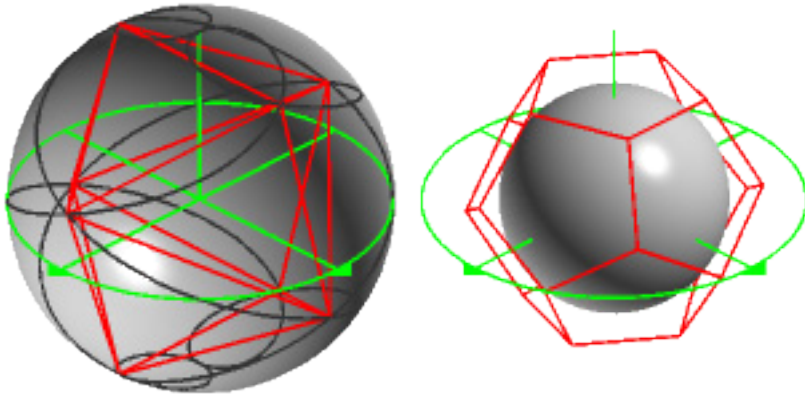


Fig. 11-5a

QSO 1(5:2) and its
inscribed polyhedron

The Platonic dodecahedron

On the left, the QSO 1(5:2) polyhedron. On the right, the Platonic dodecahedron. The QSO polyhedron appears inside a hollow unit hemisphere to remind us that it is the result of connecting the events of a QSO curve. The Platonic solid is shown in a more conventional setting with an opaque sphere ($r = 0.6$) inside the figure since there is (so far) no QSO that creates it.

One thing is certain, and that is that the QSO polyhedron is not the Platonic solid we sought. Undeterred, we count the vertices, edges and faces of the present figure. There are eight vertices, eighteen edges and twelve triangular faces. Amazingly, it's a dodecahedron, just not the Platonic dodeca. If the faces were equilateral triangles, the figure would be the snub disphenoid, one of the 92 Johnson solids. Specifically it would

be #J₈₄.⁸ Would it be fair to refer to the QSO polyhedron as the “QSO snub disphenoid”? Or, following a suggestion in chapter 7, perhaps “Burchester snub disphenoid” would suffice.⁹

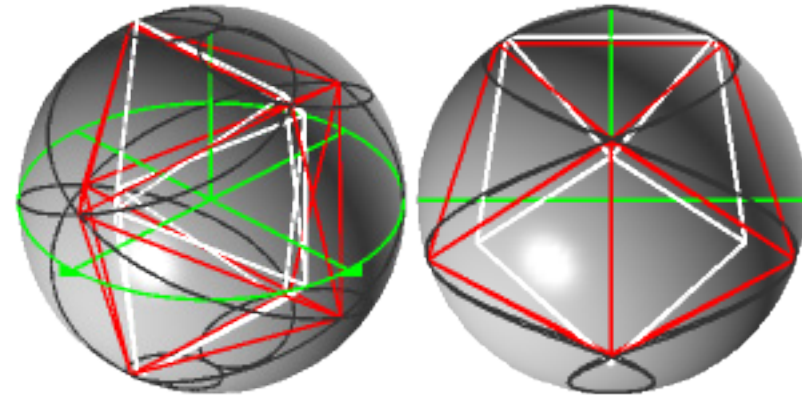


Fig. 11-5b

QSO 1(5:2) dodecahedron (red)
compared to the snub disphenoid (white)
Isometric view View from the x-axis

Here again we find that a QSO polyhedron is the polarized analog of a known geometric figure. There are six chords at 1.17557... , eight at 1.22474... , and four at 1.4802... compared to the unit radius. Like the 1(3:2) tetrahedron, the QSO 1(5:2) is an oblate figure. One wonders if all of the QSO polyhedra where $a > b$ are in fact oblate when compared to their regular

⁸ Thanks to Drs. Rachel Hastings and Rob Knapp of The Evergreen State College, Olympia, WA, for the identification of the Johnson solid. See http://en.wikipedia.org/wiki/Snub_disphenoid for more information.

⁹ See p. 116.

counterparts. The corollary would be that polyhedra generated by QSOs where $b > a$ might all be prolate.

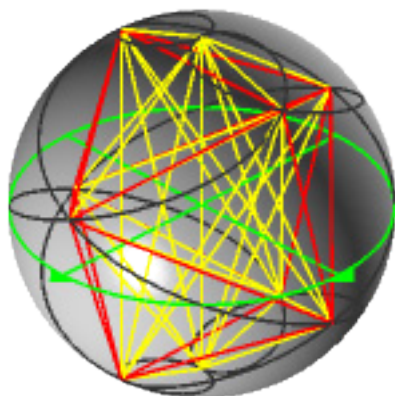


Fig. 11-5c

QSO 1(5:2) with the fully connected inscribed polyhedron

Although the fully connected 1(5:2) polyhedron has only 45 chords compared to the QSO 1(2:5) icosahedron's 66, it's an unfamiliar figure and hard to grasp visually. There are multiple surface and interior chords which seem to go every which way without order or sequence. Only the QSO trace hints at the underlying regularity. In figure 11-5c the QSO 1(5:2) polyhedron appears in red; additional chords are yellow. Table 11-5 tabulates the chords.

The QSO 1(5:2) polyhedron
4 @ 0.618034... (The Golden Mean - 1)
10 @ 1.17557... ($2 \sin 36^\circ$)
8 @ 1.22474... ($= \sqrt{1.5}$)
4 @ 1.4802...
4 @ 1.61803... (The Golden Mean)
4 @ 1.81907... ($= \sqrt{3 + \cos 72^\circ}$)
10 @ 1.90211... ($= 2 \sin 72^\circ$)
1 @ 2.0000... ($= \sqrt{4}$)
The snub disphenoid (J ₈₄)
18 @ 1.08...

Table 11-5

The chords of the QSO 1(5:2) polyhedron compared to those of the snub disphenoid (J₈₄)

Although the snub disphenoid is conventionally represented with unit edges, when inscribed in the unit sphere the edges grow by about 8%, a fact reflected in table 11-5.

We began this section with the intention of finding the Platonic dodecahedron. Although we did find a dodecahedron, the QSO figure is not the classical dodecahedron of Plato's philosophy. So far Plato's dodeca eludes us. We will return to the search in the next chapter. For now the reader is encouraged to explore the polygons and polyhedra made by dipole, tripole, and multiple QSOs, which are as interesting, as varied, and as diverse as the monopole objects.

Commencement

The *American Heritage Dictionary of the English Language* (1970) says that the verb “commence” means to begin, start, or come into existence. It derives from the Middle English word *commencen*, which comes from Old French *comencer*. *Comencer* in turn traces its origin to *cominitiare* (unattested) in Vulgar Latin which is from Late Latin *cominitiare*, a word composed of the intensifier *com-* and the root *initiare*, to begin or initiate. This is appropriate. One of the main goals of this book has been to initiate the study of Quasi-Spherical Orbits.

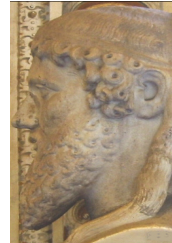
Janus



Janus was the Roman god of gates, doorways, hallways, beginnings and endings.¹ Typically

¹ Public domain photograph of a Roman statue of Janus in the Vatican Museum from <http://en.wikipedia.org/wiki/Janus_%28mythology%29>.

shown with two faces, he looks both forward and back.² In this last chapter we will try to do likewise. We will look back at what has been learned, and look forward to preview a little of what may come.



“Chance favors the prepared mind.”
--Louis Pasteur (1822-1895)

Looking back, the genesis of Quasi-Spherical Orbits perfectly illustrates Pasteur’s words. In 1960 Michael Burke was unhappy. He read widely, especially in the sciences, and he was dissatisfied with the generally accepted ways mathematics and physics conceptualized and displayed dynamic three-dimensional phenomena. The usual representation was – and to a great extent still is – to draw a two-dimensional static picture. That which could not be displayed statically and in two dimensions was said to be conceivable only in abstract mathematical terms. Such phenomena were said to be off-limits to the mathematically uninitiated.

² The month of January is named after Janus, as are janitors, the custodians of doorways and hallways. A good summary of Janus and his position in the Roman pantheon is found at <<http://www.novareinna.com/festive/janus.html>>.

The phenomenon of spin was particularly troubling. Burke asked what was spinning. The answer, he was told, was that – at least at the atomic level – “spin” is just a word used to describe a certain phenomenon. Nothing is really spinning at all. Intuitively he thought there must be a better way.

Little came of this displeasure however, until Burke had a conversation with a man who wanted to extract some of the energy generated in a centrifuge and use it for propulsion. The man and his ideas passed on into oblivion, but Burke was left with the question, “What happens when you generate centrifugal force on two axes simultaneously?” He proceeded to find out. Using his son’s Meccano® set, he built a mechanism that rotated a mass in the required way. It generated the first QSO (1:1).



Fig. 12-1

David Burke with Meccano® QSO generator, c. 1960³

³ Photograph © by Michael Burke, 1960. Used with permission.

After a long period of incubation and thoughtful waiting, the story resumes in chapter 1 where we discovered that QSOs are a subset of space curves, single dimensional lines that exist in three-dimensional space. Two-dimensional QSOs were mentioned briefly, and several limiting simplifications were made. These included using only two spin axes and specifying the angular relationship between them as 90°. QSOs were also limited to a unit radius virtual sphere. QSO (1:1) was generated with a unicycle metaphor. We learned that the dynamics of QSO curves are often obscured by the static pictures. We also learned to pay attention to more than one point-of-view.



Janus’ other face looks forward, to a time when investigators may explore the effect of relaxing some of the restrictions introduced in chapter 1. Spin axes may number more than two, for instance, and the angular relationship between them may vary. It would be interesting to find out if varying the size of the sphere on which QSOs are traced has any effect on their properties. One may wonder what relationships would be revealed between QSOs generated on spheres of different but related radii. What about concentric spheres? Many phenomena depend on distance from a center. Do QSOs behave likewise? We can also wonder what happens when the virtual sphere isn’t a sphere. Oblate and prolate QSOs, which are

generated on ellipsoidal surfaces, were mentioned in chapter 1. Variations on the theme abound.

Another area ripe for exploration is that of point-of-view. With few exceptions, notably those in chapter 4, the points-of-view in this book have been limited to views from the three Cartesian axes and the isometric view. What QSOs look like from other places is still relatively unknown. What may be learned from these other points-of-view is yet to be discovered.

Then there is the question of 2- and 3-dimensional QSOs. Two-dimensional QSOs were defined as the surfaces traced by the radius of the rotating point, but little was made of that fact. Three-dimensional QSOs haven't even been defined, let alone studied.

In physics QSO seeds a nice theory of virtual particles. Since there appears to be a minimum Planck time, and a minimum Planck length, we may speculate that there must be a minimum level of perceptibility beyond which lies the virtual. If virtual particles are unobservable, that may be because they have but a single “spin,” whatever that means. The close passage or impact of a similar entity might send one or both into a QSO. By stretching its orbit and multiplying its velocity and acceleration, the new particle would acquire mass and be catapulted into the real, i.e. observable, universe. It is the addition of a rotation or “sense of spin” that transforms the virtual into the real. One may also speculate that, instead of a close passage or impact, the two virtual particles merge. Entwined somehow, they produce a particle with not one, but two “spins” which would then be observable or “real.”



Chapter 2 described three coordinate systems in which QSOs may be generated and discussed their advantages and drawbacks. It was pointed out that QSO equations based on the spherical coordinate system were closely related to the mechanics of the rotating point itself. This makes spherical equations intuitively easier to use than equations based on other coordinate systems. The advantage of the Cartesian coordinate system is that of wide acceptance. Although less intuitive than spherical coordinates, parametric vector equations in the Cartesian system can be manipulated easily, translating and rotating QSOs in ways the spherical system cannot. One disadvantage of both spherical and Cartesian coordinates is the fact that stasis, not change, is implicit in their representations. However, a more important disadvantage was said to be the fact that nature isn't using either system. Fuller's Isotropic Vector Matrix was presented as the more realistic, but relatively unknown, alternative. The chapter closed with an extended development of 763 variations on the basic QSO equation.



A convention was established in chapter 2 to write the QSO ratio as $(\theta:\phi)$, and not $(\phi:\theta)$. However, it was noted that in the natural world the order of the rotations may in fact differ from the convention. One wonders what natural phenomena may depend on the order of the rotations. Furthermore, although Fuller's Isotropic Vector Matrix was offered as a more realistic alternative to the older systems, no one to this writer's knowledge has attempted to model QSOs in IVM coordinates. This area is ripe for further exploration. The chapter closed with the speculation that some of the 763 variations of the parametric QSO equation might be more interesting, more elegant, or more useful than the standard version. These represent 763 opportunities to further the work of QSO.



Chapter 3 was about the elements of the QSO ratio. Fractional, exponential, irrational and continuously varying ratios were discussed. The concept of a pole was

introduced and monopoles, dipoles and multipoles were briefly explored. The chapter closed with a presentation of the Event Constellation and its geometric interpretation.



Chapter 3 did not discuss imaginary numbers in the QSO ratio. Whether these have any application in QSO is unknown. When the ratio was varied continuously from QSO (1:3) to QSO (2:3), it was noted that complexity occurs on either side of simplicity, limiting and containing the simpler orbits. The closer one approached the integer ratio, the more complex the orbit got, but this pattern was not characterized mathematically. Smoothly varying the second element of the QSO ratio was just barely mentioned, and its development was left to the reader.



Events were the topic of chapter 4. Two types were discussed: the intersection event and the tangent event. A graphical display method was developed and used to analyze the timing and direction of the events of monopole QSOs 1(1:2), 1(2:1), and dipole 2(1:1) $[0,0]$ $[0,\pi]$. The chapter also

suggested a convention for listing and analyzing the events of QSOs. It was based on numbering them sequentially according to the first time the rotating point passes over an event location. It was pointed out that they can be further distinguished by noting how many and which of the rotating points make them.



Although chapter 4 was about events created by rotating points, the potentially significant topic of the velocity and acceleration of a rotating mass at the event was mentioned only in passing. There was also speculation in chapter 4 about the relationship between a surface angle of the QSO and the central angle of the icosahedron, but that investigation was left to the reader, as was the examination of the polar events of QSO 2(1:2). Although a convention for naming and analyzing events was defined, at the same time we had to wonder if there would be any advantage to alternate methods of listing or analyzing them. The polar events of QSO 1(1:2) have a 90° relationship between them. It has been suggested that this out-of-phase skewing might account for the fundamental difference between northness and southness, positive and negative, or the underlying polarity that characterizes any dipole.⁴



Where chapter 4 was about events, chapter 5 was about orbits. A recursive algorithm was developed and the orbital lengths of the first twenty-five QSOs were calculated. It was found that when these are plotted on a 3-D graph, the orbital lengths create a “landscape” with an equal-rate valley along the (n:n) diagonal. Several “dimples” were noted in the landscape, as well as the fact that the landscape is tipped – one side is higher than the other. The chapter concluded with illustrations of the first 100 monopoles as seen from all three Cartesian axes and from the isometric point-of-view.



Chapter 5 touched on, but did not explore in any meaningful fashion, the velocity and acceleration of the rotating mass around the entire Quasi-Spherical Orbit. The meaning of the “dimples” in the QSO landscape needs to be clarified, as does the relationship between them and the central valley. It would be interesting to see if these valleys of similarity have counterparts in the macro or micro worlds. When the orbital lengths are listed one above the other, beginning with the (1:1) on the lowest

⁴ Michael Burke, private communication with the author, 1992 Mar 9.

level, they are reminiscent of the energies of electron orbitals. One wonders if there is more to the resemblance than mere coincidence.

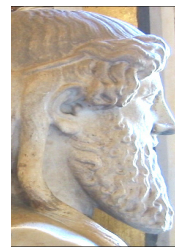
There is a potential link to string theory. In chapter 3 we saw that smoothly varying one element of the QSO ratio leads to increasingly complex orbits until the integer ratio is reached, at which point complexity gives way to simplicity. In terms of orbital length, the length of the Quasi-Spherical Orbit increases until the integer ratio, at which point it snaps back into a much shorter orbit. If the length of the orbit can be considered a wavelength, then increasing one side of the ratio by 0.1 increases the wavelength by a factor of about 10. Increasing one side of the ratio by 0.01 increases the wavelength by about 100, and so on. We find that the smaller the change in one element of the ratio, the larger the increase in orbital length.⁵ Depending on which version of string theory one considers, as many as 11 dimensions are required to describe reality at the very smallest dimensions.⁶ The theory postulates that these extra dimensions are folded within minuscule volumes of space, but cannot give specific demonstrations. QSO demonstrates that waves of immense length can be rolled into volumes of exceedingly small diameter, and that these can be easily specified, cataloged and predicted. QSO further suggests that this can be accomplished within the framework of the four known dimensions of space and time, without the extra dimensions required by string theory.

⁵ Decreasing the ratio also increases the wavelength. It's the size of the change that matters, not whether it's an increase or a decrease.

⁶ Greene, 2003, p. 307.



Chapter 6 departed from the exploration of QSOs proper to examine several techniques that have been used to display and study these curves. The early contributions of Loftus, Kelleher, and the author were detailed, as well as a number of more recent display techniques made possible by contemporary software. These included the cone and disk, the globe with latitude and longitude, and the three-in-one, a method for showing all three Cartesian views at once.



One display technique that was mentioned only in a footnote was plotting QSOs on a transparent plastic sheet such as that used in overhead projectors. The sheet could then be folded into an octahedron showing the QSO in a model that could be held in the hand. For his part, Burke suggested mapping onto a tetrahedron with the poles centered along opposed edges. Fuller's Dymaxion Sky-Ocean World Map suggests that projection onto the icosahedron would be a useful exercise.⁷

⁷ See Fuller (1946).

The discovery of the equations for the 8-trace variation of the cone and disk display, as well as the 4-trace pinwheel, was left to the reader, as were other display techniques that can translate and rotate QSOs in 3-space, slide them back and forth on any axis, or make them spin like propellers. They can also grow or shrink as the diameter of the central sphere (which is now no longer a *unit* sphere) is changed. These transformations were said to use well-known standard manipulations which readers may discover for themselves.

A display technique that was not mentioned in chapter 6 involves modeling QSOs in real materials. Such models have the advantage that they can be manipulated by hand, revealing aspects of the theory that are not suggested by the math or by staring at a screen. An example of this technique is shown next.

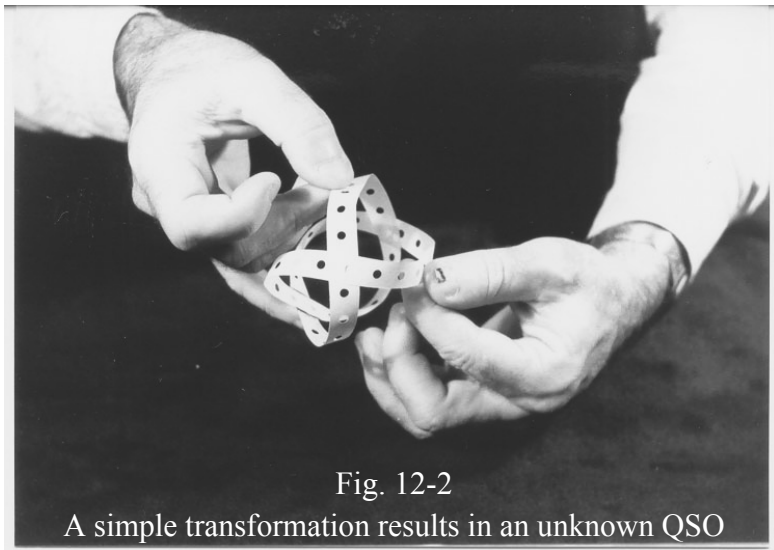


Fig. 12-2

A simple transformation results in an unknown QSO

In figure 12-2 QSO 1(1:1) is formed from the edge strips of tractor-feed printer paper (this was a while ago!). By bringing the north and south lobes of the curve together and through each other, a new curve is formed. This simple manipulation transforms the common (1:1) into a 3-event curve of unknown ratio. The radius shrinks and the angular velocity of the rotating point apparently increases. Furthermore, there no longer seems to be a polar axis – or at least the curve now seems not to go through the north and south poles. The mathematical and physical properties of such curves are yet to be determined, as is their relationship to the QSOs in this book.⁸

Mechanical devices to apply QSOs to the real world have been little explored. There have to date been only a handful, and all generated the 1(1:1). Burke's device that generated QSO 1(1:1) was built long before Loftus' computer program came along, and both Burke and the author have investigated the physical manifestations of the 1(1:1) in different ways. The applications of QSOs in the physical world are ripe for development.

⁸ In some respects the curve resembles a Quasi-Cylindrical Orbit. See Eqn. 8-4, Fig. 8-14.



Fig. 12-3
QSO 1(1:1) generator

A QSO generator designed by the author in 1996. When the vertical shaft is rotated, the red bolt head traces QSO 1(1:1).

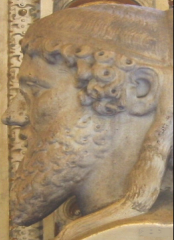


Chapter 7 looked into the relationship between QSOs and some well-known and not-so-well-known plane curves. These were the circle, the parabola, the lemniscate of Gerono, the cardioid, and the limaçon. It was also suggested that QSOs are related to epitrochoids, hypotrochoids, and to the rhodonea curves. In each case it was the projection of the QSO on one of the Cartesian planes that resembled the plane curve.

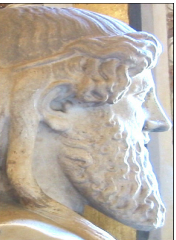


The most obvious need in this area is for convincing mathematical proofs of the claims of this chapter. Another option would be to expand the roster of plane curves subsumed by QSOs. With respect to the epitrochoids, we speculated that the QSO corresponding to an epitrochoid with variables (R, s) is of the form QSO $(R + 2s : R)$, but no proof was offered. The relationship between the hypotrochoids and the projections of the QSOs is even less clear. Finally, we noted that the rhodonea curve with $k = 1/3$ is the limaçon. This implies some interesting relationships not only between rhodonea, QSOs and the limaçon, but with the trochoid curves as well. These

relationships, if any, need to be fleshed out and examined.



Chapter 8 continued the study of the relationship between QSOs and plane curves by focusing on Lissajous figures. Although a superficial relationship seemed to exist between certain QSOs and L-Figs. (1:1), (2:1), and (3:1), we failed to find a general relationship until we introduced the idea of Quasi-Cylindrical Orbits, or QCOs. Extrapolating from the comparison between the L-Fig. (2:3) and QCO (2:3), we predicted that Lissajous figures are in general the 2-D projections of 3-D Quasi-Cylindrical Orbits. Both curves, we said, will have the form (c, s) , and both will go through the same number of cycles in 2π radians.



The formal proof of these observations was, as usual, left to persons more mathematically adventurous than the author. Furthermore, although one suspects that three-dimensional Lissajous figures are in fact Quasi-Cylindrical Orbits, this possibility has not been investigated.



Chapter 9 explored the relationship between QSOs and some well-known space curves such as the conical helix, the 3-D astroid, and the baseball seam by Gray. It was pointed out that neither the conical helix nor its 2-D cousin, Archimedes' spiral, could ever be related to any QSO because spirals and helices grow without limit whereas QSOs and their projections are limited to either the unit sphere or the unit circle. However, a relationship emerged between the 3-D astroid and QSO 1(3:2) when it was found that the tetrahedron formed by connecting the cusps of the astroid could be massaged into the QSO. Gray's baseball seam and his spherical cardioid turned out not to be related to QSOs, despite their superficial similarities. The Clelia curve yielded more positive results when it was identified with the northern halves of QSOs of the form (1:b). To close the chapter, Viviani's curve was recognized not only as being identical to QSO 1(1:1), but also as the intersection of a sphere and a cylinder.



Given that the 3-D astroid makes a tetrahedron, and that said 4-hedron can be massaged into a QSO 4-hedron, at least two questions occur. First, do any other space curves make polyhedra, and second, can any of those polyhedra also be transformed into a QSO version? With respect to Gray's baseball seam, it was pointed out that there are some interesting curves at negative k , but that these seem unrelated to QSOs. A convincing proof of that assertion would be welcome. Furthermore, although the Clelia seems perfectly matched to the northern halves of QSOs (1:b), only a single example was given for $m < 1$. This area needs to be mined for more information.



Chapter 10, Monopole Polygons & Polyhedra, began with a brief mention of Burke's discovery – and ensuing amazement – that connecting the events of QSO 1(3:2) forms a tetrahedron. The idea of a-gons and b-gons was developed, and the polygons in the (a:1) series and the (1:b) series of QSOs were examined. Chord lengths and tipping angles were calculated, and a curious reversal of orientation of the 1(1:b)

polyhedra and polygons was noted. The Loftus series of QSOs was also examined. A flip-flopping phenomenon of the Loftus polygons was attributed to precession of the figures around the z-axis, and it was observed that this phenomenon does not occur in QSOs generated with equation 2-8a. QSO 1(3:4) was developed as a way to show the assembly of the a-gons, b-gons, diagonals and diameters to make a complete polyhedron.



It was noted in the development of the 1(3:4) polyhedron that when viewed statically the QSO appears to have 10 events and 45 chords, although dynamically the true numbers are 12 events and 66 chords. The reader was (and still is) invited to figure out which chords are doubled and/or quadrupled to account for the 21 chord difference. From a chemical perspective, one wonders whether the single, double, and/or quadruple chords correspond in any way to single, double, and/or quadruple bonds in molecules. Continuing the chemical metaphor, one may wonder if there are any triple chords in QSOs.

In physics there is the problem of superdeformed nuclei. These nuclei, which are the result of an off-center collision, lose energy in steps emitting a gamma ray at each step. The emissions produce a characteristic band of energy spikes, all spaced equally apart. It turns out that the spectra of different

superdeformed nuclei are almost identical. The different nuclei have similar moments of inertia and lose angular momentum in the same steps.⁹

Burke points out that this bears a surprising resemblance to the flip-flopping characteristic of the Loftus 1(a:1) polygons. As the greater term of an integer spin ratio falls, the great circle of events flips from the xz-plane to the yz-plane to the xz-plane and so on. As the spin rate of a superdeformed nucleus decays, the integer rates, which align events, may emit a signal recognized as a gamma ray, indicating the lost energy. The gamma ray will be emitted, Burke speculates, in the transition through an irrational ratio.

By placing a “1” in front of the ratio, we limited the curves in chapter 10 to monopoles. A cursory review of multipole QSOs reveals that many QSOs make the same static figure. For example, although the dynamics differ enormously, QSOs

2(1:1) [0,0] [0,π],
 2(1:1) [0,0] [π,0],
 2(2:2) [0,0] [0,π],
 2(4:1) [0,0] [0,π],
 4(1:1) [0,0] [π/2,0] [π,0] [3π/2,0], and
 4(4:1) [0,0] [π/2,0] [π,0] [3π/2,0]

all make squares of one kind or another. When it comes to polyhedra, the situation is even more complex. QSO 2(1:2) [0,0] [0,π], the baseball seam, which in its monopole form produces only a diameter of the unit sphere along the z-axis, in its dipole form gives a regular octahedron with squares in all

three Cartesian planes.¹⁰ Regular octahedra are also produced by QSOs

2(1:2) [0,0] [π/2,0],
 2(1:2) [π,0] [0,π],
 4(1:2) [0,0] [π/2,0] [π,0] [3π/2,0], and
 8(1:2) [0,0] [0,π] [π/2,0] [π/2,π] [π,0] [π,π] [3π/2,0] [3π/2,π].

Polarized octahedra are found in QSOs

2(2:3) [0,0] [0,π],
 2(2:3) [0,0] [2π/3,0], and
 3(2:3) [0,0] [2π/3,0] [4π/3,0].

QSO 2(2:5) [0,0] [0,π] makes a polarized icosahedron which is statically similar to QSO 1(2:5) [0,0].

QSO 2(1:5) [0,0] [0,π] makes a 20-hedron too, but it's not the QSO analog to the Platonic solid. The study of these and other multipole polyhedra will surely provide many hours of enjoyment for the geometrically adept.

In table 10-2 there appears to be a relationship between the chord length and its second root in all but the pentagon. Whether this is a meaningful observation or the coincidental workings of polygons is unknown.

Table 10-4 reveals that the chords in the xy-plane, if they exist, are identical to the corresponding chords of the 1(a:1) series in the yz-plane. New in the 1(1:b) series are the diameters along the z-axis and the chords in the positive and negative z-hemispheres. A number of second roots are again apparent, but any relationship between these and the elements of the QSOs

¹⁰ This is the QSO polyhedron that was used to illustrate Fuller's great circle railroad tracks of energy in the introduction.

⁹ See Yam (1991).

remains undiscovered.

The precession of the L-QSOs around the z-axis deserves further study, as does the failure of the prediction formula in QSO 1(5:5). The problem is that there should be five 5-gons, but even with the revised definition of an event, only one can be found. Where are the other four? A similar situation occurs in all of the equal rate QSOs. One a-gon or b-gon will be found, but not the multiples suggested by the QSO ratio.

A related problem is revealed in the pattern of z-chord involvement in the polygons of the first 25 QSOs as shown in table 10-6. The pattern seems to be that the z-chord occurs only when the QSO ratio is read left to right, a is odd and b is even. However, some QSOs form a z-chord when the ratio is read the other way, while others do not need the z-chord at all. One wonders whether this pattern persists at higher frequencies.

It was mentioned that there are many other ways of connecting the events of QSO 1(5:2). Some of these involve the z-axis and some do not. These alternatives have not been explored.



Chapter 11 dealt with the Platonic solids and their relationship to QSOs. It was perhaps a little surprising that none of the Platonic polyhedra seemed to be generated by connecting the events of QSOs. What we found instead were three analogs

to the Platonic tetrahedron, octahedron and icosahedron. These were formed by QSOs 1(3:2), 1(2:3), and 1(2:5), respectively. Although all three are polarized along the z-axis, the QSO tetrahedron turned out to be an oblate figure while the QSO octahedron and icosahedron are prolate figures. Note was made of the fact that the QSO icosahedron seems to be more prolate than the QSO octahedron. The idea of a fully connected polyhedron was introduced and a formula was offered for the number of unique chords Tn needed to connect n events.

A search for the QSO analog to the Platonic dodecahedron failed to reveal any such figure. What was found instead was the snub disphenoid, the Johnson figure J_{84} . The QSO version, was predictably polarized. The missing polyhedron was the cube.

The Last Platonic

To find the QSO analog to the cube we begin with QSO 1(3:2).

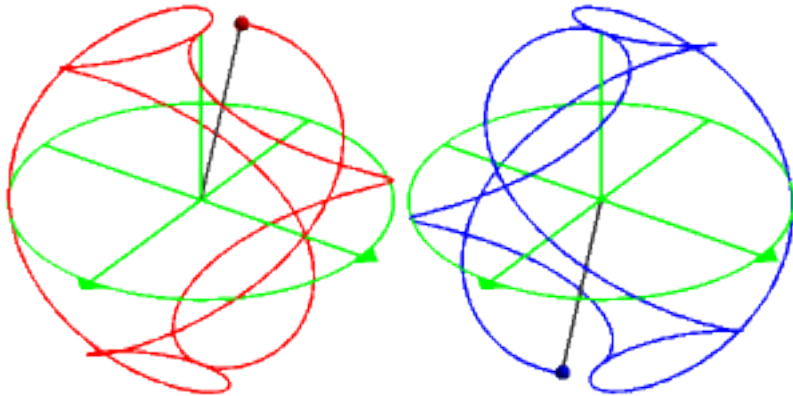


Fig. 12-4a

QSO 1(3:2) [0,0] @ 98%

Fig. 12-4b

QSO 1(3:2) [0, π] @ 98%

The familiar monopole (3:2) with phase angles of [0,0] is shown on the left at 98% of a cycle. On the right a phase angle of 180° has been added to the second rotation, resulting in an apparent 90° precession of the curve around the z-axis. Note that although the phase angle was added to ϕ , the precession of the curve is in θ .¹¹ The coordinate system in the illustrations has

¹¹ In general, increasing θ results in eastward precession around the z-axis, whereas increasing ϕ goes the other way. The precession of the curve in all cases is governed by a simple ratio. It will be left to the reader to discover the details of this behavior.

been rotated slightly away from the isometric view to allow a better appreciation of the polyhedron which will develop.

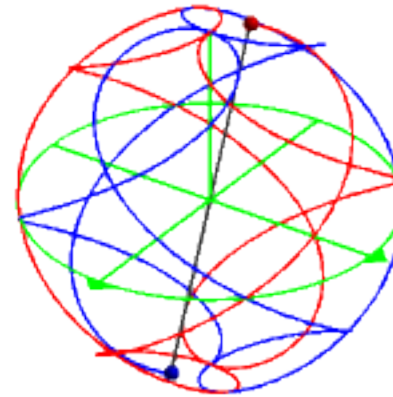


Fig. 12-5

QSO 2(3:2) [0,0] [0, π] @ 98%

Combining the two monopoles results in the dipole 2(3:2) [0,0] [0, π], shown here at 98% of a cycle.¹² This is the simultaneous energetic dipole described by Burke.¹³

¹² QSO 2(3:2) [0,0] [π,π] results in a similar static figure, but the dynamics are entirely different.

¹³ Burke, 1992, p. 4.

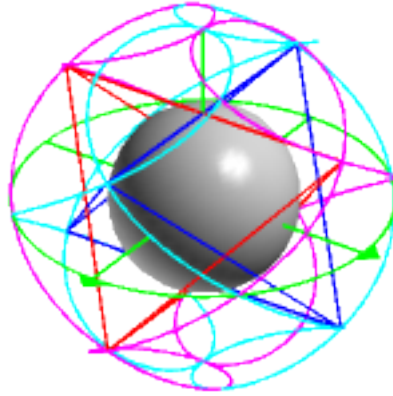


Fig. 12-6
QSO 2(3:2) [0,0] [0, π] @ 100%
with inscribed tetrahedra

As we know, each branch of the QSO generates a tetrahedron, so we draw them in. The branches themselves are traced in lighter shades while the tetrahedra take the original color of their parent curves. Things are getting a little complicated visually, so an opaque sphere is placed at the center of the system. The radius of the sphere is 0.5, the same as the distance of the horizontal edges of the tetras from the xy-plane. Thus the sphere is tangent to the horizontal edges of the 4-hedrons.

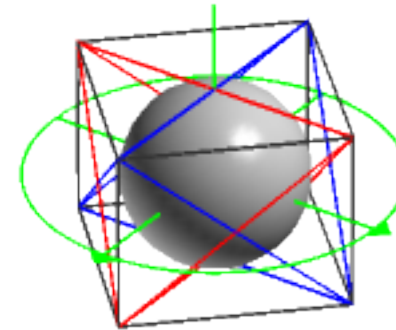


Fig. 12-7
The 2(3:2) tetrahedra generate a QSO cube

Removing the QSO traces considerably simplifies the illustration. The next step is to connect the vertices of the tetrahedra. The resulting 6-hedron looks very much like a cube. Each face is defined by two edges, one from each QSO tetrahedron. Since the tetras are polarized, we expect that the QSO 6-hedron will also be polarized. To show this we need one final graphic.

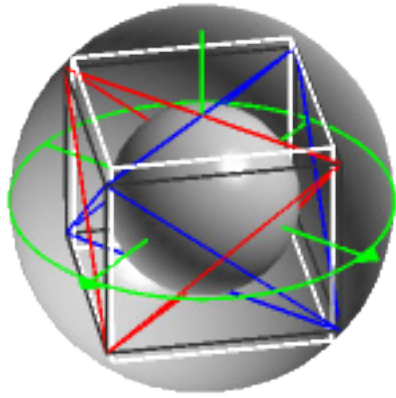


Fig. 12-8
The QSO 6-hedron (black)
compared to the
regular (Platonic) cube (white)

The two QSO tetrahedra and their related 6-hedron are compared to a regular (Platonic) cube inscribed in the unit sphere. The concave unit hemisphere provides a dark backdrop so the white figure can be seen. When the regular cube is inscribed in the unit sphere, its edges are

$$\sqrt{\frac{4}{3}} = 1.1547\dots$$

The volume is thus an irrational

$$\left(\sqrt{\frac{4}{3}}\right)^3 = 1.5396\dots$$

By way of comparison, the horizontal edges of the QSO 6-hedron are

$$\sqrt{\frac{3}{2}} = 1.2247\dots,$$

and the vertical edges are 1.0.... The volume is thus a very rational 1.50....

The missing Platonic is the dodecahedron. To understand why we have not found the Platonic dodecahedron, and why it will likely never be found among QSOs, it's necessary to take a short excursion through the synergetic geometry of Buckminster Fuller.

Fuller on Structure¹⁴

Buckminster Fuller was an original. Born eight years before the Wright brothers' first flight, by the end of his life he had taken the measure of Universe and all it contains.¹⁵ He insisted that his mathematical and geometric explorations, like all else that he did, were strictly based on experimental data. Thus when it came to understanding structure, Fuller started with an experiment.

Make a necklace, Fuller said. This particular necklace is made from a multiplicity of identical hollow tubes – soda straws will do. Lace them through with a string. Pull the string tight and tie it so that there is as little string as possible showing

¹⁴ The discussion presented here is based on that in Fuller (1975), §600.00, and especially §§608.00–610.00.

¹⁵ Fuller always capitalized "Universe" and never used the article "the."

between the straws. As you hold the necklace and manipulate it in your hands, you find that the necklace is flexible. You can easily drape it over a nearby book, bowling ball, or your pet cat. It has no structural integrity of its own. Since the dimensions of the soda straws themselves do not change, we discover that the flexibility is due solely to the angular variability between the straws.

Remove a straw and repeat the experiment. The necklace is still flexible. Repeat this operation until you have only three straws left. Now the 3-straw necklace holds its shape. It has become a structure, by which Fuller meant a self-stabilizing pattern. The triangle is the only self-stabilizing polygon, he said. The experiment with the soda-straw necklace shows that any polygon with more than three sides is unstable. Thus if structural *systems*, which are composed of many subunits, are to be similarly stable, they must be made of triangles.

Next Fuller asked how many triangles can be assembled around a vertex to make a stable polyhedron. To find out he performed another experiment. Again using soda straws or the equivalent, he constructed various polyhedra. He required that the lengths of the tubes be identical. Only the angles between the tubes were allowed to vary in any way they might. He found that three, four, or five equiangular triangles assembled around a vertex make stable polyhedra. With three triangles around each vertex you get a tetrahedron. Four triangles around each vertex result in the octahedron, and five triangles around each vertex give the icosahedron.

Fuller found, again experimentally, that any polyhedron

bound by polygonal faces with more than three sides is unstable. Only polyhedra bound by triangular faces are inherently stable. Furthermore, you can't put six equiangular triangles around a vertex because that gives the infinite plane, a concept acceptable to theoretical mathematics, but not to Fuller's experimentally based geometry. Thus there are three and only three Prime Structural Systems, the tetrahedron, the octahedron, and the icosahedron.¹⁶ The cube, which has square faces, can exist in Fuller's geometry, as it can in QSO, only as the synergetic combination of two tetrahedra.¹⁷ The Platonic dodecahedron, which has pentagonal faces, cannot exist unless it's omnitriangulated. Fuller gives a method for constructing it; QSO has yet to discover one.¹⁸ On the other hand, the J₈₄ was found in the exact location where we expected a dodecahedron. It's omnitriangulated and stable, but it's not regular and it's not a Platonic.

¹⁶ Fuller further pointed out that these three are smoothly transformable one into the other. He called this process the "Jitterbug." See Fuller (1975), §460.00.

¹⁷ Note that a single tetrahedron stabilizes the cube, but it takes two to create it. This is reminiscent of what is perhaps Fuller's best known dictum, "Unity is plural, and, at minimum, two."

¹⁸ When he learned of this situation, Burke wrote, "... it used to worry me that the 'Platonic solids' generated by QSO were 'imperfect', i.e. polarised. This now seems to me to indicate that QSO as descriptive of this universe is superior to theoretical maths in that the Universe does not contain straight lines, or symmetrical crystals, or true circles, or, presumably, non-polarised Platonic solids. All these perfect mathematical concepts ARE concepts only, generalised definitions of, in fact, infinitely [though minutely] variable classes of phenomena. One can conceive of these items, but nowhere in the universe will you [or can you] actually sight them." --Personal communication with the author, 2008 Apr 18.



Fuller's comments about structure and QSO's failure to find a polarized analog to the Platonic dodecahedron seem to put an end to the search. Still, one would like to have a convincing proof of that assertion. As far as the polarized nature of QSO polyhedra, one wonders if all of the polyhedra where $a > b$ are in fact oblate when compared to their regular counterparts. Equally, we wonder whether polyhedra generated by QSOs where $b > a$ might all be prolate. One may further question whether the observed polarization of QSOs is a result of graphing them in the Cartesian coordinate system. Perhaps Fuller's Isotropic Vector Matrix would yield perfectly regular polyhedra. As of yet these areas are *Terra Incognita*.

Finally, Fuller has suggested that the photon can be characterized as a tetrahedral energy package.¹⁹ One may ask whether Fuller's tetrahedral photons are related in any way to the 4-hedron in QSO monopole (3:2). If so, what does this imply for other basic particles?

¹⁹ Fuller, 1975, §541.30–36
-----, 1979, Color Plate 10

The Analemma

This book began with the hippopede of Eudoxus. Although Eudoxus' twin crystal spheres failed to explain the retrograde motion of the planets, they come very close to describing another astronomical phenomenon. We close with this stunning photograph of the analemma by the modern Greek astronomer Anthony Ayiomamitis.²⁰ The analemma is created by the simultaneous rotation of the Earth on two axes, the very definition of a QSO.

With the analemma we have come full circle. Eudoxus might have been familiar with this place. Perhaps he gazed at the sky-wanderers from some of these very stones.

²⁰ Sometimes called the Equation of Time, the analemma is inscribed on globes and sundials to indicate the sun's declination for every day of the year. To take a picture of the analemma you expose the film at the same time, typically local noon, at regular intervals for a year. The 44 solar images in Ayiomamitis' picture suggest that he exposed the film weekly, with a few gaps.

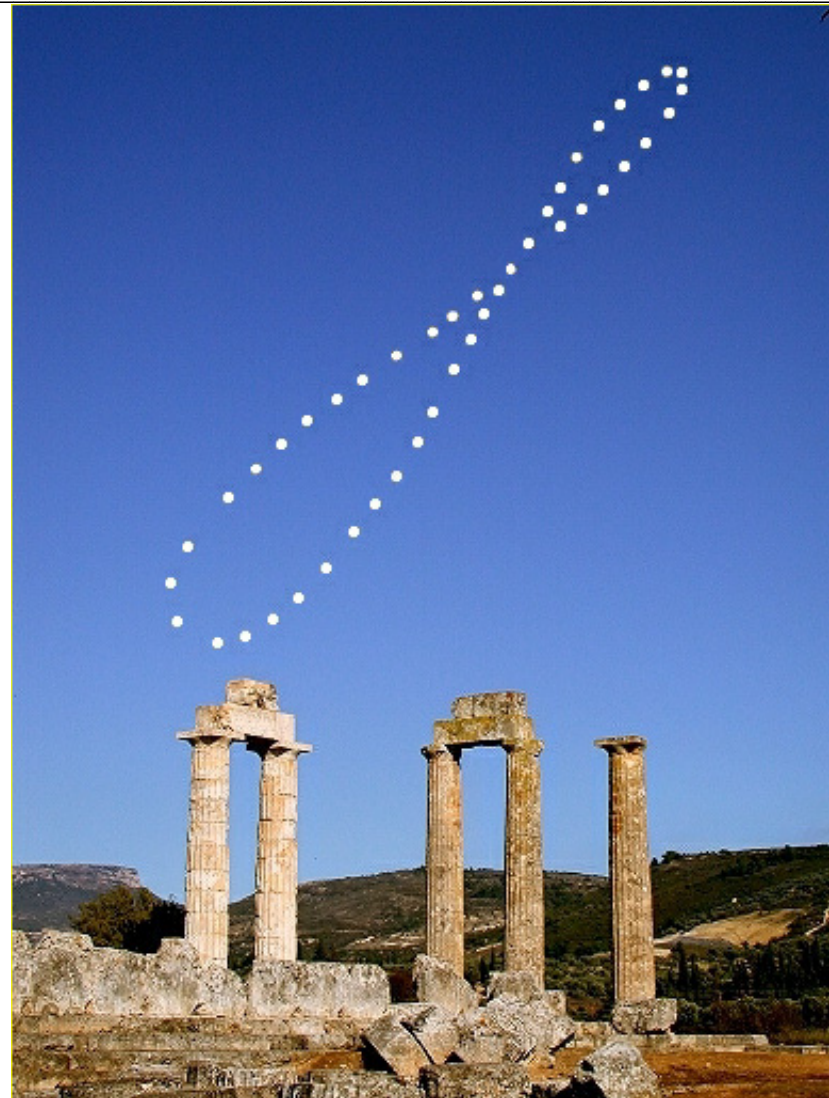


Fig. 12-9

Analemma with the Temple of Zeus (340-330 BC)²¹

²¹ Photograph © 2003 by Anthony Ayiomamitis. Used with permission.

Appendix 1

Simulating the Unicycle

The unicycle QSO generator portrayed in chapter 1 consists of eight elements:

- 1) A fork
- 2) An axle
- 3) Two small spheres to give the axle a finished look
- 4) A hub
- 5) The spokes
- 6) A small sphere that rotates in sync with one spoke
- 7) The wheel
- 8) The QSO

We will discuss each of these in turn. For completeness, we will also briefly present a tubular QSO

The Fork

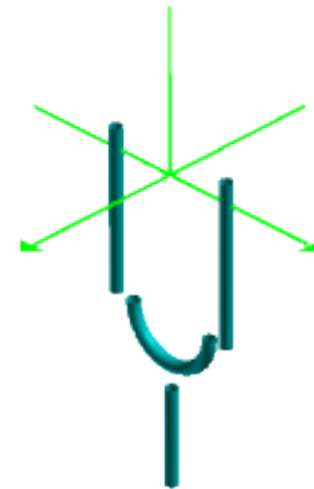


Fig. A1-1
The fork

The fork consists of four separate surfaces. In this exploded view, there are two vertical tubes at positive and negative y , a semicircular tube in the yz -plane, and a vertical tube along the z -axis.

$$\begin{bmatrix} x \\ y \\ z \end{bmatrix} = \begin{bmatrix} \cos ag - \sin ag & 0 \\ \sin ag & \cos ag & 0 \\ 0 & 0 & 1 \end{bmatrix} \begin{bmatrix} S \cos 2\pi u \\ (S \sin 2\pi u) - 0.28 \\ -v \end{bmatrix}$$

Eqn. A1-1

The vertical tube at negative y

$$\begin{bmatrix} x \\ y \\ z \end{bmatrix} = \begin{bmatrix} S \cos 2\pi u \\ S \sin 2\pi u \\ 0.6v - 1.9 \end{bmatrix}$$

Eqn. A1-4

The vertical tube along negative z

$$\begin{bmatrix} x \\ y \\ z \end{bmatrix} = \begin{bmatrix} \cos ag - \sin ag & 0 \\ \sin ag & \cos ag & 0 \\ 0 & 0 & 1 \end{bmatrix} \begin{bmatrix} S \cos 2\pi u \\ (S \sin 2\pi u) + 0.28 \\ -v \end{bmatrix}$$

Eqn. A1-2

The vertical tube at positive y

$$\begin{bmatrix} x \\ y \\ z \end{bmatrix} = \begin{bmatrix} \cos ag - \sin ag & 0 \\ \sin ag & \cos ag & 0 \\ 0 & 0 & 1 \end{bmatrix} \begin{bmatrix} 0.145 (0.28 \sin (2\pi v)) \\ 0.28 (-\cos \pi u) (1 + 0.145 (\cos (2\pi v))) \\ 0.28 (-\sin \pi u) (1 + 0.145 (\cos (2\pi v))) - 1 \end{bmatrix}$$

Eqn. A1-3

The semicircular tube

All four surfaces are generated parametrically. The introduction of parametric surfaces immediately requires variables u and v . The ranges of u and v are automatically set by the software, but they can be changed by the user. While we're at it, we'll list the ranges for x , y , z , and t as well.

$$\begin{aligned} x: & -1 \dots 1 \\ y: & -1 \dots 1 \\ z: & -1 \dots 1 \\ t: & 0 \dots 1 \\ u: & 0 \dots 1 \\ v: & 0 \dots 1 \end{aligned}$$

The diameter of the parametric tubes is

$$S = 0.04$$

To animate the curve, define

$$g = 2\pi n$$

and let n go from 0 to 1 in 100 steps.

**The Axle and
Two Small Spheres to Give the Axle a Finished Look**

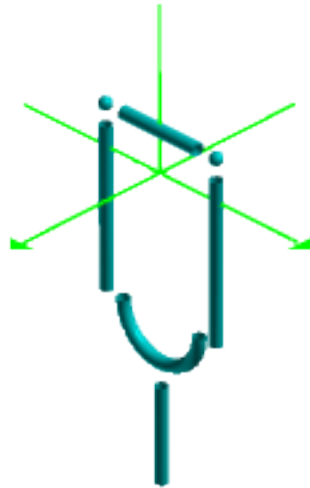


Fig. A1-2
The axle and two small spheres

An axle is added to the fork.

$$\begin{bmatrix} x \\ y \\ z \end{bmatrix} = \begin{bmatrix} \cos ag - \sin ag & 0 \\ \sin ag & \cos ag & 0 \\ 0 & 0 & 1 \end{bmatrix} \begin{bmatrix} S \cos 2\pi u \\ 0.55 v - 0.275 \\ S \sin 2\pi u \end{bmatrix}$$

Eqn. A1-5
The axle.

Since the members of the fork and axle are hollow tubes, the 90° angles at which the axle and the two vertical members of the fork meet have open ends. They appear unfinished. To give these areas a more finished look, two small spheres with the same radii as the tubing are added.

$$\begin{bmatrix} x \\ y \\ z \end{bmatrix} = S \begin{bmatrix} \cos ag - \sin ag & 0 \\ \sin ag & \cos ag & 0 \\ 0 & 0 & 1 \end{bmatrix} \begin{bmatrix} \sin 2\pi bu - \sin 2\pi av \\ \cos 2\pi bu - 7 \\ \sin 2\pi bu - \cos 2\pi av \end{bmatrix}$$

Eqn. A1-6

The small sphere at negative y

$$\begin{bmatrix} x \\ y \\ z \end{bmatrix} = S \begin{bmatrix} \cos ag - \sin ag & 0 \\ \sin ag & \cos ag & 0 \\ 0 & 0 & 1 \end{bmatrix} \begin{bmatrix} \sin 2\pi bu - \sin 2\pi av \\ \cos 2\pi bu + 7 \\ \sin 2\pi bu - \cos 2\pi av \end{bmatrix}$$

Eqn. A1-7

The small sphere at positive y

Note the placement of the diameter of the spheres in front of the rotation matrix. In this location it can be used as an On-Off switch. Set $S = 0$ and the small spheres disappear. This same trick can be used with any part of the illustration to turn it on or off from a central location.

The Hub

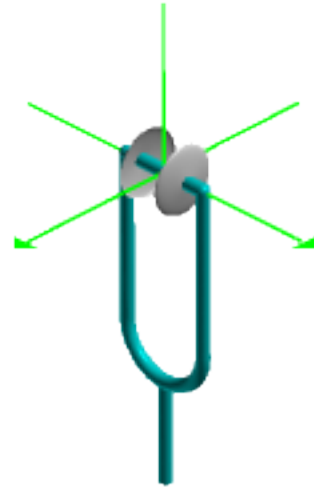


Fig. A1-3
The hub

A hub is added to the fork-and-axle assembly. The hub comes in two saucer-shaped pieces.

$$\begin{bmatrix} x \\ y \\ z \end{bmatrix} = \begin{bmatrix} \cos ag & -\sin ag & 0 \\ \sin ag & \cos ag & 0 \\ 0 & 0 & 1 \end{bmatrix} \begin{bmatrix} 0.1 (\cos 2\pi u) (1 + \cos (2\pi v)) \\ -0.05 \sin \pi v \\ 0.1 (\sin 2\pi u) (1 + \cos (2\pi v)) \end{bmatrix}$$

Eqn. A1-8
The half-hub at negative y

$$\begin{bmatrix} x \\ y \\ z \end{bmatrix} = \begin{bmatrix} \cos ag & -\sin ag & 0 \\ \sin ag & \cos ag & 0 \\ 0 & 0 & 1 \end{bmatrix} \begin{bmatrix} 0.1 (\cos 2\pi u) (1 + \cos (2\pi v)) \\ 0.05 \sin \pi v \\ 0.1 (\sin 2\pi u) (1 + \cos (2\pi v)) \end{bmatrix}$$

Eqn. A1-9
The half-hub at positive y

The Spokes

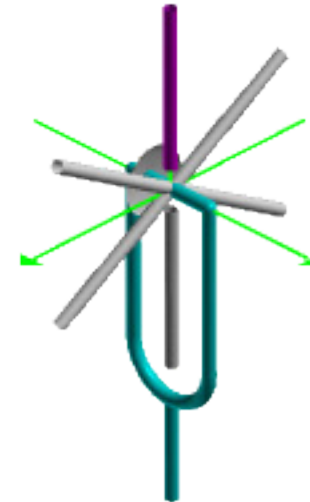


Fig. A1-4
The spokes

Although in the finished unicycle it looks like there are six spokes, there are actually only four. Two of these extend through the axle, making two spokes in one. The other two are

normal spokes, extending from the axle to the wheel. One of these is colored violet to distinguish it from the others. In this

view the half-hub nearest the reader has been removed to show the details of spoke construction.

$$\begin{bmatrix} x \\ y \\ z \end{bmatrix} = \begin{bmatrix} \cos ag & -\sin ag & 0 \\ \sin ag & \cos ag & 0 \\ 0 & 0 & 1 \end{bmatrix} \begin{bmatrix} \cos(-bg) & 0 & -\sin(-bg) \\ 0 & 1 & 0 \\ \sin(-bg) & 0 & \cos(-bg) \end{bmatrix} 0.95 \begin{bmatrix} S \sin 2\pi u \\ S \cos 2\pi u \\ v \end{bmatrix}$$

Eqn. A1-10
The violet spoke

$$\begin{bmatrix} x \\ y \\ z \end{bmatrix} = \begin{bmatrix} \cos ag & -\sin ag & 0 \\ \sin ag & \cos ag & 0 \\ 0 & 0 & 1 \end{bmatrix} \begin{bmatrix} \cos(-bg) & 0 & -\sin(-bg) \\ 0 & 1 & 0 \\ \sin(-bg) & 0 & \cos(-bg) \end{bmatrix} 0.95 \begin{bmatrix} S \sin 2\pi u \\ S \cos 2\pi u \\ -v \end{bmatrix}$$

Eqn. A1-11
The spoke opposite the violet spoke

$$\begin{bmatrix} x \\ y \\ z \end{bmatrix} = \begin{bmatrix} \cos ag - \sin ag & 0 \\ \sin ag & \cos ag & 0 \\ 0 & 0 & 1 \end{bmatrix} \begin{bmatrix} \cos(-bg + 60^\circ) & 0 & -\sin(-bg + 60^\circ) \\ 0 & 1 & 0 \\ \sin(-bg + 60^\circ) & 0 & \cos(-bg + 60^\circ) \end{bmatrix} 0.95 \begin{bmatrix} S \sin 2\pi u \\ S \cos 2\pi u \\ 2v - 1 \end{bmatrix}$$

$$\begin{bmatrix} x \\ y \\ z \end{bmatrix} = \begin{bmatrix} \cos ag - \sin ag & 0 \\ \sin ag & \cos ag & 0 \\ 0 & 0 & 1 \end{bmatrix} \begin{bmatrix} \cos(-bg + 120^\circ) & 0 & -\sin(-bg + 120^\circ) \\ 0 & 1 & 0 \\ \sin(-bg + 120^\circ) & 0 & \cos(-bg + 120^\circ) \end{bmatrix} 0.95 \begin{bmatrix} S \sin 2\pi u \\ S \cos 2\pi u \\ 2v - 1 \end{bmatrix}$$

Eqns. A1-12

The two long spokes

**A Small Sphere That Rotates
in Sync With One Spoke**

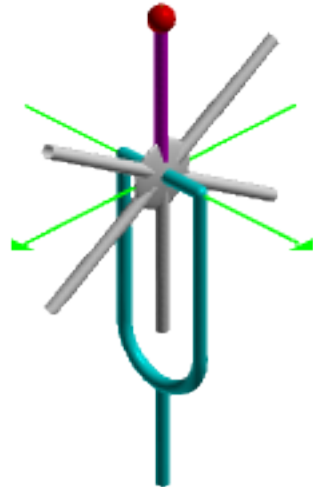


Fig. A1-5

A small red sphere is placed at the end of the violet spoke.

$$\begin{bmatrix} x \\ y \\ z \end{bmatrix} = 0.075 \begin{bmatrix} \sin 2\pi bu - \cos 2\pi av \\ \sin 2\pi bu - \sin 2\pi av \\ \cos 2\pi bu \end{bmatrix} + 0.925 \begin{bmatrix} (\sin bg) (\cos ag) \\ (\sin bg) (\sin ag) \\ \cos bg \end{bmatrix}$$

Eqn. A1-13

The small red sphere

The Wheel

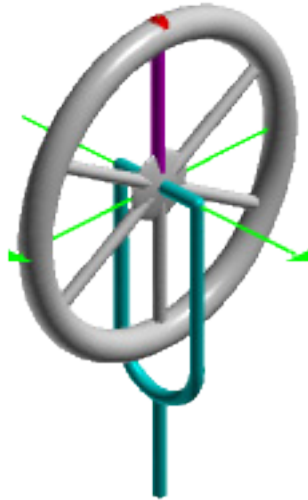


Fig. A1-6
The wheel

Adding the wheel of the unicycle obscures the ends of the spokes and all but a small portion of the red sphere, which now becomes the “patch” mentioned in chapter 1.

$$\begin{bmatrix} x \\ y \\ z \end{bmatrix} = \begin{bmatrix} \cos ag & -\sin ag & 0 \\ \sin ag & \cos ag & 0 \\ 0 & 0 & 1 \end{bmatrix} 0.9 \begin{bmatrix} (\cos 2\pi u) (1 + 0.1 \cos (2\pi v)) \\ 0.1 \sin (2\pi v) \\ (\sin 2\pi u) (1 + 0.1 \cos (2\pi v)) \end{bmatrix}$$

Eqn. A1-14
The wheel of the unicycle

The QSO

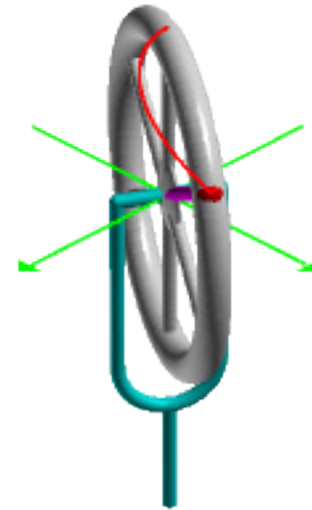


Fig. A1-7
The QSO

Without rotation QSOs do not exist, so, in order to see the QSO, we need to rotate the unicycle. Here, at 1/6 of a cycle, is the beginning of QSO 1(1:1).

$$\begin{bmatrix} x \\ y \\ z \end{bmatrix} = \begin{bmatrix} (\sin bgt) (\cos agt) \\ (\sin bgt) (\sin agt) \\ \cos bgt \end{bmatrix}$$

Eqn. 2-8a
The QSO

Clones

For a thicker, brighter line the QSO can be cloned. Define a variable f such that f is the separation between the cloned curves and the original. A convenient value is

$$f = 0.007$$

Define three variables, X, Y, and Z, such that

$$X = \begin{bmatrix} f \\ 0 \\ 0 \end{bmatrix}, Y = \begin{bmatrix} 0 \\ f \\ 0 \end{bmatrix}, Z = \begin{bmatrix} 0 \\ 0 \\ f \end{bmatrix}$$

Then duplicate equation 2-8a six times. Add X, Y, Z to three of these and subtract X, Y, Z from the other three.

$$\begin{bmatrix} x \\ y \\ z \end{bmatrix} = \begin{bmatrix} (\sin bgt) (\cos agt) \\ (\sin bgt) (\sin agt) \\ \cos bgt \end{bmatrix} + X$$

$$\begin{bmatrix} x \\ y \\ z \end{bmatrix} = \begin{bmatrix} (\sin bgt) (\cos agt) \\ (\sin bgt) (\sin agt) \\ \cos bgt \end{bmatrix} - X$$

$$\begin{bmatrix} x \\ y \\ z \end{bmatrix} = \begin{bmatrix} (\sin bgt) (\cos agt) \\ (\sin bgt) (\sin agt) \\ \cos bgt \end{bmatrix} + Y$$

$$\begin{bmatrix} x \\ y \\ z \end{bmatrix} = \begin{bmatrix} (\sin bgt) (\cos agt) \\ (\sin bgt) (\sin agt) \\ \cos bgt \end{bmatrix} - Y$$

$$\begin{bmatrix} x \\ y \\ z \end{bmatrix} = \begin{bmatrix} (\sin bgt) (\cos agt) \\ (\sin bgt) (\sin agt) \\ \cos bgt \end{bmatrix} + Z$$

$$\begin{bmatrix} x \\ y \\ z \end{bmatrix} = \begin{bmatrix} (\sin bgt) (\cos agt) \\ (\sin bgt) (\sin agt) \\ \cos bgt \end{bmatrix} - Z$$

Eqn. 2-8a
Cloned curves

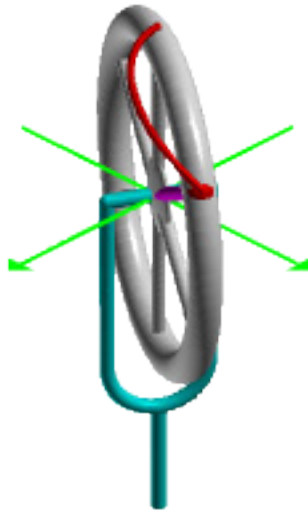
A Tubular QSO

Fig. A1-8
A tubular QSO

It is also possible to represent the QSO trace with a tubular parametric surface.

Simulating the Unicycle

$$U(t) = \sqrt{((ga)^2 + (gb)^2)^2 \sin^2 gbt + (4(ga)^2 + (gb)^2)(gb)^2 \cos^2 gbt}$$

$$V(t) = \sqrt{(gb)^6 + (ga)^2(gb)^4(3 + \cos^2 gbt) + (ga)^4(gb)^2((1 + 4\cos^2 gbt)\sin^2 gbu + 2\sin^4 gbt) + (ga)^6 \sin^4 gbt}$$

$$X(t) = ((gb)^3 + (ga)^2 gb \sin^2 gbt), Y(t) = ga(gb)^2 \cos gat \cdot \text{singbu} \cdot \cos gbt, Z(t) = ((ga)^2 + (gb)^2) \text{singbt}$$

$$X = (2 + 0.2 \sin 2\pi u) \sin 4\pi v, Y = 0.2 \cos 2\pi u + 3 \cos 2\pi v, Z = (2 + 0.2 \sin 2\pi u) \cos 4\pi v$$

Eqns. A1-15

Common terms of the tubular equation¹

$$\begin{bmatrix} x \\ y \\ z \end{bmatrix} = \begin{bmatrix} \text{singbu} \cdot \cos gau + 0.02 \left(\frac{\cos 2\pi v \cdot (-\cos gau \cdot Z(u) - 2gagb \text{singau} \cdot \cos gbu)}{U(u)} + \frac{\sin 2\pi v \cdot (-\text{singau} \cdot X(u) + \cos gau \cdot Y(u))}{V(u)} \right) \\ \text{singau} \cdot \text{singbu} + 0.02 \left(\frac{\cos 2\pi v \cdot (-\text{singau} \cdot Z(u) + 2gagb \cos gau \cdot \cos gbu)}{U(u)} + \frac{\sin 2\pi v \cdot (\cos gau \cdot X(u) + \text{singau} \cdot Y(u))}{V(u)} \right) \\ \cos gbu + 0.02 \left(\frac{(-\cos 2\pi v)(gb)^2 \cos gbu}{U(u)} + \frac{\sin 2\pi v \cdot ((ga(gb)^2 + (ga)^3) \sin^2 gbu + 2ga(gb)^2 \cos^2 gbu)}{V(u)} \right) \end{bmatrix}$$

Eqn. A1-16

The tubular QSO²

¹ Notice that the definitions of X, Y, & Z differ from those on p. 219.

² I am indebted to Chris Young of the Yahoo! Graphing Calculator users' group for these expressions.

<<http://tech.groups.yahoo.com/group/GraphingCalcUsers/>>

Appendix 2

Three-Axis Rotation

A footnote in chapter 1 says that rotation on three mutually perpendicular axes was explored by Kelleher in 1991 and by Prodaniuk in 1992. Kelleher's QSO (1:2:1) and QSO (3:4:3) are displayed here.

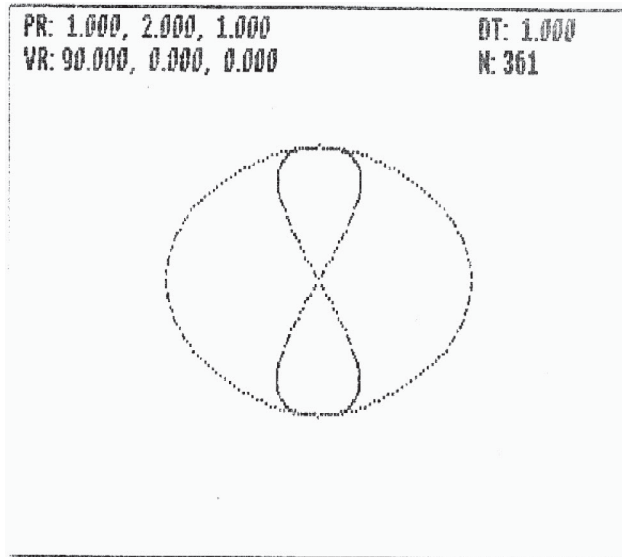


Fig. A2-1
QSO (1:2:1)¹

¹ Illustration © John Kelleher 1991. Used with permission.

PR is Kelleher's shorthand for "Point Rotation," the angular rate of rotation on each of the three axes. *VR* is "View Rotation," which indicates the point-of-view. Other than these very preliminary efforts, little is known about rotation on three axes.

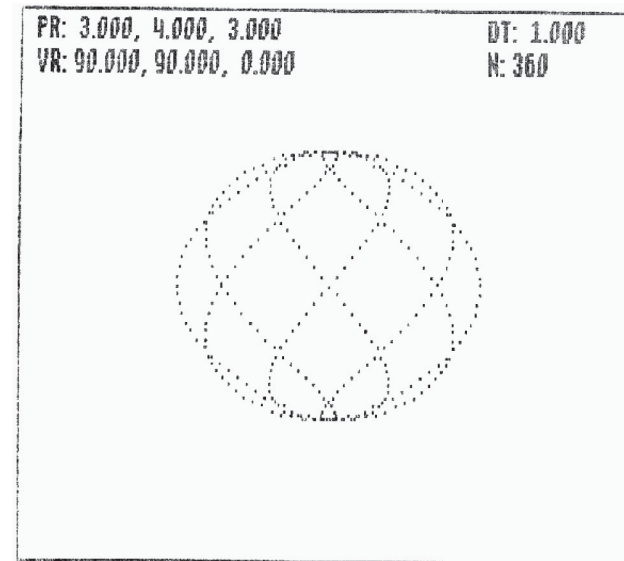


Fig. A2-2
QSO (3:4:3)²

² Illustration © John Kelleher 1991. Used with permission.

Prodaniuk's exploration of QSO (1:1:1) is next. Both views, which are from the z-axis, show a curve similar to but narrower than QSO 1(1:1)

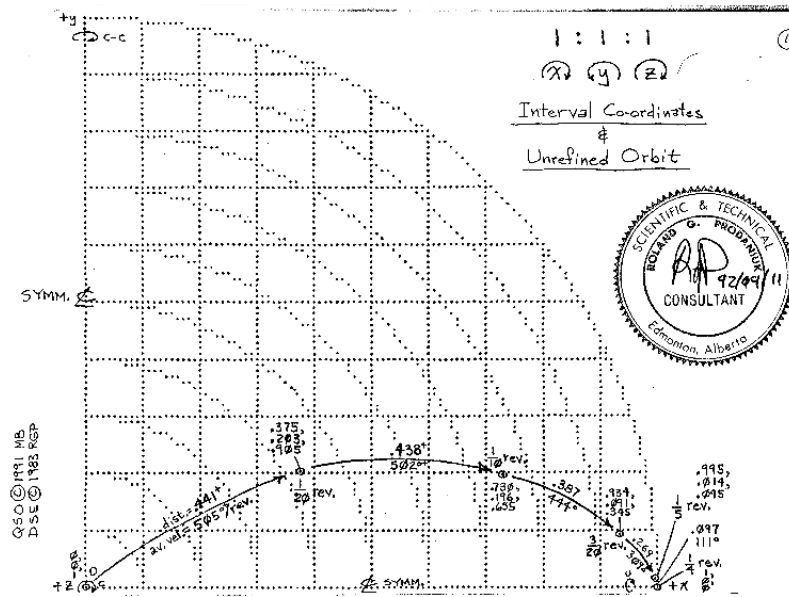


Fig. A2-3
QSO (1:1:1)³

³ Design for Scientists and Engineers (DSE) © Roland Prodaniuk 1983. Used with permission.
QSO illustration © Roland Prodaniuk 1992. Used with permission.

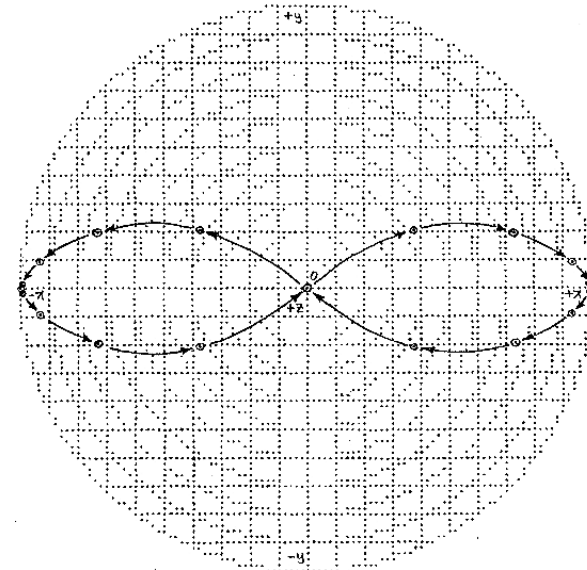


Fig. A2-4
QSO (1:1:1)⁴

⁴ Design for Scientists and Engineers (DSE) © Roland Prodaniuk 1983. Used with permission.
QSO illustration © Roland Prodaniuk 1992. Used with permission.

Appendix 3

The Octet Truss

Chapter 2 discusses Fuller's Isotropic Vector Matrix (IVM) as an alternative coordinate system for calculating and displaying QSOs. When the IVM is carried out as physical structure, it's known as the *Octet Truss*, where "octet" indicates the alternating *octahedral-tetrahedral* nature of the framework.

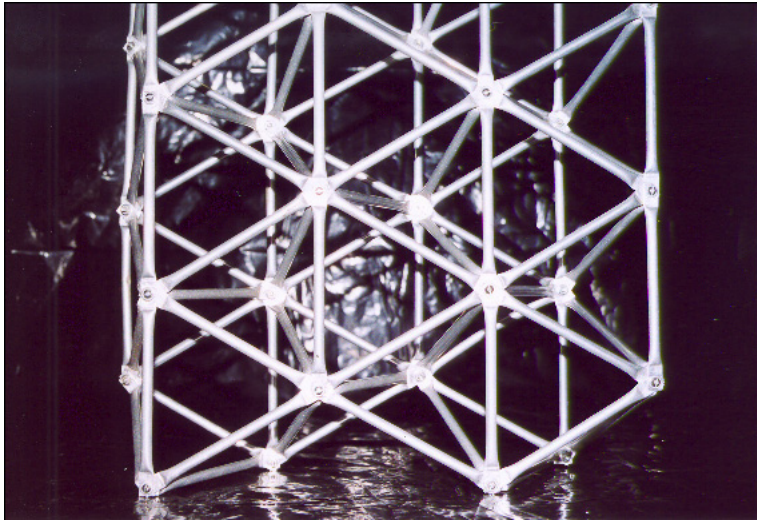


Fig. A3-1

An aluminum tube Octet Truss

Figure A3-1 shows an aluminum tube Octet Truss built by the author. The truss was constructed according to the specifications in U.S. patent #2,986,241. The material was 0.25" aluminum tubing commonly available in hobby stores. The tubing was cut to length and flattened at the ends. One-eighth-inch holes were punched in the ends, and the struts were bolted together with 4-40 x 1/2" machine screws. Finished dimensions of the truss were 44.75" x 11.5" x 3.5", making a volume of about 1801 in³. The truss weighed 27.4 oz. Density of the truss was therefore 1.52 x 10⁻² oz/in³, or about the same as expanded polystyrene foam.

The Octet Truss

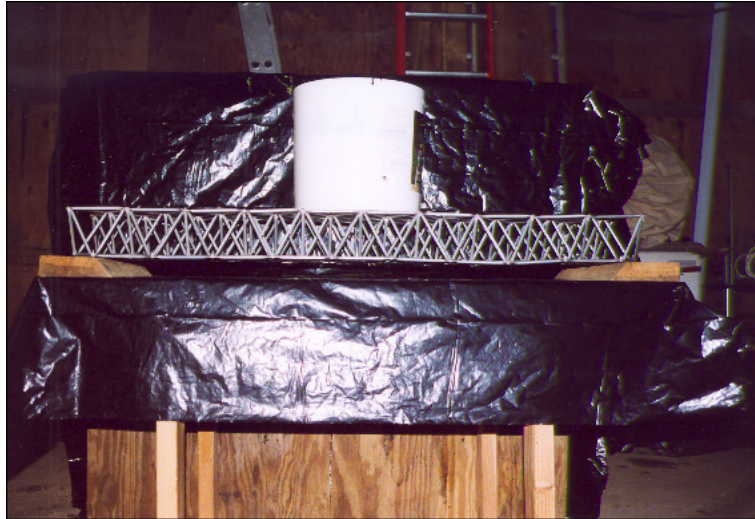


Fig. A3-2

The aluminum tube Octet Truss undergoing stress testing

The Octet Truss was positioned between two supports 40.25" apart. A bucket was placed in the center of the truss and filled with water in one pound increments. Deflection was measured from the bottom of the truss to the surface of the table. The smallest measurable unit of deflection was 1/64". At the maximum weight of 10 lb., no deflection could be measured. This is consistent with the fact that the structure of the Octet Truss is identical with the structure of natural diamond.

It was this combination of light weight and great strength that led Alexander Graham Bell to investigate tetrahedral space frames in the early 20th century.

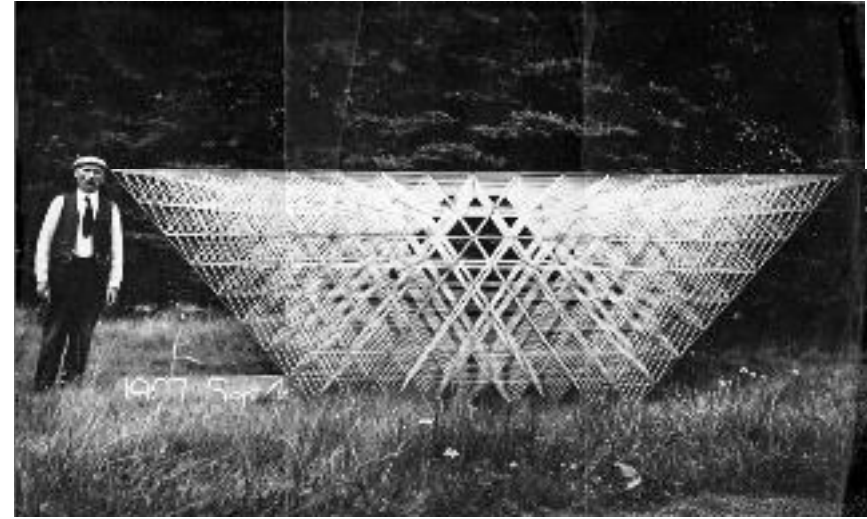


Fig. A3-3

A tetrahedral kite

Bell, who was interested in aviation from the time he was quite young, believed the safest way to get a man into the air would be with some sort of kite. He experimented extensively with kites made of tetrahedral cells.¹ One such kite is shown in the photo. The date, "1907 Sep 4," can be seen faintly written in the grass between the man's feet and the edge of the kite. By November of that year Bell would create the Cygnet, a tetrahedral kite with over 3300 cells, which would succeed in carrying a man into the air. The man in the picture is Hector

¹ Bell was granted three U.S. patents for his tetrahedral work: #757,012 for an Aerial Vehicle, #770,626 for an Aerial Vehicle or Other Structure, and #856,838 with Hector MacNeil for a Connecting Device for the Frames of Aerial Vehicles and Other Structures.

MacNeil who worked with Bell for many years building whatever experimental apparatus Bell devised.

More recently the Octet Truss has been used for everything from roofing at the Kennedy Space Center to the main structure at Biosphere 2 in Oracle, Arizona.

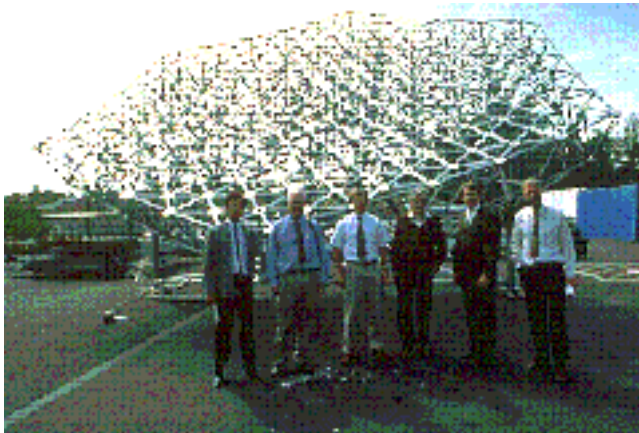


Fig. A3-4

The Hobby-Eberly Telescope primary mirror truss²

Pictured here, the primary mirror truss of the Hobby-Eberly Telescope at the McDonald Observatory, University of Texas.³ Dr. Frank Bash, the former Director of McDonald Observatory, is second from left.

² © Hobby-Eberly Telescope Partnership. Used with permission.

³ http://hyperion.as.utexas.edu/mcdonald/het/het_images/06truss_etal.html

Appendix 4

A Brief History of QSO Programming

Chapter 6 traces the early history of QSO programmers and their work. The people and their programs are detailed here.

Year	Programmer	Program	Language	Computer	Comments
1990	Loftus	3-D Combined Rotation Plotter	BASIC	IBM XT	Isometric view only
?	Crosby	Loftus, improved	BASIC	IBM 286	All four static views simultaneously and in color.
1990	Loftus	Second Stage Program	BASIC	IBM XT	Individual views of each axis in addition to the isometric
1991	Kelleher	QSO Simulator	PASCAL	Apple IIe	Views rotate around all three axes
1992	Crosby	?	BASIC?	IBM AT or better	All four views developing simultaneously
1994	Kelleher	Spin Engine of a QSO	BASIC	Apple IIgs	View rotates around any arbitrary vector

Drawing QSO Polyhedra

One of the more interesting aspects of Quasi-Spherical Orbits is the fact that when the events are connected by straight lines, they form a plethora of polygons and polyhedra. The study of these figures requires the ability to draw them. Although we will focus here on the polyhedra of chapters 10 and 11, the lessons learned will allow the reader to draw polyhedra for any QSO. The first example is from chapter 10.

QSO 1(1:3), the Oblate Hexahedron

QSO 1(1:3) forms a hexahedron, or two face-bonded tetrahedra. It consists of 10 chords: three in the xy-plane, three in the northern hemisphere of the unit sphere, three in the southern hemisphere, and one chord along the z-axis. It has five events. Three are equally distributed around the z-axis in the xy-plane, with one each at the north and south poles. Although it was not specifically indicated in chapter 10, table 10-4 clearly shows that the hexahedron is polarized in an oblate manner. The extent of the figure along the z-axis is less than it would be if the tetrahedra were regular figures. The perception is that they've been compressed along the z-axis.¹

¹ Due to its rotation, the Earth is an oblate spheroid. Its north-south axis is slightly shorter than any of its equatorial diameters.

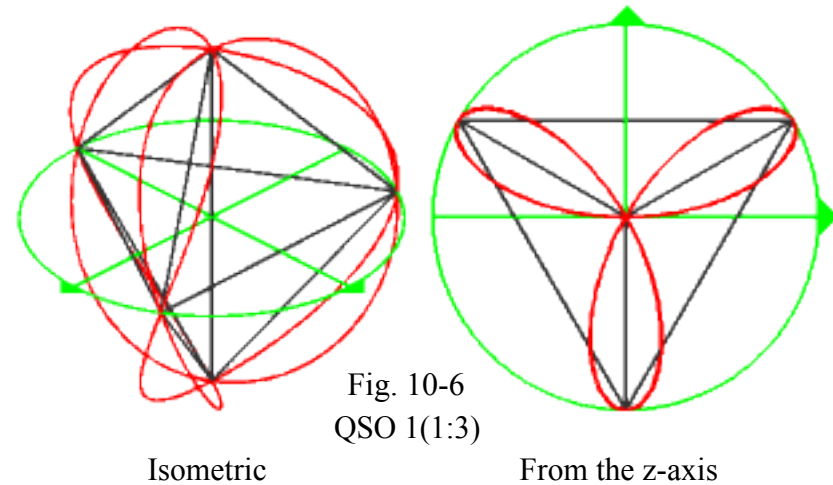


Fig. 10-6
QSO 1(1:3)

Isometric

From the z-axis

QSO 1(1:3) is shown above as it appeared in chapter 10. Although it may seem easier to begin with the chords that radiate from the z-axis, the procedure is actually simpler for the triangle in the xy-plane. In order to draw chords, we first define a new variable, angle d .

$$d = \frac{90^\circ}{b}$$

Eqn. A5-1
Angle d

where b is the second element of the QSO ratio (a:b)

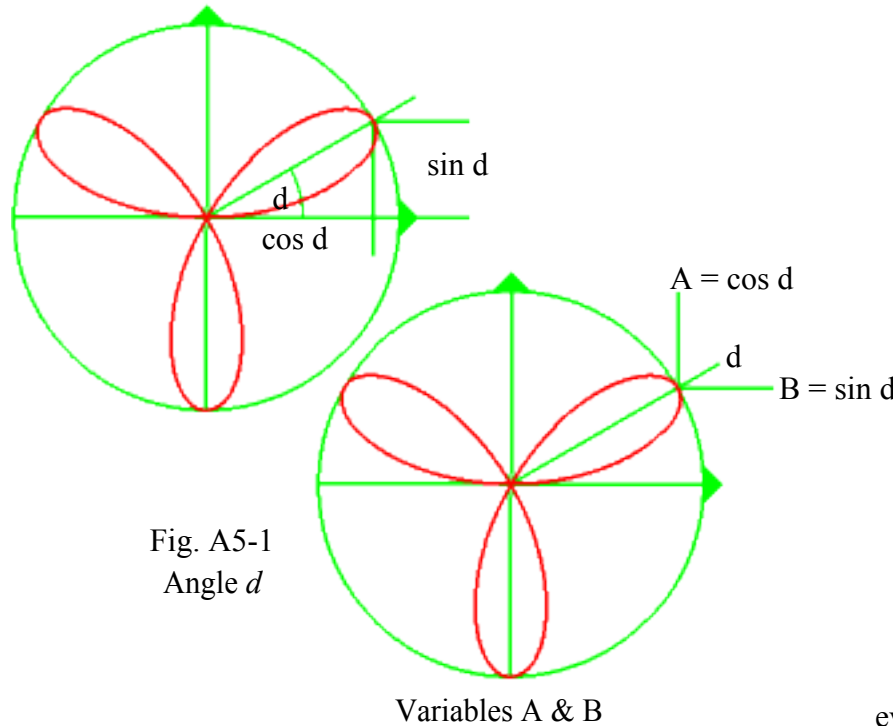
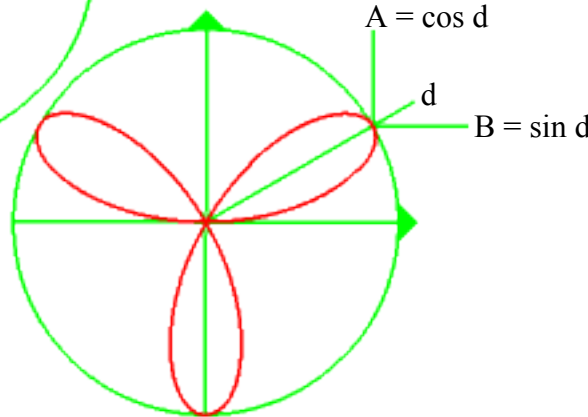


Fig. A5-1
Angle d



Variables A & B

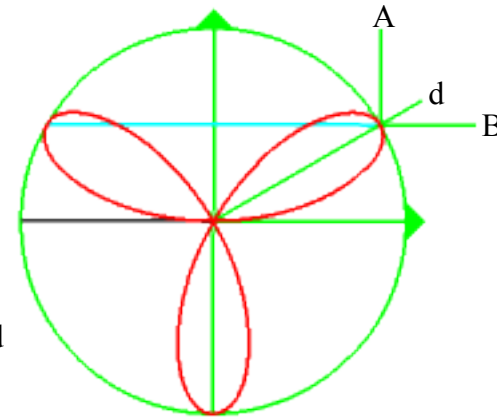


Fig. A5-2

A radial horizontal chord

$$\begin{bmatrix} x \\ y \\ z \end{bmatrix} = \begin{bmatrix} -t \\ 0 \\ 0 \end{bmatrix}$$

where $t: 0 \dots 1^3$

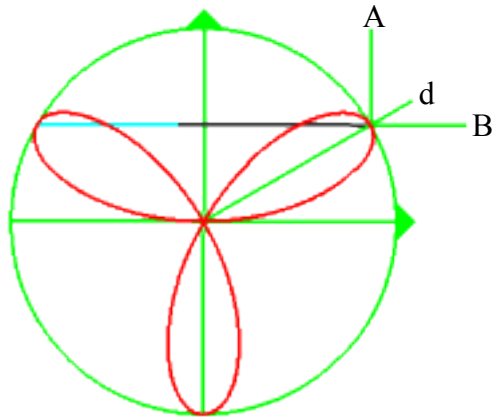
Eqn. A5-2

Angle d is shown in this view of the 1(1:3) from the z-axis. It is the angle between a line from the Origin to the event in the first quadrant of the xy-plane and the positive x-axis.² On the right, the sine and cosine of d are labeled B and A , respectively. The labels have been placed outside the unit circle in order to leave the QSO and its chords visually uncluttered. Let's move on to the horizontal chord in the xy-plane.

² Even without Eqn. A5-1, it's pretty easy to show that $d=30^\circ$. When the QSO trace reaches the event at $(A, B, 0)$, the b-rotation has rotated through 90° (see Fig. 3-1). However, the a-rotation, which rotates 1/3 as fast, has only gone through 30° .

The target chord is shown in light blue. It connects the two events in the first and second quadrants of the xy-plane. Applying standard right-hand rotation around the Origin, the chord begins at $(A, B, 0)$ and ends at $(-A, B, 0)$. Equation A5-2 draws a black radial horizontal vector along the negative x-axis. At this point we are interested only in the fact that the parametric variable t has the same sign as the target chord, so the vector is drawn right to left. It begins at the Origin and ends at $(-1, 0, 0)$. This gives t a negative sign.

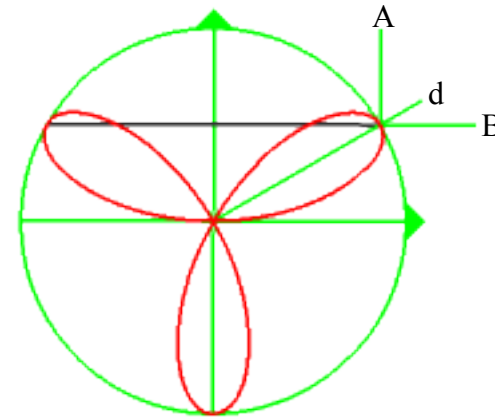
³ Although the range of the parametric variable t may be defined differently in different contexts, in this book t always goes from zero to one unless otherwise noted. See chapter 2, p. 13. For an exception, see chapter 10, p. 166, footnote 10, Loftus' equation.



$$\begin{bmatrix} x \\ y \\ z \end{bmatrix} = \begin{bmatrix} -t + A \\ B \\ 0 \end{bmatrix}$$

Fig. A5-3

Moving the vector to the beginning of the target chord



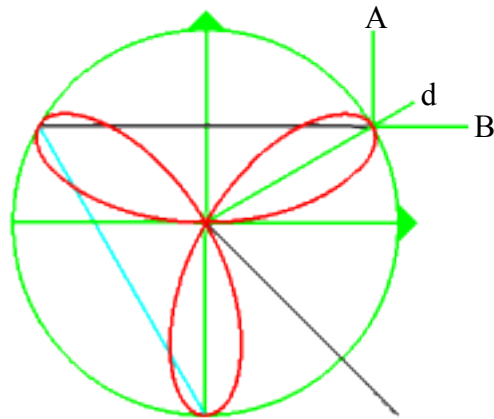
$$\begin{bmatrix} x \\ y \\ z \end{bmatrix} = \begin{bmatrix} -2tA + A \\ B \\ 0 \end{bmatrix}$$

Fig. A5-4

Completing the chord

To move the vector to the beginning of the target chord, we add A to the x-term of the vector while B is added to the y-term.

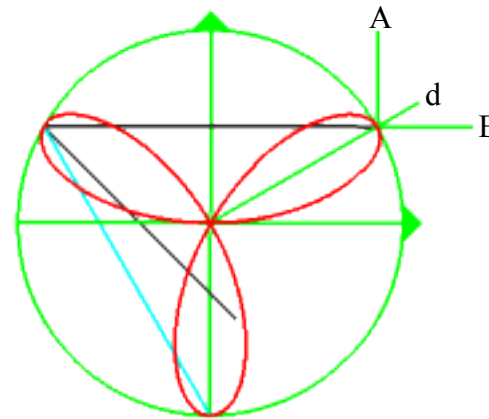
The length of the chord is $2A$, which is entered as a multiplier of t . There is no extent of the chord along the y- or z-axes, so no further changes are needed.



$$\begin{bmatrix} x \\ y \\ z \end{bmatrix} = \begin{bmatrix} t \\ -t \\ 0 \end{bmatrix}$$

Fig. A5-5
The second chord of the triangle

To draw the second chord of the triangle, we again begin with a radial vector. The vector equation is written such that all variables t have the same sign as the target chord.



$$\begin{bmatrix} x \\ y \\ z \end{bmatrix} = \begin{bmatrix} t - A \\ -t + B \\ 0 \end{bmatrix}$$

Fig. A5-6
Moving the vector to the beginning of the target chord.

Subtracting A from the x -term of the vector and adding B to the y -term moves the vector to the beginning of the target chord, but does nothing for alignment or length.

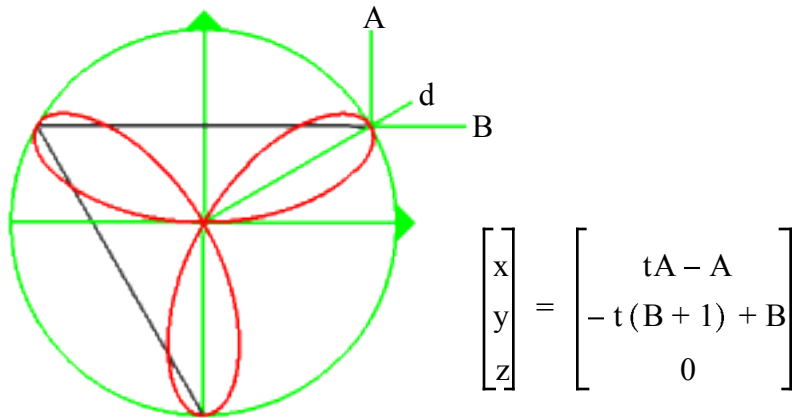


Fig. A5-7
Completing the second chord of the triangle

The length of the target chord in the x -direction is A , which is entered as a multiplier of t . In the y -direction, the length has two parts, B , from the first chord to the x -axis, and 1, from the x -axis to $(0, -1, 0)$. In order to maintain a sense of direction, the length is written as $(B + 1)$, rather than $(1 + B)$, even though the scalar values of these expressions are identical.

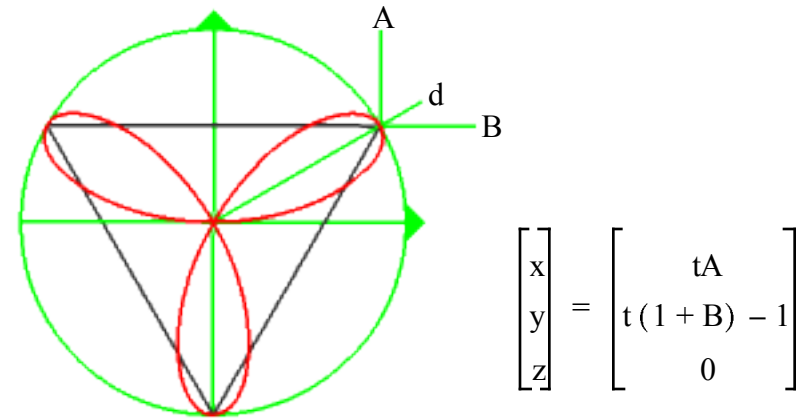


Fig. A5-8
The third chord of the triangle

The third chord of the triangle in the xy -plane is shown in Fig. A5-8. Although this chord could be created by negating the x -term of equation A5-7, in order to maintain the counterclockwise movement around the z -axis, we write equation A5-8 instead. In particular, the length of the vector along the y -axis is now written as $(1 + B)$ rather than the former $(B + 1)$. In general, this is the procedure we will follow – with increasing complexity – to draw all the chords of any polygon:

- First define a suitable angle or angles. In the present example only angle d was needed.
- Second, create a radial vector in the xy -plane such that all variables t have the same signs as the target chord.
- Third, move the vector to the starting point of the target

chord, and

- Fourth, adjust the length of the vector along all axes.

Chord Lengths

In general, the length of a vector is given by the equation

$$\sqrt{(\Delta x)^2 + (\Delta y)^2 + (\Delta z)^2}$$

Eqn. A5-9

A general expression for the length of an arbitrary vector⁴

The length of a vector along an axis is represented by the multipliers of t on that axis. In the present case, the length of the third side of the triangle is

$$\sqrt{(A)^2 + (1 + B)^2 + (0)^2} = 1.73205\dots = \sqrt{3}$$

Eqn. A5-10

The length of the third side of the triangle in the xy -plane

This is the length that was recorded for this chord in table 10-4. The reader is invited to confirm that the other two sides of the triangle are identical, making the figure an equilateral triangle.⁵

⁴ Compare this equation with equation 10-1.

⁵ QSO 1(3:1) creates an identical equilateral triangle, but in the yz -plane. See Fig. 10-2 and Table 10-2.

Chords With a Z-Term

The 1(1:3) hexahedron has three chords in the xy -plane, three in the northern hemisphere, three in the southern hemisphere, and one along the $\pm z$ -axis. We turn our attention now to drawing one of the chords in the northern hemisphere.

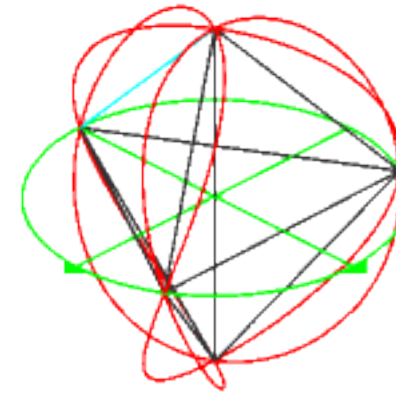


Fig. A5-9
The target chord

The first target chord in the northern hemisphere will be the one from $(0, 0, 1)$ to $(0, -1, 0)$.

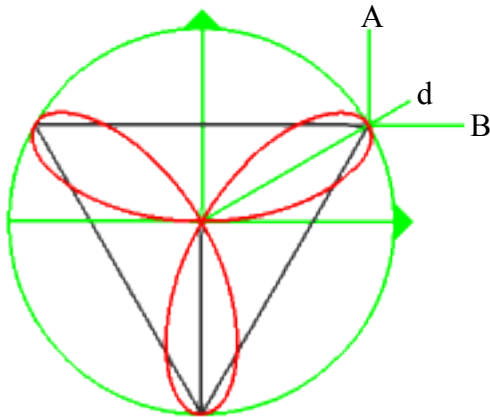


Fig. A5-10

A radial vector in the xy-plane

$$\begin{bmatrix} x \\ y \\ z \end{bmatrix} = \begin{bmatrix} 0 \\ -t \\ 0 \end{bmatrix}$$

Eqn. A5-11

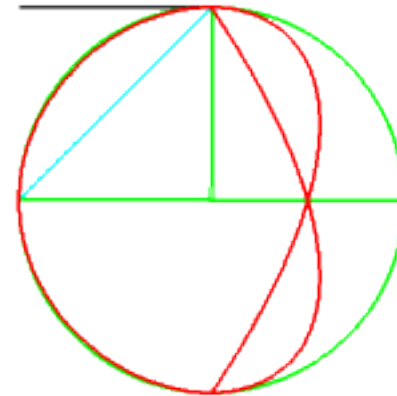


Fig. A5-11

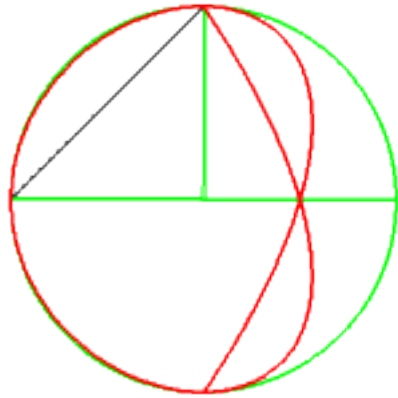
Placing the beginning of the vector at $z = 1$
View from the x-axis

$$\begin{bmatrix} x \\ y \\ z \end{bmatrix} = \begin{bmatrix} 0 \\ -t \\ 1 \end{bmatrix}$$

Eqn. A5-12

We begin, as usual, with a radial vector in the xy-plane. It starts at the Origin and extends to $(0, -1, 0)$. Equation A5-11 consists of a single variable t , which is negated to give the vector direction *from* the Origin *to* $y = -1$. Although the vector could certainly be drawn the other way, the author's personal preference is to draw from the pole to the equator.

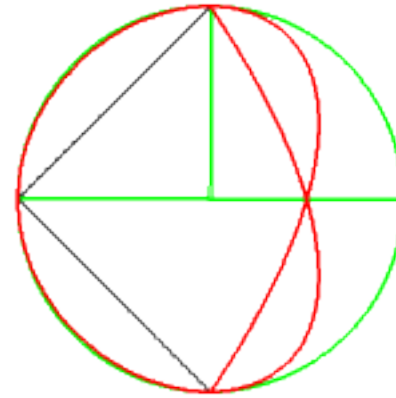
The target chord begins at $(0, 0, 1)$. This view from the x-axis shows that equation A5-12 places the beginning of the vector at $z = 1$. The green unit circle is a meridian which has been drawn in the yz-plane. On the left side of Fig. A5-11 the red QSO appears to be slightly inside the unit circle everywhere except at the equator. This attests to the fact that the QSO is not actually on the yz-plane, but slightly in front or in back of it everywhere except at $(0, -1, 0)$.



$$\begin{bmatrix} x \\ y \\ z \end{bmatrix} = \begin{bmatrix} 0 \\ -t \\ -t + 1 \end{bmatrix}$$

Fig. A5-12
Adjusting the length and direction of the vector to match the target chord

The final step in drawing the chord is to realize that the extent of the chord along the z-axis is negative t . No other changes are needed.



$$\begin{bmatrix} x \\ y \\ z \end{bmatrix} = \begin{bmatrix} 0 \\ -t \\ t - 1 \end{bmatrix}$$

Fig. A5-13
A chord in the southern hemisphere

Equation A5-14 draws the corresponding chord in the southern hemisphere. The equation reflects the author's preference for drawing from pole to equator, and not vice-versa. The reader is invited to confirm that the length of the two chords thus drawn is $\sqrt{2}$, and that the angle between them is 90° .⁶

⁶ $\sqrt{2} < \sqrt{3}$, thus verifying the oblate polarization of the hexahedron.

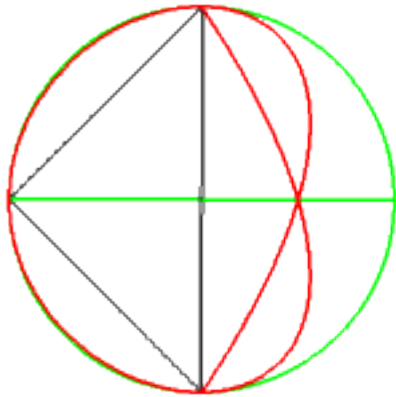


Fig. A5-14

The chord along the z-axis

$$\begin{bmatrix} x \\ y \\ z \end{bmatrix} = \begin{bmatrix} 0 \\ 0 \\ -2t + 1 \end{bmatrix}$$

Eqn. A5-15

The chord along the z-axis may be drawn from south to north or from north to south.⁷ The chord here is shown originating at the north pole and terminating at the south pole.

⁷ Although the direction of a vector is arbitrary in the static picture, when the dynamics of a QSO are considered, the order and placement of the events often suggest not only the order in which chords are created, but where they begin and end. For example, a chord cannot exist before the two events that create it. In monopoles, events are created sequentially. Therefore there must necessarily be a first and a second event before the existence of the chord. This suggests that the chord extends *from* the first event *to* the second. Multipoles, which offer the possibility of simultaneous events and multiple, overlapping chords, are more complex. For more on the order and sequencing of events, see chapters 3 and 4.

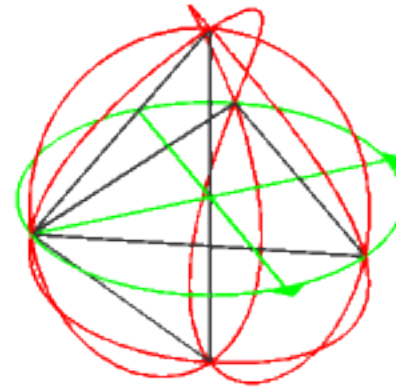


Fig. A5-15

QSO 1(1:3) with six of its 10 chords

The figure confirms that we have correctly drawn six of the ten chords of the QSO 1(1:3) hexahedron. The other four chords in the northern and southern hemispheres are similarly drawn. Their construction will be left to the reader.

QSO 1(2:3), the Prolate Octahedron

The second example of drawing a QSO polyhedron will be QSO 1(2:3), the polarized octahedron from chapter 11. We will find that whereas angle d and two variables, A & B , sufficed to draw the QSO 1(1:3) hexahedron, the QSO 1(2:3) octahedron will require four variables and a second angle to complete the figure.

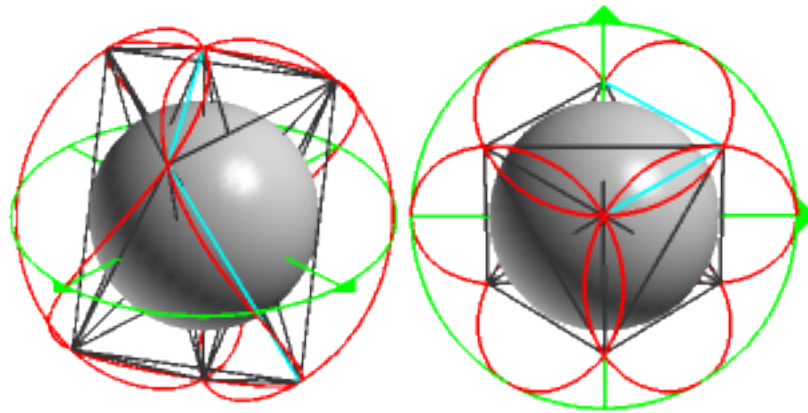


Fig. A5-16
QSO 1(2:3)

Isometric view

View from the z-axis

The QSO 1(2:3) polarized octahedron is shown in Fig. A5-16. An opaque central sphere ($r = 0.6$) has been inserted to block some of the visual confusion resulting from trying to see all 28 chords of the figure at once. The octahedron has two low-altitude tetrahedra on its northern and southern faces. One edge of the northern tetrahedron is colored light blue, as is an edge of the octahedron itself. These are the target chords for this section.

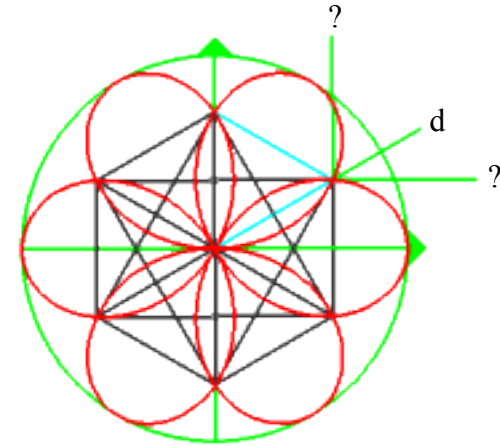


Fig. A5-17
Angle d

The first step in drawing QSO figures is to define suitable angles. This view from the z-axis shows that angle d is defined pretty much as before.

$$d = \frac{90^\circ}{b} = 30^\circ$$

Eqn. A5-16
Angle d

In fact, since $b = 3$ in both examples thus far, angle d has the same value in each. However, the coordinates of the events do not. In order to draw the chords of the 1(2:3) octahedron, a new angle will be needed. We'll call it angle c

$$c = \frac{90^\circ}{a}$$

Eqn. A5-17
Angle c

where a is the first element of the QSO ratio (a:b)

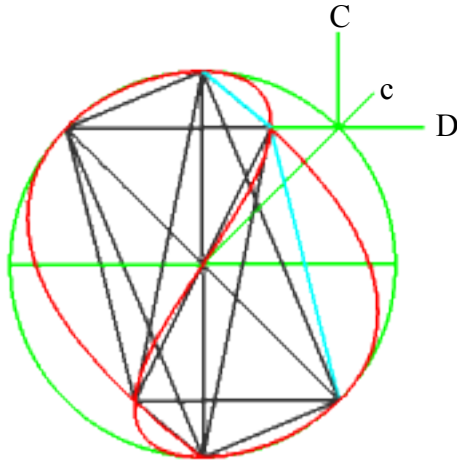


Fig. A5-18
Angle c , variables C & D

The view from the x-axis shows that the north and south non-polar events of the 1(2:3) octahedron are equidistant from the xy-plane. If the angle between the xy-plane and one of these events is c , then the events are at a distance of $\pm \sin c$ from the xy-plane, and $\cos c$ from the z-axis. This allows us to define two new variables.

$$C = \cos c \quad , \quad D = \sin c$$

Eqns. A5-18
Variables C & D

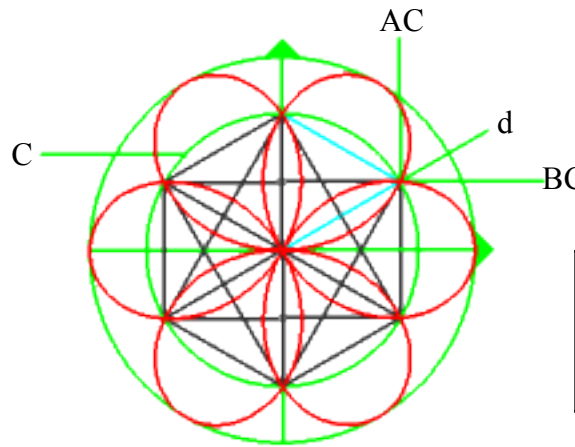


Fig. A5-19
Coordinates of the events

$$\begin{bmatrix} x \\ y \\ z \end{bmatrix} = \begin{bmatrix} tAC \\ tBC \\ -t(1-D) + 1 \end{bmatrix}$$

Eqn. A5-19
The first target chord

A circle of radius C is drawn on the view from the z-axis. The first target chord extends from $(0, 0, 1)$ to (AC, BC, D) . The x- and y-terms of the vector are written using the compound variables directly from the drawing. Negative t in the z-term indicates that the vector is drawn from the pole to the event at (AC, BC, D) . The only thing to remember here is to subtract D from the unit radius to get the extent of the vector along the z-axis. Having done so, you then add 1 to move the vector to $(0, 0, 1)$.

$$\begin{bmatrix} x \\ y \\ z \end{bmatrix} = \begin{bmatrix} -tAC + AC \\ t(C - BC) + BC \\ -2tD + D \end{bmatrix}$$

Eqn. A5-20

The second target chord

The equation for the second target chord, an edge of the octahedron itself, is somewhat more complex than those seen so far, but it follows the same rules. First write a radial vector in the xy-plane. Then move it to the beginning of the target chord, and finally write the extent of the vector along all three axes to match the chord.

QSO 1(2:5), the Prolate Icosahedron

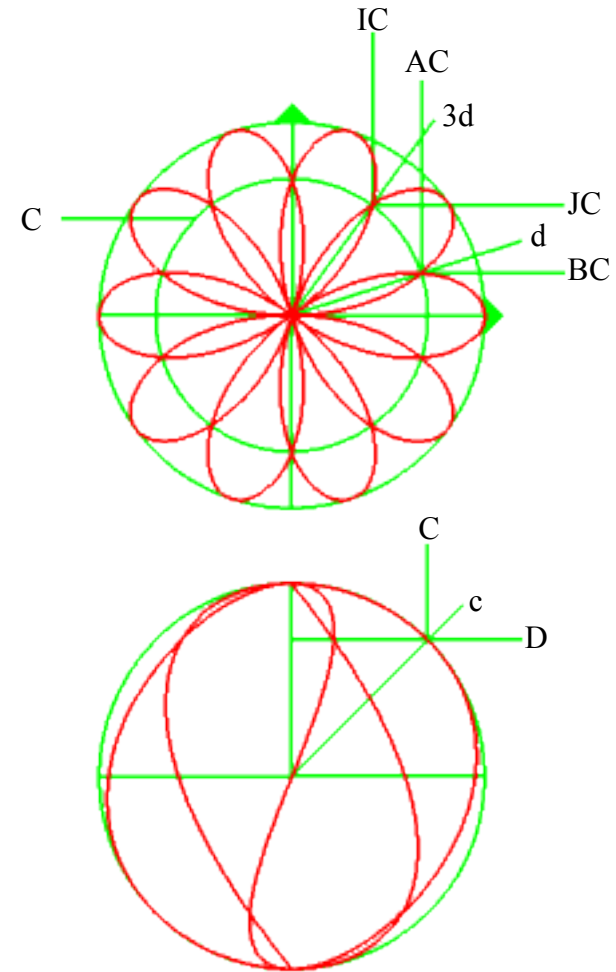
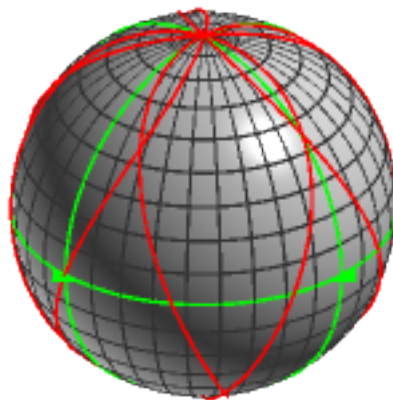


Fig. A5-20
QSO 1(2:5)

Isometric (left), z-, and x-axis views

The 1(2:5) polarized icosahedron shows angles c and d as before. Given that in the QSO ratio $a = 2$ and $b = 5$,

$$\begin{aligned} d &= 18^\circ \\ c &= 45^\circ \end{aligned}$$

The new feature in this QSO is the second angle as seen from the z-axis. It will be found that this angle is an exact multiple of angle d . In this case it is three times angle d , so rather than name it with a new letter, we'll call it angle $3d$.⁸

$$3d = 54^\circ$$

Using these three angles and their related definitions of variables A, B, C, D, I, & J, the chords may be written as before.

QSO 1(4:5), a 40-hedron

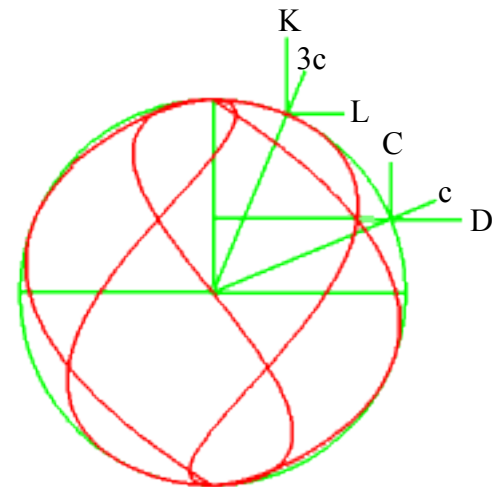
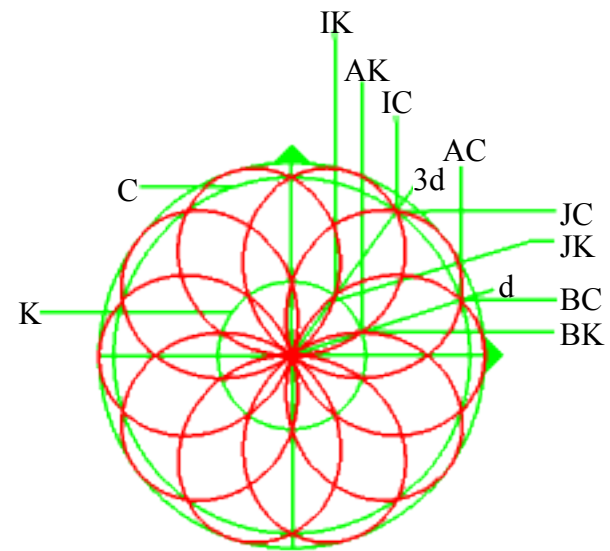
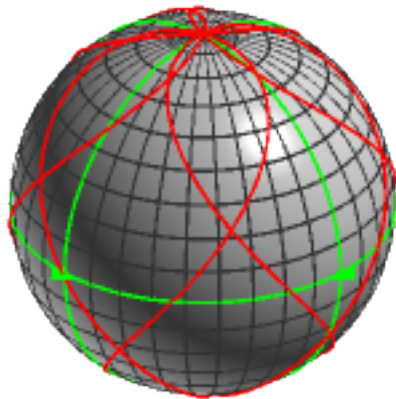


Fig. A5-21
QSO 1(4:5)

Isometric (left), z-, and x-axis views

⁸ These and all other angles associated with QSOs can be confirmed by tracing the angular rotations of the QSO as it develops.

QSO 1(4:5) creates a 40-hedron; its 22 events create 231 chords.⁹ The QSO shows increasing complexity in the number and placement of the defining angles, but no new features. Angles d and $3d$ still appear in the view from the z-axis, and their scalar values are identical to those in the previous example. However in the view from the x-axis, angles c and $3c$ differ from the previous values. Variables A, B, C, D, I, J, K, & L are needed to write the chords.

Variables Needed to Write the Chords of the First 25 QSO Monopoles

The reader is perhaps wondering why the sine and cosine variables are not named in sequence. Why, for instance, is there a gap between D and I in the previous example. The answer will be found in the following table.

⁹ These are the events counted statically. As we saw in chapter 10, p. 172, multiple passes at the poles can be seen as creating multiple overlapping events.

1:1	1:2	1:3	1:4	1:5	2:1	2:2	2:3	2:4	2:5	3:1	3:2	3:3	3:4	3:5	4:1	4:2	4:3	4:4	4:5	5:1	5:2	5:3	5:4	5:5		
		●		●			●		●					●			●		●				●			A = cos d
		●		●			●		●					●			●		●				●			B = sin d
					●		●		●		●		●		●		●		●		●		●			C = cos c
					●		●		●		●		●		●		●		●		●		●			D = sin c
													●											●		E = cos 2d
													●											●		F = sin 2d
											●			●		●					●		●			G = cos 2c
											●			●		●					●		●			H = sin 2c
				●					●					●						●						I = cos 3d
				●					●					●						●						J = sin 3d
															●		●		●		●		●			K = cos 3c
															●		●		●		●		●			L = sin 3c
																					●		●			M = cos 4c
																					●		●			N = sin 4c
0	0	2	0	4	2	0	4	0	6	2	2	0	4	6	4	2	6	0	8	4	4	6	6	0	Total variables	

Table A5-1
Variables needed for the chords of the first 25 monopole QSOs

Table A5-1 displays the first 25 monopole QSOs and the variables needed to write the chords for each. The QSOs are listed across the top of the table. On the right, the variables are

listed in order by size of their defining angle – first the unit angles d and c , and then $2d$ and $2c$, $3d$ and $3c$, and so on. The sine and cosine of angle $4d$ are not listed because they're not

needed in the first 25, although it's certainly reasonable to expect them to be needed as the QSO ratio increases. Readers wishing to explore beyond the limits of the table may need to create a more general scheme for naming the angles.

Derivation of the Total Chord Formula

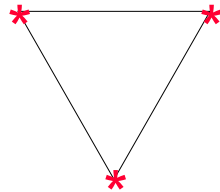
One of the main goals when drawing QSO polyhedra is to know when you've got all the chords. A total chord formula was presented without much justification in chapter 11, footnote 4. As a last offering in this appendix we will derive the total chord formula following a fairly intuitive line of reasoning. If we let a red star represent an event, then...



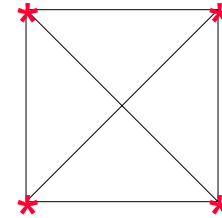
...one event has no chords...



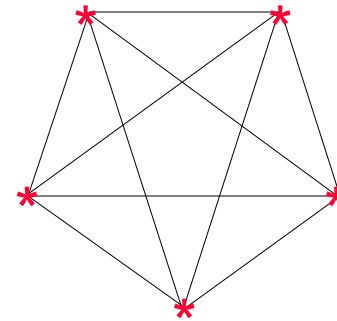
...two events have a single chord between them...



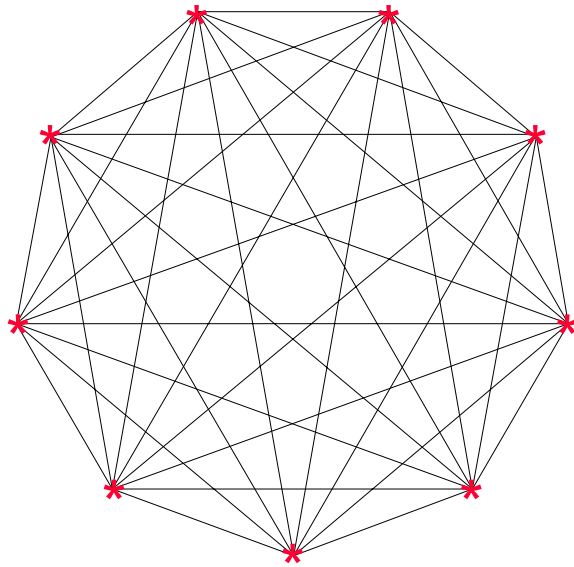
...three events, three chords...



...four events, six chords...



...five events, 10 chords...



...nine events, 36 chords...

and so on.

If there are n events, then each event is connected to $(n - 1)$ others. This results in $n(n - 1)$ chords. But if we count all chords this way, we're going to count each chord twice, once coming and once going, so the thing to do is to divide by two.

$$T_n = \frac{n(n-1)}{2}$$

Eqn. A5-21

The total number of chords between n events

References

- Avitzur, Ron 2002. *Learning math with graphing calculator*. Oakland: eeps media. <<http://www.eeps.com>>
- Banks, Robert 1999. *Slicing pizzas, racing turtles, and further adventures in applied mathematics*. Princeton: Princeton University Press.
- Brown, Kenneth A. 1988. *Inventors at work*. Redmond: Tempus Books of Microsoft Press.
- Burke, Michael 1992. *Quasi spherical orbits*. Unpublished manuscript.
- Coxeter, H. S. MacDonald (Donald) 1961, 1969. *Introduction to geometry*, 2nd ed. New York: John Wiley & Sons, Inc.
- Edmondson, Amy C. 1987. *A Fuller explanation*. <<http://www.angelfire.com/mt/marksomers/40.html>>
- Fuller, R. Buckminster 1946. Dymaxion map. U.S. Patent 2,393,676. Washington, D.C.: U.S. Patent and Trademark Office.
- 1975. *Synergetics*. New York: Macmillan Publishing Co. <<http://www.rwgrayprojects.com/synergetics/synergetics.html>> Accessed 2008 Jul 15
- 1979. *Synergetics 2*. New York: Macmillan Publishing Co.
- 1992. *Cosmography*. New York: Macmillan Publishing Co.
- Gray, Alfred 1998. *Modern differential geometry of curves and surfaces with mathematica®*, 2nd ed. Boca Raton: CRC Press.
- Greene, Brian R. 2003. *The elegant universe*. New York: W. W. Norton & Company, Inc.
- Hein, Morris 1990. *Foundations of college chemistry*, 7th ed. Pacific Grove: Brooks/Cole Publishing Company.
- Kelleher, John P. 1991. Screen shots. Personal communication, Dec. 23, 1991.
- 1994. QSO – A Newsletter of Quasi-Spherical Orbits, 2:1. Intellectual Property Associates, Clearwater, FL, March 1994.
- Kenner, Hugh 1976. *Geodesic math and how to use it*. Berkeley: University of California Press.
- Loria, Gino 1925. La finestra di Viviani in *Curve Sghembre Speciali*, 1:201–3. Bologna: Nicola Zanichelli.
- Morris, William, ed. 1970. *The American heritage dictionary of the English language*. New York: Houghton Mifflin Co.

-
- O'Connor, John J. and Edmund F. Robertson 2008. Eudoxus of Cnidus. <<http://www-history.mcs.st-andrews.ac.uk/Mathematicians/Eudoxus.html>> Accessed 2008 Nov 18.
- 2008. Jules Antoine Lissajous. <<http://www-history.mcs.st-andrews.ac.uk/Mathematicians/Lissajous.html>> Accessed 2008 Nov 18.
- 2008. Leonardo Pisano Fibonacci. <<http://www-history.mcs.st-andrews.ac.uk/Mathematicians/Fibonacci.html>> Accessed 2008 Nov 18.
- 2008. Luigi Guido Grandi <<http://www-history.mcs.st-andrews.ac.uk/Biographies/Grandi.html>> Accessed 2008 Nov 18.
- 2008. Richard Buckminster Fuller. <<http://www-history.mcs.st-andrews.ac.uk/Mathematicians/Fuller.html>> Accessed 2008 Nov 18.
- 2008. Vincenzo Viviani. <<http://www-history.mcs.st-andrews.ac.uk/Mathematicians/Viviani.html>> Accessed 2008 Nov 18.
- Prodaniuk, Roland G. 1992. Graph of the QSO 1:1:1. Personal communication, September 11, 1992.
- Roberts, Siobhan 2006. *King of infinite space*. New York: Walker Publishing Co.
- Roero, Clara S. 1986. L'Interet International d'un Probleme Propose par Viviani in *Actes de L'Université sur L'Histoire des Mathématiques* 351–79. Toulouse: Université Paul Sabatier.
- 1988. The Italian challenge to Leibnizian calculus in 1692 in *Leibniz Tradition und Aktualität*. V. Internationaler Leibniz-Kongreß, Vorträge, Hannover, 14-19 November, 1988, 803–10. Hannover: Gottfried-Wilhelm-Leibniz-Gesellschaft e.V., Niedersächsische Landesbibliothek.
- Soukhanov, Anne H., ed. 1992. *The American heritage electronic dictionary*. New York: Houghton Mifflin Company.
- Space curve gallery 2008. <<http://www.math.umd.edu/research/bianchi/Gifspacecurves/spcu.html>> Accessed 2008 Nov 18.
- Yam, Philip 1991. Spin cycle. *Scientific American* 265:16.

Index

A

- a* (a rotation, first element of the QSO ratio), 13–14, 26
 - equal-rate valley, 72
 - and monopole QSO polygons and polyhedra, 161–162, 164, 171
 - in unicycle model, 33
- Acoustic vibrations, 133
- Aenigma geometricum* (Viviani), x
- Analemma, 211
- Analytic geometry, x
- Angle in a coordinate system, 11. *See also* Phase angle; Tipping angle
 - angle c, 2c,3c, etc., 237–238, 241, 242
 - angle d, 2d, 3d, 4d, etc., 228, 237, 240, 241–242
 - definition of Phi (ϕ), 87
 - regular icosaedra in icosahedron, 67
 - use of radian to express, 11
 - use of sine/cosine to express, 16, 17, 30–32
- Archimedes' spiral, 145
- Architectural structure, 224–226
- Asclepius' staff, 50n11
- Astroid. *See* 3-D astroid; 2-D astroid
- Axes. *See also* x-axis view; y-axis view; z-axis view
 - about QSO, 2
 - colors of eight combinations of positive and negative QSO axes, 26
 - exchanging, 21–23
 - in Lissajous figure, 133
 - orthogonal system, 18n5, 20
 - reversing polarity, 23–26

- sine/cosine to express off-axis event, 61
- three-axis QSO, 222–223
- three-in-one QSO globe display, 95
- visualizing, 3–10
- x, y, and z axes in a coordinate system, 11, 16, 17
- Ayiomamitis, Anthony, 211

B

- b* (a rotation, second element of the QSO ratio), 13–14, 26
 - equal-rate valley, 72
 - and monopole QSO polygons and polyhedra, 161–162, 164, 171
 - in unicycle model, 33
- Banchoff's The Temple of Viviani, 157
- Base 720 rather than base 10, 18n6
- Baseball seam QSO, 35n1, 66–67, 71, 72
 - compared with monopole QSO (1:2), 149–151
 - event, 53
 - polar trace of Gray's, 151
- Bash, Frank, 226
- Bell, Alexander Graham, 225–226
- Bend Sinister, 72n2
- Biosphere 2, 226
- Borromeo, Clelia, 154
- Burchester cardioid, 116
- Burchester snub disphenoid, 192
- Burke, Michael, 200, 204
 - and David Loftus' QSO tool, 78, 158
 - generation of first QSO, 194–195
- Octamap suggestion, 81n6, 199

Burke, Michael, *continued*

- on Platonic solid imperfection, 209n18
- QSO tetrahedron discovery, 158, 180, 185
- simultaneous energetic dipole, 206

C

c (variable for drawing chords), 237–238

Caduceus, 50n11

Cannonball stack model, 19

Cardioid, 114–116, 121n14. *See also* Spherical cardioid relation to Pascal's *limaçon*, 117

Cartesian coordinate system, 16–18, 20, 196. *See also* Isotropic Vector Matrix (IVM); Spherical coordinate system

de Castillon, Johann, 114, 116

Chester, Robert. *See also* Octamap

- Octet Truss, 224–225

- QSO generator, 201

Chirality, 28–30

Chord length. *See also* Line

- 1(a:1) QSO polyhedra, 161–162

- 1(1:b) QSO polyhedra, 164–165

- in complete polyhedron example, 180–184
- equation, 233

- L-1(a:1) series, 167

- Platonic solids, 187, 189, 191

- snub disphenoid, 193

Chordal increments of QSO (1:1), 69, 70

Chords of polygons

- drawing, 228–233

- new angles, 228, 237–238, 240–241

- total chord number formula, 186n4, 243–244

- variables for writing chords in first 25 monopole QSOs, 241–243

- z-axis chords in first 25 monopole QSOs, 179–180

Chords of polygons, *continued*

- with z-term, 233–236

Circle

- latitude and longitude, 94

- Lissajous figure, 135

Clelia, 154–156, 203

Cone and disk display of QSO, 82–92

Cone of Phi (ϕ), 86–87

- second, 88–89

Conical helix, 145

Continuously varying QSO ratio, 40–42

Coordinate system. *See* Cartesian coordinate system; Isotropic vector matrix (IVM); Spherical coordinate system

Cosine. *See* Sine/cosine

Crosby, Athol, 79, 227

Cube. *See* Hexahedron (Cube)

Cubical 3-D astroid, 146–147

Cuboctahedron, 67

Curly brackets, 21

Curve. *See also* Lissajous figure; Plane curve; Space curve; specific types, e.g., Cardioid, Lemniscate, Viviani's window, etc.

- cloned, 219

- difference between monopole QSO (a:1) and (1:b), 164

- geometric figures from QSO curve, 158

- Gray's baseball seam, 149–151

- Loftus' QSO series, 166

- using Graphing Calculator to explore epitrochoid, 120n12

Cycle of QSO with irrational ratio, 38–40

Cycloid, 120–121

Cygnets (tetrahedral kite), 225

D

d (variable for drawing chords), 228, 237

A lower case letter “n” following a page number indicates a footnote.

Decahedron, 164, 180
 Descartes, René, 16
 Diagonal line in Lissajous figure, 135
 Diamond structure, 225
 Dipole QSOs, 44–45. *See also* Monopole QSOs
 Burke's simultaneous energetic, 206
 differences from monopole QSO figure, 204
 polarity, 198
 QSO (1:1), event examples, 62–67
 QSO (3:1), 159
 QSO (3:2), cube generated from, 206–208
 Disc and cone display of QSO, 82–92
 Dodecahedron, 185, 191–193
 dual, 191n7
 possibilities for future study, 208–210
 Drawing QSO polyhedra. *See* Chords of polygons
 Dynamic view of QSO, 8–10. *See also* Static view of QSO

E

Eight curve (Gerono). *See* Lemniscate of Gerono
 Einstein, Albert, 18
 Element of QSO. *See* Event; Pole of QSO; QSO ratio
 Ellipse in Lissajous figure, 135
 Epicycloid, 121. *See also* Cardioid
 Epitrochoid, 120–124
 Equation of Time. *See* Analemma
 Equatorial event, 66–67
 Eudoxus of Cnidus, ix–x, xii, 211
 Event, 47–50. *See also* Intersection event; Tangent event
 about, 47, 51
 and chord, 236n7, 243–244
 dipole QSOs, 62–67
 distinguishing which branch of a QSO forms, 52n1
 equatorial, 66–67

Event, *continued*
 event constellation, 49–50
 order of off-axis QSO event, 58–61
 polar, 64
 polygons and polyhedra from straight line, 228
 possibilities for future study, 198
 single- and two-pass, 172
 and their geometric figures, 158–159
 Exponential QSO, 36

F

Figure eight curve. *See* Lemniscate of Gerono
 First Light, 78
 40-hedron, monopole QSO (4:5), 240–241
 Four-gons, 181
 Fractional QSO, 33–36, 167
 Fractional ratio, 33–36
 Fuller, Buckminster. *See also* Great circle railroad tracks of
 energy; Isotropic Vector Matrix (IVM)
 definition of synergy, 2n2
 Dymaxion Airocean World patent, 81n4
 Dymaxion Sky-Ocean World Map, 199
 objections to orthogonal axis system, 18–20
 on polygon shapes, 163n6
 statement on minimum system, 10
 on structure, 208–210
 tetrahedron and octahedron, 27
 theory of energy, xi–xii

G

g (variable in QSO vector equations), 15
 Geometric curiosity of dipole QSO event, 66–67
 Geometric figure from QSO curve, 158

A lower case letter “n” following a page number indicates a footnote.

Gerono, Camille Christophe, xi, xii. *See also* Lemniscate of Gerono
 Globe display of QSO, 92–95
 with three axial views at once, 95–104
 Grandi, Guido, x–xi, xii, 128, 154
 Graphing Calculator
 about, 7n7
 and equation for epitrochoid, 121n15
 exploring epitrochoid curves with, 120n12
 note about the slider, 83n9
 problem using, for QSO globe display, 95
 use of orthogonal axes, 20
 Gray's baseball seam, 149–151
 Great circle railroad tracks of energy (Fuller), xi, 66–67, 187, 204n10

H

Handedness of a pattern. *See* Chirality
 Helix, 145
 Hexagon, 162
 Hexahedra, 165
 Hexahedron (Cube), 163, 165, 185, 189, 206–208
 monopole QSO (1:3), 228–236
 QSO 6-hedron and the Platonic cube, 206–208
 Hippopede of Eudoxus, ix–x, xii, 211
 Hobby-Eberly Telescope, 226
 Hypocycloid, 145
 Hypotrochoid, 125–128

I

Icosahedron, 67, 71, 72, 185
 monopole QSO (2:5) prolate, 239–240
 possibilities for future study, 198

Icosahedron, *continued*
 QSO 1(2:5), 189–191
 Intersection event, 51–53. *See also* Tangent event
 notation, 47
 single, 48
 Irrational QSO, 37–40, 167
 Isometric view, 50
 3-D astroid, 146
 compared with vector diagrams, 50, 53
 first 100 monopole QSOs, 77
 icosahedron, 67
 L-1(1:b) QSO and their polyhedra, 168
 Loftus' 3-D Combined Rotation Plotter, 79
 Loftus QSO polygons and polyhedra, 166, 167
 monopole (b:1) QSO polygon series, 163
 monopole QSO (1:3), oblate hexahedron, 228
 monopole QSO (2:3), prolate octahedron, 237
 monopole QSO (2:5), prolate icosahedron, 239
 monopole QSO (4:5), a 40-hedron, 240
 monopole QSO and their Platonic solid, 186, 187, 188, 189, 190
 monopole QSO polygons, 160
 monopole QSO polyhedra, 164
 monopole QSO triangle, 160
 original QSO (1:1) display, 79
 QSO (1:2), rose bud, 131
 QSO (2:1), on xy-plane, 115
 QSO L-1(1:3), 168
 Isosceles tetrahedron, 188n6
 Isotropic Vector Matrix (IVM), 18–20. *See also* Cartesian
 coordinate system; Spherical coordinate system
 carried out as physical structure, 224–226
 modeling QSO in the, 197
 possibilities for future study, 196

A lower case letter “n” following a page number indicates a footnote.

J

J84. *See* Snub disphenoid (J84)
 Janus, 194, 195
 Johnson solid, 192

K

Kelleher, John, 79, 81, 142n9, 222, 227
 Kennedy Space Center, 226

L

L-1(a:1) and 1(1:b) series. *See* Loftus QSO series
 L-figure. *See* Lissajous figure
 Left-handedness. *See* Chirality
 Leibnitz, Gottfried, x
 Lemniscate of Gerono, xi, 7
 equivalence with projection of QSO (1:1) on xz-plane,
 110–114
 and Lissajous figure, 136–138
Limaçon, x, 117–120
 relation to cardioid and spherical cardioid, 117, 154
 relation with *rhodonea*, trochoid and QSO, 131
 Line. *See also* Chord length
 monopole QSOs, 162, 165, 175, 180
 Lissajous, Jules Antoine, 133
 Lissajous figure
 about, 133
 compared with QCO (Quasi-Cylindrical Orbit), 141–144
 figure (1:1), 134–135
 figure (2:1), 135–138
 figure (3:1), 138–140
 figure (10:7), 141
 generating, 133–134

Lissajous figure, *continued*
 possibilities for future study, 202
 three-in-one QSO globe display resemblance, 101
 Loftus, David, 78–79, 158, 227
 Loftus QSO series
 L-1(a:1), 165–167, 204
 L-1(1:b), 167–169

M

MacNeil, Hector, 225–226
 Mathematical concepts, 209n18
 McDonald Observatory, 226
 Mechanical devices to display QSO, 200–201
 Monopole polygons and polyhedra. *See also* Chords of
 polygons
 about, 158–159
 a-gons & b-gons, all four series, 169–174
 a-gons & b-gons, to polyhedra, 180–184
 drawing polyhedra, 228–244
 1(a:1) series, 159–163, 169
 1(1:b) series, 163–165, 169
 Loftus L-1(a:1) series, 165–167, 204
 Loftus L-1(1:b) series, 167–169
 possibilities for future study, 203–205
 reversal of orientation, 165
 z-axis view for constructing a-gons and b-gons, 174–180
 Monopole QSOs, 42–44. *See also* Dipole QSOs; Event;
 Monopole polygons and polyhedra
 and 3-D astroid, 147–148
 and the Clelia, 154–156
 first 25, chord variables, 241–243
 first 25, orbital length, 71, 72
 first 100, 72–77
 and Gray’s baseball seam, 149–151

A lower case letter “n” following a page number indicates a footnote.

Monopole QSOs, *continued*

- in QSO landscape, 159
 - reversal of orientation, 165
 - and spherical cardioid, 152–154
 - static figure duplication, 204
 - and Viviani's curve, 157
- Multipole QSOs, 45–47, 236n7

N

- n (slider variable in Graphing Calculator software), 14, 15
- Notation. *See* QSO notation

O

- Octahedron, 66, 67, 71, 72, 185, 224
- monopole QSO (2:3) prolate, 236–239
 - produced by dipole QSO, 204
 - QSO 1(2:3), 187–189
 - and tetrahedron, 27
- Octamap, 80–81, 93
- Octet truss, 224–226
- Off-axis event, 58–61
- One-dimensional QSO space curve, 1
- Orbital length. *See also* QSO landscape
- calculating, 68–70
 - for first 25 monopole QSOs, 71
 - possibilities for future study, 198–199
 - relation with rotational rate, 72
- Orbital trace. *See also* Baseball seam QSO; Polar trace of Gray's baseball seam
- difference between one and two axes, 68
 - in quadripole QSO display, 86, 87, 90, 91
 - in three-in-one QSO globe display, 100–101
 - with tubular parametric surface, 220–221

- Origin of a coordinate system, 11
- Orthogonal system of coordinates, 18n5

 - reasons for author's use, 20
 - relationship with Fuller's IVM system, 20

P

- P (a point in a coordinate system), 11, 16. *See also* Point
- formula for location of, 11
 - Point (1, 1, 1), 11
- Parabola and plane curve, 107–110
- Parametric sphere, 103
- Particle theory, 196
- Pascal, Etienne, x, xii. *See also* Limaçon
- Pentagon, 170–171
- monopole QSOs, 162, 169–172, 177–179
 - possibilities for future study, 204
- Phase angle. *See also* Angle in a coordinate system
- dipole and multipole QSOs, 44–47, 65–66
 - Lissajous figure, 135, 141n7
 - of monopole QSO pentagon, 172
 - omission, in some examples, 48n10
- Phi (ϕ), 11, 12, 87. *See also* Cone of Phi (ϕ)
- Physics
- string theory, 199
 - superdeformed nuclei problem, 203–204
 - virtual particles, 196
- Plane, two-dimensional, 105–107
- addition of parabola to, 107–110
 - for monopole (a:1) and (1:b) QSO, 169
- Plane curve, 105. *See also* Lissajous figure; Space curve
- epitrochoid, 120–124
 - hypotrochoid, 125–128
 - and lemniscate of Gerono, 110–114
 - and the *Limaçon*, 117–120

A lower case letter “n” following a page number indicates a footnote.

- Plane curve, *continued*
 and parabola, 107–110
 possibilities for future study, 201–202
rhodonea, 128–132
- Planetary motion, ix, 211
 polar system, 42–47
- Platonic solid, 185–193. *See also* specific type, e.g.
 Dodecahedron, Icosahedron, Tetrahedron, etc.
 definition, 185
 possibilities for future study, 204, 205–208
- Point. *See also* P (a point in a coordinate system)
 five 1-gons, 174
 monopole QSO, 162, 165
- Point Rotation, 222
- Polar event
 of dipole QSOs, 64
 monopole QSO Platonic solid, 186–187, 188, 190
 monopole QSO polyhedron, 181
 and z-axis view of monopole QSO, 174
- Polar trace of Gray’s baseball seam, 151
- Pole of QSO, 42–47
- Polygons and polyhedra, 71, 72. *See also* Chords of polygons;
 Monopole polygons and polyhedra; Platonic solid;
 specific types, e.g., Line, Triangle, Tetrahedra, etc.
 can space curves make polyhedra, 203
 reversal of orientation of polyhedron, 165
 stability, 208–210
 volumes of polyhedra, 193
- Prodaniuk’s three-axis QSO, 223
- Q**
- QCO. *See* Quasi-Cylindrical Orbit (QCO)
 QEO. *See* Quasi-Elliptical Orbit (QEO)
 QSO. *See* Quasi-Spherical Orbit (QSO)
- QSO (a:b), 13–14, 26–27, 161–162, 164
 reversal of orientation, 165
- QSO (b:a), 26–32
 total variations, 32
- QSO (0:1), 135n4
- QSO (0.5:0.5), 34
- QSO (0.5:1), compared with QSO (1:2), 35
- QSO (1:0.5), compared with QSO (2:1), 35–36
- QSO (1:1), 6, 13
 axial permutations, 23
 calculating orbital length, 69, 70
 compared with irrational ratio QSO, 37–40
 compared with three-axis QSO (1:1:1), 223
 dipole version, QSO event examples, 62–67
 displayed with three axial views at once, 95–104
 early QSO display, 79–80
 equivalence to parabola when on yz-plane, 107–110
 example, ix–x
 with exchanged trig (sine:cosine) functions, 30–32
 folded Octamap examples, 81
 generating with inverted unicycle, 5–6
 how it was first generated, 195
 monopole version, and spherical cardioid, 154
 monopole version, and the Clelia, 156
 monopole version, and unicycle model, 218
 monopole version, and Viviani’s curve, 157
 monopole version, event example, 47, 48
 monopole version, example, 51–53
 monopole version, polygon, 161
 with negative axes, 24, 25
 orbital length for first 25 monopole QSOs, 71, 72
 and quadrifolium, 129
 rational ratio, 37
 reversing chirality, 29
 view from x- y- and z-axes, 31

A lower case letter “n” following a page number indicates a footnote.

-
- QSO (1:1), *continued*
 and Viviani's window, 6
 on the xy-plane, 106–107
 xz-plane projection equivalence with Lemniscate of Gerono,
 110–116
- QSO (1:2), 131
 3-D rose bud view, 131
 compared with QSO (0.5:1), 35
 folded Octamap example, 81
 monopole version, and the Clelia, 156
 monopole version, compared with Gray's baseball seam, 149
 monopole version, event examples, 48, 53–58
- QSO (1:3)
 compared with exponential QSO, 36
 continuous series into QSO (2:3), 40–42
 difference from other irrational ratio QSO, 39–40
 monopole version, and the Clelia, 156
 monopole version, drawing the, 228–236
 monopole version, event examples, 49–50
 and trifolium, 129
- QSO (1:4), monopole version, and the Clelia, 155
- QSO (1:5)
 and the Clelia, 155
 monopole version, and attendant pentagon, 170
 monopole version, five 1-gons, 174
- QSO (2:1)
 8-trace variation, 92
 cardioid, 115
 Chester's Octamap example, 81, 82
 compared with QSO (1:0.5), 35–36
 comparison with cardioid, 114–116
 globe display example, 93–95
 to illustrate Fuller's great circle of railroad tracks of energy,
 ix, 66
Limaçon, 114–116
- QSO (2:1), *continued*
 and Lissajous figure (3:1), 138–140
 monopole, dipole, and multipole QSO examples, 43–47
 monopole version, and spherical cardioid, 152
 monopole version, and the Clelia, 156
 off-axis QSO event examples, 58–61
 quadripole, 89–92
 rational ratio, 37
 and *rhodonea*, 130
- QSO (2:3), 1, 14, 15
 compared with QCO (2:3), 142–143
 compared with QSO (3:2), 27
 continuous series generated from QSO (1:3), 40–42
 monopole version, drawing the, 236–239
 monopole version, octahedron, 187–189
 and space curve, 27n13
- QSO (2:4), monopole version, z-chord, 179, 180
- QSO (2:5)
 monopole version, drawing the, 239–240
 monopole version, five 2-gons, 173
 monopole version, icosahedron, 189–191
 monopole version, two 5-gons, 170
- QSO (3:1)
 compared to the *limaçon*, 117–120
 dipole version, 159
 and Lissajous figure (3:1), 138–140
 monopole version, and spherical cardioid, 152–153
 and *rhodonea*, 131
- QSO (3:2)
 Burke's discovery of geometric figure from QSO event, 158
 compared with QSO (2:3), 27
 dipole version, cube generated from, 206–208
 monopole version, and 3-D astroid, 147–148
 monopole version, tetrahedron, 185–186
- QSO (3:4), monopole version, complete polyhedron example,

A lower case letter “n” following a page number indicates a footnote.

-
- QSO (3:4), *continued*
 180–184
- QSO (3:5), 3
 hypotrochoid examples, 125–128
 monopole version, five 3-gons, 173
 monopole version, three 5-gons, 171
 rational ratio, 37
- QSO (4:1), 3
 monopole version, and spherical cardioid, 153
 monopole version, polygon, 162, 163–164
- QSO (4:2), monopole version, z-chord, 180
- QSO (4:5)
 monopole version, drawing the, 240–241
 monopole version, five 4-gons, 172
 monopole version, four 5-gons, 171
- QSO (5:1), 31
 monopole version, and spherical cardioid, 153
 monopole version, five 1-gons, 174
 monopole version, single 5-gon, 179
- QSO (5:2)
 monopole version, and Platonic dodecahedron, 191–193
 monopole version, five 2-gons, 175
 monopole version, three 5-gons, 178
 monopole version, two 5-gons, 178
- QSO (5:3)
 epitrochoid examples, 122–124
 monopole version, five 3-gons, 176
 monopole version, three 5-gons, 178
- QSO (5:4)
 monopole version, five 4-gons, 176
 monopole version, four 5-gons, 177
- QSO (5:5), monopole version, five 5-gons, 172, 177
- QSO (1:1:1) for three-axis QSO, 223
- QSO (1:2:1) for three-axis QSO, 222
- QSO (3:4:3) for three-axis QSO, 222
- QSO (1:n) series, 32
- QSO (n:n) where n is an irrational number, 40
- QSO display. *See also* Isometric view; Unicycle model; x-axis view; y-axis view; z-axis view
- 3-D, 98
- 3-D graph of orbital length, 72
- brief history of programmers and their work, 227
- cone & disk display, 82–92
- difference from Lissajous figure display, 141
- early types, 78–81
- globe with latitude and longitude, 92–95
- possibilities for future study, 199
- significance of sphere for Platonic solid, 180
- static and dynamic, 7–10
- QSO display colors
- 1-gons, 174
- chords inside QSO, 170n10
- eight combinations of positive and negative axes, 26
- on globe with longitude and latitude, 94
- irrational ratios, 37
- QSO landscape, 72
- red and blue, 22, 23
- small red and blue spheres, 50
- QSO equation. *See also* QSO (a:b); QSO (b:a)
- in Cartesian notation, 16–17
- globe display, 93
- Loftus' equation, 165
- original, 78
- in spherical notation, 15
- total number of variations, 32
- variations, 21–32, 197
- vector equation, rearranging terms within, 99–100
- vector equation, standard form, 21
- QSO generator, 201
- QSO landscape, 72–77, 159

A lower case letter “n” following a page number indicates a footnote.

- QSO landscape, *continued*
 possibilities for future study, 198–199
 with QSO analogs of three Platonic solids, 191
 single plane polygons, 169
 z-axis chord in first 25 QSOs, 179–180
- QSO notation. *See also* Variables used to express QSO
 dipole QSO, 44
 monopole QSO, 43
- QSO ratio, 5, 197. *See also* QSO landscape
 continuously varying, 40–42
 exponential, 36
 fractional, 33–36
 irrational, 37–40
 possibilities for future study, 197
 rational, 37
 standard form, 33
- QSO trace. *See* Orbital trace
- Quadrable Florentine sail. *See* Viviani’s window
- Quadri-foilium, 129, 132
- Quadripole QSO, 89–92
- Quasi-Cylindrical Orbit (QCO), 141–144, 200n8
 QCO (2:3) compared with Lissajous figure (2:3), 144
 QCO (2:3) compared with QSO (2:3), 142–143
- Quasi-Elliptical Orbit (QEO), 2
- Quasi-Spherical Orbit (QSO). *See also* Event; Graphing Calculator; Orbital length; Pole of QSO
 cloned, 219
 coordinate system for graphic illustration, 11–20
 definition, 1, 2, 195
 definitional relation with space curve, 145
 depiction in book’s diagrams, 1
 Earth as, 211
 generating with cone and disk display system, 87–88
 history of study, 194–195
 need to look at multiple views, 184
- Quasi-Spherical Orbit (QSO), *continued*
 negative or reversed, 22
 possibilities for future study, 195–196
 properties, ix, 3, 6, 145
 properties of dynamic, 34
 and QCO (Quasi-Cylindrical Orbit), 141–144
 quadripole, 89–92
 range and depth of the concept, ix–xii
 real-world application, 200
 three-axis, 222–223
 tubular, 220–221
 variables used to express, 12–15
 vector expression for QSOs, 12
 visualizing, 3–6, 11
- ## R
- r (radius in a coordinate system), 11
- Radius vector in quadripole QSO display, 84, 87, 89–90
- Ratio. *See* QSO ratio
- Red sphere in unicycle model, 217, 218
- Reference circle for three-in-one QSO globe display, 97
- Reference sphere for three-in-one QSO globe display, 101–104
- Retrograde motion of the planets, ix
- Rhodonea*, x, xi, 128–132
 relation with the Clelia, 154–156
 resemblance of QSO (1:n) series to, 32
- Right-handedness. *See* Chirality
- Roberval’s use of *limaçon*, 117
- Roemer’s model of cardioid, 114
- Rotating circle with Cartesian axes and equator, 83, 84
 in quadripole QSO display, 91
 translucent disk display, 86
- Rotating points
 and orbital length calculation, 70

A lower case letter “n” following a page number indicates a footnote.

Rotating points, *continued*

for single QSO event, 51–52

Rotation

after reversing chirality, 28–30

of dipole QSOs, 44

exchanging, 26–28

of irrational ratio QSOs, 38–39

of multipole QSOs, 46–47

notation for whether identical or not on both axes, 13–14

and orbital length, 68, 72

order of QSOs, 12

and QSO ratio, 34

series 1(a:1) and 1(1:b) QSOs, 165

three-axis QSOs, 222–223

S

Sine/cosine

to express angle in a coordinate system, 16, 17, 30–32

to express off-axis event in QSO, 61

variables used to write chord for first 25 monopole QSOs,
241–243

Sine waves, 70, 101

Single event, 47, 48

16-hedron, 184

Snub disphenoid (J84), 192, 193, 204–205

Space curve, 1–2, 105, 202. *See also* Plane curve

about, 145

baseball seam and QSO, 149–151

Clelia and QSO, 154–156

conical helix, 1

equations, 145n1

one-dimensional QSO, 1

polyhedra from, 203

possibilities for future study, 203

Space curve, *continued*

spherical cardioid, 152–154

3-D astroid, 145–148

and Viviani's curve, 157

Sphere. *See* Red sphere; Virtual sphereSpherical cardioid, 152–154. *See also* Cardioidrelation to Pascal's *limaçon*, 154Spherical coordinate system, 11–15, 196. *See also* Cartesian
coordinate system; Isotropic Vector Matrix (IVM)Spin, 195. *See also* Axes

Spiral and QSO projection, 145

Square

monopole QSOs, 162, 172–174, 176, 180

QSO 1(3:4) polyhedron example, 181

Square brackets for dipole and multipole QSOs, 44–45

Static view of QSO, 7, 8, 10. *See also* Dynamic view of QSO

String theory and QSO orbital length, 199

T

t (parametric variable), 13Tangent event, 48, 53–58. *See also* Intersection event

Temple of Viviani, The (Banchoff), 157

Tetrahedra, 163, 165

and 4-hedron QSO monopole (3:2), 210

Tetrahedral space frames of Alexander Graham Bell, 225–226

Tetrahedron, 67, 71, 72, 185, 224

first, 158–159, 180

isosceles, 188n6

monopole QSO (1:3) oblate, 228–236

and octahedron, 27

QSO 1(3:2), 185, 185–187

and QSO astroid, 147–148

relationship to cube, 209n17

Theta (θ), 11, 12

A lower case letter “n” following a page number indicates a footnote.

Three-axis QSO rotation, 222–223
 3-D astroid, 145–148
 3-D cardioid, 152–154
 3-D Combined Rotation Plotter (Loftus), 78–79, 158
 3-D QSO, 2, 196
 3-gons, 173, 182
 Tipping angle, 162–163
 Loftus QSOs, 167
 Triangle
 Buckminster Fuller’s theory of structure, 209
 monopole QSOs, 160, 162, 163, 173, 176
 QSO 1(3:4) polyhedron example, 181
 Trifolium, xi, 129, 163
 Trigonometry. *See* Angle in a coordinate system; Sine/cosine
 Trochoid, 131
 Tubular QSO, 220–221
 2-D astroid, 145
 2-D cardioid, 152, 154
 2-D QSO, 1, 195, 196
 2-gon, 173

U
u (parametric variable), 213
 Uneventful lives of points in a 2-dimensional circular orbit, 47
 Unicycle model
 about, 3–5
 cone & disk refinement, 82–92
 manipulating, 33
 r (radius), 11
 simulating, 212–221
 Unit circle and parabola on projection of QSO (1:1), 108
 and lemniscate of Geronno, 114
 University of Texas, 226

V

v (parametric variable), 213
 Valleys of similarity 72–73, 198–199
 Variables used to express QSO, 12–15, 26n12. *See also* *a* (a rotation, first element of the QSO ratio); *b* (a rotation, second element of the QSO ratio)
 Vector Equilibrium (Fuller), 67
 View Rotation, 222
 Virtual particle, 196
 Virtual sphere, 2–3
 QSO (1:1), 6
 Viviani’s curve, 157
 Viviani’s window, x, xi, xii, 6

W

Wavelength and QSO orbital length, 199

X

x-axis view
 first 100 monopole QSOs, 74
 first six 1(*a*:1) QSOs and their polyhedra, 164
 icosahedron, 67
 monopole QSO (2:5), prolate icosahedron, 239
 monopole QSO (4:5), a 40-hedron, 240
 monopole QSO polyhedra and their Platonic analogs, 186–190
 of polygon tipping angle, 162–163
 QSO (1:1), 31
 QSO (2:3) and QCO (2:3), 143
 of three-in-one QSO globe display, 100, 101, 103
 xy-plane
 cardioid and projection of QSO (2:1), 114–116

A lower case letter “n” following a page number indicates a footnote.

xy-plane, *continued*

- circle, 105–107
- drawing chords with z-term, 233–236
- limaçon*, 117–120
- monopole QSO series, 169–174
- QSO (2:1), and *rhodonea*, 130
- QSO (3:1), and *rhodonea*, 131
- QSO (3:5), and hypotrochoid, 125–128
- QSO (5:3), and epitrochoid, 122–124
- QSO geometric shapes, 164
- vs. 3-D view of QSO (1:2), 132
- xz-plane projection of QSO (1:1), 110–113

Y

y-axis view

- first 100 monopole QSOs, 75
 - Loftus QSOs, 166, 167
 - QSO (1:1), 31
 - QSO (2:3) and QCO (2:3), 143
 - three-in-one QSO globe display, 101, 103
- Young, Chris, 221n1

yz-plane

- monopole QSO series, 169
- parabola, 107–110
- QSO geometric shapes, 164
- in unicycle model, 212

Z

z-axis view

- of the Clelia, 155
- for constructing a-gons or b-gons, 174–180
- first 100 monopole QSOs, 76
- first six 1(1:b) QSOs and their polyhedra, 164
- Graphing Calculator view of Cartesian coordinate system
 - from, 95
- Kelleher rotation QSO display, 79
- monopole (b:1) series of QSO polygons, 163
- monopole QSO (1:3), oblate hexahedron, 228
- monopole QSO (2:3), prolate octahedron, 237
- monopole QSO (4:5), a 40-hedron, 240
- possibilities for future study of QSOs, 205
- QSO (1:1), 31
- QSO (2:3) and QCO (2:3), 142
- in three-in-one QSO globe display, 101, 103
- unicycle model, 212
- in vector diagram, compared with isometric view, 54

Michael Burke



Michael Burke has been a bookseller, a farm worker, a soldier, an art director for the movies, a herd tester and a gasworks stoker. In 1960 he once again changed his employment and became a middle manager in the field of scientific laboratory supplies, where he was successful because he could “speak the language,” and because he regarded no request as too outlandish to ignore. While he was thus employed, he discovered and developed the idea of spin occurring simultaneously on two or more axes.

Michael Burke, now in his eighties, lives with his wife in Auckland, New Zealand. He may be contacted at qso.michael@gmail.com.

The author

Robert Chester is a retired teacher of English as a Second Language. He is also a private pilot, an inventor with one patent to his name, and has designed and built geodesic domes. He was a Peace Corps volunteer in the mid-1960s, and is bilingual in English and Spanish. He and Michael Burke were already discussing their mutual interest in Buckminster Fuller when, in 1991, Michael wrote, “I have at odd times been working on an idea which others seem to have overlooked.” Thus was born the collaboration that resulted in this book.

The author lives in Tumwater, WA.



Why should “spin” be of necessity a two-dimensional phenomenon?

Quasi-Spherical Orbits, or QSOs, are the dynamic three-dimensional curves that result when a point rotates simultaneously about two or more axes. Although the historical record is littered with hints, many of which are cited in this book, there are no precedents for QSOs. These intriguing curves provide insights and yield results in mathematics and physics alike.

In mathematics, QSO (1:1) is produced by equal rates of rotation on the vertical and horizontal axes. This curve also goes by the name of Viviani's Curve (Vincenzo Viviani, 1622 - 1703), although Viviani probably never thought it could be generated dynamically. The projection of QSO (1:1) on the xy -plane is a circle. On the yz -plane it's a parabola, and on the xz -plane it's the Lemniscate of Geronno. Pascal's *Limaçon* is the projection of a QSO, as are Grandi's *Rhodonea* and Lissajous' figures. Three-dimensional curves subsumed by QSOs are the Astroid, the Baseball Seam, the Clelia, and the epi- and hypotrochoids. QSOs also generate all the Platonic Solids except the dodecahedron. Instead of the regular dodecahedron, QSO (5:2) generates the Johnson solid, J84, which is, in fact, dodecahedral. It's just not the Platonic version.

On the physics side, the Hippopede of Eudoxus is a QSO, as is the analemma. QSO (1:1) appears to characterize aspects of the electron cloud of the nitrogen atom, and QSO (1:2) may describe a special-case photon orbit around a Kerr black hole. A number of QSOs seem to be related to Buckminster Fuller's “Great Circle Railroad Tracks of Energy,” while QSO (3:2) may support Fuller's suggestion of a tetrahedral photon. QSOs seed a theory of virtual particles, describe the decay of superdeformed nuclei, and explain how to fit waves of enormous length into the minuscule volumes required by string theory.

Errata

p. 241: Period to question mark.

As printed: Why, for instance, is there a gap between D and I in the previous example.

Change to: Why, for instance, is there a gap between D and I in the previous example?

p. 60: The order of Events.

Current language: *Events are listed and analyzed in the order in which the rotating point first passes through the location of the event.*

But Events are created only by a second or subsequent pass of the rotating point, so it makes more sense to list the events in the order in which they're created, i.e. by a second or any subsequent pass through that same point.

QSOs on the WWW

- 1) <http://www.youtube.com/watch?v=k9gRoo4cLTc>
- 2) <http://www.youtube.com/watch?v=pNGwa-ff9GQ>
- 3) <http://www.youtube.com/watch?v=fu6Mm9L06k>
- 4) <http://www.youtube.com/watch?v=GAg3em5NY80>
- 5) <http://www.youtube.com/watch?v=tZM7u0jJY5k>
- 6) <http://www.youtube.com/watch?v=ADfjKmUwVtQ>

<http://www.quirkyscience.com/quasi-spherical-orbits/>

<http://curvebank.calstatela.edu/qsochester98/qsochester98.htm>